PB81-236150

Proceedings of the Joint Symposium on Stationary Combustion NOx Control. Volume V: Fundamental Combustion Research and Advanced Processes

(U.S.) Industrial Environmental Research Lab.
Research Triangle Park, NC

Prepared for

Electric Power Research Inst.
Palo Alto, CA

Aug 81

U.S. Department of Commerce
National Technical Information Service
NTIS

PB81-236150

EPA-600/9-81-028e
IERL-RTP-1087a

Proceedings of the Joint Symposium on Stationary Combustion NO_x Control

Volume V

Fundamental Combustion

Research and Advanced Processes

Symposium Cochairmen
Robert E. Hall, EPA
and
J. Edward Cichanowicz, EPRI

Program Element No. N130

Prepared for

U.S. ENVIRONMENTAL PROTECTION AGENCY
Office of Research and Development
Washington, D.C. 20460
and
ELECTRIC POWER RESEARCH INSTITUTE
3412 Hillview Avenue
Palo Alto, California 94303

REPRODUCED BY
NATIONAL TECHNICAL
INFORMATION SERVICE
U.S. DEPARTMENT OF COMMERCE
SPRINGFIELD, VA 22161

TECHNICAL REPORT DATA
(Please read Instructions on the reverse before completing)

1. REPORT NO. EPA-600/9-81-028e
2. proceedings
3. RECIPIENT'S ACCESSION NO. PB81 236150
4. TITLE AND SUBTITLE Proceedings of the Joint Symposium on Stationary Combustion NO_x Control. Vol. V, Fundamental Combustion Research and Advanced Processes
5. REPORT DATE
6. PERFORMING ORGANIZATION CODE
7. AUTHOR(S) Symposium Cochairmen: Robert E. Hall (EPA) and J.E. Cichanowicz (EPRI)
8. PERFORMING ORGANIZATION REPORT NO. IERL-RTP-1087a
9. PERFORMING ORGANIZATION NAME AND ADDRESS See Block 12.
10. PROGRAM ELEMENT NO. EHE624
11. CONTRACT/GRANT NO. NA (Inhouse)
12. SPONSORING AGENCY NAME AND ADDRESS
EPA, Office of Research and Development
Industrial Environmental Research Laboratory
Research Triangle Park, NC 27711
13. TYPE OF REPORT AND PERIOD COVERED Proceedings; 10/6-9/80
14. SPONSORING AGENCY CODE EPA/600/13
15. SUPPLEMENTARY NOTES EPA-600/7-79-050a through -050e describe the previous symposium.

16. ABSTRACT

The proceedings document the approximately 50 presentations made during the symposium, October 6-9, 1980, in Denver, CO. The symposium was sponsored by the Combustion Research Branch of EPA's Industrial Environmental Research Laboratory, Research Triangle Park, NC, and the Electric Power Research Institute (EPRI), Palo Alto, CA. Main topics included utility boiler field tests; NOx flue gas treatment; advanced combustion processes; environmental assessments; industrial, commercial, and residential combustion sources; and fundamental combustion research. This volume relates to NOx control as applicable to both fundamental combustion research and advanced processes.

17. KEY WORDS AND DOCUMENT ANALYSIS

a. DESCRIPTORS		b. IDENTIFIERS/OPEN ENDED TERMS	c. COSATI Field/Group	
Pollution	Flue Gases	Pollution Control	13B	
Combustion	Engines	Stationary Sources	21B	21K
Nitrogen Oxides		Environmental Assessment	07B	
Boilers			13A	
Tests			14B	
Assessments				

18. DISTRIBUTION STATEMENT Release to Public
19. SECURITY CLASS *(This Report)* Unclassified
20. SECURITY CLASS *(This page)* Unclassified
21. NO. OF PAGES 325
22. PRICE

EPA Form 2220-1 (9-73)

PREFACE

These proceedings document more than 50 presentations given at the Joint Symposium on Stationary Combustion NO_x Control held October 6-9, 1980 at the Stouffer's Denver Inn in Denver, Colorado. The symposium was sponsored by the Combustion Research Branch of the Environmental Protection Agency's (EPA) Industrial Environmental Research Laboratory-Research Triangle Park and the Electric Power Research Institute (EPRI). The presentations emphasized recent developments in NO_x control technology. Cochairmen of the symposium were Robert E. Hall, EPA, and J. Edward Cichanowicz, EPRI. Introductory remarks were made by Kurt E. Yeager, Director, Coal Combustion Systems Division, EPRI, and the welcoming address was given by Roger L. Williams, Regional Administrator, EPA Region VIII. Stephen J. Gage, Assistant Administrator for Research and Development, EPA, was the keynote speaker. The symposium had 11 sessions:

I: NO_x Emissions Issues
Michael J. Miller, EPRI, Session Chairman

II: Manufacturers Update of Commercially Available Combustion Technology
Joshua S. Bowen, EPA, Session Chairman

III: NO_x Emissions Characterization of Full Scale Utility Powerplants
David G. Lachapelle, EPA, Session Chairman

IV: Low NO_x Combustion Development
Michael W. McElroy, EPRI, Session Chairman

Va: Postcombustion NO_x Control
George P. Green, Public Service Company of Colorado, Session Chairman

Vb: Fundamental Combustion Research
Tom W. Lester, EPA, Session Chairman

VI: Status of Flue Gas Treatment for Coal-Fired Boilers
Dan V. Giovanni, EPRI, Session Chairman

VII: Small Industrial, Commercial, and Residential Systems
Robert E. Hall, EPA, Session Chairman

VIII: Large Industrial Boilers
J. David Mobley, EPA, Session Chairman

IX: Environmental Assessment
Robert P. Hangebrauck, EPA, Session Chairman

X: Stationary Engines and Industrial Process Combustion Systems
John H. Wasser, EPA, Session Chairman

XI: Advanced Processes
G. Blair Martin, EPA, Session Chairman

VOLUME V

TABLE OF CONTENTS

Page

Session Vb: Fundamental Combustion Research

"The Fundamental Combustion Research Program," T. J. Tyson, C. J. Kau, T. L. Corley, W. R. Seeker, W. Clark, J. Kramlich, M. P. Heap, and W. S. Lanier 1

"Two Phase Processes Involved in the Control of Nitrogen Oxide Formation in Fossil Fuel Flames," J. M. Beér, A. F. Sarofim, L. D. Timothy, S. P. Hanson, A. Gupta, and J. M. Levy 43

"Gas Phase Processes Involved in the Control of Nitrogen Oxide Formation in Fossil Fuel Flames," J. M. Levy 84

Session XI: Advanced Processes

"Low NO_x Combustors for High Nitrogen Liquid Fuels," G. C. England, M. P. Heap, D. W. Pershing, J. H. Tomlinson, and T. L. Corley 115

"Fate of Coal Nitrogen During Combustion," S. L. Chen, M. P. Heap, D. W. Pershing, R. K. Nihart, and D. P. Rees 154

"System Applications of Catalytic Combustion," J. P. Kesselring, W. V. Krill, S. J. Anderson, and M. J. Friedman 181

"Fixed-Bed and Suspension Firing of Coal," S. P. Purcell, D. M. Slaughter, J. M. Munro, G. P. Starley, S. L. Manis, and D. W. Pershing 216

"Pressurized Bench Scale Testing of Low NO_x LBG Combustors," W. D. Clark, B. A. Folsom, W. R. Seeker, C. W. Courtney, and M. P. Heap 248

"Control of NO_x and Particulates Emission from SRC-II Spray Flames," J. M. Beér, M. T. Jacques, S. Hanson, A. K. Gupta, and W. Rovesti 279

THE FUNDAMENTAL COMBUSTION RESEARCH PROGRAM

By:

T. J. Tyson, C. J. Kau, T. L. Corley, W. R. Seeker,
W. Clark, J. Kramlich, and M. P. Heap
Energy and Environmental Research Corporation
8001 Irvine Blvd.
Santa Ana, CA 92705

W. S. Lanier
U.S. Environmental Protection Agency
Research Triangle Park, N.C. 27711

ABSTRACT

The Fundamental Combustion Research (FCR) Programs's goals, management structure, and output are discussed. The basic research in this coordinated effort is conducted in support of EPA's low NO_x burner development program. The most immediate objectives are, first a determination of the chemical limits of NO_x production in order to determine the lower bounds of fuel and thermal NO_x, and second, a description of fuel NO_x formation in turbulent diffusion flames with gaseous, liquid, or solid fuels. To achieve these goals, FCR's subcontracts are divided among studies in transport processes in reacting flows, gas phase chemistry, and the physics and chemistry of two-phase reacting flows. Work performed in these areas is split almost evenly between the prime contractor and subcontractors. Among the most important results to date are the characterization of pyrolysis products from a number of coals, the determination of the influence of particle size on the physical mode of devolatilization, and the initial development of gas phase kinetic schemes to model higher hydrocarbon pyrolysis and oxidation.

I. FCR-I STRUCTURE AND STATUS

The first Fundamental Combustion Research Applied to Pollution Control Program (FCR-I) had three major objectives. These were:

- To generate the understanding of combustor behavior necessary to aid the Combustion Research Branch in the development of control strategies to minimize NO_x emissions from stationary sources.
- To develop engineering models which would allow effective utilization of a large body of fundamental information in the development of new NO_x control techniques.
- To identify critical information necessary for low NO_x combustor development and to generate it in a time frame which was consistent with the needs of the CRB technology development programs.

The overall goal of the CRB, and hence, for the FCR-I program is to provide the technology for the maximum control of NO_x emissions from stationary sources. The intent of FCR-I was to develop a focused program directed at the important issues of relevance to the CRB in order that the results could be applied. The program plan emphasized well-defined priority target areas, and the ensuing research effort was always guided towards engineering solutions to specific problems. There was a conscious effort to avoid projects which did not provide information critical to the needs of the CRB. Consequently, it was necessary to isolate the relevant issues, and the program was directed away from studied of the physics and chemistry of combustion which were not relevant to the goal of the CRB.

Fifty-six percent of the annual emission of nitrogen oxides from stationary sources in this country emanate from one general combustor category, boilers firing coal or oil. The dominant characteristics in the combustors can be characterized as follows:

- The flames are large, with energy release zones whose dimensions are on the order of tens of feet.

- The time mean motion is in steady state.
- The pressure is atmospheric.
- Radiation heat transfer has a dominant impact upon exchange from the heat release zone to the cold confining walls.
- Mass and thermal transport is turbulent.
- Fuel/air contacting occurs by diffusion and particle penetration.
- Fuels are injected as solids or liquids giving rise to two-phase transport and homogeneous and heterogeneous reactions.
- The high fuel-bound nitrogen content generally requires that NO_x emissions are minimized by staged combustion with the associated generation of copious levels of carbonaceous particulates, and problems associated with the burnout of this material.

Thus, the primary initial objective of the FCR-I program was to immediately establish a subcontractor-oriented program of fundamental investigations focused on the simultaneous control of NO_x and particulates from large, confined, one-atmosphere turbulent diffusion flames burning heavy residual oil and pulverized coal.

This section of the paper will describe the initial program plan, and summarize the status of the various programs initiated by EER during FCR-I.

II. Program Structure

The combustion of pulverized coal and oil in boilers is accomplished through the use of a burner of which there are many different designs. In fact, Combustion Engineering claims that they do not use burners, just fuel and air injectors, and the whole boiler acts as the burner. For the purposes of this discussion, a burner will be considered as a device which allows fuel and air to be injected in such a way as to provide a stable flame whose characteristics are suited to a given combustion chamber. Pulverized coal is injected either through annular or axial nozzles with spreading devices. Liquid fuels are normally broken into liquids by atomizers of many different designs which produce a variety of fuel spray characteristics (spray angle, spray type, drop size). The combustion air is supplied axially without tangential momentum, or with tangential momentum which may vary acorss the burner throat which might be composed of more than one annular passage. Depending upon the fuel and air injection parameters, two different types of flames can be readily distinguished, both of which are shown in Figure 1. The top half of the sketch shows a near-field dominated burner stabilized flame. These are relatively short, high-intensity flames typical of wall-fired boilers produced with rapid fuel/air mixing and each flame is stabilized independently, although there is some flame/flame interaction. The second class of flames are typified by those used in cement kilns or corner-fired boilers where the air is injected completely axially, producing a long, simple jet flame (see the bottom half sketch in Figure 1). In a corner-fired boiler these jet flames intersect on a firing circle and mix in the fireball which occupies a significant fraction of a combustion chamber. Regardless of the type of flame, the liquid droplets or pulverized coal particles exhibit the same phenomena as their energy is converted from potential chemical energy in the fuel to thermal energy in the combustion products.

A simplified description of the phenomena occurring to solid particles and liquid droplets of fuels in turbulent diffusion flames is illustrated in Figure 1. The fuels first decompose giving a vapor and a solid product. The vapor may be ejected from the solid as a single jet from a blowhole or may vaporize uniformly from the particle or droplets. This vapor will then either undergo pyrolysis producing soot particles, or undergo gas phase oxidation. The solid remaining after devolatilization of coal is normally referred to as char. The char and soot may then undergo heterogeneous reaction which include oxidation (burnout) and possible reaction with gaseous nitrogen specie. Throughout this sequence of events the fuel droplets/particles and their products must be brought into contact with oxidant and the high temperature combustion products in order to cause decomposition and subsequent reaction. This contacting is important on a macroscale because it dictates the major flame characteristics (i.e., near-field dominated burner stabilized, or far-field dominated jet flame), and on a microscale because it ultimately dictates the production of pollutant specie. FCR-I has been primarily concerned with the phenomena associated with the conversion of the nitrogen in the fuel droplets/particles to the ultimate nitrogen oxide released from combustion chamber.

FCR-I was divided into three program areas. These were concerned with (1) transport processes in reacting systems; (2) gas phase chemistry; and (3) the physics and chemistry of two-phase systems. Figure 2 presents an overall view of the program structure divided into these major program areas, specific program elements, and support areas. This program structure was planned to lead to two major program outputs. These were:

- A description of the chemical limits of NO production in order to ascertain the lower bounds of both fuel and thermal NO production under a series of process constraints which were not limited in any way by fuel/air contacting.
- A description of fuel NO formation in turbulent diffusion flames for gas, liquid and pulverized coal systems.

This overall program was planned as a combined in-house and subcontract project effort. EER took responsibility for program planning management and synthesis of the overall program, and subcontracted to various organizations separate projects included within the various program elements. Subcontracts accounted for 70 percent of the program and were used to ensure that FCR-I had the benefit of the best scientific talent available. Every effort was made to use subcontractors who had the necessary experience and, in many cases, equipment. The main synthesis role was accomplished by EER using the analytical tools developed in one of the program areas.

The reasoning behind the division of the total program into the three major program areas can most easily be described by consideration of the phenomena occurring to solid and liquid fuels in turbulent diffusion flames. A pulverized coal particle is heated, decomposes and the fuel-bound nitrogen component is divided between that which stays with the solid (char) and that which is evolved with the volatile gases. The processes that lead to the division of fuel nitrogen are part of the physics and chemistry of two-phase systems, as are the subsequent reactions of the solid phase. Thus, two of the program elements in the two-phase program area were concerned with the thermal decomposition of the fuel and heterogeneous NO/char reactions. The fate of the volatiles depends upon the chemistry of nitrogenous specie during combustion of the gas phase pyrolysate composed primarily of hydrocarbons. This whole area was treated in the gas phase chemistry program area. The primary goal of the gas phase chemistry program was to produce a kinetic mechanism which was adequate for the description of the fate of fuel nitrogen in gaseous mixtures which were likely to be found in pulversized coal and residual fuel oil flames. Thus, the gas phase chemistry area was divided into two program elements: one experimental and one aimed at mechanism development using computer simulations. A considerable effort was expended in the development of two-phase reactor experiments. These provided coupled experiments in which both gas phase chemistry and fuel decomposition were involved.

All of the above neglected the physics of turbulent transport. In flames the particles must be mixed with high-temperature gases before they can decompose, and oxidant must be mixed with the volatile fuel fractions before they can react. These fuel/air contacting processes were treated in the program area defined as transport processes in reacting systems. Three projects were carried out in this major program area. These were concerned with turbulence;kinetics coupling, fuel injection systems, and turbulent diffusion flames.

Although each of the projects in the various program areas were planned to provide information which was of value in itself and was of direct use for data interpretation, the overall program flow was directed towards the development and verification of engineering tools. These tools could be used in the attainment of the two major goals which defined fuel NO formation in turbulent diffusion flames. It is not possible to show the overall interaction of the various program areas and program elements because of the additional complexity which would be added to Figure 2. However, it does demonstrate the importance placed upon the use of analytical tools to provide the program synthesis. Indeed, all the program elements can be considered as providing input to allow analytical tools to be developed, and the application of these tools then provides the output of the FCR program.

It was recognized from the outset that within the time frame of FCR-I the development of a unified mathematical model for NO_x production in pulverized coal flames was unattainable. The major modeling effort in FCR-I concentrated upon the development of a framework of semiempirical modular models. Thus, a complex system could be modeled using a collection of limit-case elements linked together by means of empirical knowledge of the exchange of heat and mass transfer between these elements. In its simplest application, these modular elements could be used to analyze the data generated in several of the program elements involving reactor experiments. The modules describing fuel decomposition could be applied to both reactors and turbulent diffusion flames. Recognizing how complex a pulverized-coal system is, the limit-case approach was deemed to be the most appropriate in analyzing fundamental data for application to real systems. In limit-case studies certain phenomena are assumed to dominate the process while other phenomena become suppressed, thus allowing the implications of specific phenomenological behavior to be examined. Limit-case studies could be used to define the times and temperatures needed to reach a certain total fixed-nitrogen content in a fuel-rich combustion system, or in an attempt to define to what extent heterogeneous NO reduction took place in pulverized coal flames.

Although FCR-I placed considerable emphasis on the provision of information which was necessary to provide near-term solutions, long-term research was not entirely neglected. FCR-I pioneered the use of holography and two-color pyrometry as tools to study the thermal decomposition and combustion of fuels. Activities in turbulence kinetics coupling are beginning to show considerable promise for the future. Effort was initiated to evaluate numerical techniques which could be used in the ultimate models of furnace performance. Projects such as these ensured the CRB with a balanced directed fundamental combustion research program.

The following subsections will discuss the projects in the three major program areas. Another section will describe the products of several projects which were defined as part of the Measurement Systems Program support area. Finally, this section will conclude with a review of FCR-I's achievements in the areas of modeling of fuel NO formation in reactors and flames.

III. Gas Phase Chemistry and Heterogeneous NO Reduction

The projects initiated by FCR-I in this program area were:

- Kinetic Mechanism Development, T. L. Corley, J. C. Kramlich, and W. R. Seeker, EER.
- The Modeling of Fuel Nitrogen Chemistry in Combustion, J. Levy and A. F. Sarofim, Massachusetts Institute of Technology.
- The Formation and Destruction of Nitrogenous Specie During Hydrocarbon/Air Combustion, D. W. Blair and A. Myerson.
- NO_x Formation in a Flat Opposed-Jet Diffusion Flame, W. A. Hahn and J.O.L. Wendt, University of Arizona.
- Mechanisms of NO Reduction on Solid Particles, G. G. de Soete, IFP.
- Reactor Studies, W. Clark, EER.

Kinetic Mechanism Development. T. L. Corley, J. C. Kramlich, W. R. Seeker, EER--

This project was focused on the development of a kinetic mechanism which could give an adequate prediction of the conversion of fuel nitrogen compounds to NO in gaseous systems. The major objective was to provide a validated reaction model which could then be used as one component of more complex models describing the conversion of fuel nitrogen during the combustion of coal and liquid fuels.

The total chemical kinetic mechanism describing hydrocarbon combustion and nitrogen conversion can be divided into a number of natural subsets. Starting with the most simple and proceeding to subsets which require the addition of more reactions, these subsets are:

- H_2/O_2;
- $CO/H_2/O_2$;
- NH_3/O_2;
- HCN/O_2;
- CH_2O/O_2;

- CH_4/O_2;
- $CH_4/C_2/O_2$.

Figure 3 shows the interrelationships between the various subelements. All of the final subsets are then combined to yield a complete hydrocarbon/fuel nitrogen mechanism. The following steps summarize the approach taken during this project to assemble and evaluate the mechanism.

1. Assemble elements of reaction model:
   - determine if species included are necessary and/or sufficient;
   - use accepted values for rate coefficients.
2. Select data sets for analysis:
   - ensure data sets selected provide resolution of critical questions;
   - data sets must have well-defined experimental conditions.
3. Use shock tube and flame data to identify and correct deficiencies.
4. Use completed subelement of reaction mechanism as known element of more complex systems.

It was recognized that availability of data would prevent resolution of certain questions concerning some of the subelements. In such cases calculations would be used to establish the limitations of the reaction mechanism and identify the data required to extend its range of applicability.

The shock tube system was selected as the initial basis for comparison because it is a one-dimensional system in which diffusion is not important, and temperature could be varied independently of stoichiometry and time. Depending upon the type of observations, predictions can be assessed against ignition delays, characteristic species growth constants, and time-resolved profiles. Flame data were included since the processing of fuel nitrogen in flame environments is of major interest. In flames, temperature is time- and stoichiometry-dependent, and comparison of predictions with data provides a stringent test of the mechanisms range of applicability. Evaluation of the mechanism can be based upon both its ability to predict burning velocities and to reproduce species profiles.

Step 4 of the methodology refers to the manner in which particular subelements are incorporated into more complex elements of the reaction model. After an element of the mechanism has successfully passed the appropriate tests it cannot be modified when used in the analysis of more complex elements of the reaction model unless it is shown that the discrepancies in the new system can only be corrected by changing features of the subelement. If this step is required, the modified subelement must again be checked against the relevant data to ensure consistency with the old data. This feedback cycling ensures the internal consistency of the final mechanism.

Table I summarizes the ability of the mechanism subelements to predict shock tube and flame data. Application of the procedure to elements of the reaction model indicates:

- CH_2O - CO - H_2 - O_2 system is complete
    - HCO is important for chain-branching in rich, wet CO flames
    - Decomposition and oxidation of CH_2O is slower than previous predictions
- NH_3 - O_2 mechanism requires additional analysis
    - Chain-branching path required: $NH_2 + NO = N_2 + H + OH$
    - Ignition delay controlled by: $NH_2 + O_2 = HNO + OH$
    - N_2H_i species may be important for rich processing of NH_3
    - Overall oxidation of NH_3 too slow with present mechanism
- HCN - O_2 reaction model must be compared with other data

Most of the recent work has been directed towards a description of the CH_4-O_2 mechanism which was divided into two components:

- C_1 - chemistry
    - 17 species: CH_4, CH_3, CH_2, CH, CH_3O + the CH_2O - O_2 set
    - 61 reactions

- C_1 and C_2 - chemistry
    - 23 species: C_2H_i (i = 1 to 6) + the C_1 set
    - 101 reactions

The mechanism was first examined for correlation with shock tube ignition delays and, in particular, the simulations examined the impact of various products for the reaction $CH_3 + O_2$ and the impact of the C_2 chemistry. The principal result was that CH_3O was a necessary component in the mechanism to correctly predict ignition delays. It was not possible to conclude that C_2 chemistry was necessary.

Flat flame data of Biordi et al were adequately modeled without the necessity of changing the mechanism. The flame velocities were in excellent agreement (model = 76 cm/sec; data = 80 cm/sec). The species profiles were also in excellent agreement, with the exception of CO and CO_2 (see Figure 4). This divergence is consistent with the observation that the rate of $CO + OH = CO_2 + H$ is too slow at high temperatures.

The data Harvey and MacColl (1979) provide a test of the C_2 - chemistry portion of the CH_4 mechanism; a number of C_2H_i profiles are reported. Since the flat flame was attached (i.e., burner stabilized) no flame velocity check was possible. As shown in Figure 5, the species profiles indicated that hydrocarbon intermediates were over-predicted. The inclusion of the C_2 chemistry set improved, but did not eliminate the divergence.

The Modeling of Fuel Nitrogen Chemistry in Combustion: The Influence of Hydrocarbons. J. M. Levy and A. F. Sarofim, MIT--

There are uncertainties in the currently available mechanistic and kinetic data base suitable for modeling of fuel nitrogen conversion in the presence of "simple" fuels; however, an attempt must be made to attack the problems of real fossil fuels. Real fuels introduce mechanistic complexities due to the presence of hydrocarbon specie which do not decouple easily from solution of the fuel nitrogen problem. This project was concerned with an assessment of these complexities and to the development of a methodology for dealing with them which would allow fuel nitrogen processing in real fuels to be modeled.

The ability to assess the factors affecting bound nitrogen conversion in a real-fuel, fuel-rich environment is dependent upon an understanding of hydrocarbon decay kinetics because:

1. Interactions of fuel nitrogen and hydrocarbon fragements are significant, causing recycling of NO back to HCN.
2. The radical pool (H, O, OH) which drives the fuel nitrogen chemistry is determined primarily by the hydrocarbon chemistry which dominates the system at early times.

Several approaches to the problem of treating hydrocarbons were considered:

- Detailed kinetics rejected because of time, cost and lack of detailed information.
- Global and semiglobal methods may not adequately describe the free radical pool.

Having exhausted, as impractical or inapplicable, existing methods of treating hydrocarbons, a new quasi-global method was proposed with the following general form:

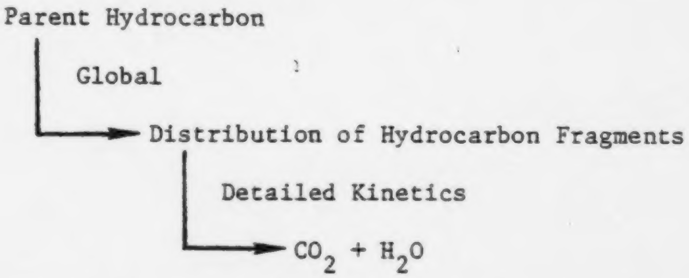

The method assumes: (1) that the initial degration of the parent hydrocarbon in the preflame zone via pyrolysis and oxidative pyrolysis is very rapid; (2) that the initial decomposition products may be represented by a relatively small set of low molecular weight, stable, and/or unstable, hydrocarbon species; and (3) that the decomposition mechanism can be justifiably represented by a global step.

The potential utility of this proposed method, referred to as the Quasi-Global Method Applied to Initial Reaction Extents (QUAGMIRE), lies in the following:

- The advantages of modeling free radical chemistry by detailed kinetics are retained, but the magnitude of the elementary reaction set required is vastly reduced;
- Unlike the quasi-global proposed by others, hydrocarbons are retained in the elementary reaction scheme.

QUAGMIRE is currently being used to model data generated in the post-flame region of flat flames doped with nitrogen specie. Initial results are encouraging and point to the need for more detailed measurement of the relevant free radicals in hydrocarbon flames in order to provide a basis for the initial global step.

The Formation and Destruction of Nitrogenous Specie During Hydrocarbon/Air Combustion. D. W. Blair, Exxon--

Earlier work at Exxon has been funded by the CRB to develop two reactors for the investigation of NO formation: a strongly backmixed jet-stirred combustor (JSC) and an adiabatic laminar quasi-plug flow combustor - the multiburner (MB). This project was continued by FCR-I to utilize this expertise and equipment in several experiments:

- Extend the measurements to include nitrogen specie other than NO.
- Investigate the impact of temperature on fuel NO formation .
- Indicate experiments on fuel nitrogen conversion with hydrocarbon fuels other than CH_4.

This information was necessary if a kinetic mechanism for fuel nitrogen oxidation was to be developed.

The following conclusions were drawn from Exxon studies:

- With both equivalence ratio and flame temperature held constant, specific hydrocarbon chemistry influences both thermal nitrogen fixation and fuel nitrogen conversion.

- Fuel chemistry is more important in the multiburner than it is in the jet-stirred combustor. The contributions of combustion environment to this difference appear to exceed those of reaction time.

- While the conversion of fuel nitrogen is dependent upon fuel nitrogen species, the dependency in the MB considerably exceeds that in the JSC. This argues that differences in combustion environment between the two combustors is important.

While there is a need for considerable additional work in this area (extending range of variables, verifying results, expanding range and areas of overlap between the several independent variables), this project has been terminated with EER and further work is not contemplated at this time.

NO_x Formation in Flat Laminar Opposed-Jet Methane Diffusion Flames. W. A. Hahn and J.O.L. Wendt, University of Arizona--

The oxidation and pyrolysis of fuel nitrogen, as ammonia, was investigated by first injecting ammonia in the fuel and then in the air, and then comparing the predicted versus measured NO profile. The good agreement between model and experiment when the ammonia was injected with the fuel indicates that the pyrolysis reactions of ammonia in the presence of fuel hydrocarbon fragments can be described by the mechanism used. When ammonia was injected with the oxidant, the poor agreement with theory indicates that the mechanism may not accurately describe ammonia pyrolysis in the presence of CO, CO_2, H_2O and oxidant.

The effect of rate of stretching on the axial NO profile is well-predicted by theory. NO formation and NO destruction mechanisms are of equal importance in these types of flames, and the experimental and theoretical results are in qualitative agreement with observed effects of increased turbulent intensity on NO formed in turbulent diffusion flames.

Mechanisms of Nitric Oxide Reduction on Solid Particles. G. G. de Soete, IFP--

The scope of the work is to provide information on:

- The mechanism of heterogeneous NO reduction under typical flame and flue gas conditions.

- Determine the reaction rates of reactions controlling the disappearance of NO, the formation of intermediates, and their transformation to molecular nitrogen.

The study performed on packed bed reactors was restricted to a general investigation of the heterogeneous NO reducing mechanism.

It has been shown that the heterogeneous reduction of NO by solids takes place via a complex series of reactions which are dependent upon the nature of the solid and the composition of the gas phase. In particular:

- When the solid contains neither hydrogen nor carbon, reduction rates are negligible at temperatures below 1100°C unless gas phase reducing agents are present.
- NH_3 has been identified as an intermediate if there is a source of hydrogen.
- HCN is produced with carbon-condensing solids.
- Oxygen can act either as an inhibitor or promoter of the NO reduction reactions.

These studies were carried out under equilibrium conditions, and any extrapolation to flame conditions should be carried out only with the same restriction.

Reactor Studies. W. D. Clark, EER--

A series of short reactor studies were carried out in-house to provide information to aid program planning and management. A high temperature plug flow reactor was built originally to test model predictions which suggested that NO decayed relatively rapidly in the absence of hydrocarbons in fuel-rich systems. Experiments indicated that this decay did not take place, and the reaction rate of the reaction CO + NO = NCO + O was found to be too high.

The reactor was modified (see Figure 6) to allow an investigation of heterogeneous effects (NO reduction and char nitrogen conversion) in a disposed phase system.

Particles were injected into NO-doped post-flame combustion gases to investigate their NO reducing potential under realistic conditions. Effects of temperature and particle concentration on the NO reducing properties of alumina, graphite, char, and anthracite coal were examined. Alumina and graphite had little effect on NO; however, char and anthracite coal caused a decrease in NO with increasing particle concentration. Alumina particles were injected into slightly lean and into lightly rich NO-doped methane combustion gases at injection point temperatures up to 1100°C. Particle concentrations up to 200 g/standard m^3 had little effect on NO. Injection of graphite particles also had little effect on NO at temperatures up to 1100°C and particle concentrations up to 70 g/sm^3.

Figure 7 shows the effects of injecting low volatile char particles into slightly rich NO-doped methane combustion gases. With the injection of char particles, NO concentration dropped sharply, CO rose due to char oxidation and volatile release, and CO_2 and temperatures fell primarily due to dilution. NO decreased with increasing feed rate (particle concentration), and returned to its initial concentration when the particle injection stopped. At an injection temperature of 900°C and a particle mass loading of 180 g/sm^3, 30 percent of the NO was reduced (after correction for reduction).

Figure 8 shows the effects of anthracite coal particles on NO. Reductions of up to 20 percent were caused by injection of anthracite into slightly rich NO-doped methane combustion products. Further increases in particle concentration had little effect on NO. Injection of anthracite particles into slightly lean undoped methane combustion gases caused a 30 PPM rise in NO. This cast doubt as to whether the observed NO reduction in the fuel-rich case was due to heterogeneous or homogeneous reactions. However, other investigators have measured negligible amounts of NH_3 and HCN in anthracite combustion, even under very fuel-rich conditions. Therefore, the observed reduction of NO by anthracite in fuel-rich combustion gases was probably due to heterogeneous reactions.

Physics and Chemistry of Two-Phase Systems

FCR-I projects which were included in this program area were oriented towards providing data on the fate of fuel nitrogen during thermal decomposition. Two investigations were initiated to study the fate of fuel nitrogen from real fuels using two-phase backmixed reactors.

Volatility of Fuel Nitrogen. R. L. Gay, A. E. Axworthy, V. H. Payne, and H. L. Recht, Rockwell International--

An experimental program measured fuel nitrogen volatility using a quartz two-stage pyrolysis reactor developed under previous CRB programs. Solid and liquid fossil fuels were heated in helium in the first stage of the reactor at selected temperatures up to 1100°C. The volatile nitrogen compounds released were measured by converting them to HCN in the second stage of the reactor at 1100°C. The HCN was collected in dilute sodium carbonate solutions and measured colorimetrically.

Samples of 20 fossil fuels which were used on other CRB programs were supplied by EER. Petroleum-based fuel oils, synthetic oils from coal and shale, and coals were studied. All of the samples tested produced the greatest yields of volatile nitrogen compounds at a first-stage temperature of 1100°C. The maximum yield of volatile nitrogen from petroleum fuel oils was 35-48 percent of the nitrogen in the sample. The yield curves increased continuously from 300°C with a slight dip at 600-750°C. The maximum volatile nitrogen yields from shale oils were 70-79 percent, while the coal liquids yielded 50 percent. The nitrogen species in shale oils were very volatile at low temperature, giving HCN yields of about 65 percent at a pyrolysis temperature of only 200°C.

The data generated by this experiment was used to correlate NO_x emissions from pulverized coal and liquid fuels. The results of this attempt were presented in Figure 9 which shows percent NO in combustion as a function of percent HCN in pyrolysis at 1100°C.

The Characterization of Coals During Thermal Decomposition. P. R. Solomon, UTRC--

UTRC had developed an in-house capability to investigate coal inorganic structure and the products of thermal decomposition. A model was available which allowed the prediction of the time and temperature dependent evolution of the major products of pyrolysis from a knowledge of the coal's functional group distribution. The model assumes that large molecular fragments ("monomers") are released from the coal "polymer" with only minor alternation to form tar, while simultaneous cracking of the chemical structure forms the light molecules of the gas. Any chemical component of the coal can, therefore, evolve as part of the tar or as an independent species. The model may be used to predict the amount of volatile fuel nitrogen evolved in pyrolysis which is essential if the formation of fuel nitrogen is to be accurately assessed.

A study was initiated to apply these concepts to the study of several coals which were being investigated in other programs. Particular attention was paid to the rate and forms of nitrogen evolution. Pyrolysis experiments were performed on Beulah, a North Dakota lignite, a Pittsburgh bituminous, Savage, a Montana lignite, and Rosa, a bituminous coal, between 400°C and 1800°C.

A rank dependence in the retention of nitrogen in the char was observed as indicated in Figure 10. The higher rank bituminous coals appear to retain much more nitrogen at high temperature than do the lignites. Possible explanations for this could be the higher oxygen content or the smaller aromatic cluster size in the lignite. Figure 11 shows some interesting aspects of the evolution of nitrogen during pyrolysis. At temperatures below 1200°C, nitrogen balance is obtained by measuring the tar and char nitrogen, HCN and NH_3. At higher temperatures, there appears to be some missing material indicating some other nitrogen form evolved which is not determined. Of the gaseous species, HCN yields are substantially higher than NH_3 and the ease of evolution of these two gases at low temperature appears to be rank-dependent. As an example of this, efforts have already begun to utilize the kinetic parameters derived in this experiment in the cool reactor models being developed as part of the Analytical Tool Development Support Area.

The Physical and Chemical Effects Occurring During the Thermal Decomposition of Coal Particles and Oil Droplets. W. R. Seeker, G. S. Samuelsen, J. D. Trolinger, and C. F. Hess, EER/SDL--

The events occurring during the thermal decomposition of liquid droplets and coal particles in the initial stages of heat release in turbulent diffusion flames are of considerable significance to the designers of low pollutant emission combustors. In pulverized coal flames the partition of fuel nitrogen between the volatile and char fractions, for example, will impact the production of fuel NO. Moreover, since the fate of fuel nitrogen in the volatiles is dictated by the environment in which they react, their conversion to NO or N_2 will depend upon the degree to which they mix with the bulk flow before reacting. In liquid fuel flames the minimum achievable NO_x emissions is quite often related to the trade-off between NO_x and smoke emissions. Therefore, the factors controlling the formation of particulates under fuel-rich conditions are germane to the problem of low NO_x burner design for liquid fuels.

Earlier studies supported by FCR-I demonstrated that holography could be used to observe the behavior of coal particles during combustion. The approach taken in the present study was to observe particles/droplets under well-controlled conditions which simulated those encountered in real systems. This was accomplished by the construction of a reactor which allowed the particles/droplets to be injected into high temperature gases whose temperature and composition could be varied. Diagnostics were designed to allow visualization of the particles/droplets during combustion, both by holygraphy and high-speed photography. Two-color particle pyrometry was employed to measure particle temperatures, and solid and gaseous samples were extracted to investigate the variation of composition with time.

The major goals were to explore the effects of controllable parameters on combustion phenomena and pollution formation. The specific parameters investigated included the following:

- The effect of coal type. The coals selected were those used in other CRB programs.
- The effect of particle/droplet size.

- The effect of particle number density.
- The effect of environment, i.e., either reducing or oxidizing.
- The effect of relative velocity between the particles and background gas.
- Exploratory investigation using liquid droplets.

Initial evaluations of the results obtained in this study to date on the physical phenomena which occur during the thermal decomposition of pulverized coal particles indicates that:

- Volatile coal fractions are ejected from coal particles in jets, and that for large bituminous coal particles these jets produce a trail of small particles.
- Coal composition and volatile evolution rate influences particle temperature.
- Large soot structures can be formed from the bulk gases produced when bituminous coal particles decompose.

Pollutant Formation from Combusting Pulverized Coal Clouds. P. M. Goldberg, H. Tong, and R. Kendall, Acurex--

The objective of this experimental study was to provide information on the mechanisms of coal combustion and subsequent oxides of nitrogen formation under conditions similar to those found in the near-burner region of a high-intensity pulverized coal flame. A jet-stirred reactor system is utilized in this study to simulate this type of combustion environment. The conditions in the stirred combustor approximate those found in flames when a high degree of recirculation is present. In addition, a stirred reactor is capable of operating over a wide range of coal concentrations at high temperatures and residence times ranging from about 20 to 100 msec.

An overview of the experimental program plan by tasks is presented in Table II. Referring to the table, the first goal of the program was to design a well-mixed coal reactor capable of operating over a residence time range of 20 to 200 milliseconds. After completing the design and fabrication, noncombusting mixing studies were to be conducted to verify that a high level of gas phase mixing exists in the reactor. Once gas phase mixing performance was verified, subsequent experiments were to be directed at quantifying particle mixing behavior. Combustion experiments were to begin after the completion of this task.

The original experimental plan was modified somewhat during the course of this program. Instead of one reactor, two similar reactors were designed to cover the residence time ranges of about 20 to 60 and 50 to 100 msec, respectively, during combustion testing. The gas phase mixing efficiency of the longer time scale reactor (SRII) was examined using a "cold" model reactor in conjunction with an He tracer method. Attempts have been made to quantify particle mixing in the SRII cold model by using a light attenuation technique. Experiments indicate that good mixing is achieved in SRII. However, the particle mixing study results indicate that the particle residence time might be longer than the gas residence time. The results also indicate that the particle residence time may vary significantly less than that of the gas.

The combustion results show that devolatilization may be essentially completed in the SRII residence time range. The exhaust concentrations and temperature dependence on equivalence ratio is similar to those expected in larger time scale systems. This might lead to the conclusion that enhanced volatile yields play a major role in combustion.

It has been observed that fuel nitrogen conversion is correlatable with equivalence ratio, reaction efficiency, and temperature. The trends in these correlations show similarities with other experimental work. It was also found that the nitrogen depletion of the char corresponds roughly to the weight loss exhibited by the char, although a limited range of weight loss has been examined to date (75-95 percent).

Pollutant Formation During the Combustion of Residual Fuel Oils in Backmixed Reactors. M. J. Murphy and A. Levy, Battelle/Columbus--

This program was included in FCR-I in an attempt to relate the production of NO_x from burning residual fuel oils to fuel nitrogen in these fuels and to the combustion variables such as spray droplet size, fuel properties and time/temperature history. This objective was addressed through the use of a well-stirred reactor fired on fuel oil having the capability of variable residence time, stoichiometry and droplet parameters (size and fuel composition). The program was organized into three tasks:

1. Design, Construct and Test a Reactor Model,
2. Construct and Test the Actual Reactor,
3. Demonstrate Reactor Operation and Data Acquisition.

The performance of the well-stirred reactor design (Task 1) has been verified by extensive cold flow testing. Criteria for well-mixedness were found to be met satisfactorily with the selected design. Measurements of gas residence times were performed on the cold flow model using laser extinction techniques applied at the exhaust duct.

Technical problems associated with the prototype combustor have led to the design of the current combustor configuration. This combustor has eight fuel jets utilizing Sonicore nozzles and eight air jets fired into a cylindrical chamber. The chamber dimensions were selected to allow a residence time range between 20 and 200 msec at a firing rate variable between 100,000 to 1.5×10^6 Btu/hr. Emissions data have been collected for natural gas burning over a stoichiometry range of 0.6 to 1.60 as a function of residence time. The combustor has been successfully fired for extended periods on a No. 6 fuel oil to equivalence ratios greater than 2.0.

Transport Processes in Reacting Systems

The major program areas discussed in the two previous sections were concerned with types of reactants and their probable products which would be found in heavy liquid or pulverized coal flames. The projects included in the program area defined as Transport Processes in Reacting Systems were concerned with problems associated with reactant mixing.

An Experimental Approach to the Study of Heavy Oil Spray Combustion in Shear Layers. A. Vranos, UTRC--

This program was included during FCR-I and consisted of two phases: (1) design and fabrication of an apparatus, and (2) preliminary combustion experiments. A unique shear-layer mixing and combustion apparatus was developed (see Figure 12) which simulates high-shear diffusive combustion with heavy oil droplet injection as found in the near-field combustion zone of boilers and furnaces. The apparatus provides: (1) two-dimensional mixing and combustion of uniform streams of air and rich combustion products fed from opposite sides of a splitter plate; (2) uniform injection of a monodisperse heavy oil spray into the shear layer by means of a linear array of fuel injectors located beneath the combustor wall; (3) control of droplet path, residence time, and extent of vaporization; (4) control of hot- and cold-stream inlet properties; and (5) three-dimensional probing of the flow field.

The experimental phase of the program consisted of: (1) verification of uniform properties of the hot and cold streams at the splitter plate trailing edge; (2) demonstration of high injection velocities and uniform droplet size and penetration with Nos. 2, 5, and 6 oils in vibrating multicapillary injectors; (3) determination of stable flow regimes as a function of primary and secondary stream velocities; (4) flame stability and flashback studies; (5) high-speed cinematography of the shear layer with injection of Nos. 2 and 6 fuel oil; and (6) preliminary flame probing.

The Application of Droplet-Sizing Interferometry and Holography to the Measurement of Spray Droplet Size. C. F. Hess, W. D. Bachalo, SDL--

Two optical techniques were used to characterize the droplet field produced by a Sonicore nozzle under laboratory conditions. Droplet-sizing interferometry (DSI) and holography were used to obtain the size and velocity of fuel droplets in the presence of a surrounding airstream. The experiments were performed under cold conditions to provide data on droplet size and velocity correlations, size stratification, and droplet evaporation.

Due to the complex nature of the flow (two phases, small droplets, high number densities, recirculation, etc.) nonintrusive measuring methods must be used to avoid disturbing the flow. The methods must also have very high resolution since the droplets can be very small and move at high speeds. The techniques must be flexible enough to access the measuring volume from any direction since physical obstacles will be present in most combustion applications. Droplet sizing interferometry proved to be a very strong technique with which to study these fuel sprays since it meets the criteria listed above. Holography was also used since it provided a quick profile of the shape of the plume and its resolution was adequate to confirm the results obtained with the DSI.

It was found that:

- The DSI instrument proved to be very powerful for the study of fuel sprays in that:
  - it measures the size and velocity of individual droplets;
  - it provides a point measurement;
  - it can be used to distinguish air velocity from droplet velocity.
- Holography is adequate for sizing droplets, but the analysis of holograms is very time-consuming.

Spray Characterization. W. R. Seeker and G. S. Samuelsen, EER--

A program was established to help explain data obtained on a CRB-funded development program which showed the dependency of NO_x emission in fuel oil combustion on atomizing nozzle type, and nozzle operating conditions. Toward this end, a cold chamber spray rig, patterned after the combustion system, was built for the purpose of characterizing nozzle spray behavior. As the initial step in the program, nonintrusive optical techniques are being applied and evaluated for (1) consistency of data measured, and (2) applicability to studying the spray behavior most likely important to NO_x emission. The optical techniques include diffraction, visibility, and holography.

At this juncture in the program the visiblity measurements have been concluded. Significant differences were found to exist between these data and data acquired in an independent program conducted at the IFRF. It appears that these differences can be attributed to:

1. Difference between the spray rig configuration and properties of the fuel used on the two studies;
2. Differences associated with the actual parameters being measured such as size distributions averaged across the spray (line

integrated) as opposed to point measurements, and size distribution measured in terms of volume versus number which must be transposed.

3. Differences associated with the resolution limits of the various instruments. For example, when taking holograms through dense sprays, the resolution limit is known to increase to near 20 μm. There is uncertainty associated with the defined resolution limits of some of the newer techniques which must be well-defined in order to directly compare with other instruments.

Development of a Coherent Flame Model for Turbulent Chemically-Reacting Flame. F. E. Marble, and J. E. Broadwell, CIT/TRW--

A coherent flame model was applied to a methane air turbulent diffusion flame with the objective of describing the production of nitric oxide. The example of a circular jet of methane discharging into a stationary air atmosphere was used to illustrate application of the model. In the model, the chemical reactions take place in laminar flame elements which are lengthened by the turbulent fluid motion and shortened when adjacent flame segments consume intervening reactant. The rates with which methane and air are consumed and nitric oxide generated in the strained laminar flame are computed numerically in an independent calculation.

Detailed Measurements of Long Pulverized Coal Flames for the Characterization of Pollutant Formation. R. Payne, IFRF--

This program was initiated to provide experimental data which could be used both for model development and to provide a mechanistic understanding of nitrogen processing in flames of this type.

Six "long" coal flames were produced with the same burner under similar boundary conditions. The differences between these flames were mainly due to air and fuel input velocities and temperatures which have a direct effect on the mixing characteristics and the coal heating rates. A comprehensive set of flame data was generated. Despite the many difficulties encountered in making measurements in such flames, particularly for sampling in regions of high temperature and solid concentrations, the consistency between the various measurements is generally good. Indications are that globally, the combustion is controlled by mixing and that the influence of fuel kinetics is basically the same in all cases. In particular, NH_3 concentrations were always very low, while HCN was found to form very rapidly and in large amounts.

Measurement Systems Support

Three efforts were carried out in this Program Support Area:

- a study to assess the accuracy of chemiluminescent analyses when measuring NO in combustion products after calibration with NO in nitrogen;
- tests to standardize the use of ion-specific electrodes for HCN and NH_3 analysis; and
- a study to assess the problem of sampling sulfur and nitrogen specie in "dirty" flames.

Analytical Tool Development

The major integration function in the FCR-I program was to be carried out through the use of mathematical models. The models were developed in close accord with the experimental investigations. These models include a description of the following phenomena:

- particle thermal history, including the existence of particle supertemperatures,
- finite rate thermal decomposition,
- heterogeneous chemical behavior,
- finite rate gas phase chemistry,
- fluid mechanics and ballistics of turbulent transport in two-phase systems,
- complex flow fields associated with the near-field of highly swirl-stability combustors,
- the interaction between turbulent unmixedness and chemistry.

These modeling efforts have resulted in a hierarchy of analysis codes. Treatment of the fully-coupled finite rate processes associated with particle heat up, thermal decomposition, heterogeneous reactions, and gas phase chemistry was emphasized. The codes can handle with ease and efficiency as many as 200 such coupled processes, although often such complexity is not warranted.

In the course of developing an understanding of the dominant mechanisms governing complex and poorly understood behavior, it is often necessary to start with a large coupled system and, through sensitivity analysis, reduce it in such a manner that it contains first-order phenomena only. A good example of a situation requiring such an approach is the development of an understanding of NO_x generation in p.c. flames. The complexities of HCN, NH_i, and C_2 chemistry, in conjunction with finite rate devolatilization, defies a simple intuitive understanding and requires complex analysis in order to generate such intuition.

The decomposition of coal is described assuming that the coal is composed of an arbitrary number of functional groups; the quantification and characterization of these is provided by utilization of independent experimental data (the work of Solomon; The Characterization of Coals During Thermal Decomposition). These functional groups are envisioned to decompose by one or more parallel paths with Arrhenius-like rate behavior. A given species may evolve from more than one functional group, and the functional groups can exchange between themselves with an equilibrium composition that is temperature-dependent. This generalized model lends itself easily to the incorporation of observations from many different investigators.

The hierarchy of models developed during FCR-I allow a description of the following systems:

- Simple Reactors
- Simple Diffusion Flames
- Long Turbulent Diffusion Flames

Simple Reactor Models--

These operational codes are routinely used for the analysis of well-stirred (SR) and plug flow (PF) reactors for both gas and coal. The SR module assumes either a perfectly stirred exponential distribution of particle residence times, or it will accept as input an arbitrary distribution obtained from experimental evidence, as will the PF module. The heat loss or heat-loss distribution can be specified as appropriate. The modules can be coupled, and the PF can receive additional combustion air and fuel in a staged fashion. These coupled reactors are ideally suited for simple modular modeling of combustion system performance (ignition stability, energy release distribution, heat transfer) and pollutant formation as a function of fuel, burner and furnace characteristics.

Simple Laboratory Diffusion Flames--

These codes provide for the analysis of fundamental experiments on laminar one- and two-dimensional diffusion flames. In addition to simple coaxial flames, this code will describe behavior in opposed-jet flames. The mathematical solution for such a system proves to be self-similar with all properties independent of the radial coordinate with the exception of the radial velocity.

Long Turbulent Diffusion Flames--

This code represents the most ambitious, and perhaps the most satisfying, output of FCR-I. It is directly applicable to a large class of industrial furnaces. This operational code treats long coaxial turbulent p.c. diffusion flames typified by tunnel furnace flames stabilized through convective backflow along the walls, as well as by radiation from the flame to the incoming particles. The model and its free shear layer equivalent can also be used as modular elements in conjunction with the idealized stirred and plug flow reactors in the modular modeling of staged systems and high swirl-stabilized burners.

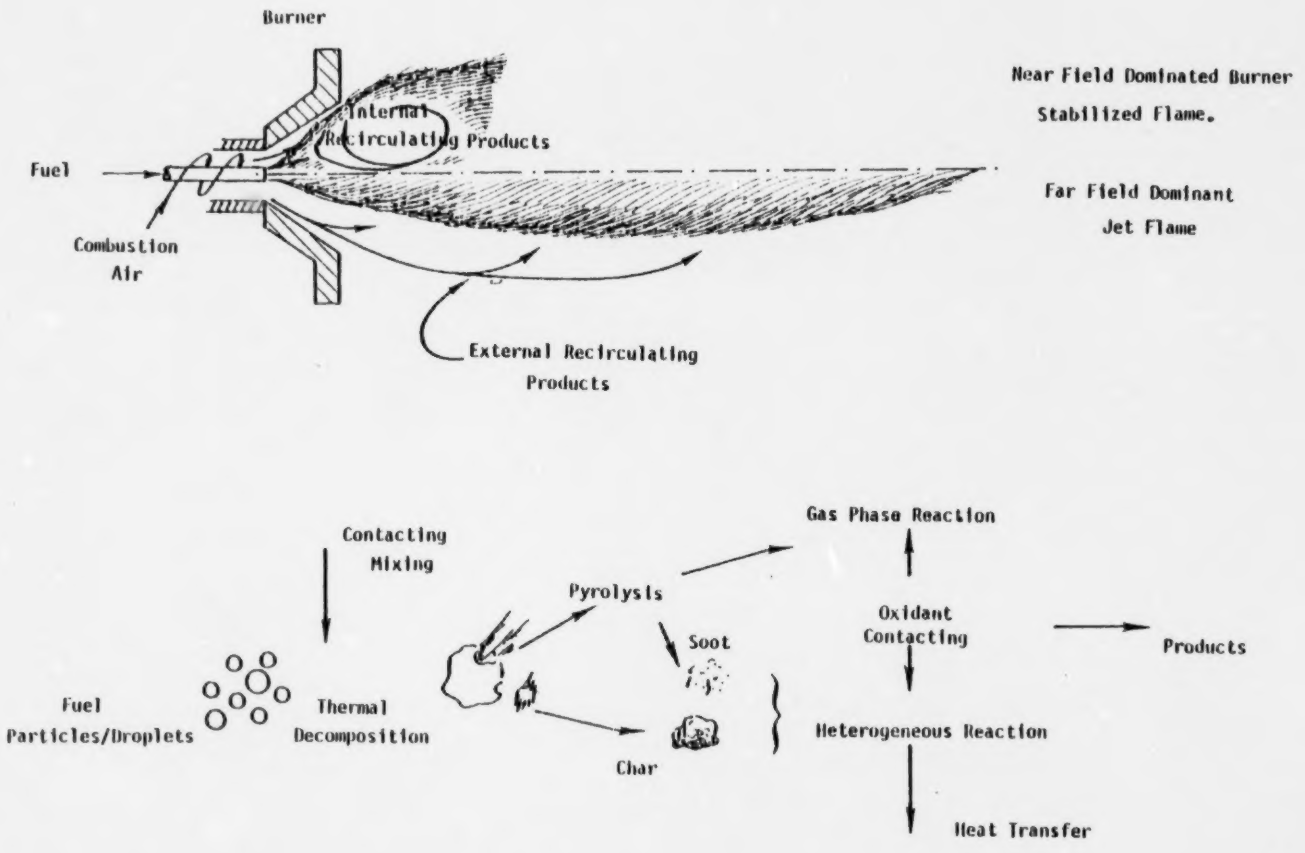

Figure 1. Solid Liquid Fuel Processing in Turbulent Diffusion Flames.

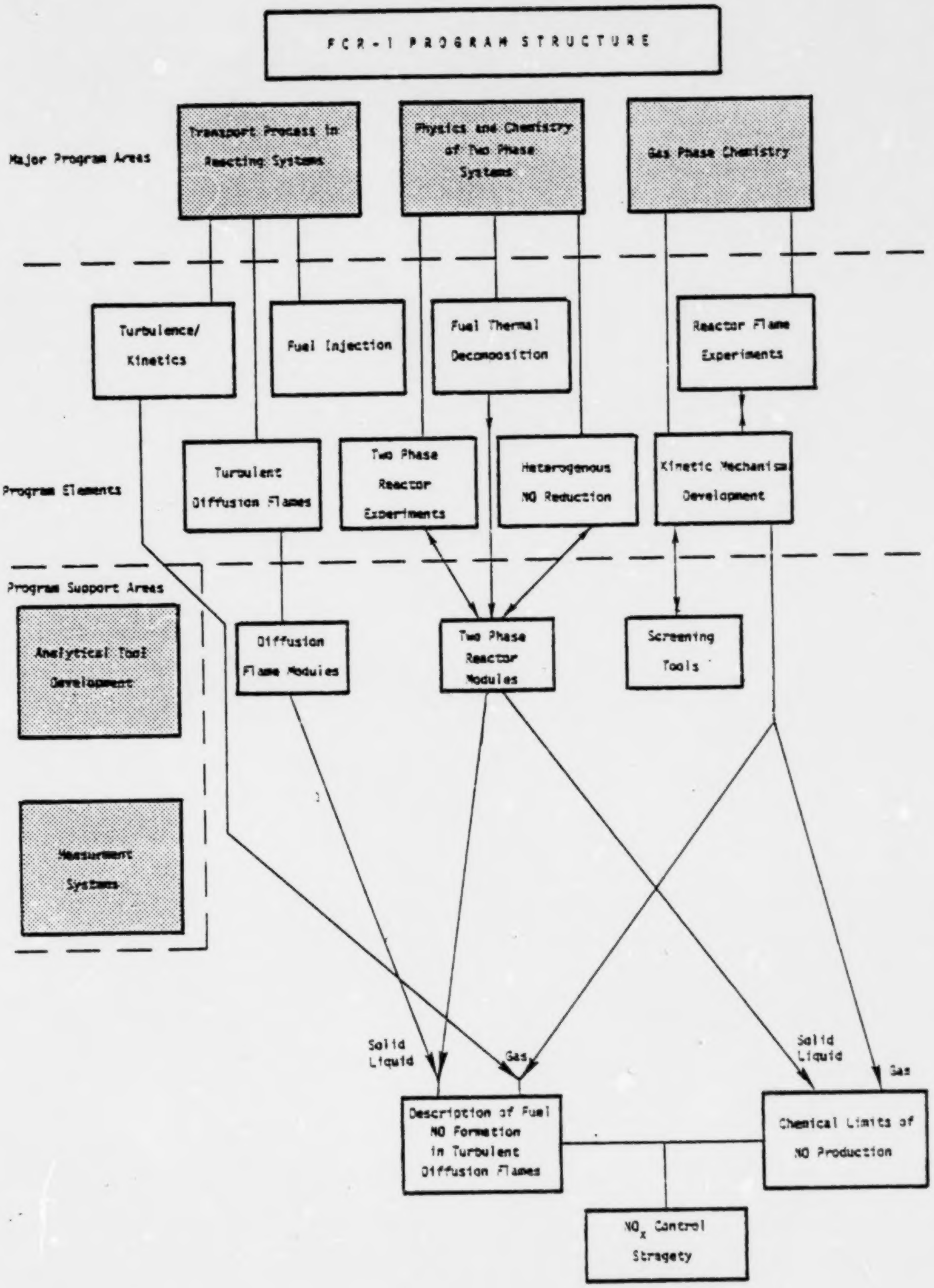
FCR-I PROGRAM STRUCTURE
Major Program Areas
Transport Process in Reacting Systems
Physics and Chemistry of Two Phase Systems
Gas Phase Chemistry
Turbulence/ Kinetics
Fuel Injection
Fuel Thermal Decomposition
Reactor Flame Experiments
Program Elements
Turbulent Diffusion Flames
Two Phase Reactor Experiments
Heterogenous NO Reduction
Kinetic Mechanism Development
Program Support Areas
Analytical Tool Development
Measurement Systems
Diffusion Flame Modules
Two Phase Reactor Modules
Screening Tools
Solid Liquid
Gas
Solid Liquid
Gas
Description of Fuel NO Formation in Turbulent Diffusion Flames
Chemical Limits of NO Production
NO_x Control Stragety

Figure 2. FCR-I Program Structure.

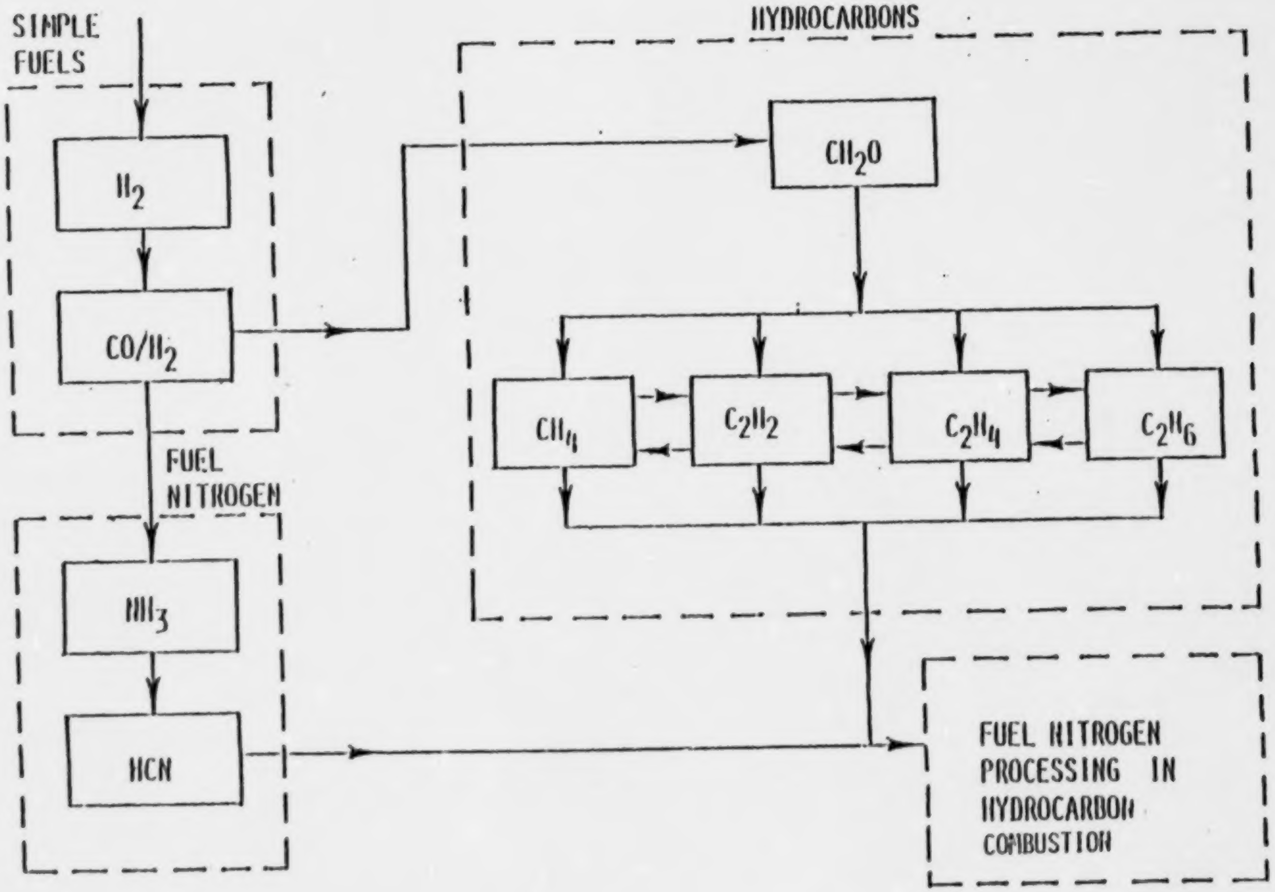

Figure 3. Overview of Kinetic Mechanism.

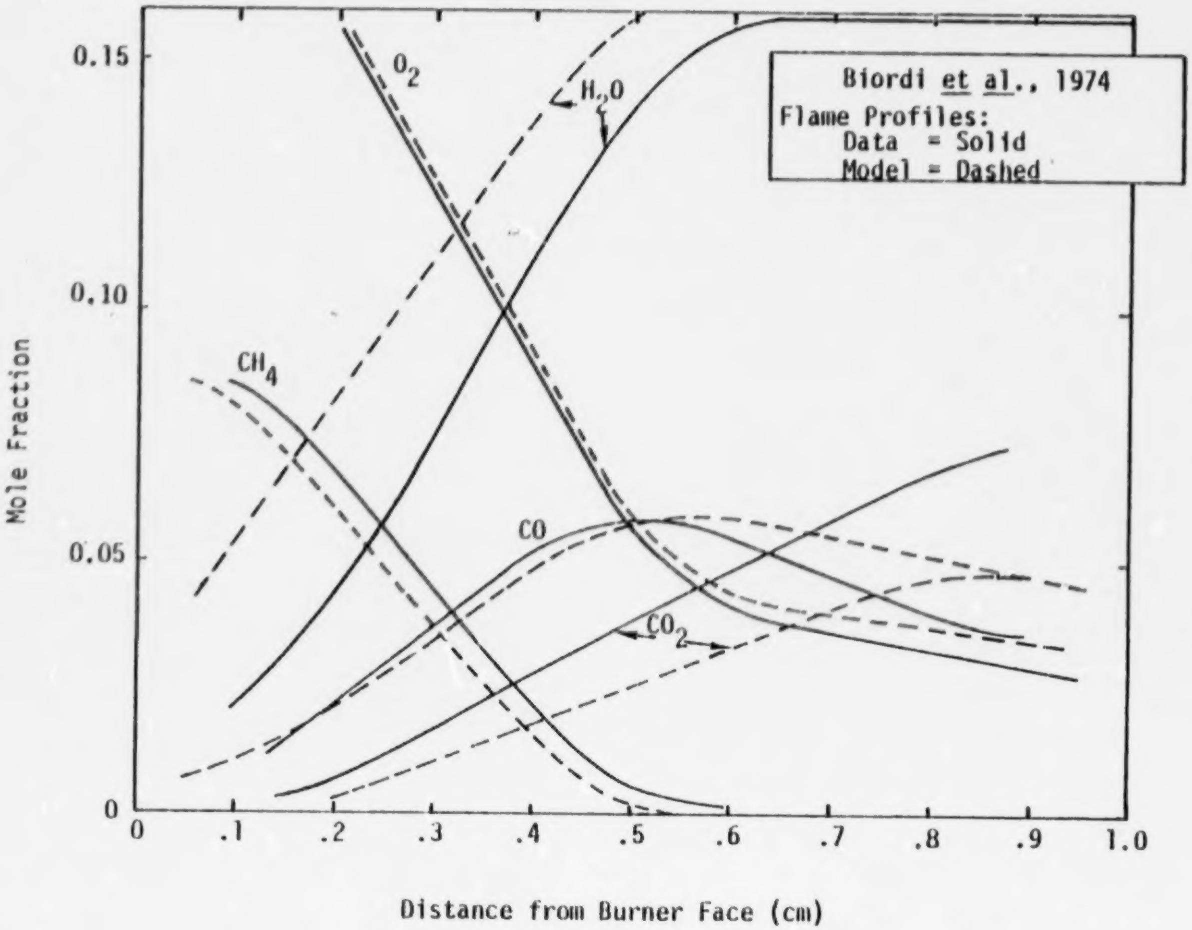

Figure 4. Comparison of Gas Phase Mechanism to CH_4/Air Flame Profiles of J. C. Biordi et al (15th International Symposium on Combustion, p.917, 1974)

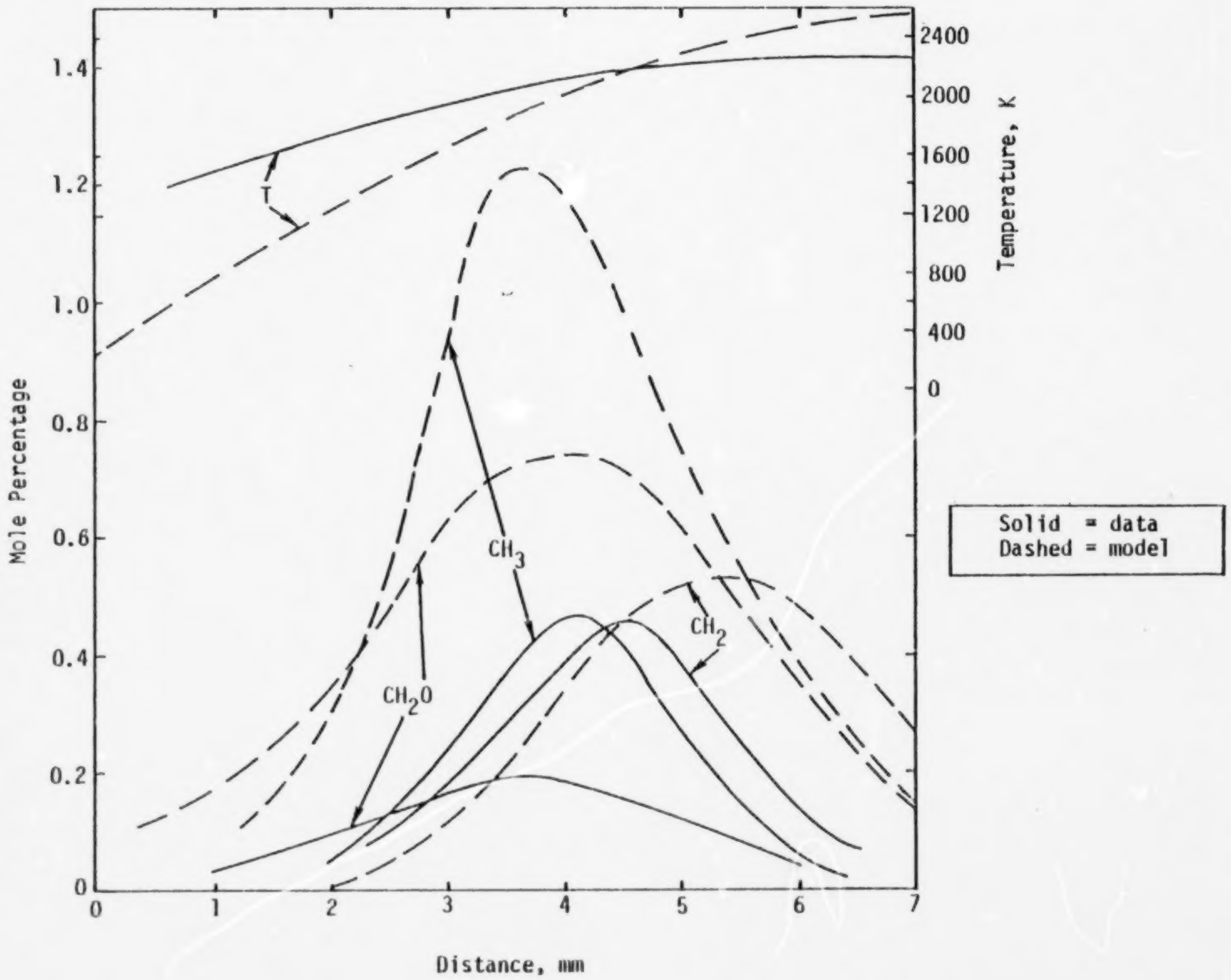

Figure 5. (17th International Symposium on Combustion, p. 857 (1979))
Stoichiometric CH_4-O_2-Ar Flame Profiles From R. Harvey and A. MacColl

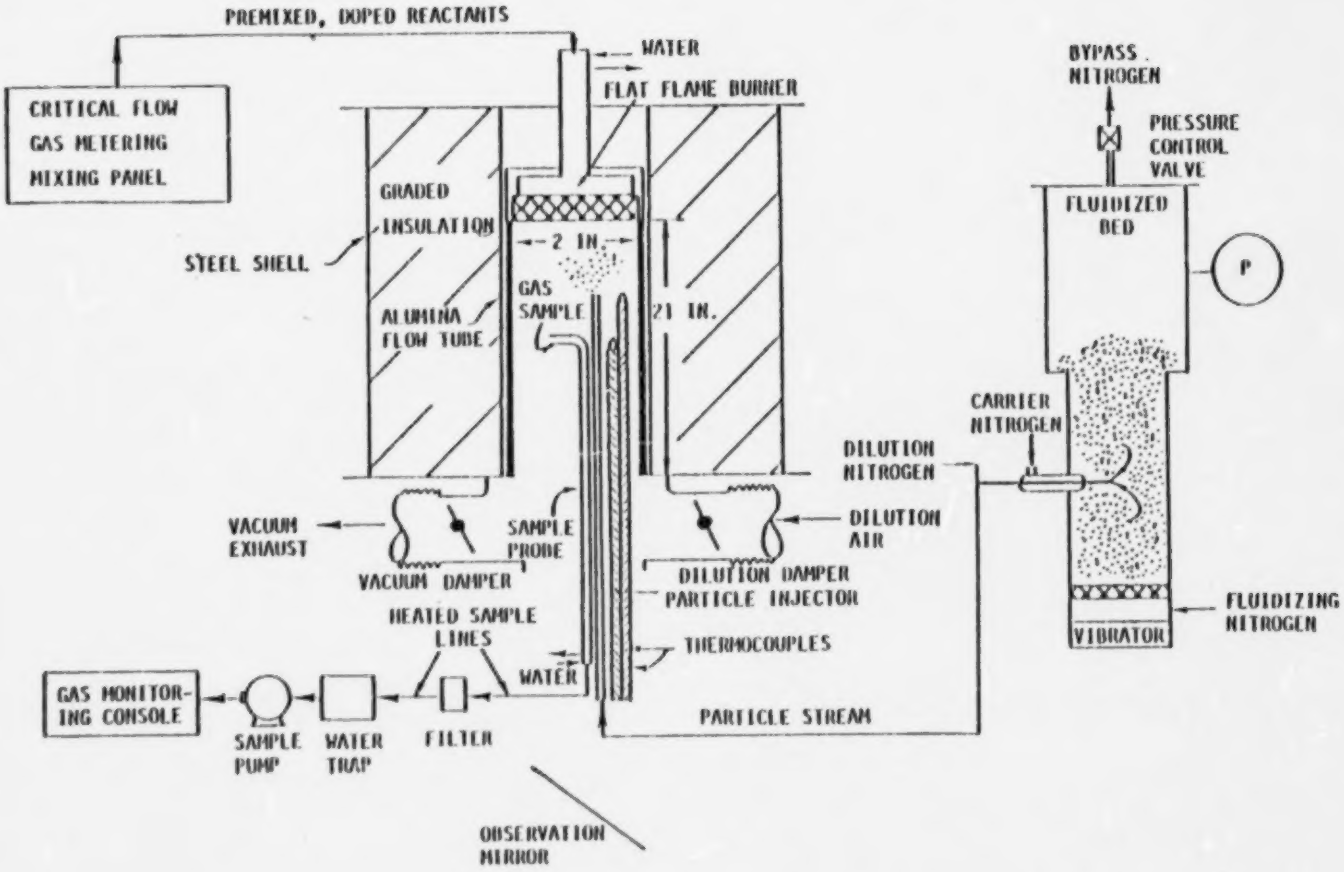

Figure 6. Heterogeneous Reactor System.

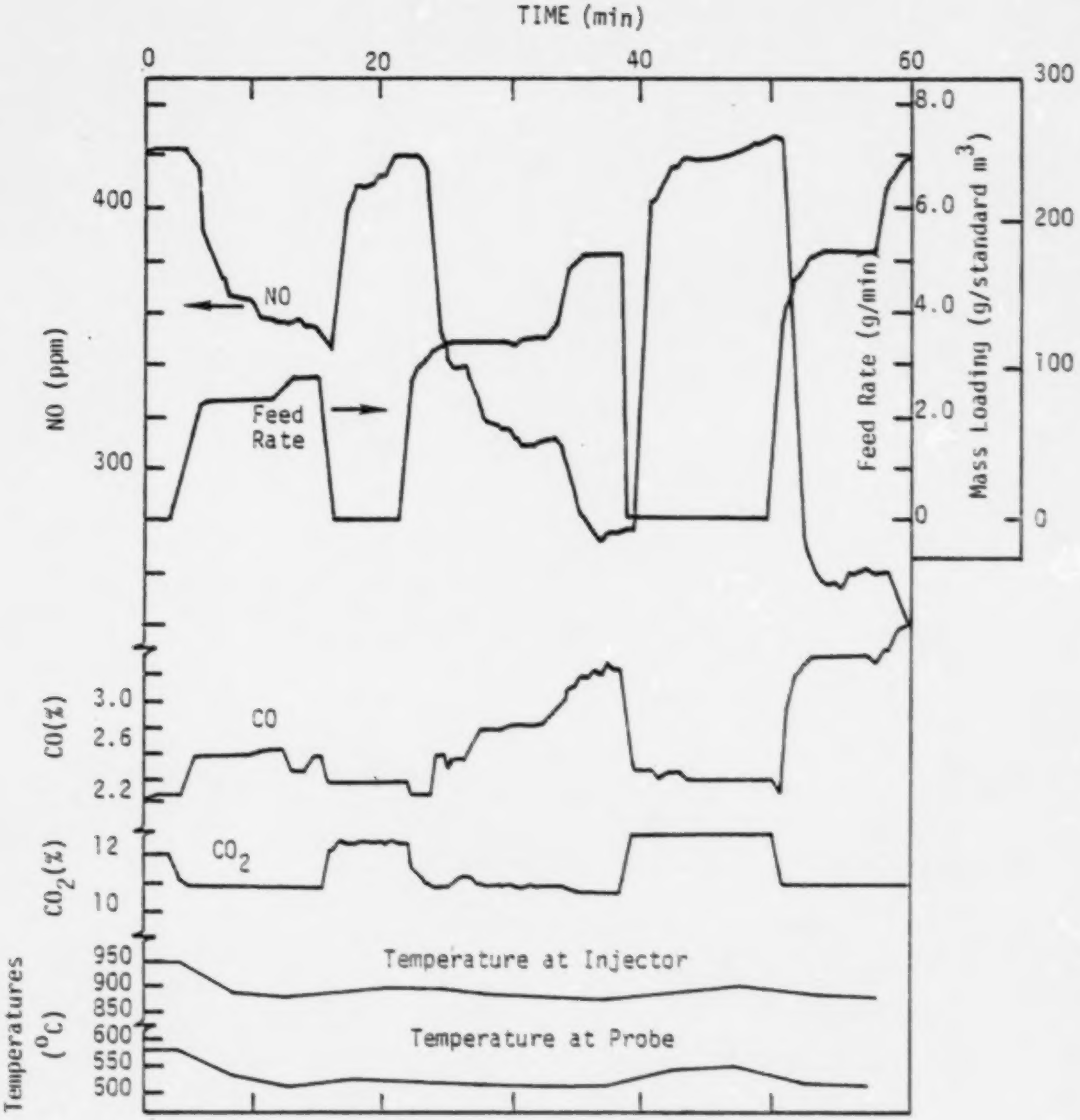

Figure 7. Heterogeneous Effects of Coed Char.

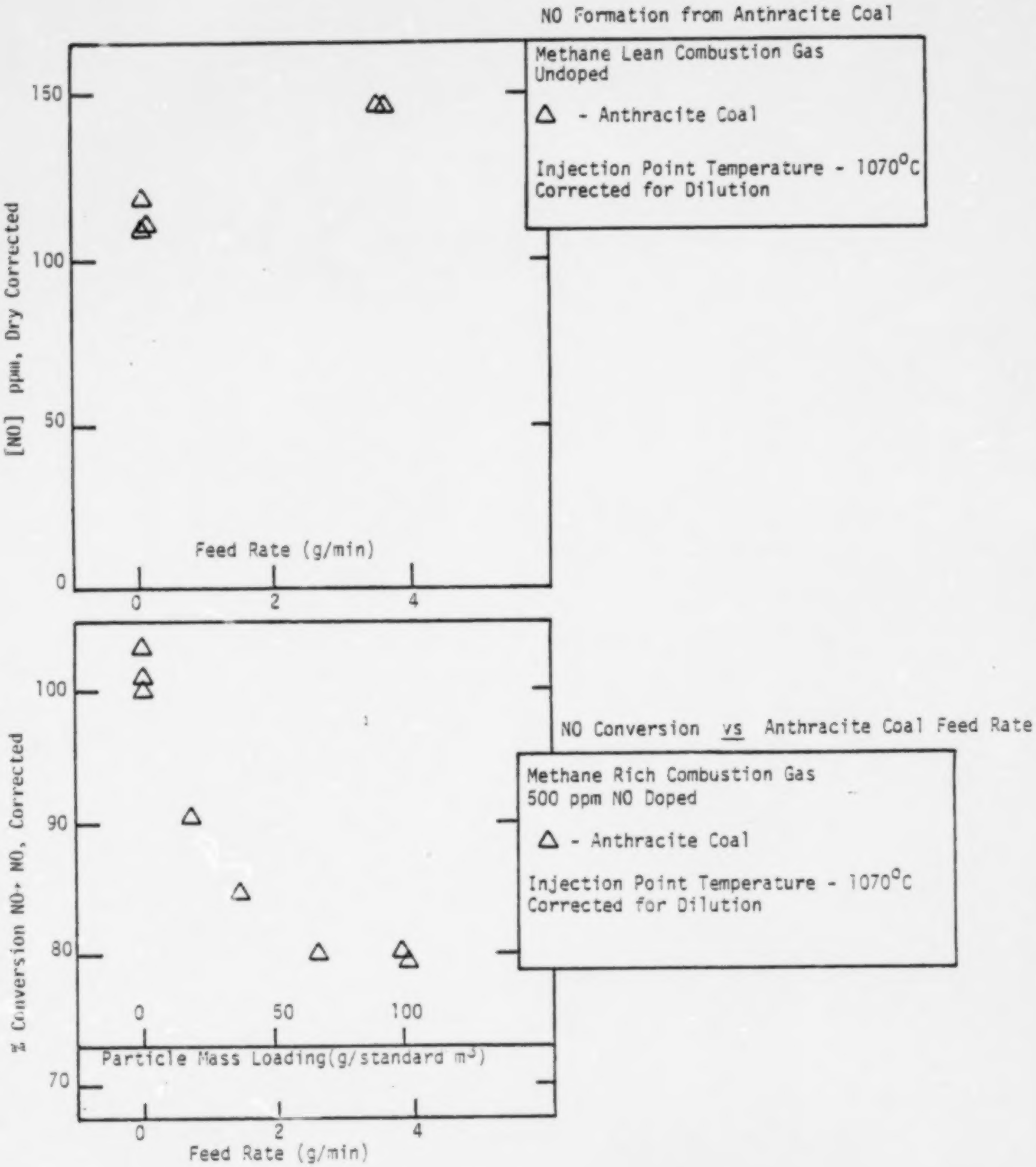
NO Formation from Anthracite Coal

NO Conversion vs Anthracite Coal Feed Rate

Figure 8. Heterogeneous Effects of Anthracite Coal.

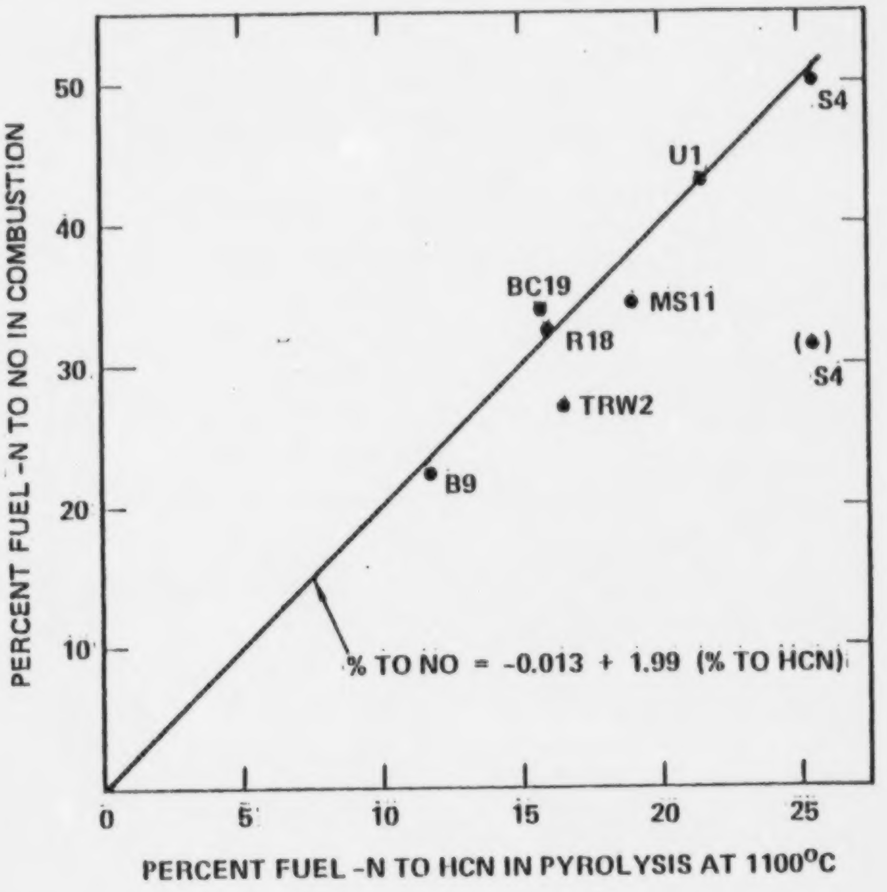

Figure 9. Percent NO in Combustion vs Percent HCN in Pyrolysis at 1100°C.

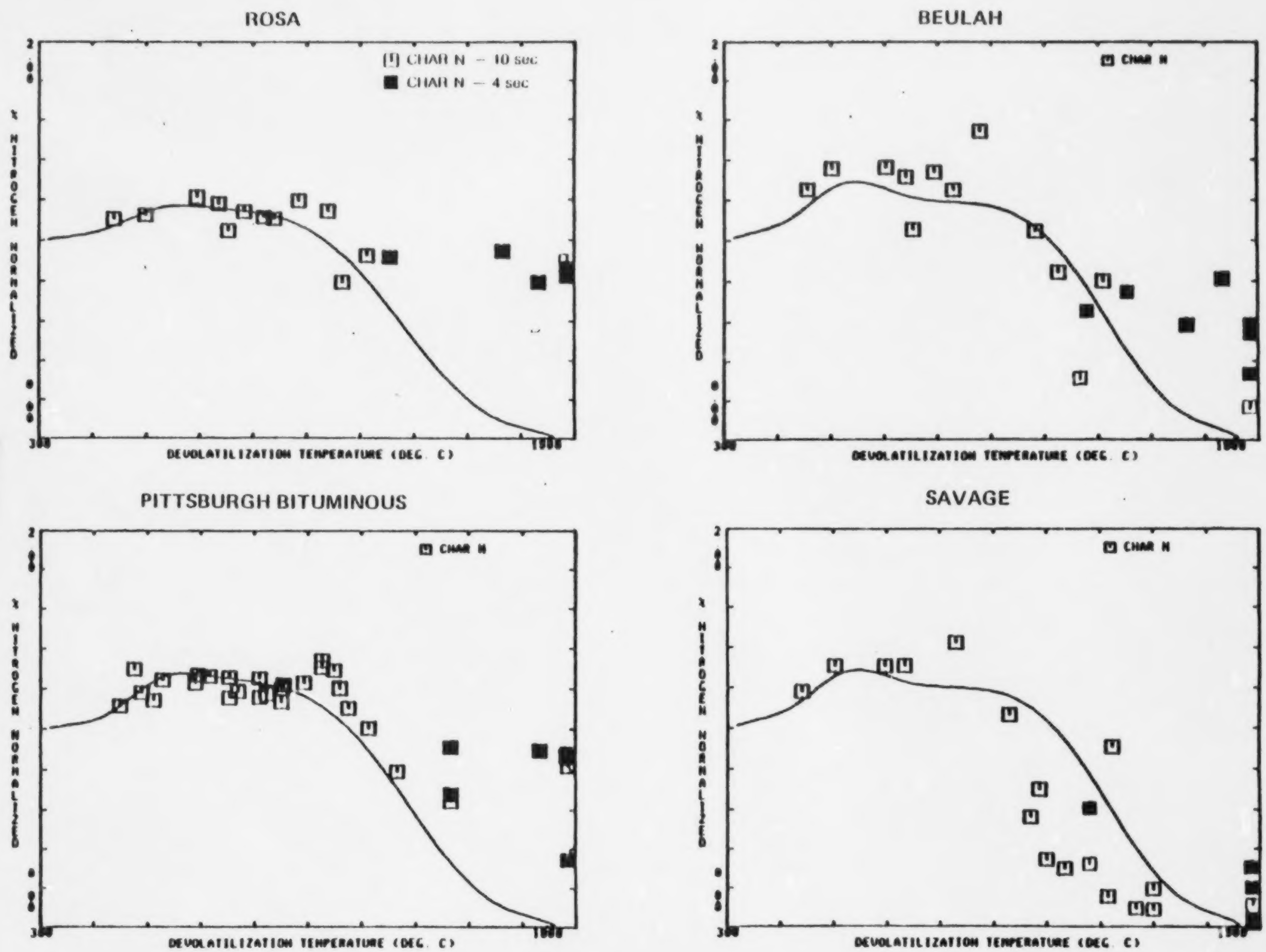

Figure 10. Temperature Dependence of Nitrogen Retention in Chars.

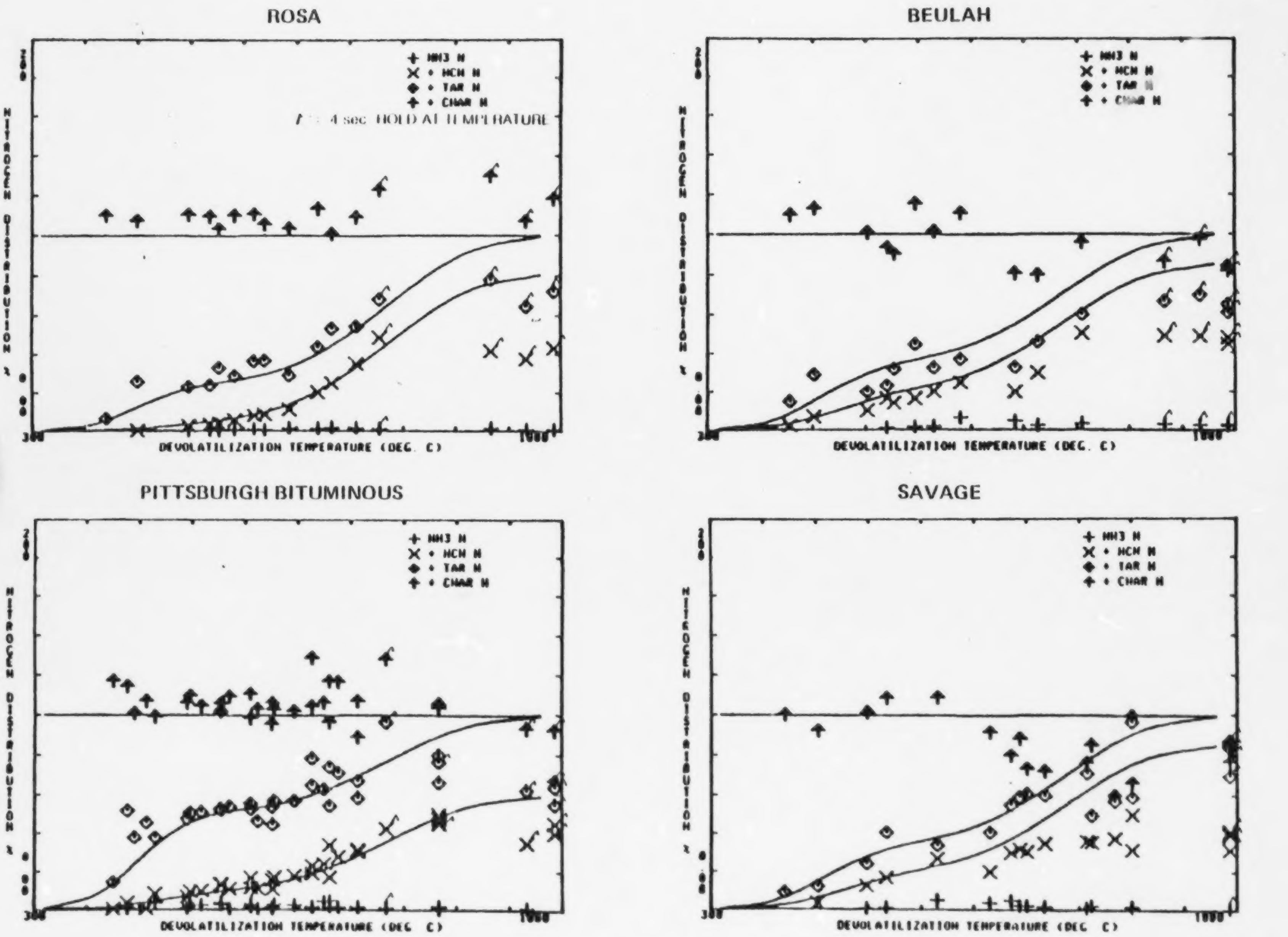

Figure 11. Evolution of Nitrogen from Lignites and Bituminous Coals.

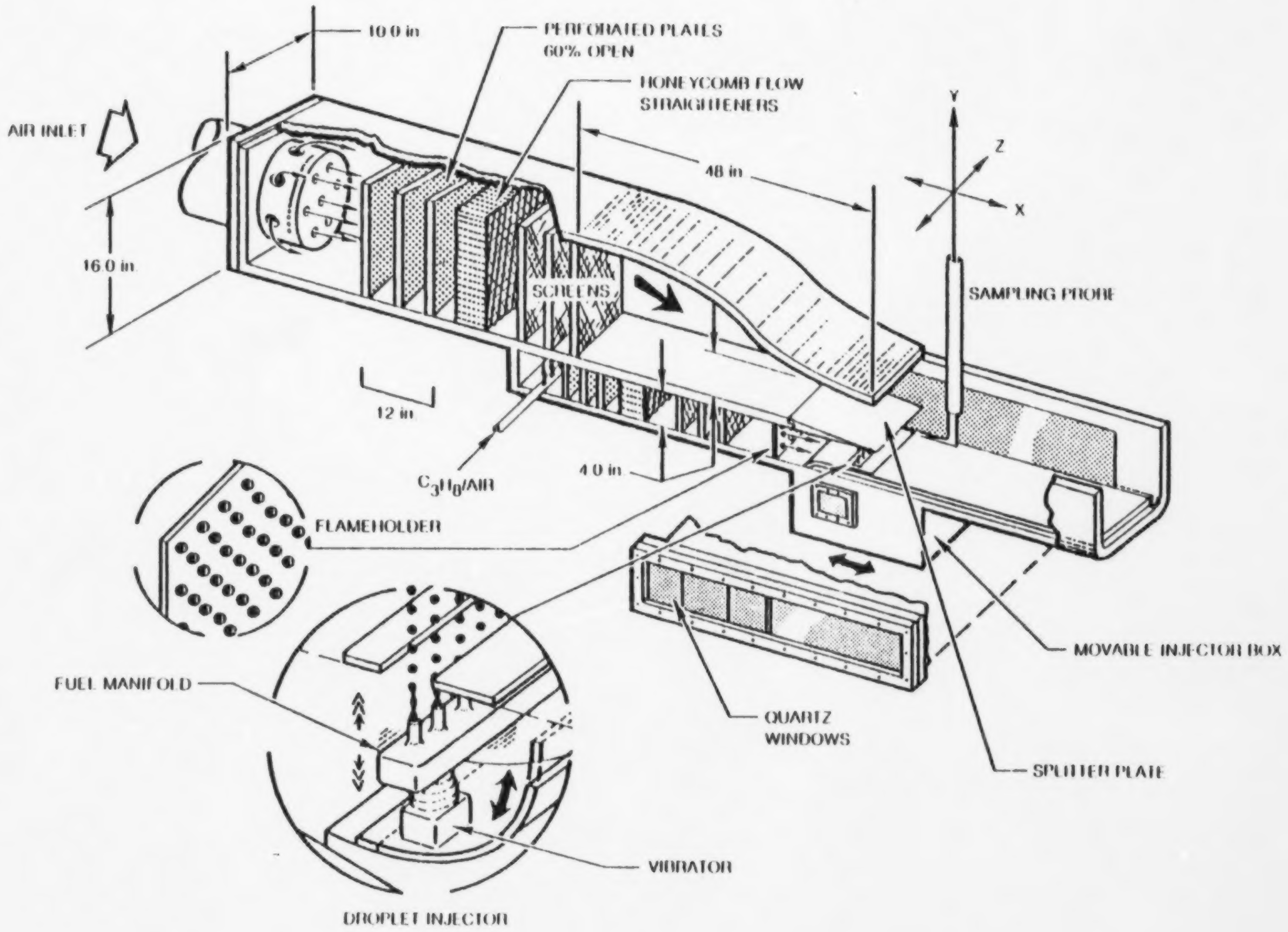

Figure 12. Heavy Oil Spray Combustor.

TABLE I. MECHANISTIC DEVELOPMENT PROGRAM RESULT SUMMARY

Experimental System	Reactants	Measured	Quality of Comparison (a)
Shock Tube	H_2-O_2	Ignition Delay	***
		Exponential Growth Constants for OH	***
Flat Flame Burner	H_2-O_2	Freely Propagating Burning Velocity	***
		Flame Temperature and Species Profiles	**
Shock Tube	CO-H_2-O_2-Ar	(1) Exponential Growth Constant	***
		(2) Exponential Growth Constant for CO	***
		(3) Time for CO to Reach a Given Value	* (b)
Flat Flame	CO-air	Freely Propagating Burning Velocity	* (c)
Shock Tube	CH_2O-O_2-CO-Ar	Ignition Delay	***
Shock Tube	CH_4-O_2-Ar	Ignition Delay	**
Flat Flame Burner	CH_4-O_2 CH_4-O-Ar	(1) Freely Propagating Burning Velocities	***
	CH_4-air	(2) Flame Temperature and Species Profiles	**
Shock Tube	NH_3-O_2-Ar	Ignition Delays	***
Shock Tube	NH_3	Pyrolysis Profiles	* (d)

(a) Quality of comparison: *** = excellent; ** = good; * = fair.

(b) Cause by rate of CO + OH → CO_2 + H being too low above 2000°K.

(c) Difficult to estimate water content of reactants from most papers. Modeled burning velocity is a strong function of water content when water is a trace specie.

(d) Suggested that additional species (i.e., N_2H_i) were necessary to correctly model NH_3 pyrolysis.

TABLE II. ACCUREX STIRRED REACTOR PROGRAM PLAN

Task	Description
1	Design stirred reactor to be well-mixed on gas over the residence time range between 20-200 msec
2	Verify (optimize) gas mixing intensity using a "cold" model of the reactor
3	Qualtify coal particle mixing vehavior in the stirred reactor
4	Proceed with coal combustion tests • Covering the reactor residence time range at equivalence ratios up to 4 • Performing wet sieving tests and chemical analysis on selected char samples • Using conventional gas analysis, supplemented with NH_3 and HCN measurements during selected tests

TWO PHASE PROCESSES INVOLVED IN THE CONTROL OF NITROGEN OXIDE FORMATION IN FOSSIL FUEL FLAMES

By:

J. M. Beér, A. F. Sarofim, L. D. Timothy, S. P. Hanson,
A. Gupta, and J. M. Levy
Department of Chemical Engineering and the Energy Laboratory
Massachusetts Institute of Technology
Cambridge, Massachusetts 02139

ABSTRACT

The conversion of fuel-nitrogen to nitric oxide in flames is dependent upon a number of physical and chemical factors, three of which are discussed in this paper: the rate of evolution of fuel nitrogen by heavy fuel oils, the temperature-time history of burning coal particles, and the kinetics of the reduction of NO by char.

Measurements of the nitrogen evolution of a stream of 150 μm fuel droplet injected into a heated helium stream were made for a Raw Paraho Shale oil and an Indo-Malaysian residual fuel oil. The nitrogen evolution during vaporization of the dispersed oil droplets is found to depart significantly from that obtained under equilibrium distillation. For a Paraho shale oil the rate of nitrogen evolution under the rapid heating experienced by the droplets is retarded relative to that observed under equilibrium conditions. By contrast preferential vaporization of the nitrogen was observed for an Indo-Malaysian residual fuel oil. The temperature-time history and burning times of coal particles burning singly were determined by two-color optical pyrometry in order to provide insights on the role of volatile combustion on nitric oxide formation. The burning times and intensity traces showed that 100 μm particles of a bituminous coal produced a detached volatile flame which was not evident during the combustion of smaller 40 μm particles. The last part of the paper summarized data on the kinetics of NO reduction by char, the enhancement of the rate of reduction in the presence of CO and the inhibition of the reduction reaction by H_2O.

ACKNOWLEDGEMENT

We are grateful for the proficient laboratory assistance of Mr. Anthony Modestino. The two-color pyrometer studies were ably performed by Diana Altrichter. Support for this work from the U.S. Environmental Protection Agency is gratefully acknowledged. The authors gratefully acknowledge guidance and advice from Steve Lanier and Blair Martin.

SECTION 1

INTRODUCTION

Control of fuel nitrogen conversion to NO_x in the process of combustion of high-nitrogen content fuels requires understanding the chemical transformations of fuel nitrogen during the inital pyrolysis and subsequent combustion of coal particles and fuel droplets which can lead to the formation of molecular nitrogen and nitrogen oxides in variable proportions. Schematic pathways of fuel nitrogen transformations during pyrolysis and oxidation in combustion processes are illustrated in Fig 1. In coal combustion the fuel nitrogen evolves during the devolatilization of the coal and the subsequent combustion of the individual char particle. The fraction of fuel nitrogen evolved with the volatiles varies with coal type, particle size and temperature. In the case of fuel oil droplets the fuel nitrogen becomes available for reaction in the gas phase through vaporization; in multicomponent fuel droplets the nitrogen evolution will therefore depend on the distribution of fuel nitrogen over the various boiling fractions, the droplet size and the rate of droplet vaporization. Understanding the details of the non-equilibrium distillation process is necessary for determining the nitrogenous product distribution and hence the rate at which nitrogen containing compounds become availabe for gas phase reactions. The first two parts of this paper are concerned with the presentation and discussion of results of experimental studies on the evolution of fuel nitrogen from coal particles and fuel oil droplets under conditions similar to those in practical flames.

In heavy fuel oil droplets the nitrogen concentration distribution is normally biased towards the higher molecular weight hydrocarbons. Heavy fuel oils are not completely vaporizable and the amount and nature of the coke residue depends, for a given oil type, on the drop size and the rate of vaporization. It can therefore be expected that the evolution of nitrogen from a heavy fuel oil droplet during its vaporization in a flame will be significantly different from the results of equilibrium distillation obtained under slow heating conditions. For the study of fuel nitrogen evolution in small fuel droplets representative of those in fuel sprays of industrial flames, a laminar flow reactor was developed with provision for controlling the droplet size and the thermal and chemical environment of freely suspended monosize droplet streams. Results are presented in this paper of the time resolved nitrogen evolution from a shale oil and residual petroleum fuel oil. These results illustrate the effect of rapid heating of multicomponent fuel droplets upon the fuel nitrogen evolution and the significant departure from results of equilibrium distillation under high rates of droplet vaporization.

The second part of the paper presents measurements of the temperature-time history of pulverized coal particles during combustion. In earlier work carried out by Pohl and Sarofim (1) and by Cheng (2) the rate of evolution of fuel nitrogen during pyrolysis and combustion of pulverized coal particles was determined. While the thermal environment of the devolatilizing particles in an inert atmosphere is well defined, the combustion of volatiles in oxidizing atmospheres makes this less well determined. The existence of a volatile flame, the chemical composition of the volatiles, the position of the volatile flame in relation to the particle surface all influence the temperature-time history of the thermally decomposing, devolatilizing coal particle. The development of a two color optical temperature measurement technique capable of following the variation of the particle temperature during combustion made it possible to obtain additional information of the interaction between the volatile flame and the devolatization and combustion of coal particles.

The third part of the paper deals with the heterogeneous reduction of NO on a char surfare. This reaction can play an important role in reducing the formed NO concentration in coal combustion processes. In an earlier study Pereira and Beer (3) have obtained data on the rate of reduction of NO in fluidized coal combustors; Chan (4) and Sprouse(5) have determined kinetic parameters of this reaction in the fluidized coal combustion temperature range and Song (6) obtained kinetic data relevant to pulverized coal combustion. In the following, results of laminar flow reactor experiments are presented including time resolved reaction product concentration variation (CO_2, CO) and NO-Char reactors rates as affected by CO and water vapor in the feed gas.

The three studies presented in this paper are self contained separate investigations which, however, are closely interrelated through their contribution to the better understanding of the details of the transformations of fuel nitrogen in pulverized coal and liquid fuel spray flames.

SECTION 2

FUEL-NITROGEN EVOLUTION FROM VAPORIZING HEAVY FUEL OIL DROPLETS

For the study of fuel-nitrogen evolution from liquid fuel droplets during pyrolysis and oxidation a laminar flow reactor was designed with provision for feeding a monosize droplet array into a laminar gas stream and the capability of intercepting the droplets after a chosen residence time by a fast quenching sampling probe. Results of experiments with the pyrolysis of 150 μm droplet streams of Raw Paraho Shale and Indo-Malaysian residual petroleum fuel oil are presented in Figs 2 and 3. Equilibrium distillation data for these two fuels are shown in Figs 4 and 5 respectively. The data points in Figs 2 and 3 are calculated from the weight loss due to vaporization between the point of the droplet injection and their capture by the sampling probe, and from the nitrogen concentration of the residue collected at the sampling position. The equilibrium distillation curves (Figs 4 and 5) were obtained by slowly heating the fuel oil at atmospheric pressure. The distillation curves show that in the shale oil the nitrogen is quite uniformly distibuted over the different boiling fractions in contrast to the heavy petroleum fuel oil where the nitrogen is concentrated in the high temperature boiling fractions. Under conditions of rapid heating, however, the above trend is reversed. The shale oil droplet at the beginning of its vaporization yield little nitrogen and the distillation curve shifts more and more to the left as the furnace temperature and hence the vaporization rate is increased. Once the low nitrogen content, low boiling fraction compounds are vaporized the slope of the distillation curve is maintained at nearly 45° indicating that the fraction of nitrogen evolved relative to the fraction of mass vaporized is constant. The heavy petroleum fuel shows, however, a different picture; here the nitrogenous compounds are concentrated in the high boiling fractions and after an initial period in which little nitrogen is released, rapid nitrogen evolution follows resulting in a much higher total nitrogen loss per vaporized mass then under equilibrium distillation conditions. While the details of the non equilibrium distillation-pyrolysis process are far from being completely understood it is thought that the nature of the nitrogen evolution in heavy fuel oil droplets can be explained by diffusional limitation of the mass transfer within the liquid droplet. At high rates of vaporization the low nitrogen content, low boiling fraction is depleted at the particle surface because the transport of the low boiling compounds from the interior of the drop to the surface is slow compared to its removal from the surface by vaporization. As a consequence, the nitrogen concentration at the surface increases and, as the temperature increases to the boiling point of this surface layer, nitrogen evolves at a strongly increased rate. The low boiling fraction trapped in the droplet is superheated; this can increase the drop size by internal vaporization and in the limit can disrupt the droplet by microexplosions. The unexpected trend in the nitrogen evolution from heavy fuel oil droplets and shale oils under rapid heating conditions has important implications for staged combustion applications. It is clear that equilibrium distillation may provide a poor measure of the time over which the majority of the fuel nitrogen is released, a parameter of importance in locating the point of injection of the secondary air. It is emphasized, that the above data are based on a limited number of experiments and cover limited ranges of the variables. Further investigations are in process to better understand the effects of high rates of vaporization upon the departure from equilibrium distillation.

SECTION 3

MEASUREMENT OF TEMPERATURES AND BURNING TIMES OF COAL PARTICLES

In as much as the release of the bound nitrogen in coal is kinetically controlled (1), it is important to determine the temperature time histories of burning coal particles and how they are influenced by coal composition. A major uncertainty in predicting the temperature is the influence of volatiles the composition of which varies greatly from coal to coal and which may burn either heterogeneously at the particle surface or in detached flames. The following sections provide some preliminary data on the influence of coal composition of the temperature and burning time.

EXPERIMENTAL METHOD

A two-color pyrometer has been developed for measuring the temperatures and burning times of individual coal particles (7). A dilute stream of coal particles is produced by elutriating coal into a hypodermic needle at a controlled rate from a vial in which the coal level is maintained constant. The resulting coal stream is discharged as a jet and particles withdrawn from an appropriate position in the jet are injected along the axis of a laminar flow furnace (Fig 6). The radiation from the burning particles is focused on to an optical fiber which is sighted along the axis of the furnace. The optical fiber splits the radiation and feeds it throught two narrow band pass filters with band centers at 450 and 550 nanometers. The intensity of the burning particle at the two wavelengths is then measured using photomultiplier tubes. The particle temperatures are obtained from the ratio of the intensities at the two wavelengths assuming that the particle emissivity is not a function of wavelength. The signals from the photomultiplier tubes were measured with a Bascom-Turner model 8110 digital recorder that can sample simultaneously on two channels. Reference calibration signals were produced by a chopped signal from a tungsten strip lamp viewed throught the furnace.

RESULTS

Experiments were conducted with five coals (Illinois No.6, Utah No.1, Alabama Rose, North Dakota Beulah, and Montana Savage), two size fractions (38-45 μ and 90-105 μ), furnace temperatures of 1250 and 1700 K, and oxygen mole fractions of 0.15 to 1.0. For each condition the burning profiles for a large number of particles were obtained. Selected results will be presented mostly for the Illinois #6 bituminous coal and the Montana Savage lignite since the behavior of these coals bracket most of the others.

An illustration of the photomultiplier output is shown in Fig 7 for lignite particles burning in 15 and 20 percent oxygen. Each trace shows a steep rise following ignition, followed by a slower decay. The traces provide information on burning time, temperature, and changes in surface area with time during combustion. The burning times are well approximated by the duration of each signal, the temperatures are obtained by two-color pyrometry assuming the particles are gray emitters, and the decrease in area with combustion can be inferred from the decay in intensity with time during combustion.

Temperatures traces for combustion of Illinois #6 coal particles in streams containing from 15 to 100 percent oxygen is shown in Fig 8. The irregulatities in the curves are believed to be experimental errors involved in taking the ratio of the two signals and the background noise. The peaking in temperature in 100 percent oxygen concentrations is seen in many particle traces and is believed to be real. The average burning temperature of Illinois #6 coal was consistently higher than that of the Montana lignite (Fig 9). Although this is expected, on the basis of the higher heating value of the bituminous coal the story is more complicated as will be discussed below.

Burning times for the 90-105 μ Montana lignite and Illinois #6 are shown as function of oxygen partial pressure in Fig 10. At the high temperatures of the study, the burning times are expected to be diffusion limited and given by

$$t = \frac{\rho_c RT d^2}{8\alpha D P X_{O_2}}$$

where ρ_c is the density of the coal,

$D P$ is the product of diffusivity and total pressure,

X_{O_2} is the oxygen mole fraction,

d is the particle diameter,

α is the weight of coal that reacts with a mole of oxygen.

Calculated burning times are found to be in good agreement with measurements for the lignite when it is assumed that the products of combustion are CO and H_2O. The burning times for the bituminous coal (Illinois #6) are, however, considerably lower than the predicted values. This could be explained either by particle swelling (the product $\rho_c d^2$ varies inversely with size if a particle swells uniformly) or by the combustion of volatiles in detached flames. Previous studies in this laboratory have shown that the swelling of bituminous coals is small at temperatures above 1800 K, and would not be sufficient to explain the observed reduction by a factor of two to three in burning times. The formation of a volatile flame, however, would reduce the oxygen requirements for the combustion of the residual char by approximately the correct amount. Supplemental evidence for this explanation of the reduction of burning times is provided by the intensity traces obtained during combustion.

During the combustion of the Illinois No.6 coal in gases containing less than 75 percent oxygen an intense signal at relatively short times was observed signalling the formation of a luminous flame (Fig 11). This peak corresponding to the combustion of volatiles becomes increasingly marked as the oxygen partial pressure is decreased. Similar formation of volatile peaks have been reported in the literature, based on the combustion of larger coal particles at lower temperatures and time resolved measurements on CO_2 (8) and NO (9). In the present study no volatile peaks were observed for the lignite, but this would be expected since the soot which provides the luminous signal is expected to be formed in significant amounts only for the bituminous coals.

The formation of a volatile flame is expected when the rate of volatile evolution exceeds the rate of the diffusion to the particle surface of the oxygen needed for its combustion. As the oxygen diffusion rate is increased, by increasing oxygen concentration the volatiles burn heterogeneously at the particle surface as soon as they are evolved and no distinct volatile flame is seen. Consistent with this hypothesis is the failure to detect volatile flames when 40 μ particles were burned, since the diffusion rate will increase as the particle size is decreased. For the smaller bituminous particles the burning times were in good agreement with the diffusion limited estimates, when it was assumed that the oxygen diffusing to the surface was that required to burn the char and volatiles; this provide further support for the postulate that the volatiles burn heterogeneously when the oxygen diffusion rate is sufficiently high. The effect of particle size on burning time is shown in Fig 12. The data suggest that the volatile combustion undergoes transition from detached flame to heterogeneous surface oxidation in the size range found in pulverized coal flames. This is consistent with the predictions of Howard and Essenhigh (10).

The above interpretation of the data are preliminary but provide interesting insights on the variation that can be expected in burning temperatures and burning times, as the coal type, size, and ambient conditions are varied. These changes in particle temperature and mode of volatile combustion will influence fuel nitrogen release rates and the efficiency of conversion.

SECTION 4

NO/CHAR REACTIONS AT PULVERIZED COAL FLAME CONDITIONS

Nitric oxide produced early in pulverized coal flames may be subsequently reduced by char generated by the partial combustion of coal. Indirect evidence for the importance of NO reduction reactions in coal combustors is provided by the observation in pilot-scale combustors that the NO concentration passes through a maximum and undergoes substantial reduction in the latter stages of combustion, particularly under fuel-rich conditions (11). That the rate of reduction of NO observed in coal flames is much higher than that in the combustion products of gaseous or liquid fuels suggests that coal products, such as ash or char, may be responsible for the reduction.

This section of the paper provides data on the NO/char reaction under conditions of interest to pulverized coal flames for possible use in assessing the role of char in reducing NO. It covers research under the EPA grant which has also been presented at the 18th Symposium (International) on Combustion. Extensive studies of the reduction of NO by carbonaceous solids have been carried out in the temperature ranges of interest for automobile exhaust-reactors (12-14) and fluidized bed combustors (15-18). These data show a strong influence of secondary reactants such as CO, H_2, and O_2 on the rate of the NO/char reaction. The results of these studies are not directly pertinent to the temperatures in combustors since the extent of surface coverage by adsorbed species varies markedly with temperature.

Kinetics of the NO/char reaction under conditions of interest to pulverized coal combustion were obtained in a laminar flow furnace for the temperature range of 1250 to 1750 K.

Size graded, pulverized char particles are fed into the furnace in a helium (carrier) stream, where they are rapidly heated to the furnace temperature by conduction from the surrounding main-gases and by radiation from the furnace walls. The main gases (consisting of an NO/He mixture with varying amounts of CO and H_2) are heated by passage through an alumina honeycomb/flow-straightener prior to entering the furnace. Furnace temperature of up to 1750 K can be achieved. The reaction is quenched by passage of the products from the heated zone through a water-cooled section at the base of the furnace. The char is collected on a cold, sintered bronze disk and the composition of the effluent gases are measured by a chemiluminescent analyzer (NO) and non-dispersive infrared (NDIR) analyzers (CO, CO_2). The composition of the gases may also be monitored in cold-flow prior to entry to the furnace.

The experiments were performed in the laminar flow furnace as follows. Nitric oxide of a certified concentration in helium was flowed through a calibrated mass flow controller and mixed with an additional helium stream to yield the desired NO (typically about 950 ppm) in cold flow. The total flow rates were determined from the NO dilution factor (i.e., by using NO itself as a tracer) and the known NO flow rate or, in some cases, by measurement of the additive flow rates by passage through calibrated mass flow meters. Upon subsequent additions of CO or H_2O, the helium flow was reduced until the initial NO concentration was restored. Char feeds were timed, and the weight of char fed was measured (by difference) to determine the char feed rate. The duration of each char feed was typically 60 to 210 seconds at approximately 0.1 gm/min.

During the char feed, a steady state is achieved in the furnace. Thus, from measurement of the entrance and exit NO concentrations, knowledge of the furnace volume gas flow rate and char feed rate, it is possible to derive the effective rate constant for the reduction of NO on the char surface. The char was produced by heating a pulverized Montana lignite in a crucible to its asymptotic weight loss under an inert atmosphere at 1750 K, followed by size-grading to 44-53 μm. The elemental analysis of the char is 84.4% carbon by weight, 0.16% hydrogen, 0.215% nitrogen, and 0.76% sulfur.

RESULTS AND DISCUSSION

Rate of the NO/Char Reaction and Influence of Additives.

A trace of the temporal variation of NO in the effluent gas is shown in Fig. 13. The experiment was designed to obtain the rate of the NO/char reaction and also to show the effect fo CO upon the net reduction of NO. 956 ppm NO in helium was fed at a rate of 3.0 l/min into the laminar flow furnace which was maintained at 1250 K. The first drop in NO concentration follows the introduction of the char transport gas (carrier gas) at a rate of 115 ml/min. After the NO concentration stabilized, the char was fed at a rate of 0.16 gm/min. for a period of about 60 seconds (the interval shown between the char feed on and off designations in Fig 13). The resultant dip in the NO trace provides a measure of the NO/char reaction. The displacement in time between the response in the NO concentration trace and the step changes in the char feed reflect the holdup of gases in the furnace and sampling train. The total amount of NO consumed was determined from an integration of the measured deficit in NO concentration and the gas flow rate.

The effect of CO on the NO/char reaction rate was determined by introducing CO (1.4%) into the NO/He stream (a corresponding amount of helium was removed to avoid altering the NO level by dilution), waiting for the NO concentration to stabilize, and then feeding char into the heated NO/He/CO mixture. This sequence of operations provided a means of separating the NO reduction by CO at the walls from that occuring at the char surface. Examination of the concentration trace in Fig 13 shows that the wall catalyzed reaction causes the NO concentration to decrease from 922 ppm NO to about 860 ppm. The extent of this reduction, varies with wall conditioning. Once the NO trace had stabilized, the char was again introduced for a short interval and the incremental NO reduction due to ractions at the char surface measured. The remainder of the trace in Fig 13 shows a two-step increase in NO concentration to its original concentration as a consequence of sequentially stopping the carrier gas stream and then eliminating the wall reactions by turning off the CO stream. For the conditions of the experiment in Fig 13 (T = 1250 K, NO_{inlet} = 165 ppm), the influence of CO on the NO/char reaction appears to be that of a slight enhancement; the extent of the reaction is small and the value is uncertain. Repeated measurements showed a consistent slight enhancement of the NO/C reaction in the presence of 1.4% CO. Fig 14 shows the reproducibility of the NO/char reaction as the char feed was cycled on and off.

A previous study in this laboratory (6) has shown the NO/char reaction to be first order in NO in the concentration range of these experiments. The effective rate for the additive free NO/char reaction was determined, and is reported in Fig 15. The rate coefficient for the NO/char reaction based on the external surface area of the particle is given by

$$\frac{d\,NO}{dt} = 4.8 \times 10^{4} \exp \frac{-34.70 \text{ K cal}}{RT} A_E P_{NO} \text{ moles/sec}$$

where A_E is the external surface area of the char in m^2/gm and P_{NO} is in atmospheres. The internal surface area as measured by N_2 BET is 20.3 m^2/gm. Because it is known that N_2 may give a poor measure of the microporous structure, the rate coefficient was not reduced to intrinsic rate.

The enhancement of the NO/char reaction rate by CO is slight. The results of the increase in rate constant from the addition of 1.4% CO to the gas stream are shown in Table I. The increase in rate is a consequence of an increase in active sites by the reaction of CO with any surface oxides.

The rate of the NO/char reaction decreases as increasing amounts of water vapor are added to the reactant gases as shown in Fig 16. Water was added by flowing a metered stream of helium through a thermostated bubbler connected to the furnace through heated gas-transfer lines. Flow rates were corrected accordingly. The effect of H_2O on the NO/char reaction is seen to become insignificant as the temperature is raised.

Mechanistic Considerations.

The above observations of the NO/char reactions can be rationalized by the following kinetic scheme (4). The reduction of NO by carbon is probably through dissociation of the NO on the surface with a rapid surface diffusion of the dissociated atoms to form N_2. The oxygen produced by the dissociation is strongly chemisorbed and will inhibit further reaction, i.e.,

$$NO + 2C \longrightarrow C(N) + C(O) \tag{1}$$

$$C(N) + C(N) \longrightarrow (N_2)_g + 2C \tag{2}$$

where C represents a surface carbon, C(N) and C(O) adsorbed nitrogen oxygen atoms. The chemisorbed oxygen can either desorb to produce CO or react with CO to form CO_2, i.e.,

$$C(O) \longrightarrow (CO)_g \tag{3}$$

$$C(O) + CO \longrightarrow (CO_2)_g + C \tag{4}$$

The inhibition of the NO/C reaction by H_2O, or any other oxidant, is then explained by the formation of the chemisorbed oxygen layer. As the temperature is increased, enhancement of the rate of activated decomposition of the chemisorbed oxygen by reaction such as (3) is expected to decrease the steady-state coverage of the surface by the oxide layer; this is consistent with the decrease in the inhibitory effect of H_2O at the higher temperatures. The role of CO in enhancing the NO/char reaction is then by reaction with the chemisorbed oxygen (Reaction 4) to increase the available active sites. The decrease of enhancement by CO of the NO/char reaction with increasing temperature is consistent with the expected change with temperature of the chemisorbed oxygen layer.

Product Distribution in the High-Temperature NO/Char Reaction.

To supplement the understanding of the high-temperature NO/char reaction mechanism a careful attempt was made to identify the distribution of reaction products (CO and CO_2) in the high temperature furnace, and to check for closure of the oxygen material balance. A minor experimental difficulty resulted from a residual emission of a small amount of CO from the char, necessitating measurement of a CO "baseline" by feeding the char through the furnace under an inert atmosphere but the same total gas flow rate as that used in the experiments with NO, for each set of experimental conditions.

As was to be discovered later, however, this CO could react with NO to form CO_2. Therefore, in order to minimize the relative contribution of this effect, as well as in order to minimize the instrumental error associated with measurement of very small CO and CO_2 concentrations, the concentration of the NO introduced into the furnace was increased ten-fold from about 1,000 to about 10,000 ppm. Because of the first-order nature of the NO/char reaction, this did not influence the NO conversion. A representative data trace, showing NO depletion and CO and CO_2 formation as a function of time is shown in Fig 6. NO depletion begins when the char feed is turned on, and ends when the feed is turned off. Quantities of NO, CO and CO_2 destroyed or formed are determined either from the integrated areas under the peaks, or from direct reference to the NDIR instrument calibration curves for the "flat", steady-state signals attained at the peak maxima. Great care was taken to repeatedly calibrate the analytical instruments. For this purpose, multiple manufacturer "calibration" gas tanks were used. Instrument calibrations are believed accurate to within a few percent.

The results of experiments run in triplicate with the freshly devolatilized char and high entrance NO concentrations ($\sim$ 9500 ppm, typically) are shown in Table II. Repeated efforts were made to close the oxygen balance, but results converged to around 75%. Repetition of the 1750 K experiments several weeks later yielded results within 0.1% of those shown in the table. Insofar as the measurements are believed to be accurate to within 10%, given the care in calibration of flow rates and instrument responses, the source of the missing oxygen is currently unknown. Thus, it is possible, for example, that the missing oxygen is re-adsorbed on the char surface in the cooling section of the furnace. A rough calculation for one data point (D-178A), using a measured B.E.T. surface area of $20 m^2/gm$ and an area of $10 \mathring{A}^2$ per surface site reveals that the quantity of missing oxygen is just marginally more than that required to form monolayer on the char surface. The CO_2 surface area is expected to be an order of magnitude larger so that the results are consistent with the expected fractional occupancy of total sites.

Further reference to Table II reveals a systematic variation in the CO to CO_2 ratio detected, the ratio increasing with temperature. In fact, we speculate that the data support the idea that the primary product of the NO/char reaction at these temperatures is CO, the CO_2 being formed in a secondary reaction of the CO with the excess NO. As has been observed in past experiments with added CO, a reaction, apparently catalyzed by the walls of the reactor, does occur between CO and NO, forming CO_2 as a product.

To illustrate the feasability of this premise, experiments were performed at each furnace temperature, in which CO and NO, at the levels detected in the effluent stream, were fed through the hot furnace in the absence of a char feed, and the CO_2 formed was measured. An example, corresponding to the data of Fig 17 left, is shown in Fig 17 right. From the known flow rates and char feed times, a lower limit to the CO_2 formed in the char experiments could, thereby, be determined. The results are shown in Table III. Note that these represent only approximate estimates because only exit concentrations of CO and NO were reacted. More accurate assessment of the magnitude of the CO/NO reaction extent would require knowledge of the CO and NO axial profiles, knowledge of the (apparatus dependent) reaction rate, and integration over the furnace hot zone. Since the reaction is surface catalyzed, it may will proceed further during the char feed when a dispersed catalyst is present. In any case, carbon monoxide formation accounts for of the order of 90 percent of the total carbon oxides formed (Table II with corrections from Table III); the small amount of CO_2 observed may be due to secondary surface catalyzed NO/CO reactions which are difficult to eliminate in the experiment.

CONCLUDING COMMENTS

The rate of reduction of NO by char has been determined over the temperature ranges of interest in pulverized coal flames. The NO/char reaction at combustion temperatures is found to be enhanced slightly by the presence of CO and inhibited slightly by water vapor, with both effects decreasing with increasing temperature. The observations are consistent with a hypothesis that the inhibition of the reaction is due to the tying-up of active sites by chemisorbed oxygen and that the enhancement by CO is due to reduction of the chemisorbed oxygen. The data also suggest that the primary product of the NO/char reaction at elevated temperatures is CO, CO_2 being formed by surface-catalyzed secondary reaction with NO.

REFERENCES

1. Pohl, J.H., and A.F. Sarofim. Devolatilization and Oxidation of Coal Nitrogen. 16th Symposium (International) on Combustion, The Combustion Institute, 1976. p.491.

2. Cheng, I. Coal Nitrogen Conversion to NO_x During Simultaneous Oxidation and Pyrolysis. S.M. Thesis, M.I.T., Cambridge, Mass., 1978.

3. Pereira, F.J., J.M. Beer, J.M. Gibbs, and A.B. Headley. NO_x Emission from Fluidized-Bed Coal Combustors. 15th Symposium (International) on Combustion, The Combustion Institute, 1974. p.1149.

4. Chan, L.K. Nitric Oxide Reduction by Char in a Fixed Bed Reactor. Sc.D. Thesis, M.I.T., Cambridge, Mass., 1980.

5. Sprouse, A.M. Reduction of Nitric Oxide by Coal Char in a Fluidized Bed. S.M. Thesis, M.I.T., Cambridge, Mass., 1974.

6. Song, I. Fate of Fuel Nitrogen During Pulverized Coal Combustion. Sc.D. Thesis, M.I.T., Cambridge, Mass., 1974.

7. Altrichter, D.M. Optical Determination of Time Temperature Profiles for Single Particle Coal Combustion, S.M. Thesis, M.I.T., Cambridge, Mass., 1980.

8. Jungten, H., and K.H. Van Heek. Fuel Processing Technology, 2:261-293, 1979.

9. Pereira, F.J., and J.M. Beer. NO Formation from Coal Combustion in a Small Experimental Fluidized Bed. Second European Symposium on Combustion, French Section, Orleans, France, 1975.

10. Howard, J.B., and R.H. Essenhigh. Mechanism of Solid Particle Combustion with Simultaneous Gas-Phase Volatiles Combustion. 11th Symposium (International) on Combustion, The Combustion Institute, 1967. p.399.

11. Wendt, J.O.L., D.W. Pershing, J.W. Lee, and J.W. Glass. Pulverized Coal Combustion: NO_x Formation Mechanisms under Fuel Rich and Stage Combustion Conditions. 17th Symposium (International) on Combustion, The Combustion Institute, 1979. p.77.

12. Shelef, M., and K. Otto. Simultaneous Catalytic Reaction of O_2 and NO with CO and Solid Carbon. Journal of Colloid and Interface Science, 31;73, 1969.

13. Edwards, H.W. Interaction of Nitric Oxide with Graphite. A.I.Ch.E. Symposium Series No.126, 68:91, 1972.

14. Shepard, W.M. A Kinetic Study of the Reaction of Nitric Oxide and Activated Carbon. Ph.D. Thesis, Clemson University, S. Carolina, 1974.

15. Pereira, F.J. NO_x Emissions from Fluidized Coal Combustion. Ph.D. Thesis. University of Sheffield. Sheffield, England. 1975.

16. Furusawa, T., and K. Kunii. Kinetic Study of Nitric Oxide Reduction by Carbonaceous Materials. Society of Chemical Engineering, Japan, 1977.

17. Beer, J.M., A.F. Sarofim, L.K. Chan, and A.M. Sprouse. NO Reduction by Char in Fluidized Combustion. Fifth International Conference of Fluidized Bed Combustion, Washington, D.C., 1977.

18. DeSoete, G.G.. Mechanism of Nitric Oxide Reduction of Solid Particles. Fifth EPA Fundamental Combustion Research Workshop, Newport Beach, Cal., 1980.

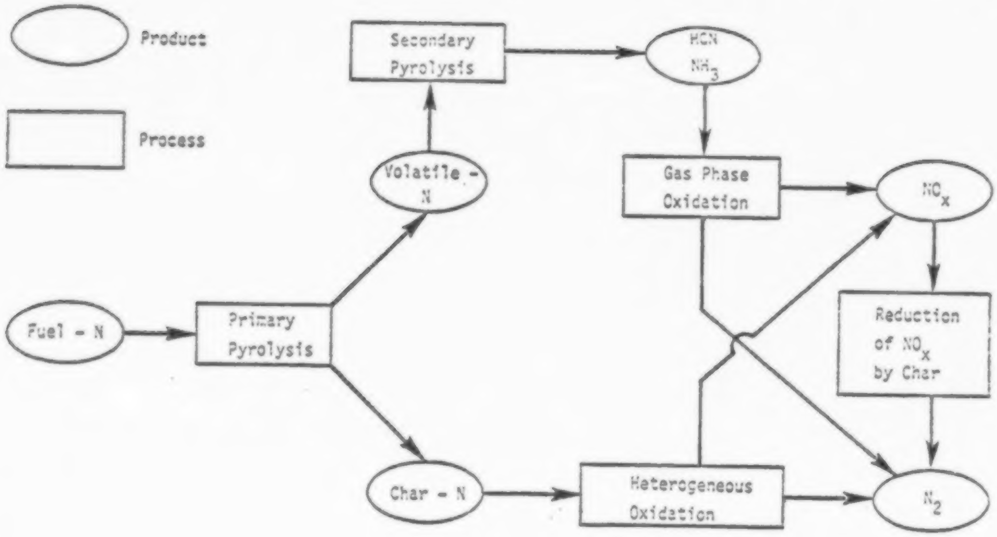

Fig 1. Schematic of Process Occuring During the Formation of Nitric Oxide from Coal Nitrogen. An Oxidative Pyrolysis Route is not Shown

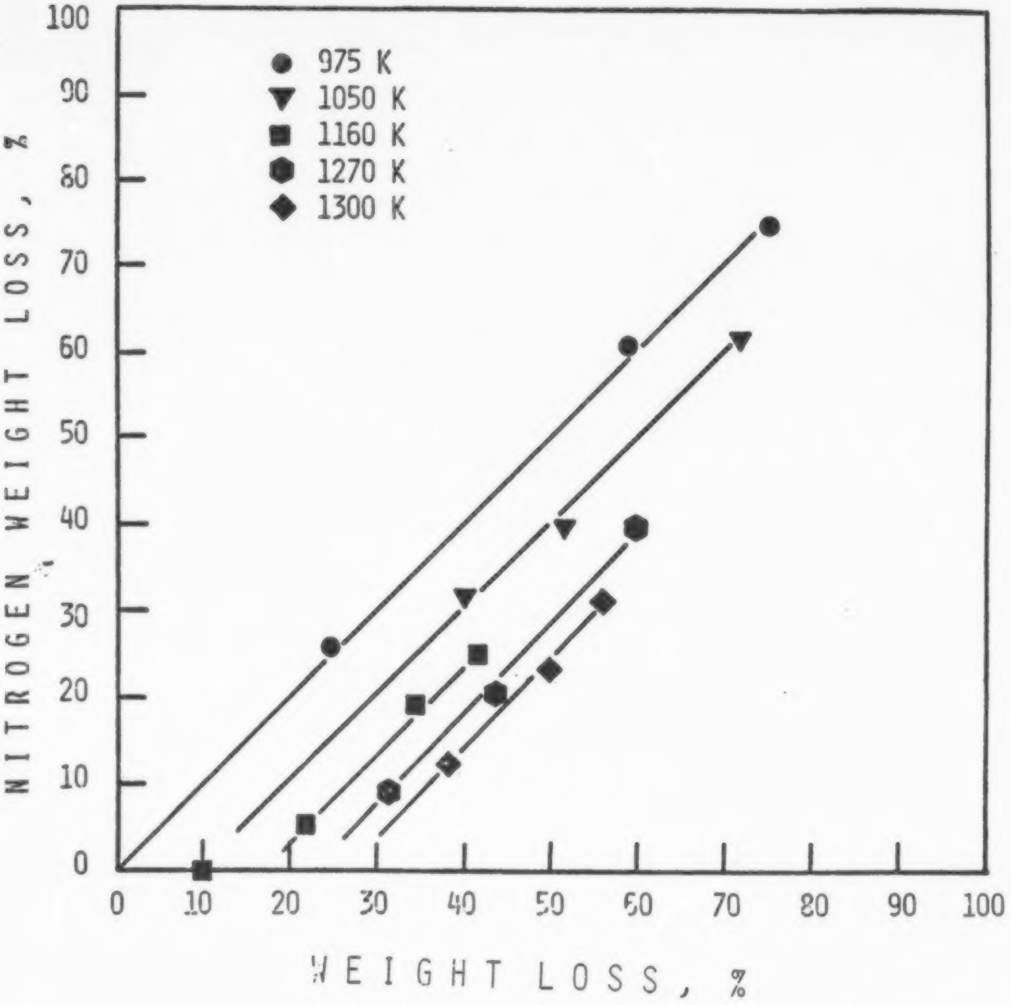

Fig 2. Nitrogen Evolution from 150μm Droplet Array of Raw Paraho Shale Oil

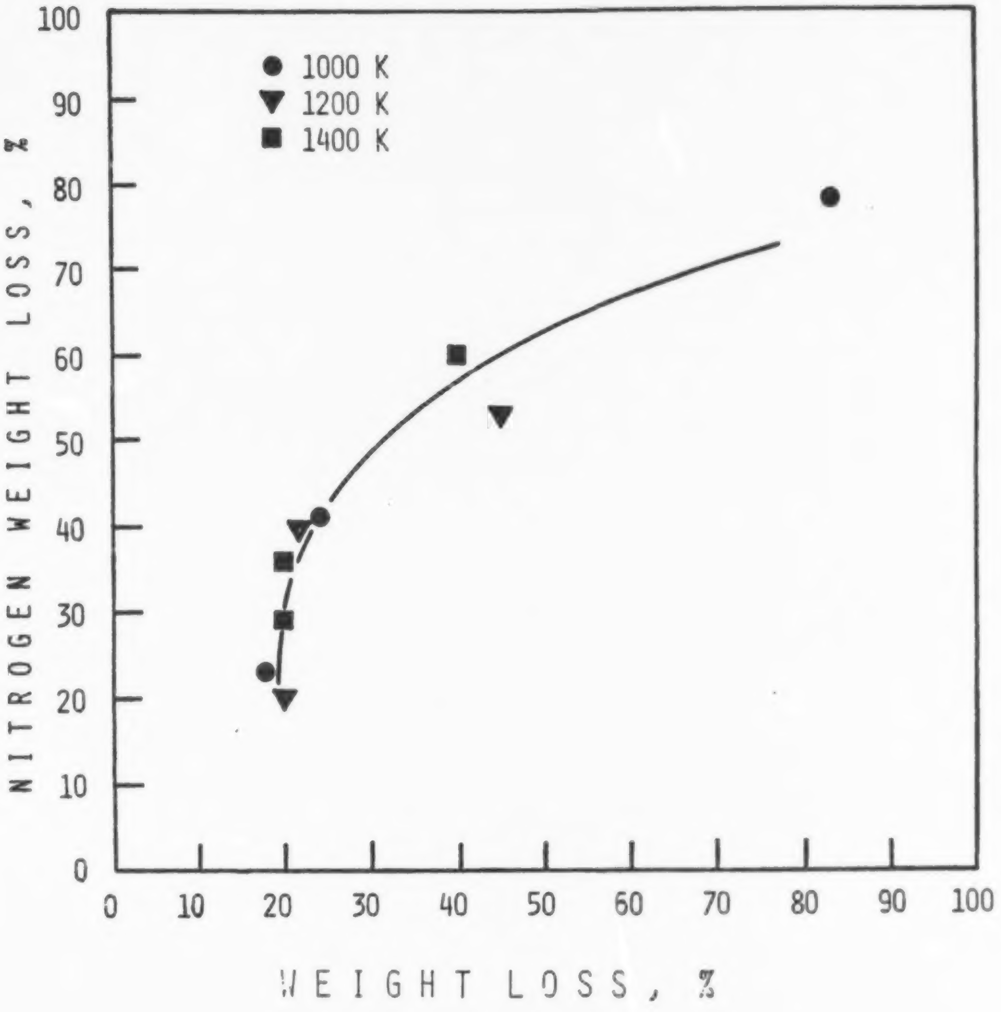

Fig 3. Nitrogen Evolution from 150 um Droplet Array of Indo-Malay #6 Oil

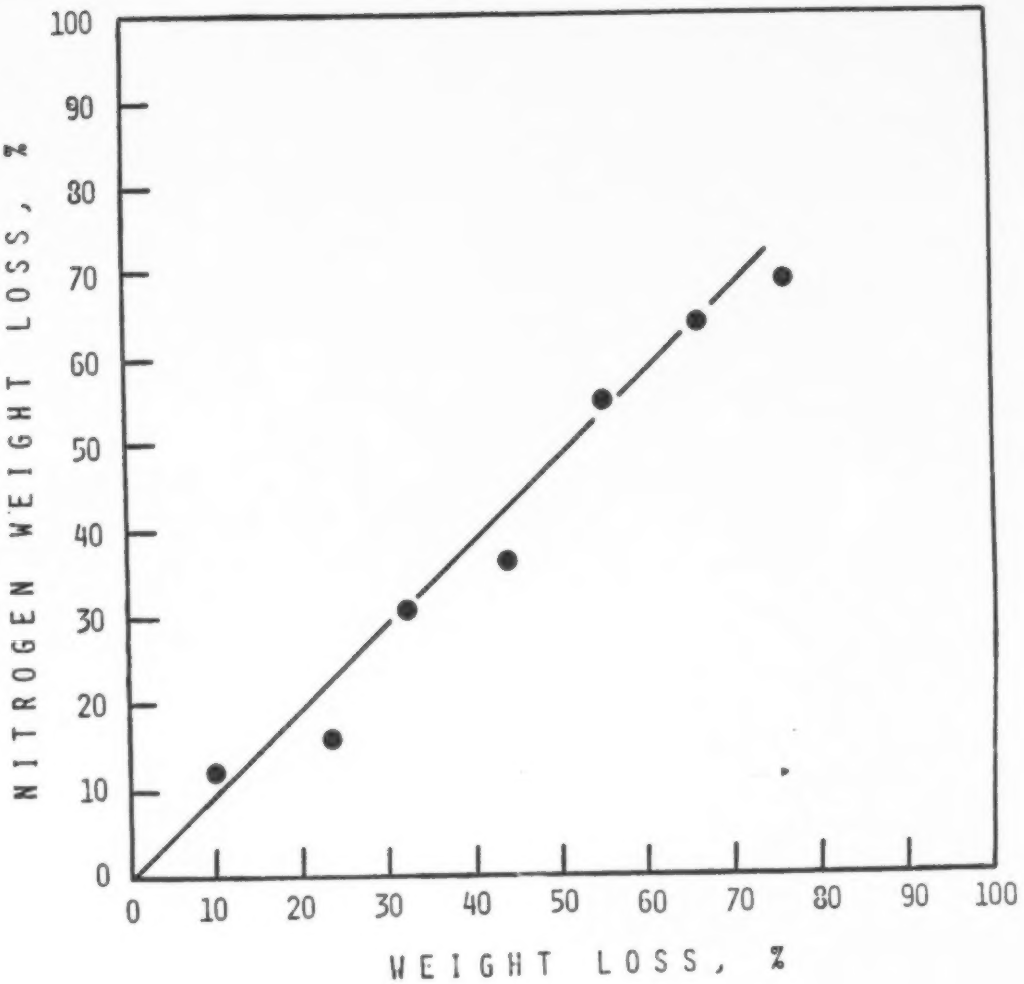

Fig 4. Nitrogen Evolution from the Equilibrium Distillation of Raw Paraho Shale Oil at Atmospheric Pressure

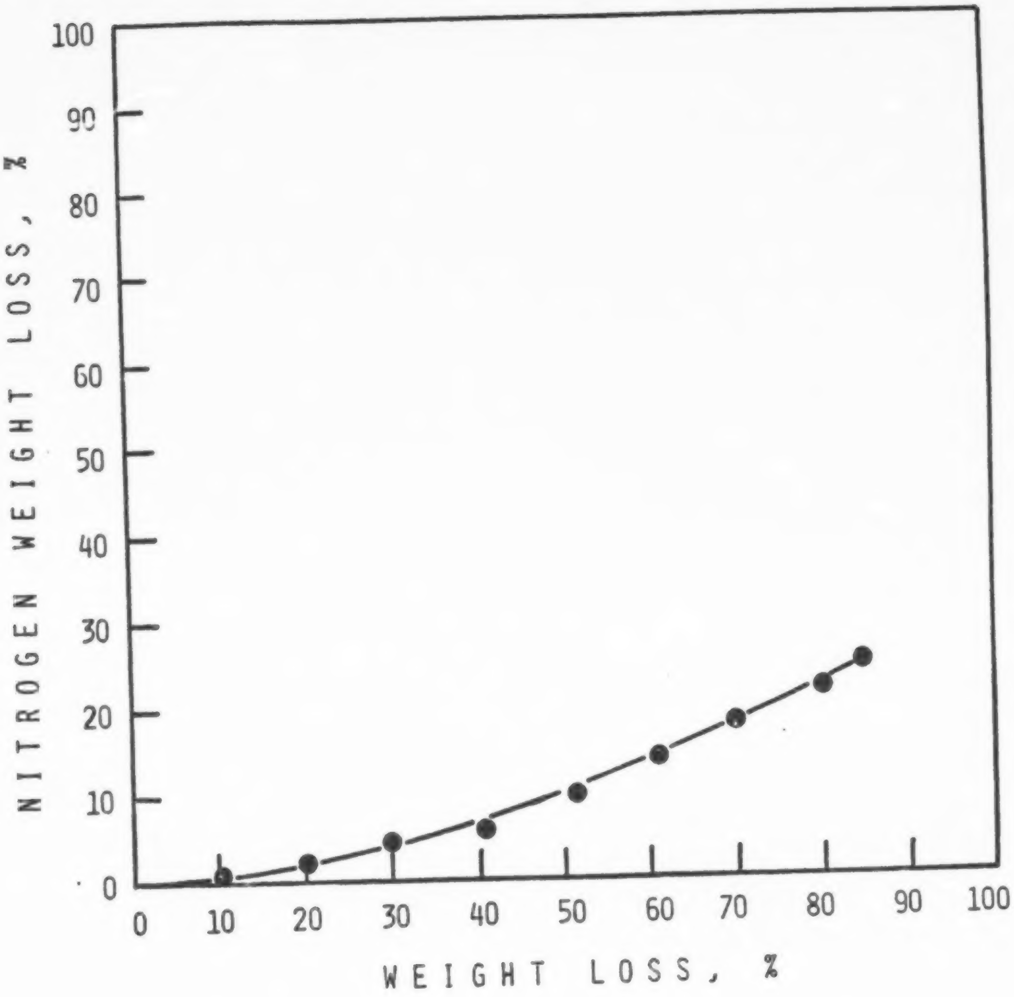

Fig 5. Nitrogen Evolution from the Equilibrium Distillation of Indo-Malay #6 Oil at Atmospheric Pressure

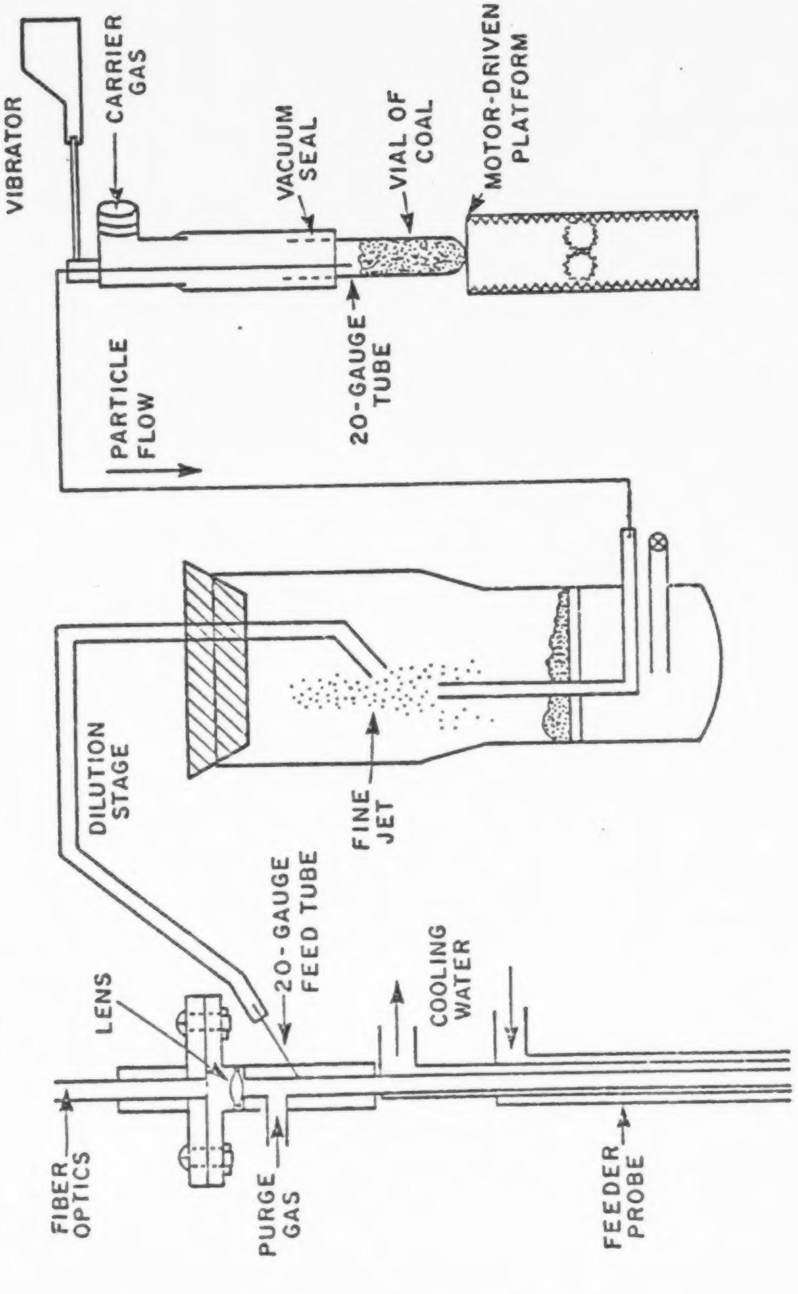

Fig 6. Two Stage Single Particle Feed System

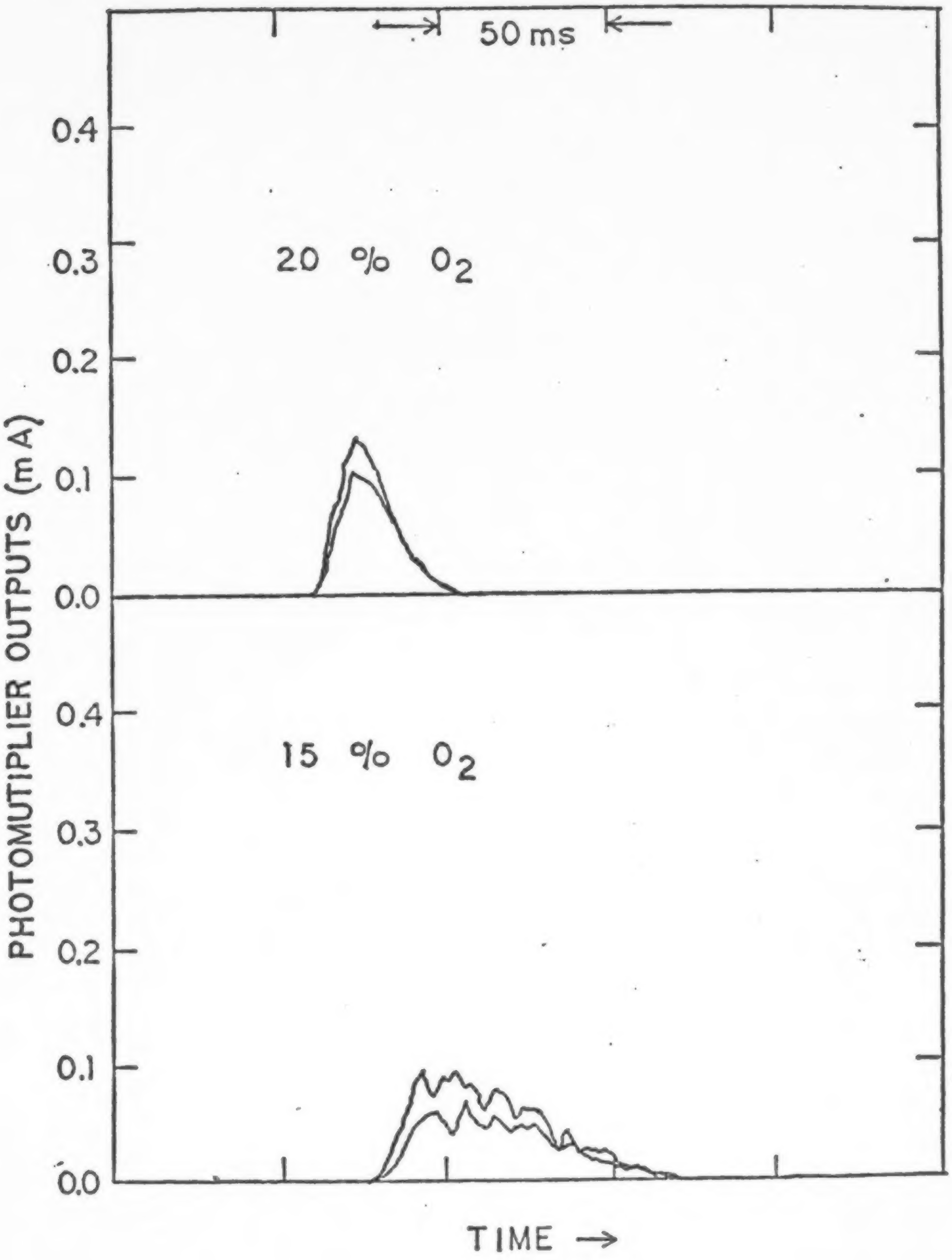

Fig 7. PMT Outputs for Montana Lignite in 15% and 20% Oxygen

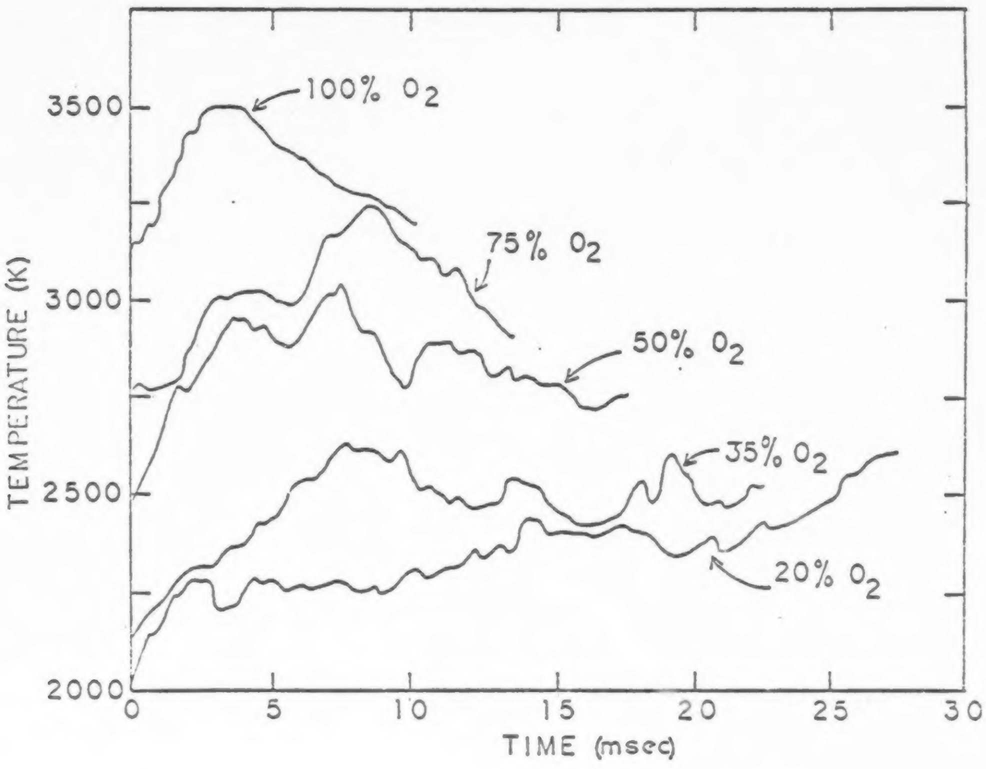

Fig 8. Typical Temperature Traces for Illinois #6 at Five Oxidizing Conditions

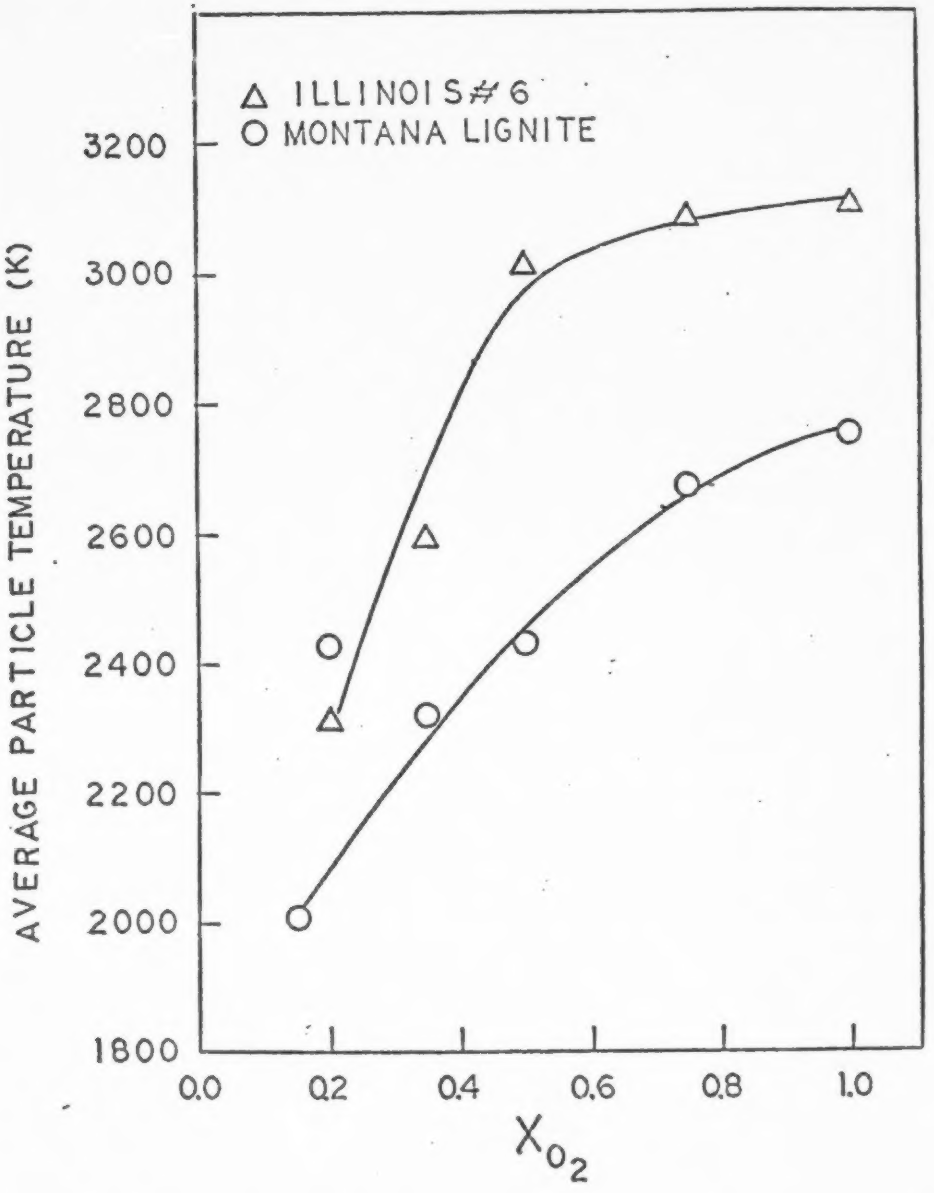

Fig 9. Average Particle Temperature Traces for Montana Lignite and Illinois #6 at 1700 K

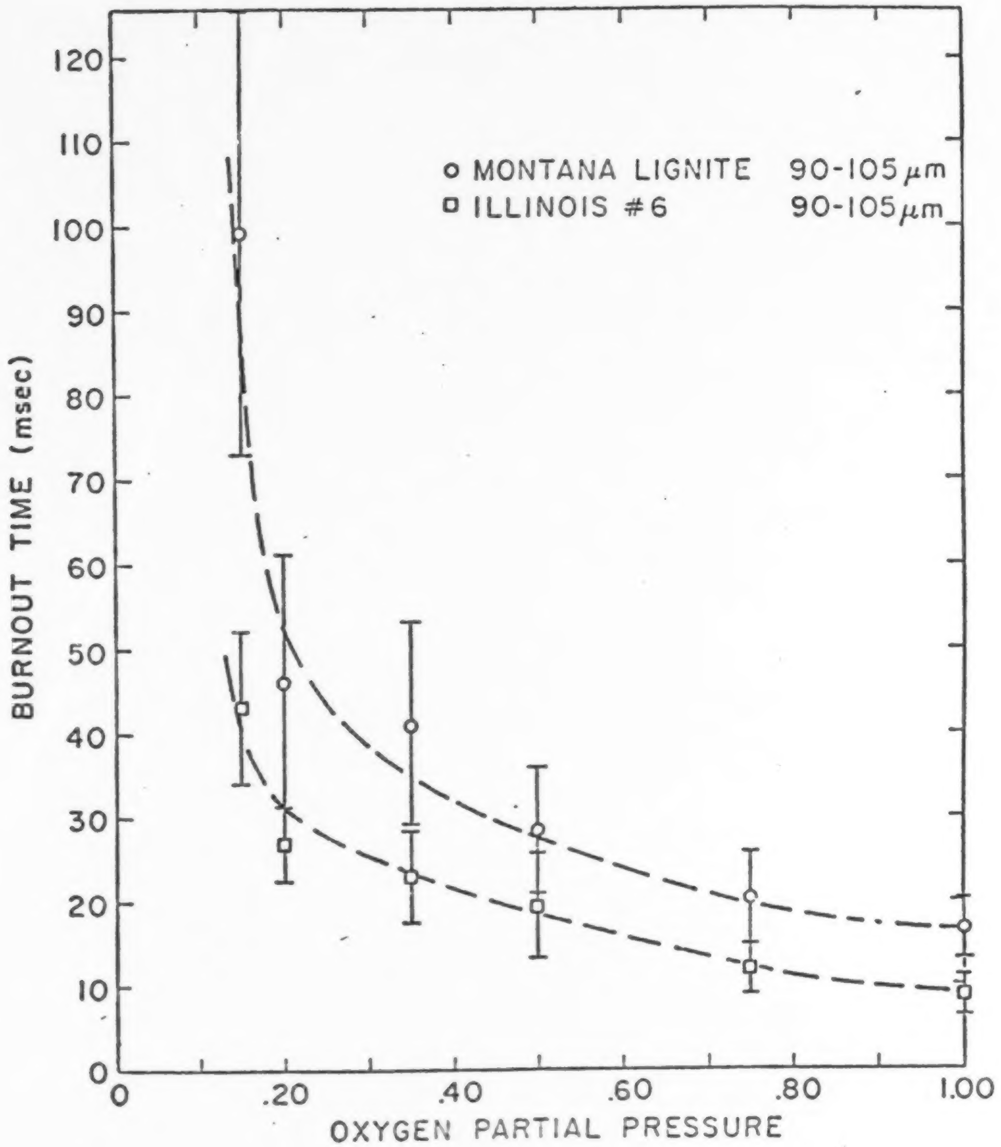

Fig 10. Average Burning Times for Montana Lignite and Illinois #6 at 1700 K

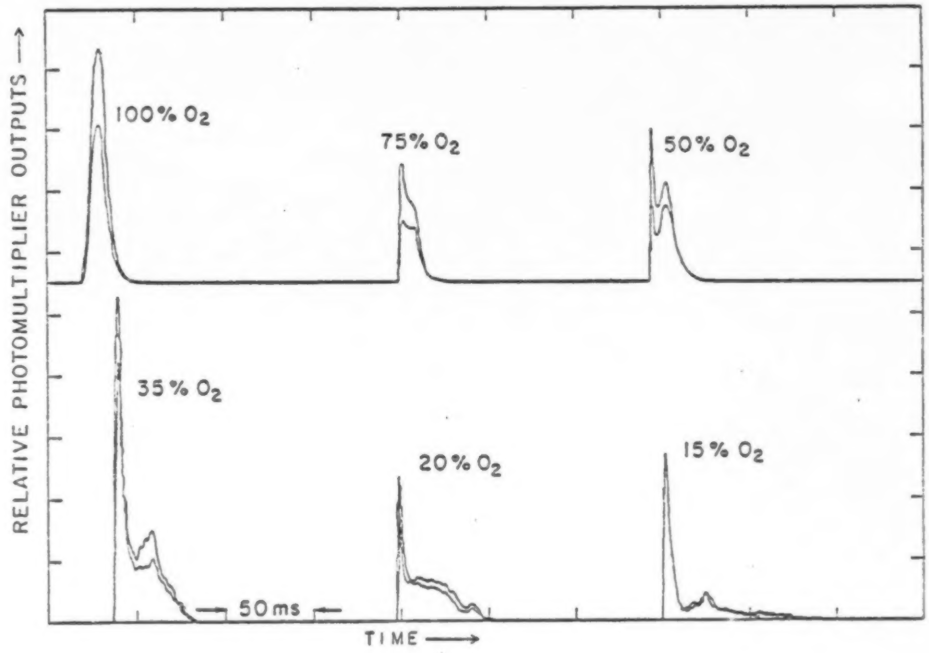

Fig 11. PMT Outputs for Illinois #6 at Six Oxidizing Conditions

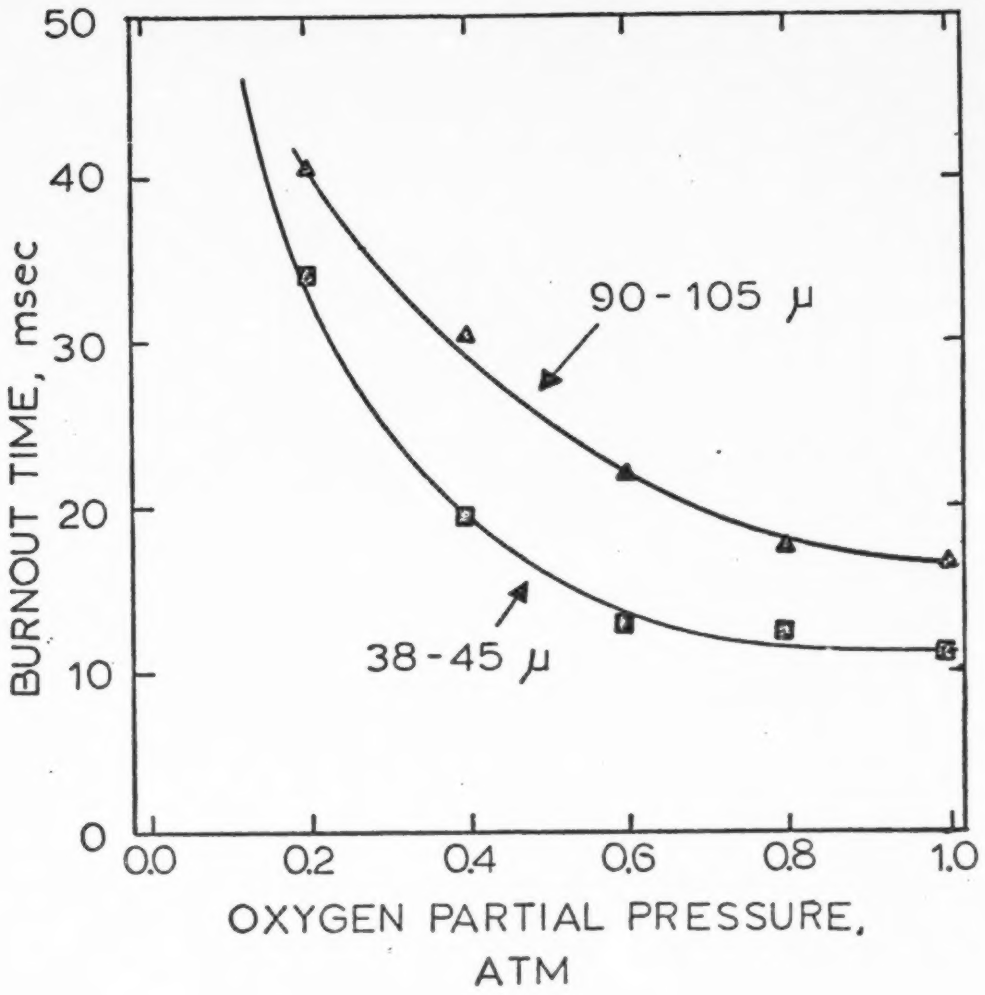

Fig 12. The Effect of Oxygen Partial Pressure and Particle size on the Burning Times of a North Dakota Beulah Coal. Furnace Temperature 1250° K

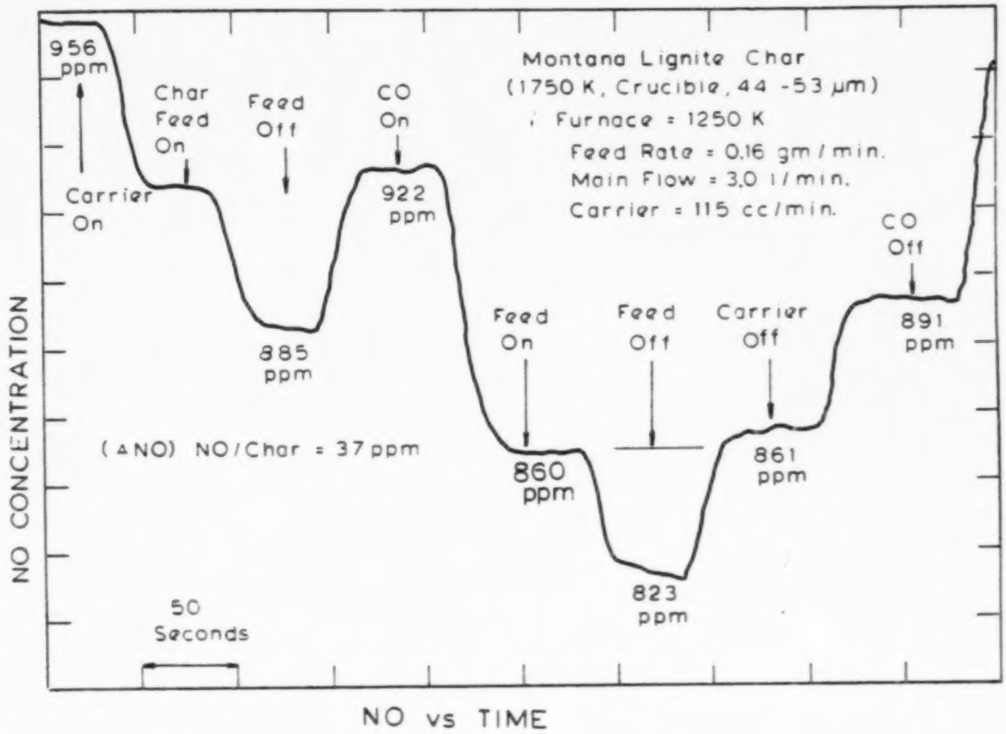

Fig 13. NO Reduction by Reaction with Char and Enhancement of the Effect by Added CO at 1250 K in the Laminar Flow Furnace

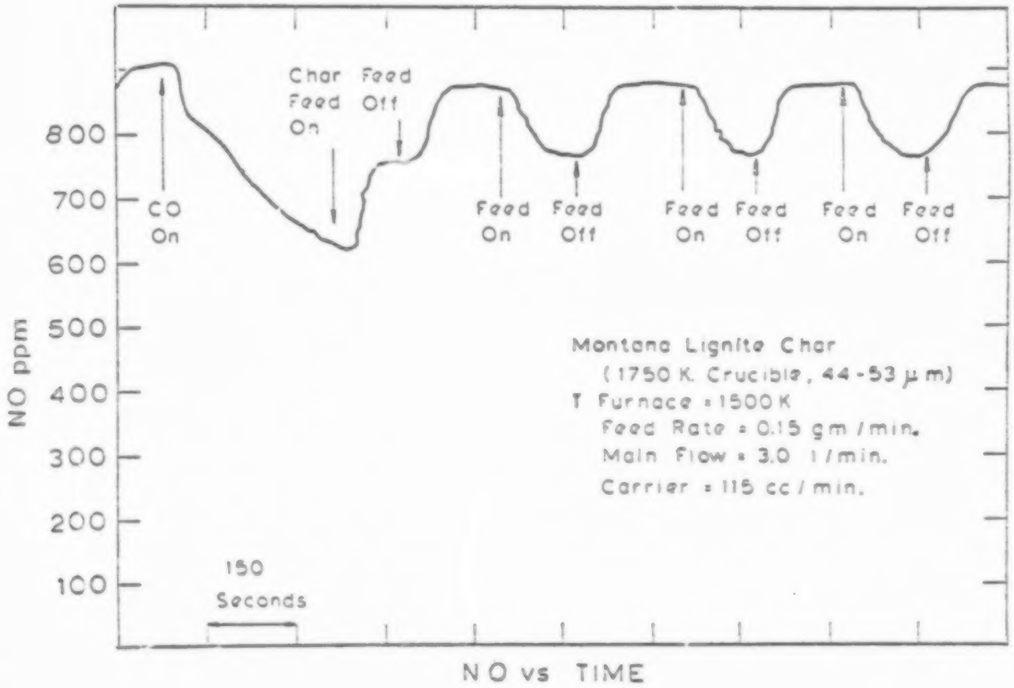

Fig 14. Poisoning of the Surface Catalysis of the NO/CO Reaction at 1500 K in the Laminar Flow Furnace

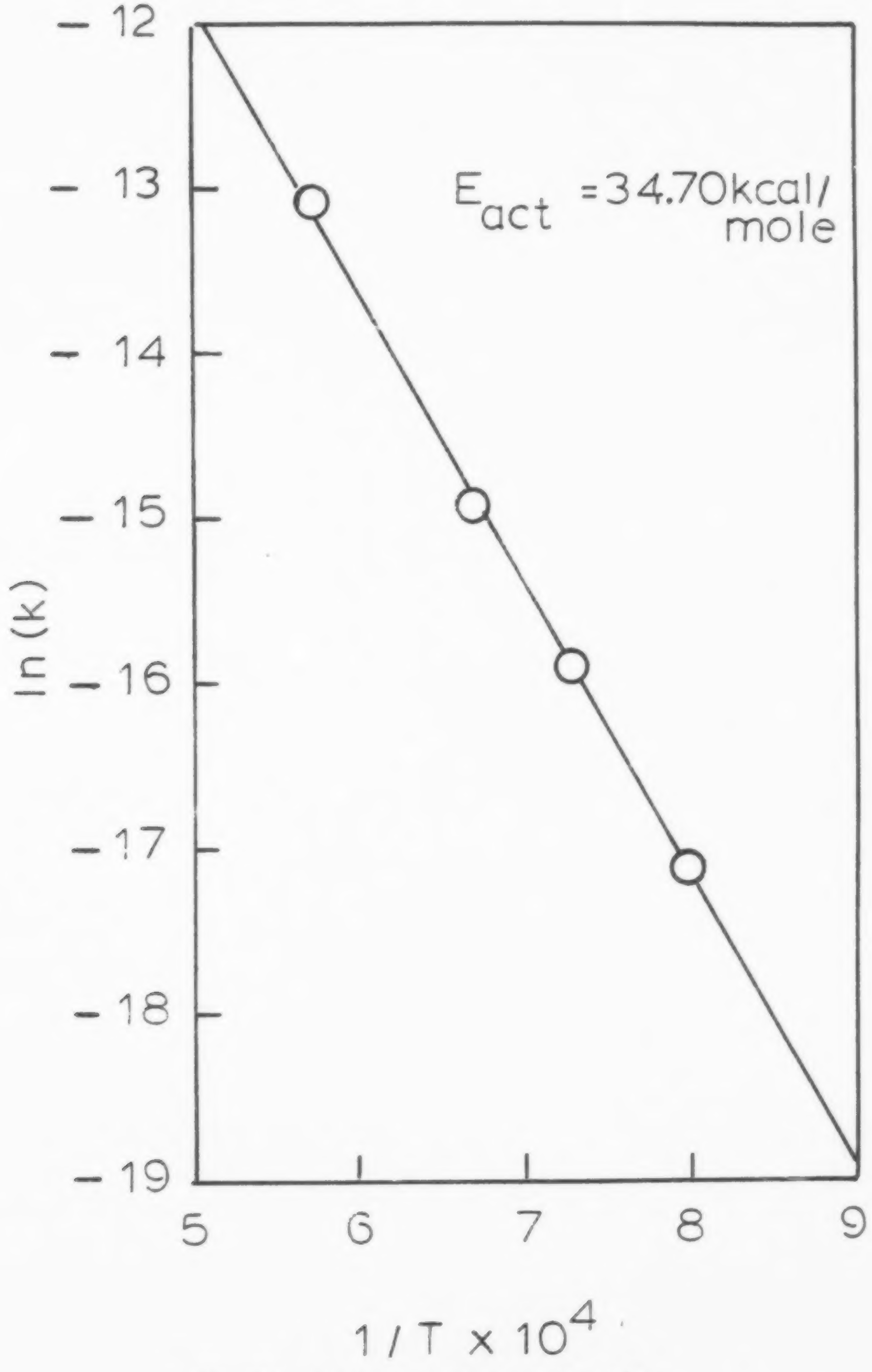

Fig 15. Arrhenius Plot of the NO/ Char Reaction Rate Constant

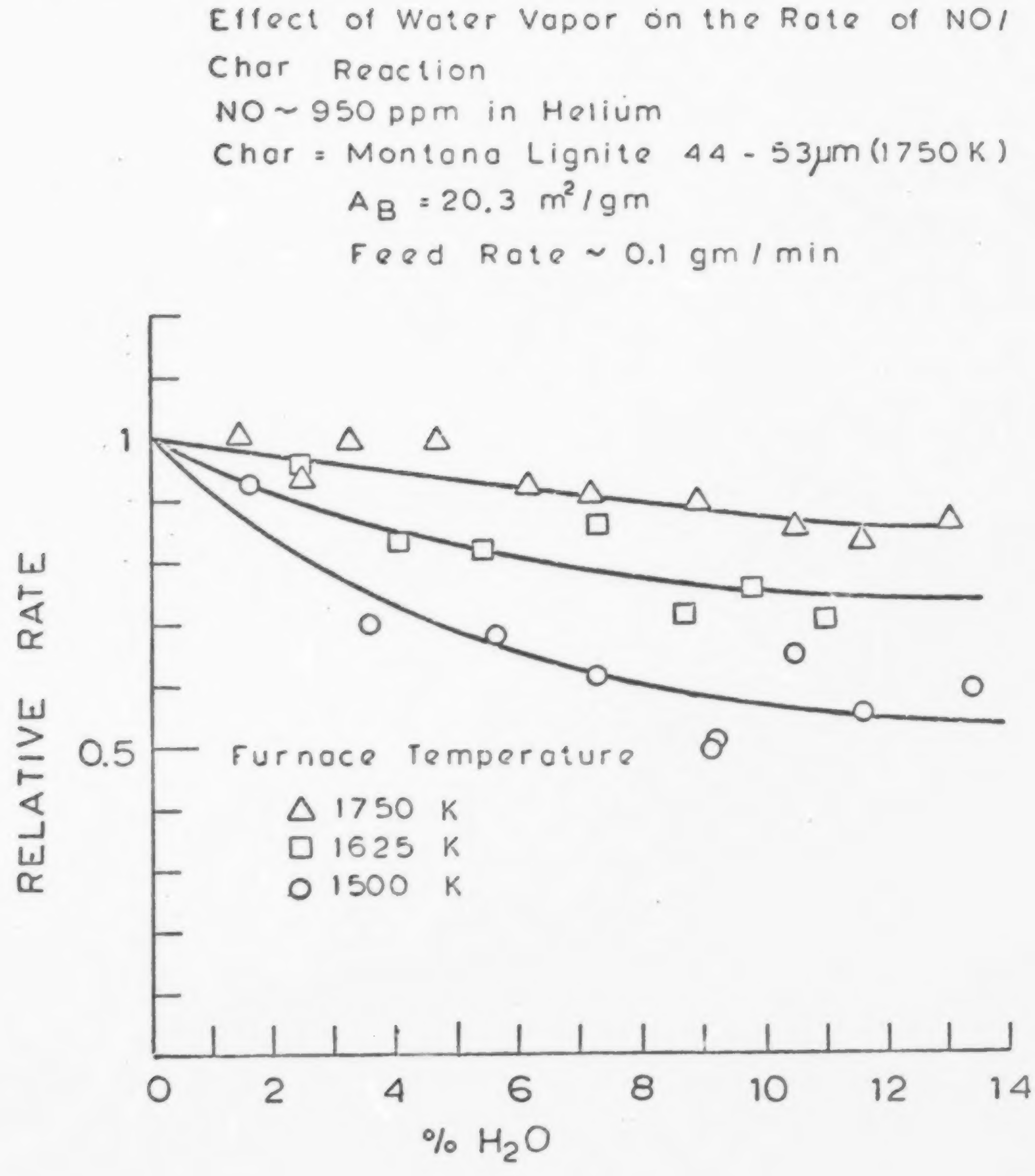

Fig 16. Inhibition of the NO/ Char Reaction Rate in the Presence of Water Vapor

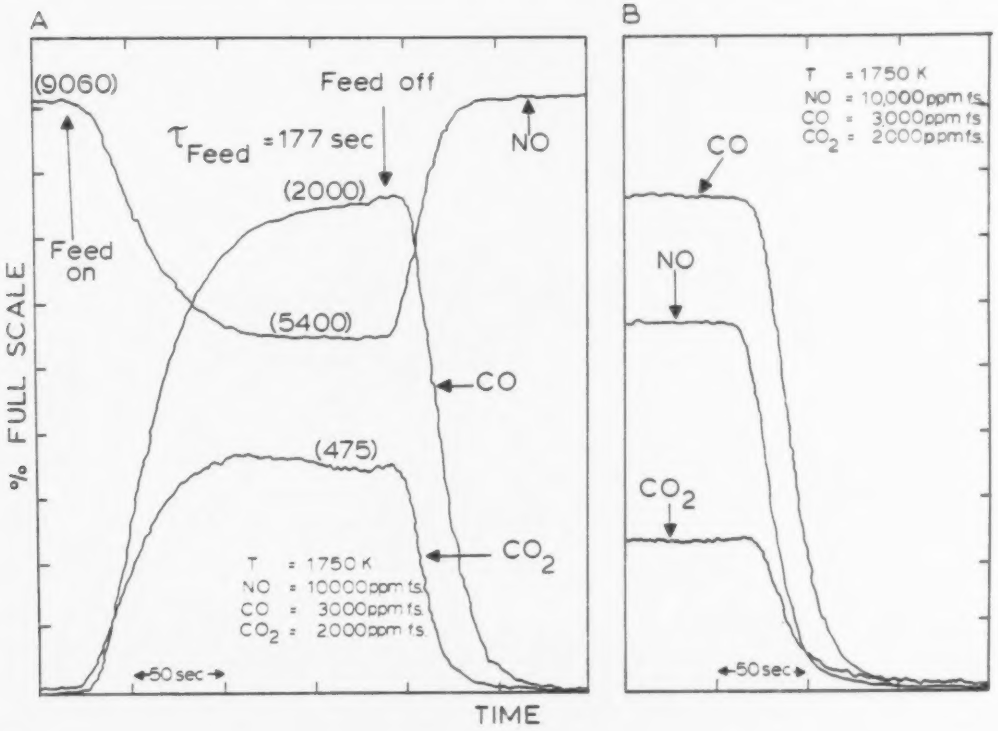

Fig 17. (a) CO and CO_2 Product Distribution from the NO/Char Reaction at 1750 K. Montana Lignite Char (Produced in a Crucible at 1750 K). 44-52 μm Feed

(b) CO_2 Formation by the Surface Catalyzed Reaction of NO with CO at 1750 K.

Rate = 0.10 gm/minute. Total Flow Rate = 3.13 l/min.

TABLE I. ENHANCEMENT OF NO/CHAR REACTION RATE BY ADDED CO (1.4%).

T Furnace	k_{CO}/k	
1300 K	1.28 1.27	1.28
1600 K	1.28 1.09 1.05	1.14

TABLE II. OXYGEN MATERIAL BALANCES IN THE NO/CHAR REACTION.

Run	Furnace Temp.	Oxygen Balance*		CO/CO_2**
D-211 A	1500 K	72.5%	67.0%	0.78
D-208 A	1500 K	64.1%		0.78
D-205 A	1500 K	64.3%		0.78
D-178 A	1625 K	77.2%	75.5%	2.53
D-175 A	1625 K	76.1%		2.62
D-172 A	1625 K	73.1%		2.64
D-193 A	1750 K	78.2%	77.3%	4.27
D-190 A	1750 K	77.3%		3.80
D-187 A	1750 K	76.5%		3.90

Notes:

* Oxygen balance is computed as $$\frac{CO + 2(CO_2) - (CO)_{BASELINE}}{(NO)_{inlet} - (NO)_{observed}}$$

** CO to CO_2 ratio is corrected by substraction of baseline CO from measured CO.

TABLE III. CO_2 FORMED BY REACTION OF NO WITH CO.

Run	Furnace Temp.	% CO_2 Accounted for by CO/NO Reaction	
D-211 A	1500 K	73.7%	77.3%
D-208 A	1500 K	79.2%	
D-205 A	1500 K	78.9%	
D-178 A	1625 K	55.6%	60.4%
D-175 A	1625 K	61.3%	
D-172 A	1625 K	67.4%	
D-193 A	1750 K	74.8%	73.3%
D-190 A	1750 K	73.8%	
D-187 A	1750 K	71.4%	

GAS PHASE PROCESSES INVOLVED IN THE CONTROL OF NITROGEN OXIDE FORMATION IN FOSSIL FUEL FLAMES

By:

J. M. Levy
M.I.T. Energy Laboratory
Cambridge, Massachusetts 02139

ABSTRACT

Optimization of a control strategy for NO_x emissions from fossil fuel combustion requires an understanding of the mechanistic chemistry of fuel-nitrogen conversion. Computational capabilities are demonstrated to be quite accurate in the presence of simple fuels. but break down somewhat in the presence of hydrocarbons. A quasi-global method for computing fuel-nitrogen conversion in a higher hydrocarbon environment is described, and the current status of modeling bound nitrogen profiles in a C_1/C_2 environment is presented.

A. Introduction

With the depletion of natural gas and petroleum reserves (which are lacking or low in nitrogen content - and, hence, relatively low in the emission of NO_x formed from the nitrogen bound in the fuel), and the increasing substitution of coal, coal-derived liquids, residual fuel-oils, and shale oils (which are high in nitrogen content), NO_x emissions, which are already unacceptably high in several urban areas, are bound to increase unless an abatement strategy is developed and implemented. Insofar as the mechanism by which fuel-bound nitrogen is converted to NO_x is complex, and insofar as early attempts (1,2) to reduce NO_x emissions by empirical adjustment of combustion parameters (e.g., temperature, fuel/air ratio, degree of mixedness, etc.) utilizing conventional combustors have achieved only a fraction of their full potential, a more fundamental elucidation of the NO_x formation mechanism has become essential in order to achieve the desired engineering goal of modifying the combustion process in such a way as to favor the conversion of fuel-bound nitrogen to the desired (combustion) end product, N_2, rather than to the undesired product, NO.

It is well understood that for any condensed phase fuel, combustion may proceed through parallel homogeneous and heterogeneous processes wherein the fuel is initially heated and undergoes devolatilization followed by rapid homogeneous gas phase oxidation of the volatile species and, if a devolatilized residue remains, slower heterogeneous burnout of the char. This is apparently the case for the combustion of pulverized coal and residual fuel oils. Distillate oils, however, may well burn entirely in the gas phase as a diffusion flame surrounding a shrinking, evaporating droplet. Certain fuels, of course, are gaseous from the outset.

Of primary interest here is the chemistry of volatile fuel-nitrogen conversion. Traditional gaseous fuels (natural gas) contain little or no bound nitrogen - although it is projected that the products of coal gasification which undergo a high temperature desulfurization may well contain significant quantities of ammonia. In addition, light distillate oils which for coal and shale-derived fuels may have nitrogen contents in excess of 1% by weight burn entirely in the volatile phase.

For fuels which leave a devolatilized residue, the relative significance of gas phase (versus heterogeneous) processes on NO_x formation is less obvious. The distribution of nitrogeneous species between volatiles and char has recently been studied (3,4,5,6,7) for pulverized coal combustion for temperatures ranging from 1250 to 1750° K. The results (for a Montana Lignite) demonstrate that at higher temperatures under fuel lean conditions, as much as 80% of the NO_x formed may originate in the volatile phase. This reflects the fact that at high enough temperatures, nearly all of the nitrogen in coal can be driven into the gas phase (3). Indeed, even under conditions (1750° K) where 70% or more of the fuel nitrogen is volatilized during the course of the experiments (5), for equivalence ratios above about 1.5, over 50% of the NO_x originates from the char! These results reflect the long established facts that increases in fuel nitrogen concentration (8) and equivalence ratio (8,9,10) in the gas phase all tend to lower the conversion efficiency to NO_x. The strategy for controlling NO_x emission, therefore, is to drive as much fuel nitrogen as possible into the gas phase in a primary fuel rich zone (7,8,9,10,11) where the reaction kinetics can be "engineered" to minimize conversion to NO_x, as opposed to the alternative of allowing the nitrogen to remain in the char where subsequently it will be partially converted to NO_x in the fuel lean secondary combustion zone (12). Clearly, optimizing this reaction engineering (minimizing NO_x emissions) is best achieved through a true understanding of the gas phase reaction mechanism. Insofar as the residence times in typical combustors are too short to achieve chemical equilibrium in the burnt gases, it is necessary to consider the time dependent flow of nitrogeneous species through the many sequential and competing reaction pathways leading to NO_x and N_2 formation, in order to develop a methodology for maximizing or minimizing certain product yields - i.e., both the elementary reaction pathways and reaction rates must be considered.

Unfortunately, trace emissions from rich stationary source combustors are the product of several, lumped chemical/physical processes, and even if the problems of coupling finite-rate chemistry with complex flow-fields are neglected for the moment, the necessity of computing NO_x levels to within the ppm range places rather stringent requirements on the mechanistic accuracy of whatever model is invoked.

Despite residual uncertainties in the currently available mechanistic and kinetic data base, adequate if imperfect, modeling of fuel-nitrogen conversion in the presence of "simple" fuels can now be achieved (11,13,14). Unfortunately, however, real combustion systems, i.e. real fossil fuels, present incremental mechanistic complexities which do not decouple easily from solution of the fuel-nitrogen problem. It is to an assessment of these complexities and to the development of a methodology for dealing with them that this paper is addressed.

B. The Fuel-Nitrogen Mechanism

A large literature has appeared recently directed towards the experimental elucidation of the mechanistic details of fuel-nitrogen conversion under flame conditions (8,15). Synthesis of these observations into a master reaction set has been the subject of other studies reported elsewhere (16,17,18). Validation and refinement of the reaction set, based upon efforts to model independent data under as broad a range of conditions as possible, is an ongoing effort (11,13).

Initial attempts (18) by this author to construct a comprehensive fuel nitrogen mechanism utilized the method of Engleman (19) in which all species expected to be present are permitted to inter-react via elementary reactions. Rate constants were selected from tabulated estimates (made, generally, by the method of Johnston (20)). The method, however, suffers from the limitation of often necessitating the use of an impractically large reaction set (especially when combined with hydrocarbon mechanisms. See below.), and, additionally, is limited in its accuracy by the capability to select, a priori, all species, including intermediates, which are present. Recent suggestions by Branch et al. (21) of mechanistic refinements to the NO/NH_3 reaction set underline this limitation. Current efforts have, therefore, tended back towards the use of a much smaller, conceptually clearer, fuel nitrogen reaction set.

To this end, equal success has been achieved in modeling the post-flame zones of several nitrogen-doped hydrocarbon flames using the "minimum subset" of fuel nitrogen reactions shown in Table I, as with the larger master set. It is cautioned, however, that the full range of applicability of this minimum subset is not yet established. Thus, for example, though significant contribution to the destruction of NO by reaction with NH_2 is precluded in modeling post-flame data in the range of 2000 K, recent indications (22) of the very strong inverse temperature coefficient of the effective $NO + NH_2$ rate constant suggest that that mechanistic addition may still prove appropriate at lower temperatures.

An example of the modeling success achievable is indicated in Figure 1, showing the data of Haynes (23) in the post-flame gases of a rich ($\phi = 1.52$), atmospheric pressure, ethylene/oxygen/nitrogen flame doped with 700 ppm of ammonia. In view of Haynes' rather flat temperature profile (22 degree variation over 9.6 msec) and the arbitrariness of any assumed rate of heat loss, modeling was performed isothermally at an average temperature of 2010 K. Calculations were in plug-flow, initialized assuming partial equilibration of the radical pool, and were performed on an IBM 360/65 using a computer code written at MIT for the integration of the stiff rate equations. Essential to the discussion to follow is the observation that no hydrocarbon species were observed in the post-flame zone of this flame.

Contrasting with the results of Figure 1 are those shown in Figure 2 for Haynes' richer ethylene/air flame ($\phi = 1.66$) doped with 500 ppm NO. The major distinction in this flame is the "breakthrough" of hydrocarbons (roughly 0.2% of the total flow) into the post-flame zone. The results of Figure 2 were generated by ignoring the hydrocarbons. Although the fits to the concentration profiles are not really bad, better success in fitting the HCN and NO profiles has been achieved (see below) through consideration of the pertinent hydrocarbon chemistry. (Ammonia profiles remain systematically in error). It should be clearly noted, also, that the influence of hydrocarbons upon fuel-nitrogen chemistry is potentially much greater in the highly backmixed environment of a practical combustor than may be suggested by Figure 2. This is demonstrated by a series of computations performed (using a detailed hydrocarbon mechanism) on a methane/air system doped with 1% ammonia. In these calculations, a well-stirred reactor (WSR) section of varying residence time fed a plug-flow reactor (PFR) section, also of varying residence time, such that the total residence time remained approximately constant. Bound nitrogen concentrations are shown in Fig. 3 for an adiabatic calculation at a fuel/air equivalence ratio of 1.33, and demonstrate nicely that for a fixed total reaction time, HCN exit concentrations (the major product of fuel-nitrogen/hydrocarbon interactions) are increased with increased stirred reactor residence time. This conclusion follows logically, of course, from the recognition that strong backmixing necessarily increases the possibility for reaction between hydrocarbon and nitrogeneous fragments.

C. The Hydrocarbon Problem

The results of Figure 2 serve in miniature to demonstrate that additional mechanistic complexities arise in the computation of fuel-nitrogen chemistry when hydrocarbons are present. Indeed, predictive modeling of bound-nitrogen emissions in a real-fuel, fuel-rich environment can be seen to be dependent upon the capability to model hydrocarbon decay kinetics for the following reasons:

(1) Interactions of fuel-nitrogen and hydrocarbon fragments may be quite significant, especially in recycling NO back to HCN. Omission of this class of reactions is consistent with the enhanced NO profile and diminished HCN profile calculated in Figure 2. Also,

(2) the radical pool (H,O,OH) which drives the fuel-nitrogen chemistry is determined primarily by the hydrocarbon chemistry which dominates the system at early times.

Insofar as fuel-rich operation contributes to NO_x abatement strategies, it seems necessary to model hydrocarbon burnout if ppm-level accuracy is to be demanded of a fuel-nitrogen mechanism. Unfortunately, however, aside from having only the most phenomenological knowledge of the specifics of the interactive reactions between hydrocarbons and nitrogenous species, even modeling the combustion of methane - the simplest of hydrocarbons - currently comes close to straining the state-of-the-art. In addition, the validity of generalizing conclusions applicable to design considerations of real fuel systems based upon computations using methane as a model hydrocarbon fuel is still not, *a priori*, clear. Indeed, methane is an atypical fuel in that

(1) its H/C ratio of 4 greatly exceeds the H/C ratios of fuels of interest (H/C might equal 1.3, for example, for a coal-derived liquid),

(2) its combustion details might simulate paraffin-type species, but many fuels of practical nature are highly aromatic in character, and

(3) even as a paraffin, methane may be atypical in that methyl recombinations may be of unusual significance in its combustion mechanism.

Two questions of significance have, therefore, been identified.

(1) To what extent can the results of NO_x modeling in the presence of methane be taken as representative of fuels of practical interest? And, in order to answer that question,

(2) how can the combustion kinetics of higher hydrocarbons, more representative of fuels of practical interest, be modeled for the purpose of predicting fuel-nitrogen conversion to NO_x?

D. Methodology for Dealing with Higher Hydrocarbons

1. Detailed Kinetics

In this method, all species of significance and all essential elementary reactions of each specie are identified, resulting in an extensive set of coupled rate equations which describe the kinetic behavior of the system. This, of course, is the most correct way to characterize the system. The method suffers, however, from the limitations that:

(a) For higher hydrocarbons, even straight chain paraffins, neither a complete set of species nor, certainly, of reactions is known - i.e., with few exceptions, the detailed combustion mechanisms are simply not available.

(b) Theoretical synthesis of combustion mechanisms for higher hydrocarbons (as performed for CH_4, for example, by the method of Engleman (19,24) is impractical because the magnitude of the problem grows exponentially (25) with the number of carbon atoms, resulting in reaction sets impractically large for computational studies, and because, in any event, virtually none of the elementary reaction rate constants are known. Additionally,

(c) Even if such an approach were viable, the time and cost necessary to screen such reaction sets down to reasonable sizes, as well as the current dearth of experimental data necessary for model validation would render the method impractical.

Detailed kinetics are therefore rejected as a viable method of modeling the combustion chemistry of fuels of practical interest.

2. The Global and Semi-Global Methods

In this method, hydrocarbon burnout is modeled by a single "global" (or overall) relation of the form

$$CnHm + (n + \frac{m}{4})\ O_2 \rightarrow nCO_2 + \frac{m}{2}\ H_2O$$

for which a rate expression must be empirically determined. Even as a first estimate, this method really has little basis in theory, and has been shown to be applicable only where a single major heat release step is involved, thereby excluding its applicability to hydrocarbon oxidation. In any event, the method completely overlooks elementary reaction kinetics and intermediate radical formation and is of no utility in computing NO_x levels.

Hydrocarbon oxidation can be conceived of occuring, however, in two overlapping heat release steps: a rapid oxidation of the hydrocarbon to carbon monoxide and hydrogen (or water), followed by subsequent oxidation of the CO (and H_2). It is possible, therefore, to develop a semi-global method utilizing two (or more) sequential global steps and one(or more) stable intermediate species to describe the overall combustion process. Thus, for example

$$C_nH_m + (\frac{n}{2} + \frac{m}{4})\ O_2 \rightarrow nCO + (m/2)H_2O$$

followed by

$$CO + 1/2\ O_2 \rightarrow CO_2$$

This method has been used with some success (26) for the relatively simple case of methane oxidation, but again, in any case, suffers from the limitation of completely neglecting intermediate, radical species essential to prediction of trace NO formation levels.

A conceptually similar, but somewhat more detailed semi-global method has been under development by Dryer (27) for application to hydrocarbon burnout. In this method, paraffin oxidation has been separable into three global steps of the form

$$\text{Alkane} \rightarrow \text{Alkene} \rightarrow CO \rightarrow CO_2$$

Although this may be regarded as a significant improvement over two-step semi-global modeling for purposes of modeling heat release, it offers little practical improvement for purposes of modeling NO levels. Additionally, empirical rate expressions characterizing each global step are currently available only for paraffins up to butane. No rates are yet available for aromatic systems.

3. The Quasi-Global Method

In this method, the simple global step

$$C_nH_m + \frac{n}{2} O_2 \rightarrow nCO + \frac{m}{2} H_2$$

is followed by an elementary reaction mechanism (which is well known) for the $H_2/CO/O_2$ system. Because the time scale for CO burnout is long compared with the global conversion of the parent hydrocarbon to CO, a certain amount of modeling success may be achieved by assuming the global step to occur at an infinite rate - especially if attention is focussed primarily upon post-flame reactions - although, following the work of Edelman and Fortune (28), a finite rate expression for the global step may also be used to enhance modeling accuracy. Utilization of detailed kinetics for the CO/H_2 oxidation admits free radical chemistry to the mechanism, thus opening the door to computations coupling the detailed kinetics of fuel-nitrogen conversion with hydrocarbon burnout.

Several serious limitations to this method, however, must be noted:

(a) Although a degree of "elementary" reaction chemistry is preserved in modeling the CO/H_2 oxidation step via detailed kinetics, the actual temporal history of the free radical pool may be seriously miscalculated. Thus, attempts to model thermal-NO_x formation (29) in a methane flame by means of the quasi-global method have proven inadequate largely due to errors in the computed oxygen atom levels.

(b) The nature of the global step is such as to remove all consideration of hydrocarbons from the model. However, as suggested by Figure 3 above, "recycling" of NO to form HCN in fuel-rich systems via reactions with hydrocarbons (e.g., CH + NO → HCN + O) is a limiting factor in bound nitrogen decay in the presence of hydrocarbons, and must be considered in developing staging strategies to eliminate bound nitrogen from the combustor exhaust stream. Omission of all hydrocarbons from consideration is tantamount to neglect of many of the processes which require modeling.

(c) Distinction among different hydrocarbon fuels is not readily apparent in any other manner other than purely stoichiometric in the quasi-global model, although differences in molar enthalpies of fuels should lead to somewhat different computed time/temperature histories. Of course, the degree to which mechanistic chemistry differences (rather than temperature differences) distinguish NO_x emission levels from the combustion of different hydrocarbons is currently unclear (no definitive experimental data are currently available), and the hope is that mechanistic differences (for example, the distribution of intermediate hydrocarbon fragments) will prove to have only a second order influence upon NO_x levels. However, construction of a computational model which a priori neglects such considerations does seem less desirable than one which permits them.

It is concluded, therefore, that the quasi-global method, as currently utilized, is, if not inapplicable to the modeling of NO_x emissions from higher hydrocarbons, at least undesirable as a method with adequate predictive capabilities.

4. Development of a New Quasi-Global Method - QUAGMIRE

Having exhausted, as impractical or inapplicable, all existing methods of treating hydrocarbons of which we are aware, we have proposed a new quasi-global method of the following, general form:

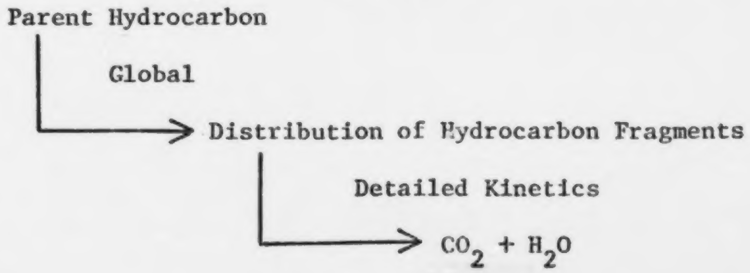

The basis underlying this hypothesized method rests upon the assumptions that the initial degradation of the parent hydrocarbon in the preflame zone via pyrolysis and oxidative pyrolysis routes is very rapid; that the initial decomposition products may be represented by a relatively small set of low molecular weight, stable and/or unstable hydrocarbon species; and, of course, that the decomposition mechanism can be justifiably represented by a global step.

The potential utility of the method lies in the following:

(a) The advantages of modeling free radical chemistry by detailed kinetics are retained, but the magnitude of the elementary reaction set required is vastly reduced. Again, this reflects the exponential-like growth in reaction set magnitude with number of carbon atoms in the parent specie. If only hydrocarbon fragments with relatively few carbon atoms are present following the global step, then the magnitude of the reaction set - given by the union of the combustion reaction sets of the fragment species - will be small relative to the (hypothetical) reaction set of the parent hydrocarbon.

(b) Whereas, even if the magnitude of the problem could be handled computationally, the detailed combustion mechanism of the parent hydrocarbon is generally unknown, detailed combustion mechanisms of many of the hydrocarbon fragments, which may be assumed to predominate at flame conditions, are known or are in varying stages of development.

(c) Unlike the quasi-global method of Edelman and Fortune, hydrocarbons are retained in the elementary reaction scheme.

(d) To the extent that an initial global step is applicable according to the method of Edelman and Fortune, the approximation should be more accurate here. This reflects a reduction in the mechanistic size of the global step, or, more significantly, a reduction in the magnitude of the reaction time or extent encompassed by the global step. That is, whereas the method of Edelman and Fortune takes a giant global step nearly to the postflame zone (where hydrocarbons have disappeared and CO has formed), it is arguable that the global step proposed here is completed in the preflame zone or early into the primary reaction zone (30) - which is where much of the essential fuel-nitrogen chemistry occurs! Thus, the global step may be regarded as faster on a time scale pertinent to fuel-nitrogen conversion. The probability of miscalculating the concentration/time history of the radical pool, for purposes of modeling NO_x emissions, is concurrently reduced.

In distinction to the quasi-global method of Edelman and Fortune, the technique proposed here may be referred to as the Quasi-Global Method applied to Initial Reaction Extents (QUAGMIRE). Details of QUAGMIRE, including justification of its computational applicability and discussion of associated research questions are presented elsewhere (31).

E. Modeling of Fuel-Nitrogen Conversion in a Hydrocarbon Environment

It can be shown (31) that the detailed kinetic mechanisms of combustion of the C_1 and C_2 species under fuel-rich conditions are the basic building blocks of QUAGMIRE. Recent developments in this area have been rapid and substantial, and have laid an adequate foundation upon which it is possible to develop QUAGMIRE. Olson & Gardiner (32) have published a methane mechanism which includes chemistry through the C_4 species, although the formaldehyde reaction rates should, probably, be updated by Dean's (33) more recent shock tube measurements. Through extensive modeling of shock tube data, Gardiner (34) has concluded that his is the best existing methane mechanism, although Gardiner (35) has also identified inadequacies in it in modeling C_2 chemistry. Levy (31), however, has rectified at least one of the residual C_2 problems in Gardiner's mechanism by demonstrating that the products of hydroxyl attack upon acetylene do not feed strongly into the CH_i set, but are better modeled as running through a ketene intermediate to formaldehyde. Accordingly, in an attempt to model Haynes' rich, fuel-nitrogen doped ethylene/air post-flame hydrocarbon decay data (Figure 2), Gardiner's modified reaction set was combined with the minimum subset fuel-nitrogen mechanism of Table I, a small subset of CH-generating reactions borrowed from the Engleman (24) methane reaction set compilation shown in Table II (Gardiner's set does not include CH), and a small set of postulated hydrocarbon/fuel-nitrogen interactions, shown in Table III, of which all but one are gleaned from Engleman's compilation (24), the remaining dominant (global) reaction of CH_3 with NO being taken from Haynes' (17,23) analysis. The resulting reaction mechanism of 102 reactions in 36 species is integrated to yield the results shown in Figure 4, which demonstrate nicely the desired hydrocarbon decay data, as well as coupled fuel-nitrogen profiles improved over those of Figure 2.

The prognosis for establishment of an adequate C_2 modeling capability in the near future does, therefore, look quite bright, although the reader should not be misled into believing that either C_1 or C_2 mechanisms can yet be considered to be adequately characterized. Thus, free radical profiles computed for the hydrocarbon "breakthrough" case fall far below the measured values. This demonstrates a residual problem with Gardiner's C_1/C_2 mechanism, and indicates the need for further developments of the elementary hydrocarbon mechanisms. It should be noted that excessive radical destruction is also predicted for this system (36) by the newly published mechanism of Westbrook (37). In this regard, it is vital that additional data, similar to those of Haynes (23), be obtained for validation or refinement, under post-flame conditions pertinent to practical fuel-nitrogen chemistry, of the mechanistic hydrocarbon chemistry developments which are generally derived from shock tube studies.

F. Summary

Capabilites to model fuel-nitrogen conversion in the absence of hydrocarbons under aerodynamically clean conditions have been demonstrated, although the mechanistic chemistry of the amines still requires refinement. Modeling capabilities under conditions of hydrocarbon "breakthrough", however, are limited by the necessity to model higher hydrocarbon oxidation. This problem, however, may be reduced in computational magnitude through a quasi-global method which limits necessary hydrocarbon mechanisms to C_1 and C_2 species. Although not yet fully developed, available C_1 and C_2 mechanisms are improving. Additional experimental data are required, however, for refinement and validation of C_1 and C_2 reaction sets; elucidation of hydrocarbon fragment distributions in the post-flame zone as a function of parent higher hydrocarbon, equivalence ratio and temperature; and provision of a data base for the modeling of the coupled chemistry of fuel-nitrogen conversion in a higher hydrocarbon environment.

REFERENCES

1a. Turner, D.W., and C.W.Siegmund, "Staged Combustion and Flue Gas Recycle: Potential for Minimizing NO_x from Fuel Oil Combustion", American Flames Research Committee Flame Days, Chicago, September, 1972.

b. Turner, D.W., R.L.Andrews, and C.W.Siegmund, "Influence of Combustion Modifications and Fuel Nitrogen Content on Nitrogen Oxide Emissions from Fuel Oil Combustion", AIChE Symposium Series 68, 55 (1972).

c. Siegmund, C.W. and D.W.Turner, "NO_x Emissions from Industrial Boilers: Potential Control Methods", J. Eng. Power, p.1-6, January, 1974.

2a. Bartok, W., A.R.Crawford, and G.J.Piegari, "Systematic Field Study of NO_x Emission Control Methods for Utility Boilers", Esso Research and Engineering Co., Report No. GRU. 4GNOS.71 to the Office of Air Programs, Research Triangle Park, North Carolina, December 1971.

b. Martin, G.B. and E.E.Berkau, "An Investigation of the Conversion of Various Fuel-Nitrogen Compounds to Nitrogen Oxides in Oil Combustion", AIChE Symp. Ser. 68, 126, 45 (1972).

c. Heap, M.P., T.M.Lowes, R.Walmsley, and H. Bartelds, Burner Design Principles for Minimum NO_x Emissions, Proceedings Coal Combustion Seminar, Research Triangle Park, N.C., EPA Report No. EPA 650/2-73-021, Sept. 1973

3. Pohl, J.H., "Fate of Fuel Nitrogen", SC.D. Thesis, M.I.T. (1976).

4. Pohl, J.H., and A.F.Sarofim, "Devolatilization and Oxidation of Coal Nitrogen", Sixteenth Symposium (International) on Combustion, The Combustion Institute, p. 491, Pittsburgh (1977).

5. Song, Y.H., "Fate of Fuel Nitrogen During Pulverized Coal Combustion", Sc.D. Thesis, M.I.T. (1978).

6. Song, Y.H., J.M. Beér and A.F. Sarofim, "Fate of Fuel Nitrogen During Pyrolysis and Oxidation", Second Annual Symposium on Stationary Source Combustion, New Orleans, LA (1977).

7. Levy, J.M., J.H.Pohl, A.F.Sarofim, and Y.H.Song, "Combustion Research on The Fate of Fuel-Nitrogen Under Conditions of Pulverized Coal Combustion" EPA Report EPA-600/7-78-165 (August, 1978).

8. Fenimore, C.P., "Formation of Nitric Oxide from Fuel Nitrogen in Ethylene Flames", Comb. and Flame, 19, 289 (1972).

9a. DeSoete, G.G.,"Le Mecanisme de Formation D'Oxyde Azotique a Partir D'Ammoniac et D"amines Dans Les Flammes D'Hydrocarbures", Revue de L'Institute Francais Du Petrole 28, 95 (1973).

b. DeSoete, G.G. and A. Queraud, "Formation D'Oxyde D'Azote Dans Les Flammes: Formation D'Oxyde D'Azote A Partir De L'Azote Du Combustible. C-Addition de NO Dans Les Melanges Inflammables", Report No.I.F.P. No. 21.681, Institute Francais Du Petrole, Rueil Malmaison, France (1973).

10. Sarofim, A.F., G. C. Williams, M. Modell, and S. M. Slater, "Conversion of Fuel Nitrogen to Nitric Oxide in Premixed and Diffusion Flames", AIChE Symposium Series 148, Volume 7, 51 (1975)

11. Levy, J.M., J.P.Longwell, A.F.Sarofim, T.L.Corley, M.P.Heap and T.J. Tyson, "NO_x Abatement in Fossil Fuel Combustion: Chemical Kinetic Considerations," Proceedings of the Third Symposium on Stationary Source Combustion, Vol. IV, EPA-600/7-79-050, p.3 (March, 1979).

12. See, also, Pershing, D.W. and J.O.L.Wendt, "Pulverized Coal Combustion: The Influence of Flame Temperature and Coal Combustion on Thermal and Fuel NO_x", Sixteenth Symposium (International) on Combustion, The Combustion Institute, p. 389, Pittsburgh (1977).

13. Corley, T.L., "Development of a Kinetic Mechanism to Describe the Fate of Fuel Nitrogen in Gaseous Systems," Fifth E.P.A. Fundamental Combustion Research Workshop, Newport Beach, California, January, 1980.

14. Heap, M.P., T.J.Tyson, J.E.Cichanwicz, R.Gersham, C.J.Kau, G.B.Martin and W.S.Lanier, "Environmental Aspects of low BTU Gas Combustion," Sixteenth Symposium (International) on Combustion, The Combustion Institute, p.535 (1977).

15. Recent examples include:
    a. Fenimore, C.P., "Reactions of Fuel-Nitrogen in Rich Flame Gases," Comb. and Flame 26, 249 (1976).
    b. Morley, C., "The Formation and Destruction of Hydrogen Cyanide from Atmospheric and Fuel-Nitrogen in Rich, Atmospheric-Pressure Flames," Comb. and Flame 27, 189 (1976).
    c. Haynes, B.S., "Reactions of Ammonia and Nitric Oxide in the Burnt Gases of Fuel-Rich Hydrocarbon-Air Flames", Comb. and Flame 28, 81 (1977).
    d. Haynes, B.S., "The Oxidation of Hydrogen Cyanide in Fuel-Rich Flames," Comb. and Flame 28, 113 (1977).

16. Sarofim, A.F., J.H.Pohl, and B.R.Taylor, "Strategies for Controlling Nitrogen Oxide Emissions During Combustion of Nitrogen Bearing Fuels," AIChE 69th Annual Meeting, Chicago (1976).

17. Haynes, B.S., "Kinetics of Nitrogen Oxide Formation in Combustion," in Progress in Astronautics and Aeronautics, Volume 62 (C.T.Bowman and J.Birkeland, eds.), Alternative Hydrocarbon Fuels: Combustion and Chemical Kinetics, American Institute of Aeronautics and Astronautics (1978).

18. Levy, J.M., J.P.Longwell and A.F.Sarofim, "Conversion of Fuel-Nitrogen to Nitrogen Oxides in Fossil Fuel Combustion: Mechanistic Considerations," Report to Energy and Environmental Research Corp. by the MIT Energy Laboratory. EPA FCR Program (1978).

19. Engleman, V.S., "Detailed Approach to Kinetic Mechanisms in Complex Systems," J. Phys. Chem., 81, 2320 (1977).

20a. Mayer, S.W., L.Schieler, and H.S.Johnston, "Computation of High-Temperature Rate Constants for Bimolecular Reactions of Combustion Products," Eleventh Symposium (International) on Combustion, The Combustion Institute, p. 837, Pittsburgh (1966).

b. Tunder, R., S.Mayer, E.Cook, and L.Schieler, Aerospace Corporation Report TR-1001 (9210-02)-1 (1967).

21. Branch, M.C., J.A.Miller, and R.J.Kee, "Chemical Kinetics of the $NH_3/NO/O_2$ System," 1979 Fall (Western States Section) Combustion Meeting The Combustion Institute, WSS Paper No. 79-38, Berkeley, California, October, 1979.

22a. Hack, W., H.Schacke, M.Schröter and H.G.Wagner, "Reaction Rates of NH_2 Radicals with NO, NO_2, C_2H_2, C_2H_4 and Other Hydrocarbons," Seventeenth Symposium (International) on Combustion, The Combustion Institute, p. 505 (1979).

b. Silver, J.A., C.M.Gozewski, and C.E.Kolb,"Chemical Kinetics of the NH_3/NO Reaction System Under Combustion Exhaust Flow Conditions," to be presented at the Eighteenth Syposium (International) on Combustion, Waterloo, Ontario, August, 1980.

23. Haynes, B.S., "The Formation and Behavior of Nitrogen Species in Fuel Rich Hydrocarbon Flames," Ph.D. Thesis, University Of New South Wales, Sydney, Australia (1975).

24. Engleman, V.S., "Survey and Evaluation of Kinetic Data on Reactions in Methane/Air Combustion," EPA Report, EPA-600/2-76-003 (1976).

25. Cohen, R.C., "The High Temperature Oxidation and Pyrolysis of Ethane," Ph.D. Thesis, Princeton University, Department of Aerospace and Mechanical Sciences (1972).

26a. Dryer, F.L., "High Temperature Oxidation of Carbon Monoxide and Methane in a Turbulent Flow Reactor," Ph.D. Thesis, Princeton University, Department of Aerospace and Mechanical Sciences (1972).

b. Dryer, F.L., and I. Glassman, "High Temperature Oxidation of CO and CH_4" Fourteenth Symposium (International) on Combustion, The Combustion Institute, Pittsburgh, PA p.987 (1973).

27. Dryer, F.L., and I. Glassman, "Combustion Chemistry of Chain Hydrocarbons," in Progress in Astronautics and Aeronautics, Volume 62, (Bowman, C.T. and J. Birkeland eds.) Alternative Hydrocarbon Fuels: Combustion and Chemical Kinetics, American Institute of Aeronautics and Astronautics (1978).

28. Edelman, R.B. and O.F.Fortune, "A Quasi-Global Chemical Kinetic Model for the Finite Rate Combustion of Hydrocarbon Fuels with Application to Turbulent Burning and Mixing in Hypersonic Engines and Nozzle," AIAA Paper No. 69-86 (1969).

29. Bowman, C.T. and A.S.Kesten, "Kinetic Modeling of Nitric Oxide Formation in Combustion Processes," presented at the Fall Meeting, Western States Section of the Combustion Institute, Paper No. 71-28, Irvine, California (October, 1971).

30. Millikan, R.C., "Non-equilibrium Soot Formation in Premixed Flames," J. Phys. Chem. 66, 794 (1962).

31. Levy, J.M., "Modeling of Fuel-Nitrogen Chemistry in Combustion: The Influence of Hydrocarbons," Fifth E.P.A. Fundamental Combustion Research Workshop, Newport Beach, California, January, 1980.

32. Olson, D.B. and W.C.Gardiner, Jr., "Combustion of Methane in Fuel-Rich Mixtures," Comb. and Flame 32, 151 (1978).

33a. Dean, A.M., B.L.Craig, R.L.Johnson, M.C.Schultz, and E.E.Wang,"Shock Tube Studies of Formaldehyde Pyrolysis," Seventeenth Symposium (International) on Combustion, The Combustion Institute, p.577 (1979).

b. Dean, A.M., R.L.Johnson, and D.C.Steiner, "Schock Tube Studies of Formaldehyde Oxidation," in press 1979.

34. Olson, D.B. and W.C.Gardiner, Jr., "An Evaluation of Methane Combustion Mechanisms," J. Phys. Chem. 81, 2514 (1977).

35. White, J.N. and W.C.Gardiner, Jr., "An Evaluation of Methane Combustion Mechanisms: 2 - Comparison of Model Predictions with Experimental Data from Shock-initiated Combustion of C_2H_2, C_2H_4, and C_2H_6," J. Phys. Chem. 83, 562 (1979).

36. Levy, J.M., unpublished results.

37. Westbrook, C.K., "An Analytical Study of the Shock Tube Ignition of Mixtures of Methane and Ethane," Comb. Sci. and Technology 20, 5 (1979).

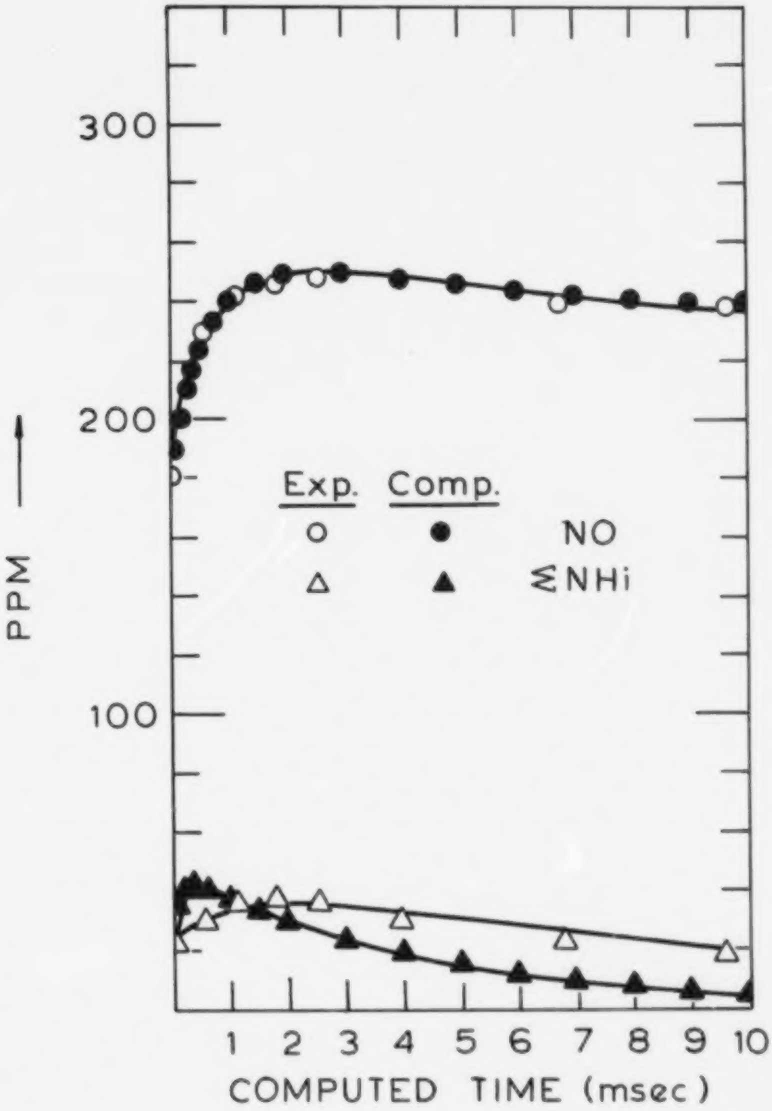

Figure 1a. Post-flame zone of a $C_2H_4/O_2/N_2$ flame doped with 700 PPM NH_3 ($\phi = 1.52$, T = 2010 K) modeled with the Reaction set of Table I. Data from Haynes [23].

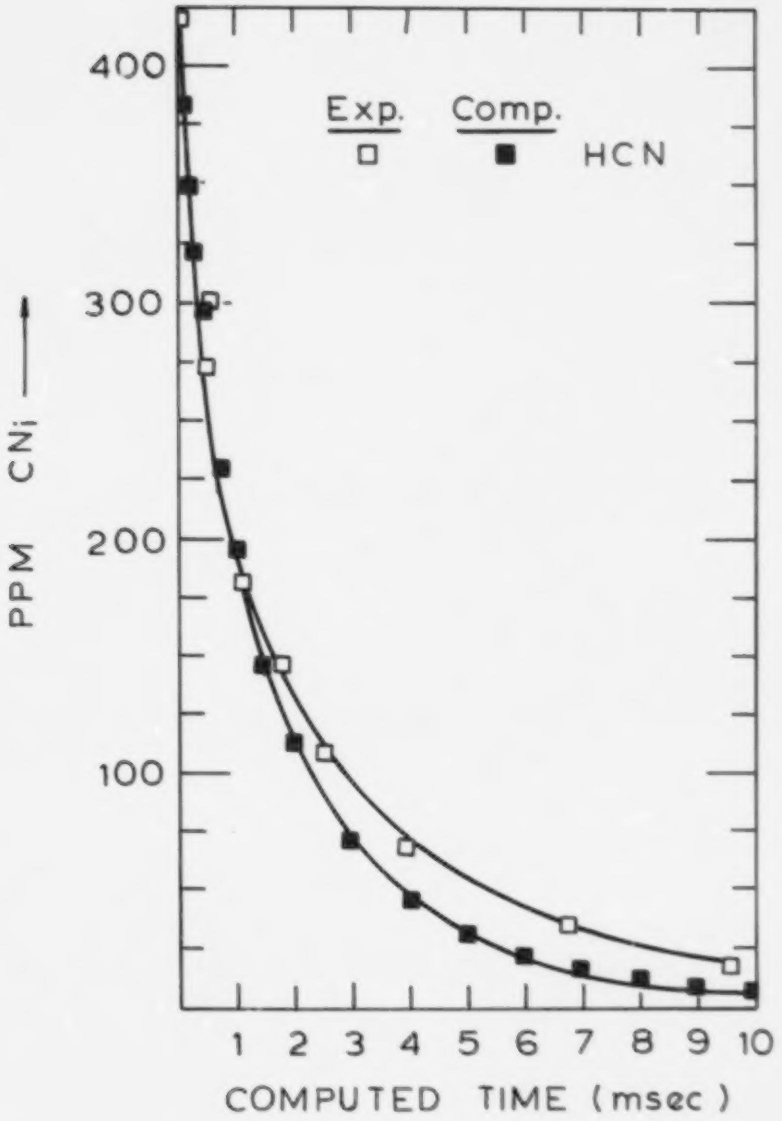

Figure 1b. Post-flame zone of a $C_2H_4/O_2/N_2$ flame doped with 700 PPM NH_3 (ϕ = 1.52, T = 2010 K) modeled with the Reaction set of Table I. Data from Haynes [23].

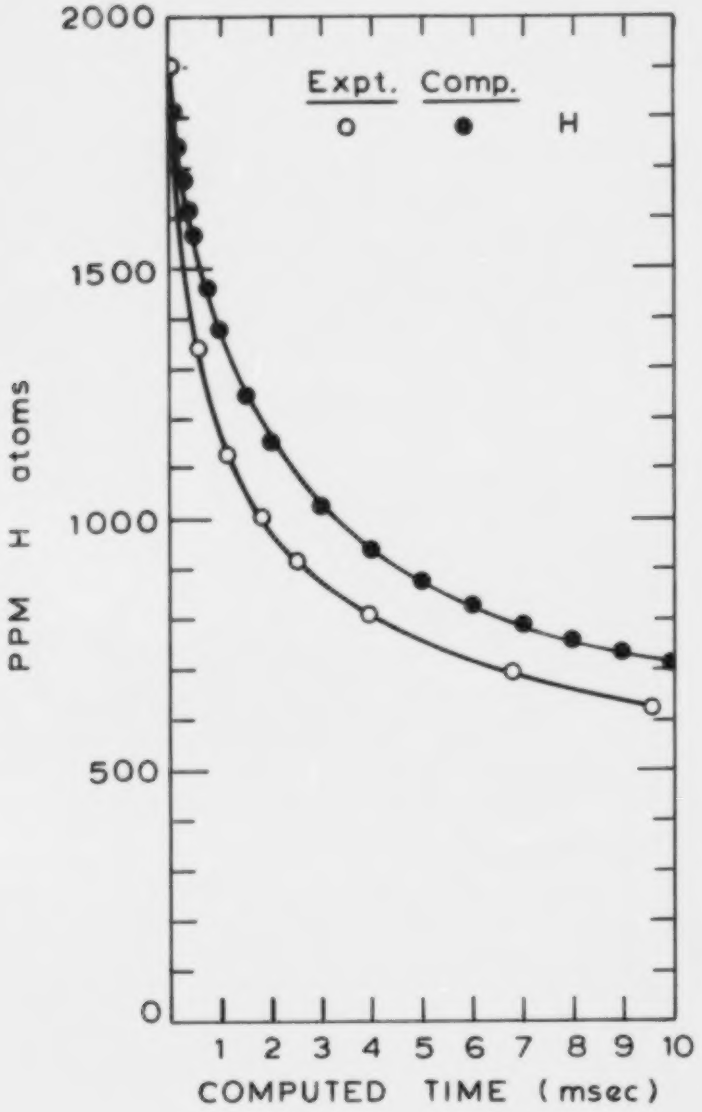

Figure 1c. Post-flame zone of a $C_2H_4/O_2/N_2$ flame doped with 700 PPM NH_3 (ϕ = 1.52, T = 2010 K) modeled with the Reaction set of Table I. Data from Haynes [23].

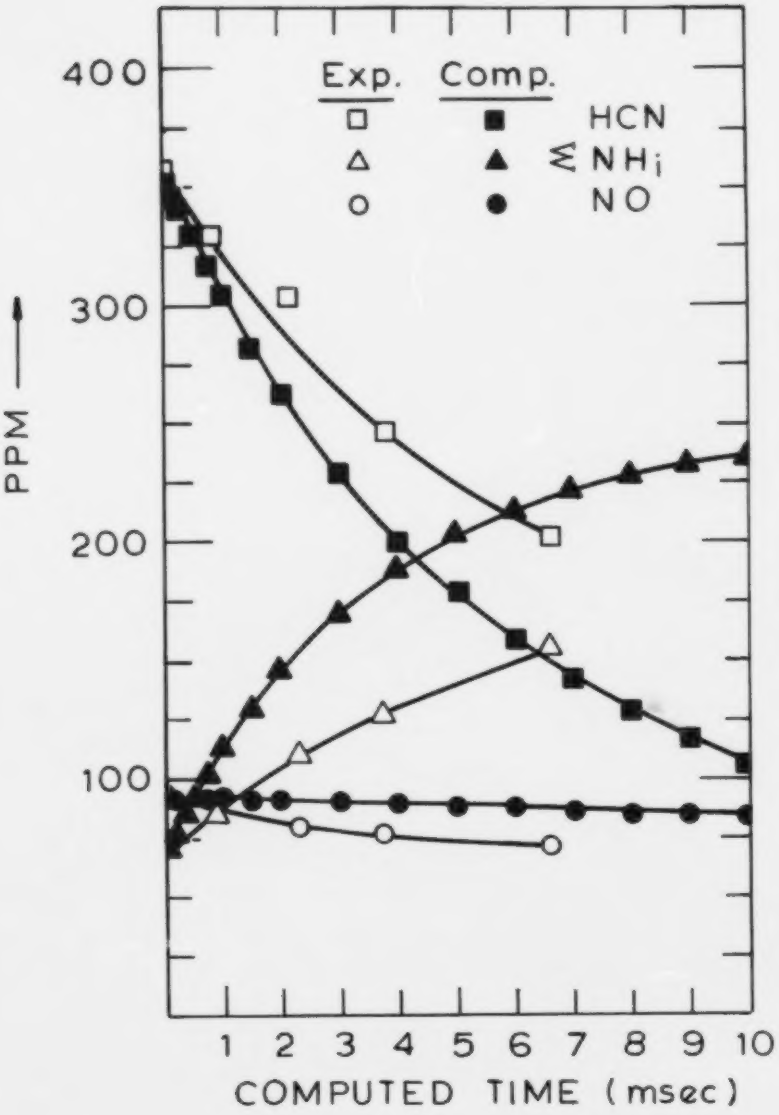

Figure 2a. Post-flame zone of a C_2H_4/air flame doped with 500 PPM NO (ϕ = 1.66, T = 2000 K) modeled with the hydrocarbon-free reaction set of Table I. Data from Haynes [23].

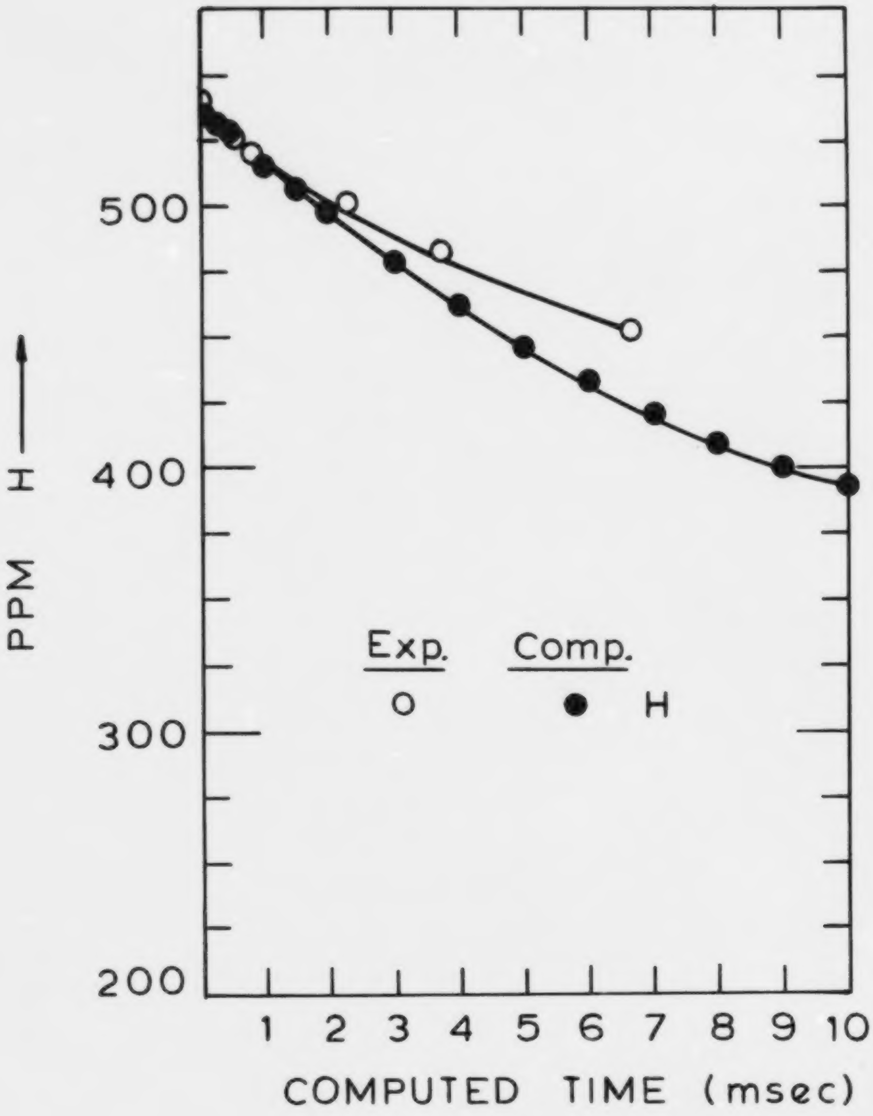

Figure 2b. Post-flame zone of a C_2H_4/air flame doped with 500 PPM NO (ϕ = 1.66, T = 2000 K) modeled with the hydrocarbon-free reaction set of Table I. Data from Haynes [23].

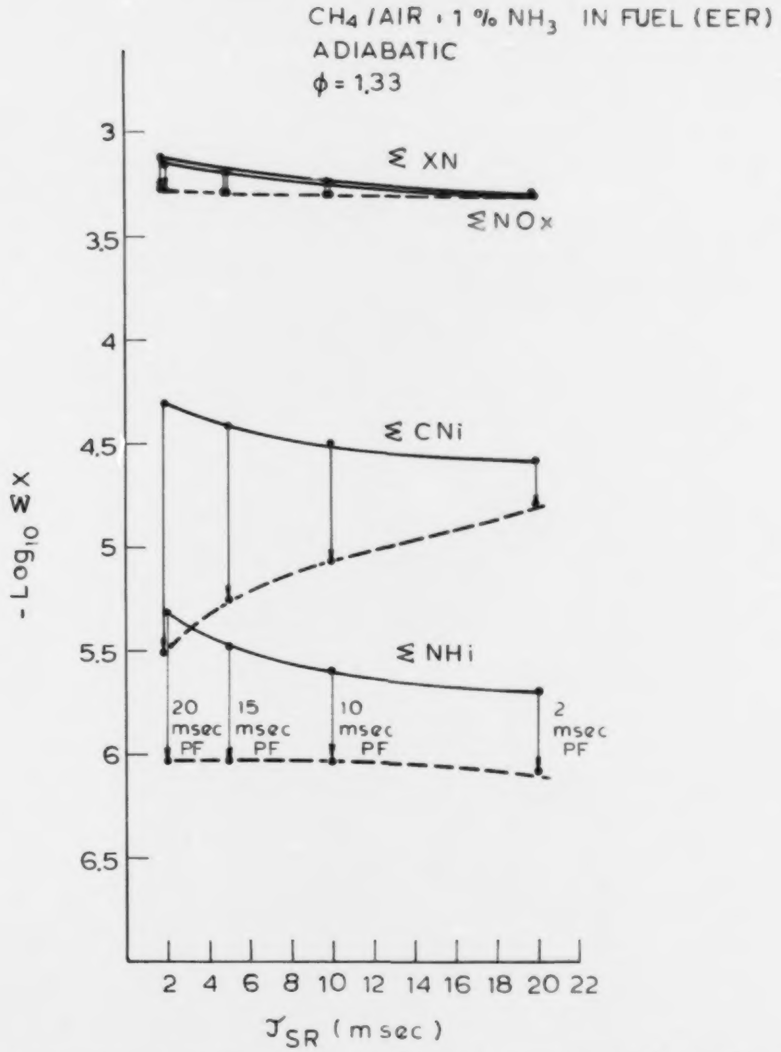

Figure 3. Species mole fractions as function of residence time (τ_{SR}) in an adiabatic stirred-reactor. CH_4/air flame doped with 1% NH_3, $\phi = 1.33$. The vertical lines denote the effects of varying times in plug-flow following the stirred-reactor section, the plug-flow residence times being (from left to right) 20 msec, 15 msec, 10 msec and 2 msec. The dashed lines denote species concentrations for combined stirred-reactor and plug-flow sections. Thus, $\Sigma CN_i = 4.88 \times 10^{-10}$ for $\tau_{SR} = 2$ msec, but falls to 3.08×10^{-6} after an additional 20 msec in plug-flow (total reaction time = 22 msec), whereas $\Sigma CN_i = 2.51 \times 10^{-5}$ for $\tau_{SR} = 20$ msec, but falls to 1.51×10^{-5} after an additional 2 msec in plug-flow.

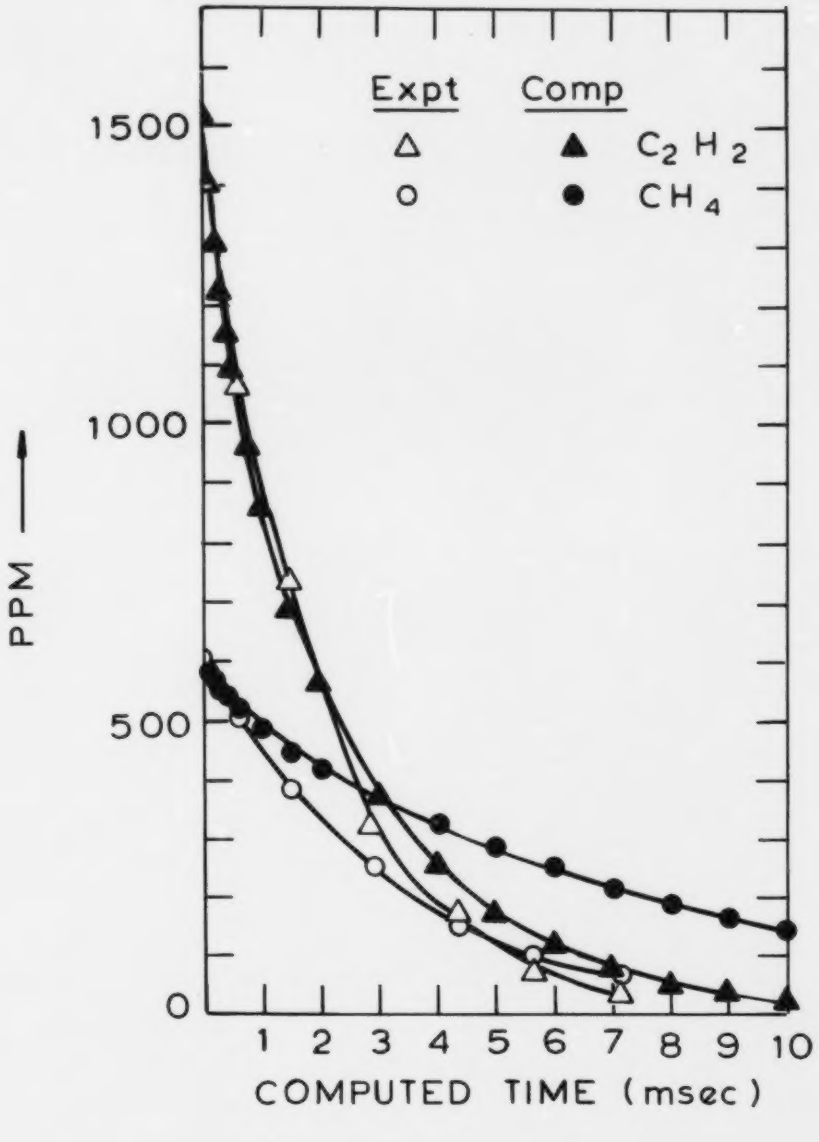

Figure 4a. Post-flame zone of a C_2H_4/air flame doped with 500 PPM NO ($\phi = 1.66$, T = 2000 K) including hydrocarbon "breakthrough", modeled with Gardiner's reaction set [32] altered to include a ketene intermediate, supplemented by the reactions of Tables I-III. Data from Haynes [23].

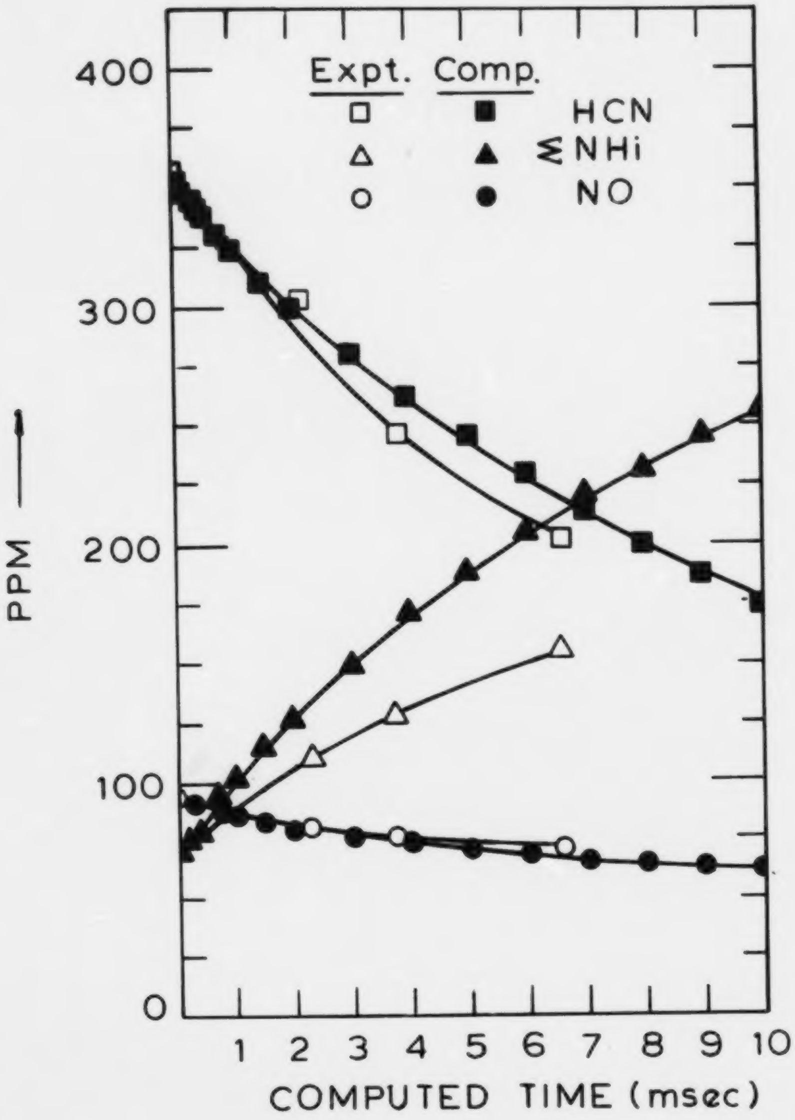

Figure 4b. Post-flame zone of a C_2H_4/air flame doped with 500 PPM NO (ϕ = 1.66, T = 2000 K) including hydrocarbon "breakthrough", modeled with Gardiner's reaction set [32] altered to include a ketene intermediate, supplemented by the reactions of Tables I-III. Data from Haynes [23].

TABLE I. SIMPLIFIED FUEL-NITROGEN REACTION MECHANISM*

Rate constant, $k_f = AT^n \exp(-E/RT)$

	REACTION	A (cm^3/mole-sec)	n	E (cal/mole)	REFERENCE
1	$HCN + OH \rightarrow CN + H_2O$	2.00×10^{11}	0.60	5000.	b
2	$CN + H_2 \rightarrow HCN + H$	3.16×10^{12}	0	5000.	c
3	$CN + OH \rightarrow NCO + H$	5.60×10^{13}	0	0.	d
4	$HCN + OH \rightarrow HNCO + H$	4.00×10^{11}	0	0.	e
5	$NCO + H_2 \rightarrow HNCO + H$	3.20×10^{11}	0	0	a
6	$NCO + H \rightarrow NH + CO$	3.00×10^{14}	0	0	a
7	$HNCO + H \rightarrow NH_2 + CO$	1.00×10^{13}	0	0	a
8	$NH_3 + H \rightarrow NH_2 + H_2$	5.00×10^{11}	0.50	2000.	f
9	$NH_3 + OH \rightarrow NH_2 + H_2O$	1.39×10^{11}	0	1600.	m,n,o
10	$NH_2 + H \rightarrow NH + H_2$	3.50×10^{10}	0.79	4460.	g
11	$NH_2 + OH \rightarrow NH + H_2O$	3.00×10^{10}	0.68	1300.	f
12	$NH + H \rightarrow N + H_2$	1.00×10^{12}	0.68	1900.	f
13	$NH + OH \rightarrow N + H_2O$	5.00×10^{11}	0.50	2000.	f
14	$NO + H \rightarrow N + OH$	1.34×10^{14}	0	49200.	h
15	$N + NO \rightarrow N_2 + O$	3.10×10^{13}	0	344.	i
16	$NH + NO \rightarrow N_2O + H$	9.00×10^{9}	0.75	0.	j
17	$N_2O + H \rightarrow N_2 + OH$	7.60×10^{13}	0	15101.	k
18	$N_2O + M \rightarrow N_2 + O + M$	1.42×10^{14}	0	51280.	l
19	$NH + NH \rightarrow N + NH_2$	3.60×10^{11}	0.55	1900.	f
20	$N + NH_3 \rightarrow NH_2 + NH_2$	2.10×10^{11}	0.50	23160.	f
21	$NH + N \rightarrow N_2 + H$	6.30×10^{11}	0.50	0.	q,r
22	$NH_2 + NH_2 \rightarrow NH + NH_3$	1.70×10^{11}	0.63	3600.	f,p

REFERENCES - TABLE I

*For a discussion of reactions 1 - 18, see Reference [a].

[a] Foster, D.E., J.B.Heywood, J.C.Keck, J.P.Longwell, A.F.Sarofim, and B. R.Taylor, "Control of NO_x Emissions from Combustion of Fuels Derived from Shale and Coal," Summary Technical Progress Report, October 23, 1978. Prepared for the Department of Energy, under Contract EX-76-A-01-2295, The Energy Laboratory, MIT.

[b] Tunder, R., S.Mayer, E.Cook, and L.Schieler, Aerospace Corp., Thermochemistry Research Dept., Aerospace Report No. TR-1001 (9210-02)-1, AD 813 485 (1967).

[c] Benson, S.W., D.M.Golden, and R.Shaw, "Estimating the Kinetics of Combustion," EPA Report EPA-600/2-75-019 (1975).

[d] Haynes, B.S., "The Formation and Behavior of Nitrogen Species in Fuel-Rich Hydrocarbon Flames," PhD. Thesis, The University of New South Wales (1975).

[e] Estimate, this work.

[f] Bahn, G.S., Reaction Rate Compilation for the N-O-H System, Gordon and Breach (1968).

[g] Mayer, S.W., L.Schieler, and H.S.Johnston, "Computations of High-Temperature Rate Constants for Bimolecular Reactions of Combustion Products," Eleventh Symposium (International) on Combustion, The Combustion Institute, Pittsburgh, PA (1967).

[h] Flower, W.L., R.K.Hanson, and C.H.Kruger, "Kinetics of the Reaction of Nitric Oxide with Hydrogen," Fifteenth Symposium (International) on Combustion, The Combustion Institute, p.823 (1974).

[i] Baulch, D.L., D.D.Drysdale, and A.C.Lloyd, "Critical Evaluation of Rate Data for Homogeneous Gas-Phase Reactions of Interest in High Temperature Systems, Vol. 4, "The University of Leeds 2, England (1969).

[j] Roose, T.R., R.K.Hanson, and C.H.Kruger, "Decomposition of NO in the Presence of NH_2," presented at the 11th Annual International Shock Tube Symposium, Seattle Washington, (1974).

[k] Baulch, D.L. et al., Evaluated Kinetic Data for High Temperature Reactions, Volume 2, CRC Press (1973).

[l] Monat, J.P., R.K.Hanson, and C.H.Kruger, "Kinetics of Nitrous Oxide Decomposition," Combustion Science and Technology, 16, 21-28 (1977).

[m] Dove, J.E. and S.N.Wing, "Shock Tube Studies of the Reactions of Hydrogen Atoms: I - The Reaction of $H+NH_3 \rightarrow H_2+NH_2$", Can. J. Chem., 52, 1171 (1974).

[n] Zellner, R. and I.W.Smith, "Rate Constants for the Reactions of OH with NH_3 and HNO_3," Chemical Physics Letters, 26 (1) (1974).

[o] Perry, R.A., R.Atkinson and J.N.Pitts, Jr., "Rate Constants for the Reactions of $OH+H_2S \rightarrow H_2O+SH$ and $OH+NH_3 \rightarrow H_2O+NH_2$ Over the Temperature Range 297-427°K," The Journal of Chemical Physics, 64 (8) 3237 (1976).

[p] Mayer, S.W. and L.Schieler, Aerospace Corp. Report TR-66 (8210-02)-3 (June, 1966).

[q] Engleman, V.S., "Survey and Evaluation of Kinetic Data on Reactions in Methane/Air Combustion, EPA Report, EPA-600/2-76-003 (1976).

[r] Benson, S.W., D.M.Golden, R.W. Lawrence and R.Shaw, Quarterly Progress Report No. 2, EPA Grant #R-800798 (Feb. 1973).

BEGIN FIRST LINE OF TEXT HERE
TYPING GUIDE SHEET
CENTER OF PAGE
TOP OF IMAGE AREA
DROPPED HEAD, BEGIN SECTIC HERE

TABLE II. REACTIONS INVOLVING CH TO BE APPENDED TO THE OLSON AND GARDINER MECHANISM

$$k_f = AT^N \exp\{-E/RT\}$$

	Reaction	A(cm^3/mole-sec)	N	E(Cal/mole)
1	$CH_2 + H = CH + H_2$	3.16×10^{11}	0.70	5,000
2	$CH_2 + OH = CH + H_2O$	5.00×10^{11}	0.50	6,000
3	$CH + CO_2 = CHO + CO$	1.00×10^{10}	0.50	6,000
4	$CH + OH = CHO + H$	5.00×10^{11}	0.50	10,000
5	$CH + O_2 = CHO + O$	5.00×10^{11}	0.50	6,000
6	$CH + O = CO + H$	5.00×10^{11}	0.50	0

All rates from Engleman, V.S., "Survey and Evaluation of Kinetic Data on Reactions in Methane/Air Combustion," EPA Report EPA-600/2-76-003 (1976)

BOTTOM OF IMAGE AREA OUTSIDE DIMENSION FOR TABLES AND ILLUSTRATIONS
BEGIN LAST LINE OF TEXT
3/8"

PAGE NUMBER
EPA-287 (Cin.)
(4-76)

TABLE III. HYDROCARBON FRAGMENT/FUEL-NITROGEN INTERACTIONS

$k_f = AT^N \exp\{-E/RT\}$

	Reaction	A(cm^3/mole-sec)	N	E (Cal/mole)	Ref.
1	$CH_4 + CN = CH_3 + HCN$	3.16×10^{11}	0.70	5,000	a
2	$CH_2 + N_2 = HCN + NH$	1.00×10^{14}	0	60,000	b
3	$CH_2 + NO = CH_2O + N$	1.60×10^{12}	0	7,000	a
4	$CHO + N = CH + NO$	1.00×10^{14}	0	48,600	c
5	$CHO + N = HCN + O$	1.00×10^{14}	0	0	a
6	$CHO + N = CO + NH$	2.00×10^{11}	0.50	2,000	a
7	$HCN + N = CH + N_2$	2.50×10^{11}	0	16,000	b
8	$HCN + O = CH + NO$	1.00×10^{14}	0	72,000	b
9	$CN + NH = CH + N_2$	1.00×10^{14}	0	40,000	b
10	$CH_3 + NO = \ldots = HCN + H_2O$	2.20×10^{11}	0	0	d

References

[a] Engleman, V.S., "Survey and Evaluation of Kinetic Data on Reactions in Methane/Air Combustion," EPA Report, EPA-600/2-76-003 (1976).

[b] Benson, S.W., D.M. Golden, R.W. Lawrence, R. Shaw and R.W. Woolfolk, "Estimating the Kinetics of Combustion: Including Oxides of Nitrogen and Sulfur," EPA Report, EPA-600/2-75-019 (1975), and estimates based thereon.

[c] Estimate based upon Engleman (Reference [a]).

[d] Haynes, B.S., "Kinetics of Nitrogen Oxide Formation in Combustion," in *Progress in Astronautics and Aeronautics, Vol. 62: Alternative Hydrocarbon Fuels: Combustion and Chemical Kinetics*, (C.T. Bowman and J. Birkeland, eds.) American Institute of Aeronautics and Astronautics (1978).

LOW NO_x COMBUSTORS FOR HIGH NITROGEN LIQUID FUELS

By:

G. C. England, M. P. Heap, D. W. Pershing,
J. H. Tomlinson, and T. L. Corely
Energy and Environmental Research Corporation
8001 Irvine Boulevard
Santa Ana, California 92705

ABSTRACT

The results of bench-scale experiments in a 21-kW tunnel furnace show that under unstaged combustion conditions total and fuel NO_x emissions from twenty-six petroleum and alternative liquid fuels correlate well with fuel nitrogen content. The optimization of staged combustion parameters in the fuel-rich primary zone was studied in order to provide direct guidance for advanced low-NO_x burner designs for evaluation in a 900-kW pilot-scale combustor. Detailed in-flame measurements were made in addition to exhaust measurements to quantify the influence of first-stage stoichiometry and temperature on the fate of fuel nitrogen species. Exhaust NO_x emissions were found to be directly related to the amount of total fixed-nitrogen species ($TFN = NO+HCN+NH_3$) leaving the first stage. Increasing the temperature of the primary zone decreased TFN concentration resulting in lower exhaust NO_x emission.

ACKNOWLEDGMENTS

These investigations were carried out under United States Environmental Protection Agency (EPA) Contracts 68-02-3125 and 68-02-2624. The support and assistance of Mr. W. S. Lanier and Mr. G. B. Martin, the Project Officers, has been appreciated. The authors also wish to acknowledge the assistance of their colleagues, R. K. Nihart, J. A. Naccarato, and J. G. Llanos, in conducting the experiments; and they wish to express their gratitude to W. C. Rovesti of EPRI, J. E. Haebig of Gulf Research, and L. Lukins of the U. S. Navy, for their help in obtaining several alternative fuels.

SECTION 1

INTRODUCTION

Combustion of liquid fuels derived from petroleum sources accounts for a significant fraction of fossil fuel consumption in stationary combustors. As petroleum reserves grow smaller, the United States is projected to place heavy reliance on coal, the most abundant fossil fuel available, in the search for new energy supplies. Coal can be burned directly or converted into either a liquid or a gaseous fuel. A balanced fuel economy necessitates that in the future many industrial users will burn petroleum- and coal- or shale-derived liquid fuels. Since these liquid fuels have relatively high nitrogen content and low hydrogen-to-carbon ratios, there will be the potential for adverse environmental impact due to the increased emission of combustion-generated pollutants unless preventative measures are taken (1-2). The pollutant of major concern in this paper is nitrogen oxides (NO_x). The paper addresses the impact of switching from a petroleum fuel to a shale- or coal-derived liquid, and on the mechanisms of combustion modification techniques used to control NO_x emissions from all liquid fuels.

Alternative liquid fuels can be broadly classified as those synthesized from the products of coal gasification, and those derived directly as liquids. The fuels in the first category tend to be clean, low-boiling-point fuels such as alcohols, and are essentially free from nitrogen and sulfur; thus, their impact upon pollutant emissions is minimal. The liquids in the second category may be compared to crude petroleum oils containing a wide range of hydrocarbon compounds with boiling points from $300^{\circ}K$ to greater than $900^{\circ}K$. The bound nitrogen content of crude synfuels is generally higher than petroleum crudes, and for many applications it might be necessary to upgrade the fuel by removing the nitrogen. Recognizing that alternative liquid fuels contain more bound nitrogen than the petroleum fuels that they would be replacing, one key factor in their production is to what extent combustion modification will allow control of NO_x emissions and reduce the necessity for substantial denitrification, thereby reducing the cost of synfuels.

Nitrogen oxides produced during combustion emanate from two sources. Thermal NO is formed by the fixation of molecular nitrogen and its formation rate is strongly dependent upon temperature (3). Fuel NO is formed by the oxidation of chemically-bound nitrogen in the fuel by reactions with a weak temperature dependence, but a strong dependence upon oxygen availability (4-5-6-7). Thus, those emission control techniques which minimize peak flame temperature by the addition of inert diluents (e.g., cooled recycled combustion products or water addition) minimize thermal NO formation, but have a minor impact upon fuel NO production. Staged heat release (staged combustion) provides the most effective NO_x control technique for nitrogen-containing fuels because fuel NO formation is mainly dependent upon local stoichiometry. It can be accomplished either by separating the combustion chamber into two zones and dividing the total combustion air into two streams, or by appropriate burner design which promotes localized fuel-rich conditions.

Minimizing fuel NO_x formation requires the existence of a fuel-rich primary combustion zone to maximize the conversion of fuel nitrogen to molecular nitrogen since the fate of fuel-bound nitrogen is strongly controlled by the reactant stoichiometry. Many studies (8-12) have shown that under fuel-rich conditions the efficiency of conversion to N_2 increases significantly. Thus, there are two fuel nitrogen reaction paths leading to the production of N_2 or NO, namely:

Path A. Fuel-lean

$$XN + \text{Oxidant} \rightarrow NO + \ldots$$

Path B. Fuel-rich

$$XN + \ldots \rightarrow N_2 + \ldots$$

The objective of staged combustion emission control techniques is the provision of conditions which maximize N_2 production via Path B. Two factors of practical importance are the residence time and the stoichiometry required to maximize N_2 production in the fuel-rich primary zone.

If the residence time is insufficient, then the original fuel nitrogen species will exist in the gaseous state as some XN compound which can be converted to NO in the second-stage heat release zone. The stoichiometry required to achieve minimum XN concentrations at the exit of the primary stage will be determined by (1) the rate of evolution of nitrogen species from the fuel; (2) the inevitable distribution of stoichiometries from fuel-rich to fuel-lean which occurs because the primary zone is supplied by a diffusion flame; and (3) the overall temperature of the primary zone. From equilibrium considerations the total fixed nitrogen (TFN given by $NO + HCN + NH_3$) is a minimum at approximately 65 percent theoretical air with levels less than 10 ppm depending upon temperature and fuel C/H ratio. Exhaust NO_x emissions are considerably greater than levels predicted by equilibrium, suggesting the existence of kinetic limitations in the fuel-rich primary stage.

NO_x formation during combustion of alternate fuels is not well-understood; however, recent test results have indicated that replacing a petroleum oil with a coal- or shale-derived liquid may result in a major increase in NO_x emissions. Bench-scale experiments (13) have shown that the smoke and combustion characteristics of the SRC II coal liquids are equivalent to light oil, but uncontrolled NO_x emissions are high due to the 0.8 to 1.2 percent N in the fuel. Pilot-scale SRC II studies (14-16) have demonstrated that both fuel blending and staged combustion are effective in reducing NO_x emissions and that improved atomization, increased preheat, and increased excess O_2 increase NO_x. Full-scale testing (17) has confirmed the need for optimized combustion modifications. Similar results have also been achieved during bench-scale (18) and field tests (19) with shale-derived liquids.

The results presented in this paper represent a portion of a study to investigate the influence of spray properties, fuel composition, stoichiometry and thermal environment on pollutant formation in liquid fuel flames. The technical approach is experimental, involving parallel programs in two combustors of different scales:

- a downfired 21 kW (70,000 Btu/hr) refractory-lined tunnel furnace, and
- a 900 kW (3,000,000 Btu/hr) cold wall axisymmetric combustor which simulates the firetube of a package boiler.

This paper focuses on recent small-scale results on the relationship between fuel chemistry and exhaust emissions under both excess air and staged combustion conditions. In particular, the optimization of staged combustor parameters in the fuel-rich primary zone were studied to provide direct guidance for advanced low-NO_x burner design. Twenty-six liquid fuels (3 distillate oils, 14 petroleum residual oils, 5 shale- and 4 coal-derived liquids) were burned in the tunnel furnace and, in addition to exhaust concentrations, in-flame measurements were made to quantify the influence of first-stage temperature and stoichiometry on the fate of fuel nitrogen species.

SECTION 2

EXPERIMENTAL SYSTEMS

TUNNEL FURNACE

The downfired tunnel furnace illustrated in Figure 1 was designed to allow utilization of commercially-available spray nozzles, and yet be capable of testing with artificial atmospheres. This combustor, which has been described in detail elsewhere (6), was 2.1 m long and 20 cm in inside diameter. The walls consisted of insulating and high temperature castable refractories and the full-load firing rate was 0.53 cc/sec, which corresponds to a nominal heat release of 20 kW. All airstreams were metered with precision rotameters. The main combustion air was preheated with an electric circulation heater; the atomization air was not preheated. In certain tests the "air" was enriched or replaced with varying amounts of carbon dioxide, argon, and oxygen, all of which were supplied from high-pressure cylinders.

Fuel and air entered the combustion chamber through the burner illustrated in Figure 1. The combustion air was introduced axially (without swirl) and a long refractory burner exit was used (L/D = 5.0). The interchangeable fuel injection system consisted of a 19 mm diameter stainless steel tube which contained the atomizing air supply tube, the fuel oil supply tube, a cartridge heater for final oil temperature control, and a chromel/alumel thermocouple positioned in the injector tip, prior to the nozzle for accurate oil temperature measurement. A commercial air-assisted ultrasonic oil atomizer (capacity 0.55 cc/sec) was used in this investigation because it provided adequate atomization of the heavy liquid fuels at relatively low flow rates. The drop-size distribution was narrow and centered at 20 microns (6). The tip of the fuel nozzle was positioned at the beginning of the burner divergent section (as shown in Figure 1); and, in general, the visible flame front was displaced one to four nozzle diameters from the nozzle tip.

ANALYTICAL SYSTEM

Exhaust concentrations were monitored continuously using a chemiluminescent analyzer for NO and NO_x, a NDIR analyzer for CO and CO_2, and a paramagnetic analyzer for O_2. The flue gas was withdrawn from the stack through a water-cooled, stainless steel probe using a stainless steel/Teflon sampling pump. Sample conditioning prior to the instrumentation consisted of an ice bath water condenser and glass wool and Teflon fiber filters. All sample lines were 6.3 mm Teflon and all fittings 316 stainless steel.

In-flame temperature measurements were made with a standard suction pyrometer containing a platinum/rhodium thermocouple. In-flame gas samples were withdrawn with a long, stainless steel water-quench probe. HCN and NH_3 were absorbed in a series of wet impingers and concentrations determined using specific ion electrodes. Sulfide ion interference was minimized by the addition of lead carbonate (20). Hydrocarbons were measured using a water-cooled probe, heated sample line, and an FID analyzer.

FUELS

Figure 2 illustrates the wide spectrum of composition for the distillate oils (half-filled symbols), heavy petroleum liquids (open symbols), and alternative liquid fuels (solid symbols) investigated to date. The petroleum-derived fuels had sulfur contents ranging from 0.2 to 2.22 percent with a maximum nitrogen content of 0.86. The nitrogen content of the alternative fuels range from 0.24 to 2.5 percent. Table 1 lists the complete chemical analysis and physical properties of each fuel as determined by an independent laboratory. The shale liquids included crude shale from the Paraho process (A3) and four refined products: diesel fuel marine (DFM, A1) residual fuel oil (A5), a 520-to-850°F distillation cut (A7), and a 5.75/1 medium/heavy SRC II blend (A6), a heavy SRC II distillate (A9), and an SRC II blended with the donor solvent (A4).

SECTION 3

EXCESS AIR RESULTS

PETROLEUM LIQUIDS

To define the influence of fuel composition on total and fuel NO_x emissions, each oil was tested under similar conditions in the tunnel furnace. Fuel NO_x formation was determined by substitution of the combustion air with a mixture of argon, oxygen, and carbon dioxide. The argon replaced the nitrogen, thereby eliminating thermal NO_x formation and the CO_2 provided the proper heat capacity so that flame temperatures were matched. Total and fuel NO_x emissions were measured with an air preheat level of $405 \pm 5^{\circ}K$ and an atomization pressure of 15 psig. Figure 3 presents a composite plot for total and fuel NO_x (defined by argon substitution) as a function of weight percent nitrogen in the fuel for a wide range of petroleum and blended distillate fuels. In Figure 3 the various symbols represent different base fuels (see Table I for symbol key). Those symbols shown with a line refer to distillate or residual fuels doped with pyridine or thiophene. It can be seen that both total and fuel NO_x increase with increasing fuel nitrogen content, and that total fuel nitrogen level is the dominant factor controlling fuel NO_x formation in this system. The form of the nitrogen does not appear to significantly influence fuel NO formation under excess air conditions, as doping with a volatile nitrogen compound (pyridine) resulted in NO_x emission similar to that from a less volatile residual oil of the same nitrogen content. Since the data is for a system where very fine oil droplets (approximately 25 micron mean diameter) are well-dispersed in the oxidizer under hot fuel-lean conditions, it is not surprising that fuel NO_x emissions are somewhat higher than those achieved in practical systems.

ALTERNATIVE FUELS

Figure 4 presents a composite plot of total and fuel NO_x for the range of petroleum fuels together with alternative fuels and mixtures. The Paraho shale was mixed with the same low sulfur oil used by Mansour (19). Synthoil could not be pumped without blending and the results presented in Figure 4 refer to 80 and 90 percent Synthoil blends with distillate oil. The SRC II blend refers to a mixture of SRC II and the donor solvent. Under the conditions tested, fuel NO_x emissions increase approximately linearly with increasing fuel nitrogen and it can be seen that the fate of fuel nitrogen in alternative fuels is similar to that in petroleum-derived fuels. Figure 5 presents the fuel NO_x data plotted as a percentage of the fuel nitrogen converted to fuel NO_x. For low fuel nitrogen contents, the conversion decreases rapidly (from greater than 90 percent) as fuel N increases. Eventually, however, the conversion becomes almost independent of fuel nitrogen content; hence, the linear dependence shown in Figure 4.

The absolute level of the fuel N conversion can be influenced by altering the fuel/air contacting and/or the fuel atomization (2), but the results obtained in this study suggest that fuel nitrogen is the only first-order fuel composition parameter controlling NO_x formation in fuel-lean flames. This conclusion applies to petroleum-, coal-, and shale-derived liquid fuels. However, there appear to be second-order effects where the volatility of the fuel nitrogen compound does have an influence upon fuel NO_x formation. Comparison of the data for the fuels with fuel nitrogen content of approximately 0.24 percent indicates that the highest conversion is achieved with a shale-derived distillate fuel with a large volatile nitrogen fraction.

SECTION 4

STAGED COMBUSTION RESULTS

POTENTIAL FOR NO_X CONTROL

Staged combustion, i.e., the operation of a combustion system in which the fuel originally burns under oxygen-deficient conditions, provides the most cost-effective control techniques established to date for reducing fuel NO_x. Figure 6 shows the influence of primary zone stoichiometric ratio on total NO_x emissions for two coal-derived and two shale-derived liquids under staged combustion conditions and 3 percent overall excess O_2. All the data in Figure 6 were obtained in the tunnel furnace with ultrasonic atomization and with a first-stage residence time of approximately 800 ms. As the primary zone becomes more fuel-rich, NO_x emissions decrease dramatically to a minimum and then increase again. This trend is in agreement with previously-reported data on petroleum fuels (21).

FUEL CHEMISTRY

First Stage Stoichiometry

In an effort to better understand the mechanisms of NO formation under staged combustion conditions, the original furnace was modified to allow in-flame sampling of the XN (NO, HCN, NH_3) species and cooling of the first-stage and/or second-stage combustion products, as illustrated in Figure 7. A "radiation shield" (choke) was installed near the top of the furnace to minimize the effects of downstream changes on the fuel vaporization zone. A secondary air injection ring and cast refractory choke were installed at 41 in. to insure isolation of the first stage. Variable cooling was achieved by insertion of multiple stainless steel water-cooling coils.

Figures 8, 9, and 10 show typical results of the detailed in-flame measurements made at the exit of the first stage for a distillate oil (D1-Alaskan diesel), a high nitrogen residual oil (R-14-Kern County, California) and an alternative liquid fuel (A8—+850°F shale fraction). These measurements were made on the centerline of the furnace at a distance of 104 cm (approximately 630 msec) from the oil nozzle. Detailed radial measurements indicated that the concentration profile was essentially uniform at this location. All of the in-flame data are reported on a dry, as-measured basis. After each in-flame measurement, second-stage air was added at 107 cm and exhaust NO_x measurements were also made (shown on a dry, 0% O_2 basis). In general, decreasing the first-stage stoichiometric ratio reduced the NO concentration leaving the first stage. However, below a stoichiometric ratio of approximately 0.8 significant amounts of NH_3 and HCN were measured. Thus, there exists a minimum in exhaust NO_x concentrations because of a competition between decreased first-stage NO and increased oxidizable nitrogen species such as HCN. Figures 9 and 10 indicate that the petroleum-derived oil (0.83 percent N) and the heavy shale liquid (2.49 percent N) produce large amounts of HCN. In addition, both fuels exhibited a minimum in TFN at a first-stage stoichiometry of approximately 0.8.

Data for the Alaskan diesel oil (Figure 8) also show the presence of much smaller but significant concentrations of HCN and NH_3, although this fuel is essentially nitrogen-free. Total conversion of the fuel nitrogen would produce 21 ppm TFN at SR_1=0.7. This confirms previous work (10-12) which demonstrated that reactions involving hydrocarbon fragments and N_2 or NO can produce HCN.

Hydrocarbons

The rapid increase in HCN concentration below SR_1=0.8 was accompanied by an increase in hydrocarbon content of the partially oxidized combustion products. Figure 11 summarizes the in-flame hydrocarbon measurements for the Alaskan Diesel (D1), three petroleum-derived residual oils (Indonesian-R4, Alaskan-R9, Kern County-R14), three alternative liquids (SRC-II heavy distillate-A9, crude shale-A3, heavy shale fraction-A8) and methane containing 0.75 weight percent nitrogen as NH_3(⌀). Hydrocarbon concentrations correlate well on the basis of first-stage stoichiometry. At very low stoichiometric ratios the distillate oil (◆) and CH_4/NH_3 produced slightly higher hydrocarbon concentrations than the heavier liquid fuels.

XN Distribution

Figure 12 shows typical results on the percentage of the original fuel nitrogen existing as either NO, NH_3 or HCN at various stoichiometric ratios for four fuels. Above SR_1=0.8, NO was the dominant TFN species; at lower stoichiometries HCN dominated with all fuels tested except the CH_4/NH_3. Axial profiles with the liquid fuels indicate that near SR_1=0.8, significant amounts of NH_3 may be formed early in the rich zone but they decay rapidly. These data are in strong contrast to similar results obtained with pulverized coal (20) which indicate that the preferred TFN species is a strong function of coal composition.

In general, both the alternate and petroleum-derived liquid fuels behaved very similarly with the exception of the Kern County, California crude (R14). It produced less HCN under rich conditions, and this tendency cannot be readily associated with common fuel properties. Hydrocarbon and nitrogen distillation data indicated that in terms of equilibrium volatile evolution the Kern County fuel is intermediate among the liquids tested. The Indonesian oil was the lightest of the liquid fuels and it produced the highest TFN concentration at the minimum (SR_1=0.8).

SECOND-STAGE NO_X FORMATION

Exhaust NO_x emissions in a staged combustor result from conversion of TFN exiting the first stage and any thermal NO_x production during burnout. Thermal NO_x production was not considered to be significant in this study because changes in heat extraction in the burnout region had almost no effect on final emissions. Figure 13 shows exhaust NO_x emissions as a function of total fixed nitrogen in the first stage at stoichiometries between 0.5 and 0.8 for all fuels. The form of this correlation can be compared with that presented in Figure 3 for excess air conditions since the second stage burnout can be considered an excess air flame. Exhaust emissions increase with increasing oxidizable nitrogen content, but the conversion efficiency decreases as the TFN concentration increases. There are three possible explanations for the data scatter shown in Figure 13: (1) TFN is not indicative of the oxidizable nitrogen compounds that are leaving the first stage; (2) TFN conversion in the burnout zone is dependent upon the form of the TFN;

and (3) TFN conversion is also dependent upon the oxidation of the partial products of combustion at the exit of the fuel-rich zone.

IMPACT OF THERMAL ENVIRONMENT

The TFN concentrations shown in Figure 12 are in excess of equilibrium levels and Sarofim and co-workers (25) have suggested that increasing the temperature of the primary zone would prove beneficial. The results presented in Figure 14 were obtained with the shale crude (A3) to demonstrate the impact of first- and second-stage heat removal on the fate of fuel nitrogen. Figure 14a indicates that adding the radiation shield with cooling coils in both the first- and second-stage (hence, increasing the temperature of the vaporization zone) reduced the minimum NO_x emissions and shifted the optimum stoichiometry more fuel-rich. Figure 14b shows that removing the water cooling coils from the first stage reduced the exhaust emissions. Removing the second stage coils did not alter the minimum level; however, it did shift the minimum SR more fuel-rich. Thus, the optimum thermal environment has a high temperature vaporization zone, a hot, rich hold-up zone, and a cooled second stage (Figure 14c).

The axial profiles (22) provide an explanation for this shift in the minimum emission levels. Heat extraction in the first stage impacts the rate of decay of TFN. Under cold conditions, both NO and HCN essentially freeze, whereas without heat extraction the initial rate of decay for all three species is much faster leading to low TFN concentrations at the exit of the fuel-rich first stage. It should be noted that heat extraction also affects the rate of CO oxidation.

SECTION 5

DISCUSSION

NO_x control via staged combustion involves operating the first stage of the combustor at some optimum stoichiometry before adding air to complete combustion. Measurements within the rich first stage show that at this optimum stoichiometry NO, HCN and NH_3 co-exist. For more fuel-rich conditions TFN exists mainly as HCN and NH_3, and for conditions less fuel-rich than the optimum, NO is the primary fixed nitrogen species. Two factors influence the stoichiometry at which minimum exhaust NO_x emissions occur: (1) the fuel type, and (2) the temperature of the primary zone. The data presented in Figure 14 clearly indicate that an increase in the first-stage temperature results in a decrease in NO_x emissions. The implication of this data with respect to practical low NO_x burner designs utilizing the staged combustion concept appears to be that heat loss from the fuel-rich first stage should be minimized in order to optimize NO_x control for liquid fuels.

Figure 15 presents the results of calculations made with an idealized plug flow well-stirred reactor sequence and a kinetic mechanism for methane-air-fuel nitrogen mixtures. The latter stages of the rich zone in the tunnel furnace may approximate to plug flow conditions, but this reactor sequence does not attempt to model the details of the initial mixing and heat release. The kinetic mechanism (23) contains 36 species and 184 reactions and represents an attempt to develop an adequate set which has been validated against a diverse body of experimental data including ignition delay times, flame speeds and species profiles. A methane plus ammonia mixture was used as the fuel to simulate an experimental system without liquid drops. The model results are in qualitative agreement with the experimental data. As the first stage becomes more fuel-rich the NO concentration decays, and the HCN and NH_3 concentrations increase (Figure 15a). The predicted distribution of nitrogenous species is in agreement with the experimental data. The three isothermal conditions shown in Figure 15b were chosen because they include the range of temperatures measured in the furnace. The model results reveal two of the same trends which were observed experimentally: (1) minimum TFN decreases with increasing temperature, and (2) the stoichiometry at which the minimum occurs becomes more fuel-rich as the temperature increases. Thus, the data and the calculations both indicate that a high temperature fuel-rich zone favors lower NO_x emissions.

The information presented in Figure 13 on the conversion of TFN to NO during burnout suggests that there might be a combination of certain fuel and nitrogen species which would minimize the second-stage conversion to NO. The presence of hydrocarbons leaving the first stage could affect second-stage NO formation. Folsom, et al (24) have shown that in a simple diffusion flame the conversion (or retention) of NH_3, HCN or NO is affected by the CH_4 content of the fuel. NH_3 conversion is low when hydrocarbons are present, but hydrocarbons are necessary for the reduction of NO or HCN. Thus, the minimum NO emission may depend upon the production of an optimum TFN/fuel mixture for burnout. The presence of HCN in the rich zone is strongly linked to the existence of hydrocarbons as shown in Figure 16. The line corresponds to results obtained from the model calculations at $1650^\circ K$. If HCN is undesirable for the ultimate reduction of NO it appears that the temperature should be sufficient to oxidize all of the hydrocarbon species within the rich zone.

SECTION 6

CONCLUSIONS

The results of the bench-scale studies on the influence of fuel properties and thermal environment indicate that:

- With liquid fuels, fuel nitrogen content is the primary composition variable affecting fuel NO formation. NO_x emissions increase with increasing fuel nitrogen. Alternative liquid fuels correlate with the high-nitrogen petroleum oils.
- Staged combustion dramatically reduces both fuel and thermal NO_x formation. Minimum emissions occur at a primary zone stoichiometric ratio between 0.75 and 0.85 depending on the combustion conditions.
- First-stage stoichiometry determines the dominant TFN species. Below SR_1=0.8 HCN is the dominant species, and above SR_1=0.8, NO is the dominant species. NH_3 concentrations at the first-stage exit generally accounted for less than 20 percent of the fuel nitrogen.
- Exhaust NO_x emissions are directly related to the TFN concentration at the first-stage exit. NO_x control for high-nitrogen fuels is most effective when a rich primary zone is held at an optimum stoichiometry to minimize the TFN concentration. This concentration is further minimized by increasing the temperature of the fuel-rich zone.

REFERENCES

1. Mansour, M. N. and M. Gerstein. Correlation of Fuel Nitrogen Conversion to NO_x During Combustion of Shale Oil Blends in a Utility Boiler. In: Proceedings of Symposium on Combustion of Coal and Synthetic Fuels, American Chemical Society, March 1978.

2. Heap, M. P. et al. Control of Pollutant Emissions from Oil-Fired Package Boilers. In: Proceedings of the Stationary Source Combustion Symposium, EPA-600/2-76-1526, NTIS, Springfield, Virginia, 1976.

3. Bowman, C. T. Kinetics of Nitric Oxide Formation in Combustion Processes. In: Proceedings of Fourteenth Symposium (International) on Combustion, The Combustion Institute, Pittsburgh, Pennsylvania 1973.

4. Martin, G. B. and E. E. Berkau. An Investigation of the Conversion of Various Fuel Nitrogen Compounds to NO in Oil Combustion. In: Proceedings of AIChE Symposium Series No. 126, 68, 1972.

5. Turner, D. W., R. L. Andrews, and C. W. Siegmund. Influence of Combustion Modification and Fuel Nitrogen Content on Nitrogen Oxide Emissions from Fuel Oil Combustion. In: Proceedings of AIChE Symposium Series No. 126, 68, 1972.

6. Pershing, D. W., J. E. Cichanowicz, G. C. England, M. P. Heap, and G. B. Martin. The Influence of Fuel Composition and Flame Temperature on the Formation of Thermal and Fuel NO_x in Residual Oil FLames. In: Proceedings of Seventeenth Symposium (International) on Combustion, The Combustion Institute, Pittsburgh, Pennsylvania, 1979.

7. Heap, M. P. NO_x Emissions from Heavy Oil Combustion. International Flame Research Foundation Report for Contract 68-02-0202, IJmuiden, Holland, 1977.

8. Malte, P. C. The Behavior of NH and CN in Nitrogen-Doped High Intensity Recirculative Combustion. Paper presented at the WSS Combustion Institute, Berkeley, California, October 1979.

9. Takagi, T., T. Tatsumi, and M. Ogasawara. Nitric Oxide Formation from Fuel Nitrogen in Staged Combustion: Roles of HCN and NH_i. Combustion and Flame, 35, 17, 1979.

10. Fenimore, C. P. Studies of Fuel Nitrogen species in Rich Flame Cases. In: Proceedings of Seventeenth Symposium (International) on Combustion, The Combustion Institute, Pittsburgh, Pennsylvania, 1979.

11. Haynes, B. S. Reactions of NH_3 and NO in the Burnt Gases of Fuel-Rich Hydrocarbon-Air Flames. Combustion and Flame, 28, 81, 1977.

12. Gerhold, B. W., C. P. Fenimore, and P. K. Dederick. Two Stage Combustion of Plain and N Doped Oil. In: Proceedings of Seventeenth Symposium (International) on Combustion, The Combustion Institute, Pittsburgh, Pennsylvania, 1979.

13. Haebig, J. E., B. D. Davis, E. R. Dzuna. Preliminary Small-Scale Combustion Tests of Coal Liquids. Environmental Science Technology, 10:3, 243, 1976.

14. Muzio, L. J., and J. K. Arand. Small-Scale Evaluation of the Combustion and Emissions Characteristics of SRC Oil. Paper presented at the ACS Fuel Chemistry Symposium, Anaheim, California, March 1978.

15. Downs, W., and A. J. Kubasco. Characterization and Combustion of SRC-II Fuel Oil. EPRI Report No. FP-1028, Palo Alto, California, 1979.

16. Mansour, M. N. Factors Influencing NO_x Production During the Combustion of SRC-II Fuel Oil. Paper presented at the WSS Combustion Institute, Berkeley, California, October 1979.

17. Hersch, S., B. F. Piper, D. J. Mormile, G. Stegman, E. G. Alfonsin, and W. C. Rovesti. Combustion Demonstration of SRC-II Fuel Oil in a Utility Boiler. Paper presented at the ASME Winter Annual Meeting, New York, New York, December 1979.

18. Dzuna, E. R. Combustion Test of Shale Oils. Paper presented at the CSS Combustion Institute, Columbus, Ohio, April 1976.

19. Mansour, M. N., and M. Gerstein. Correlation of Fuel Nitrogen Conversion to NO_x During Combustion of Shale Oil Blends in a Utility Boiler. Paper presented at the ACS Symposium on Combustion, Anaheim, California, March 1978.

20. Chen, S. L., M. P. Heap, R. K. Nihart, D. W. Pershing, and D. P. Rees. The Influence of Fuel Composition on the Formation and Control of NO_x in Pulverized Coal Flames. Paper presented at the WSS Combustion Institute, Irvine, California, 1980.

21. England, G. C., D. W. Pershing, J. H. Tomlinson, and M. P. Heap. Emission Characteristics of Petroleum and Alternate Liquid Fuels. Paper presented at the AFRC NO_x Symposium, Houston, Texas, October 1979.

22. England, G. C., M. P. Heap, D. W. Pershing, R. K. Nihart, and G. B. Martin. Mechanisms of NO_x Formation and Control: Alternative and Petroleum-Derived Fuels. Paper presented at the Eighteenth Symposium (International) on Combustion, The Combustion Institute, Waterloo, Canada, August 1980.

23. Corley, T. L. Development of a Kinetic Mechanism to Describe the Fate of Fuel Nitrogen in Gaseous Systems. Paper presented at the Fifth E.P.A. Fundamental Combustion Research Workshop, Newport Beach, California, 1980.

24. Folsom, B. A., C. W. Courtney, and M. P. Heap. The Effects of LBG Composition and Combustor Characteristics on Fuel NO_x Formation. Paper presented at the ASME Gas Turbine Conference and Exhibit and Solar Energy Conference, San Diego, California, 1979.

25. Sarofim, A.F., J. H. Pohl and B. R. Taylor. Mechanisms and Kinetics of NO_x Formation: Recent Developments. Paper presented at the 69th Annual Meeting AICHE, Chicago, Illinois, 1976.

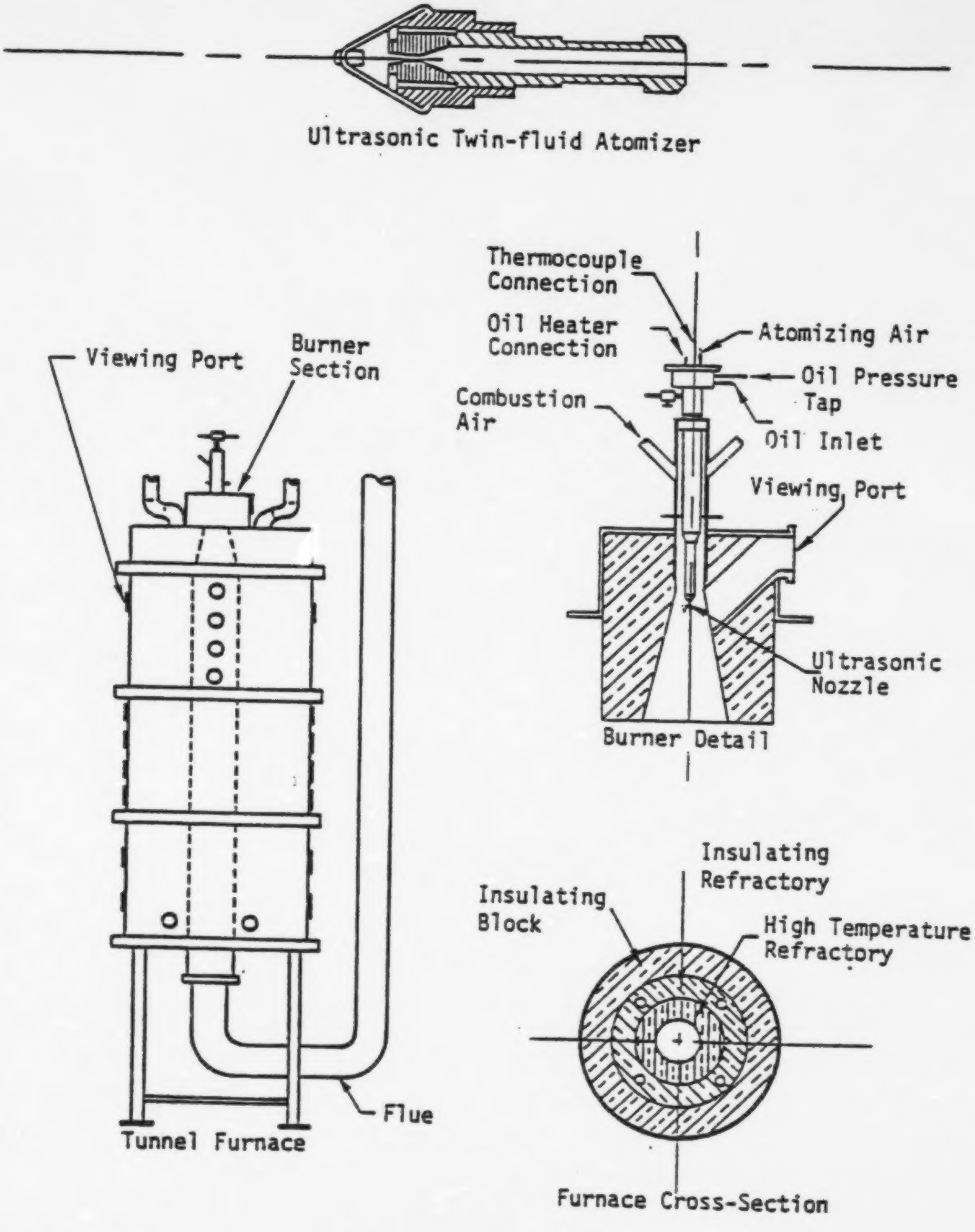

Figure 1. Details of the Tunnel Furnace System.

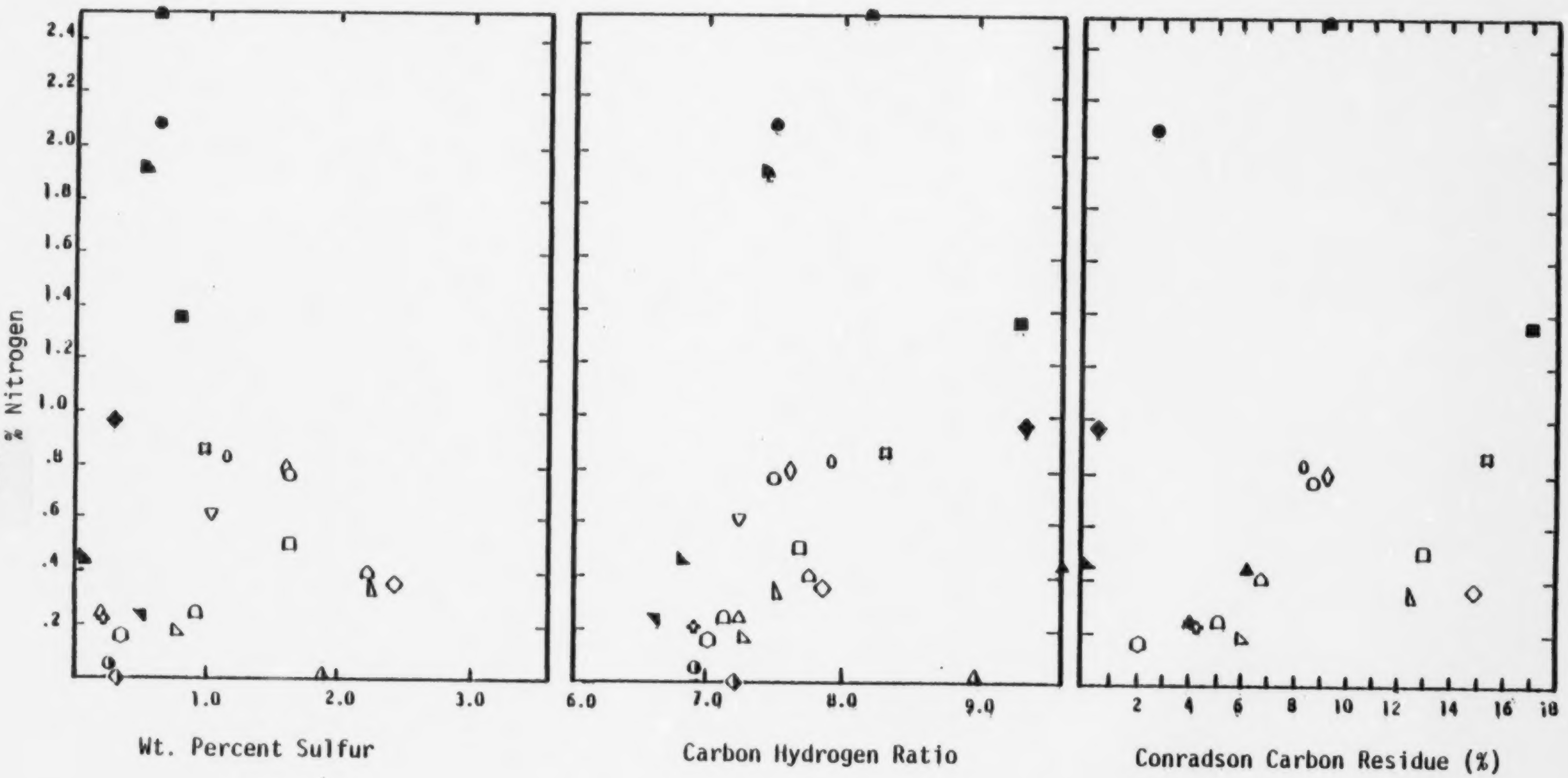

Figure 2. Properties of Fuels Tested.

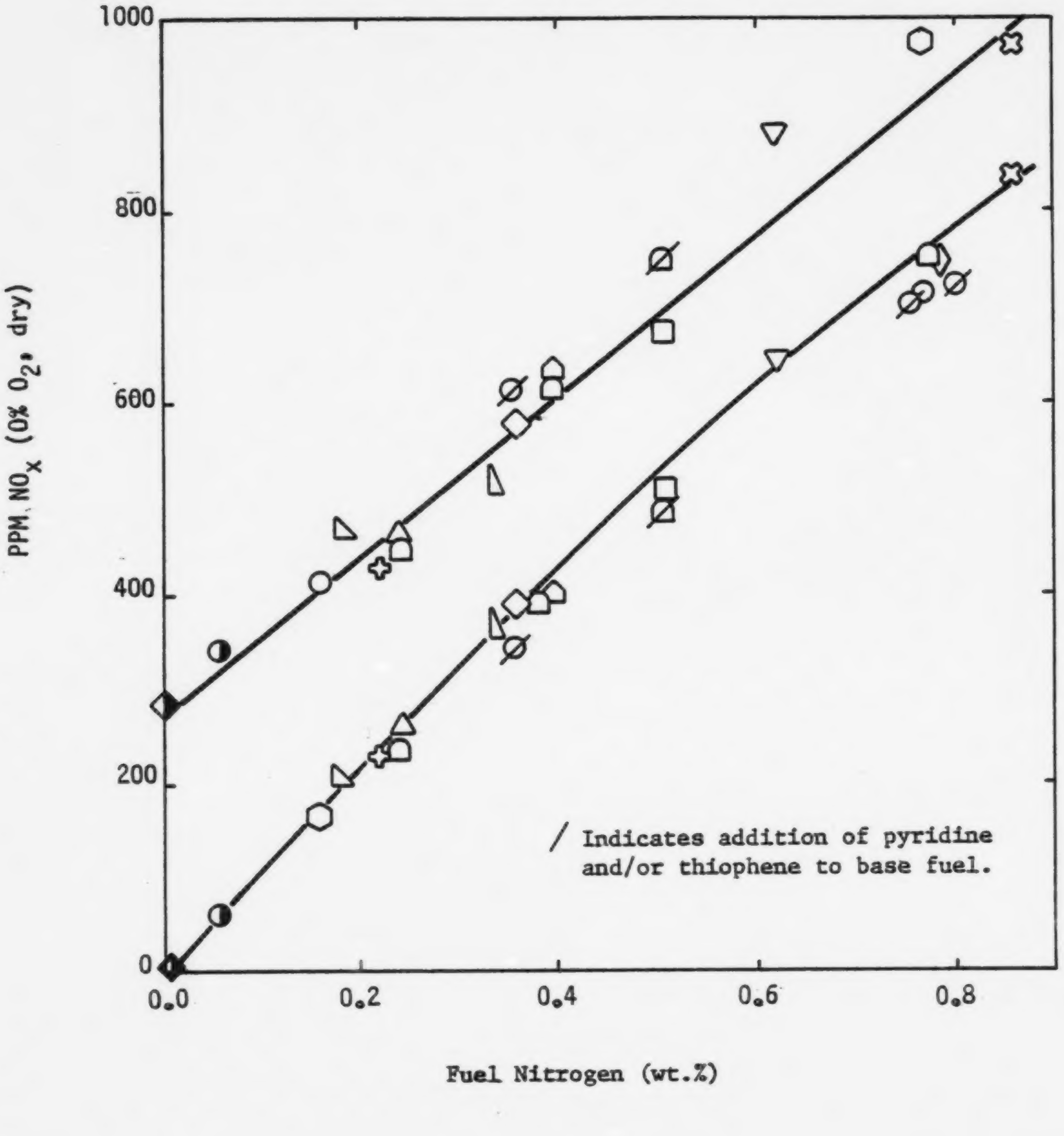

Figure 3. Total and Fuel NO$_x$ Emissions from Pure and Doped (pyridine and thiophene Petroleum Fuels-Tunnel Furnace.

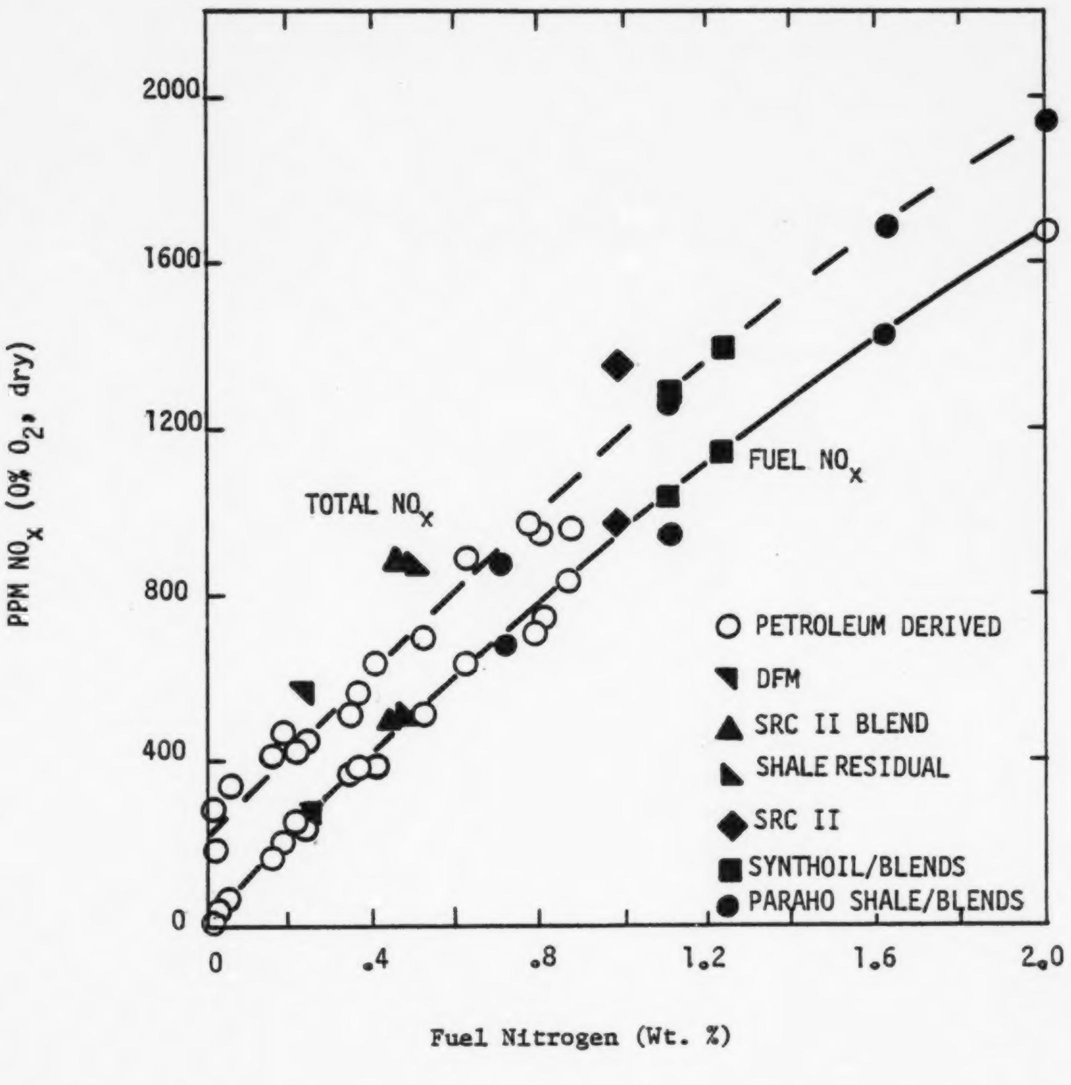

Figure 4. The Effect of Fuel Nitrogen Content on Total and Fuel NO_x (5% Excess Oxygen).

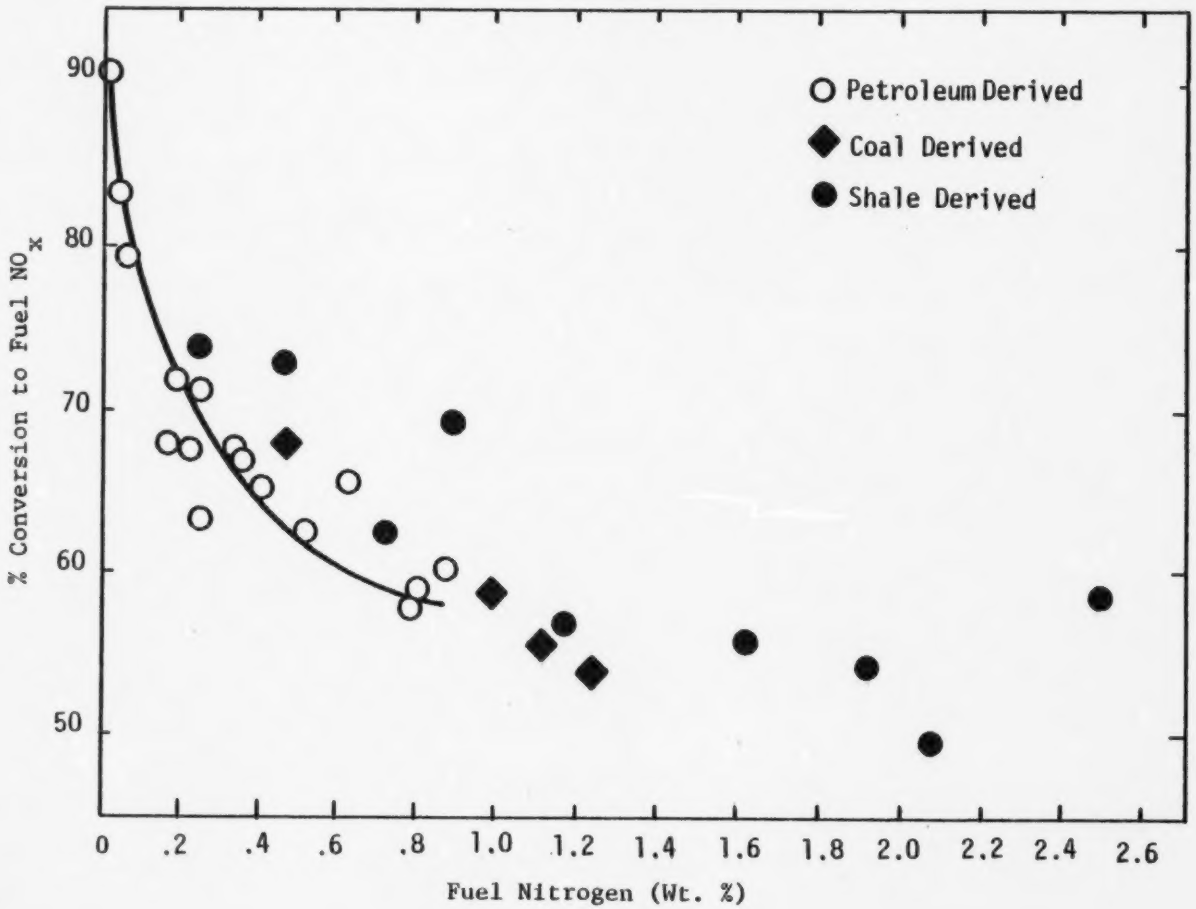

Figure 5. Fuel Nitrogen Conversion - Comparison of Alternate and Petroleum Derived Fuels.

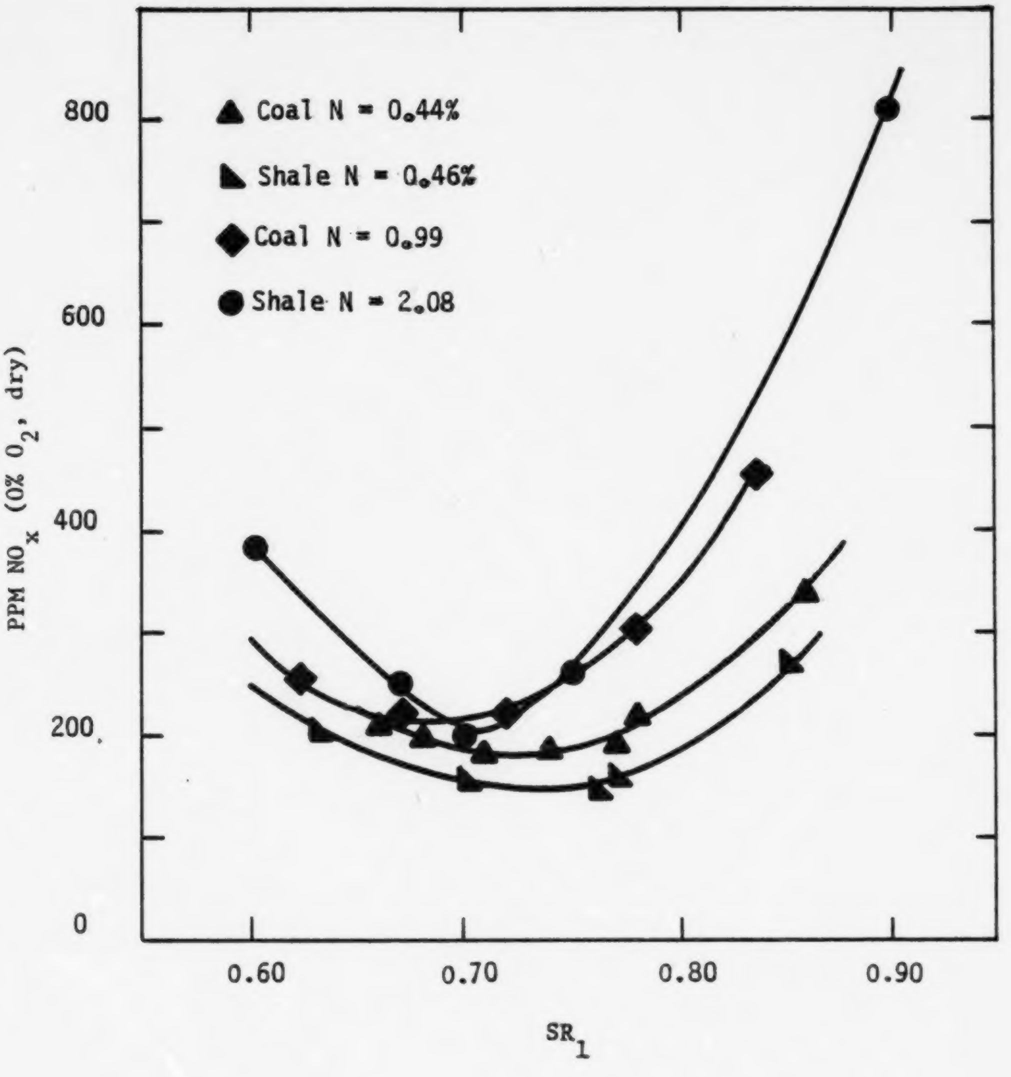

Figure 6. Minimum NO$_x$ Levels Achieved with Alternate Fuels. (Tunnel Furnace Primary Zone Residence Time .83 Sec.)

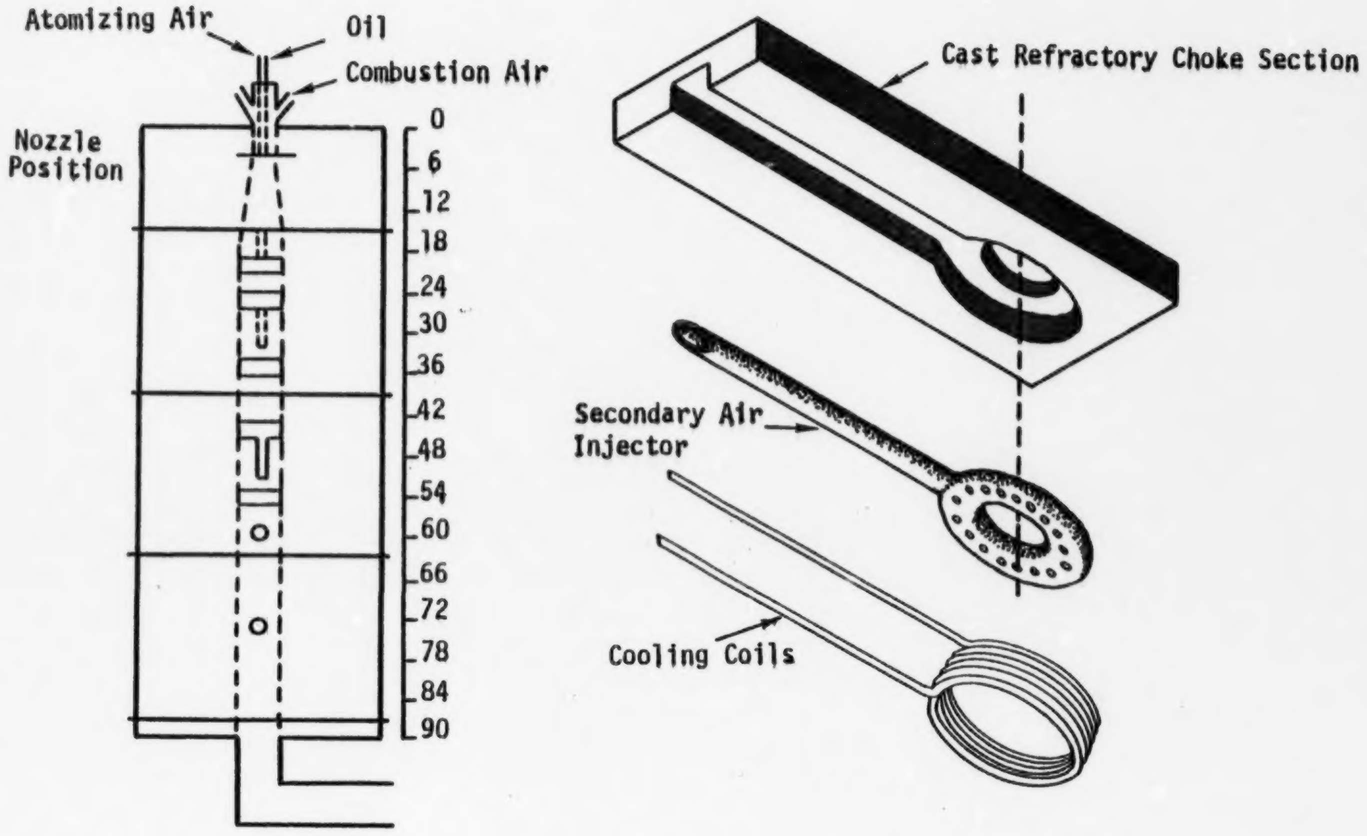

Figure 7. Modified Tunnel Furnace.

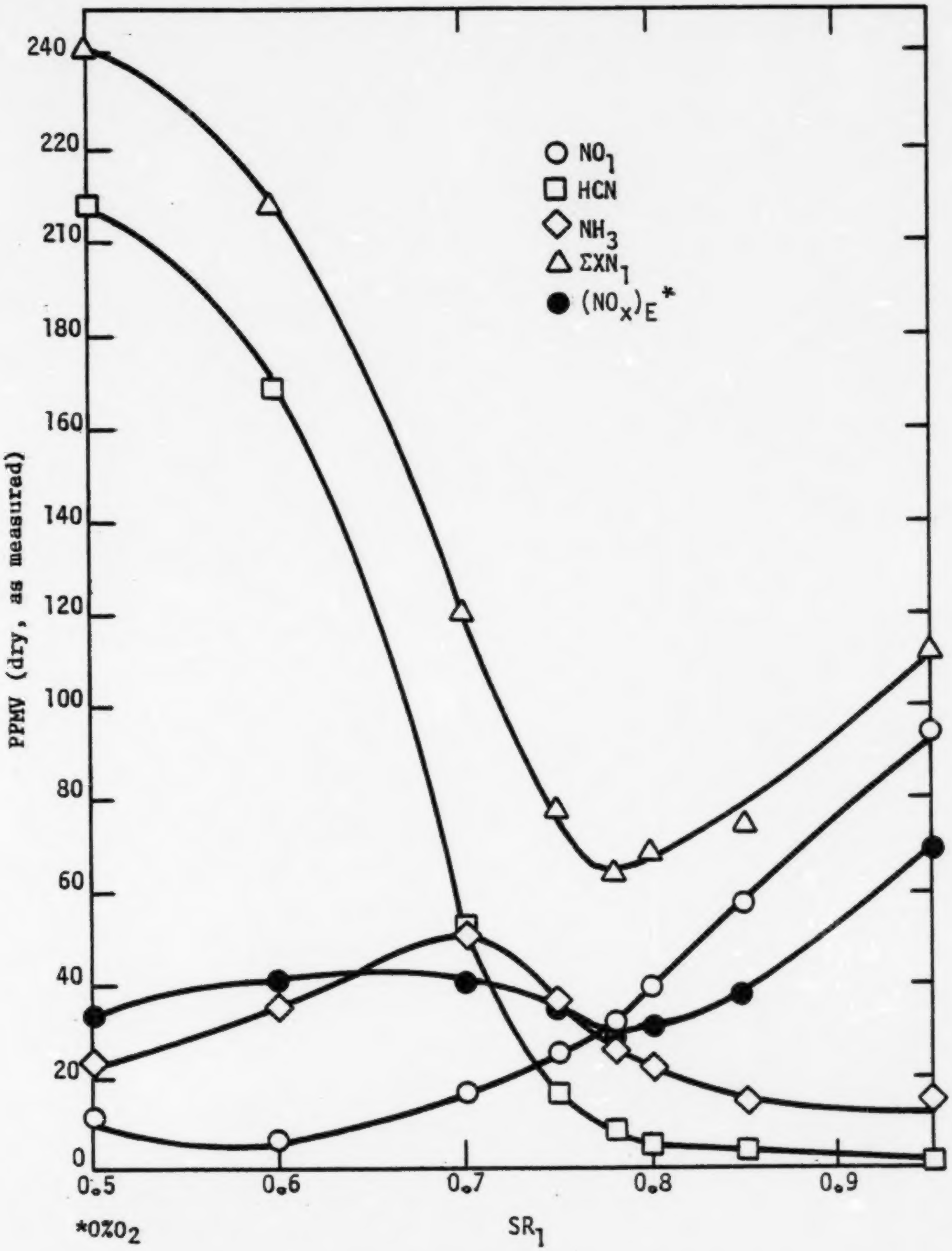

Figure 8. Detailed In-Flame Species Measurements with Alaskan Diesel Oil (D1).

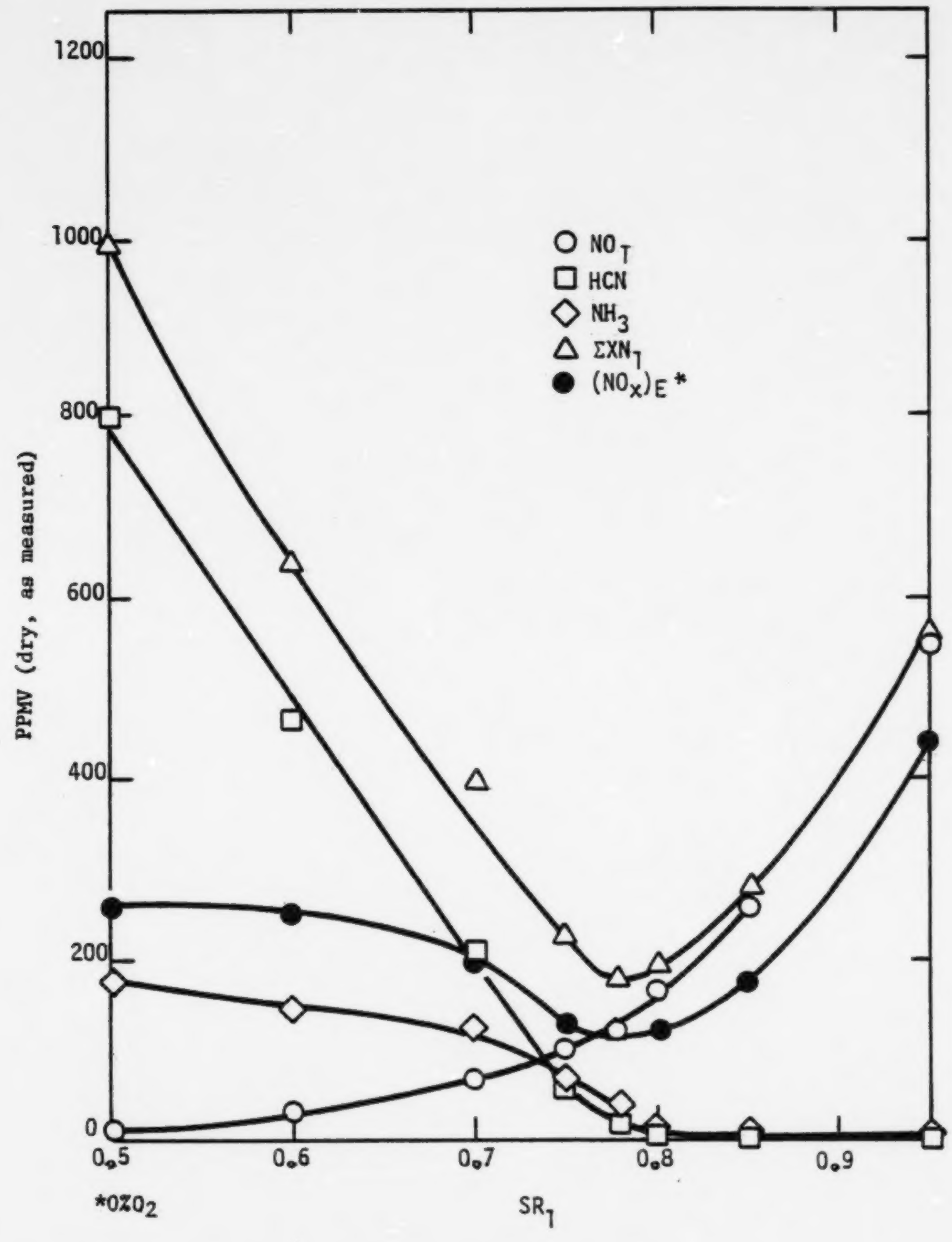

Figure 9. Detailed In-Flame Measurements with Kern County Crude Oil (R14).

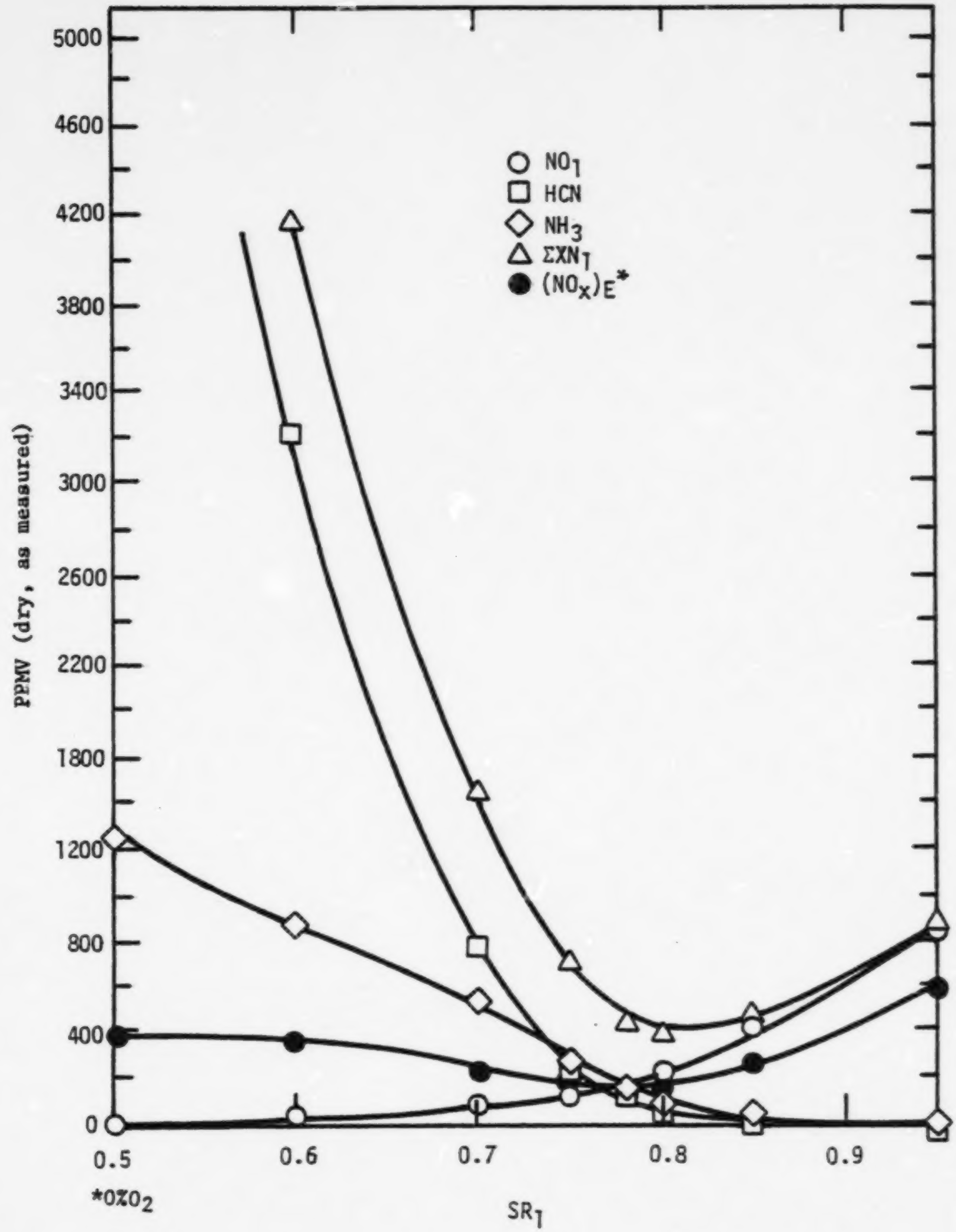

Figure 10. Detailed In-Flame Measurements With +850°F Shale Fraction (A8).

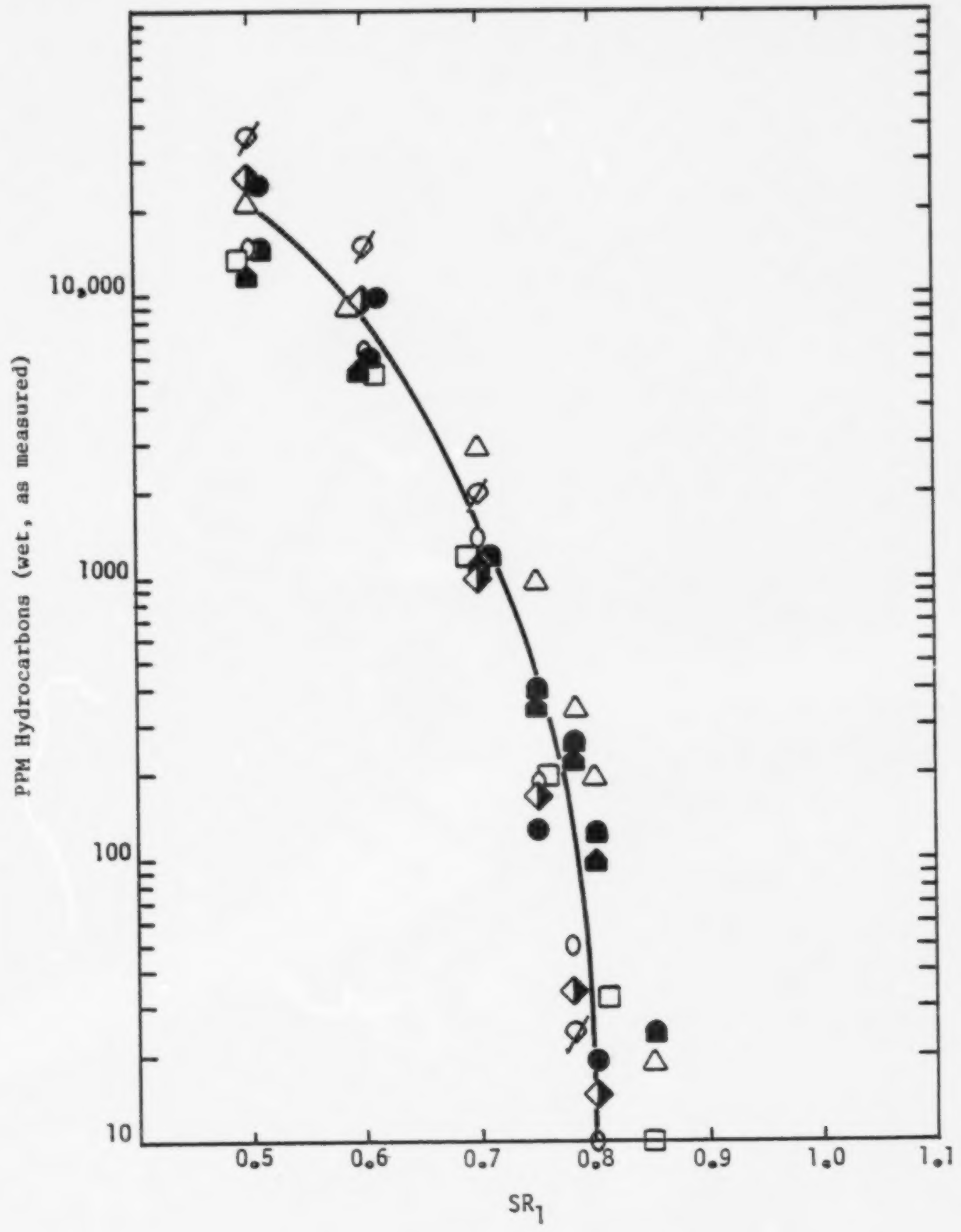

Figure 11. First Stage Hydrocarbon Production.

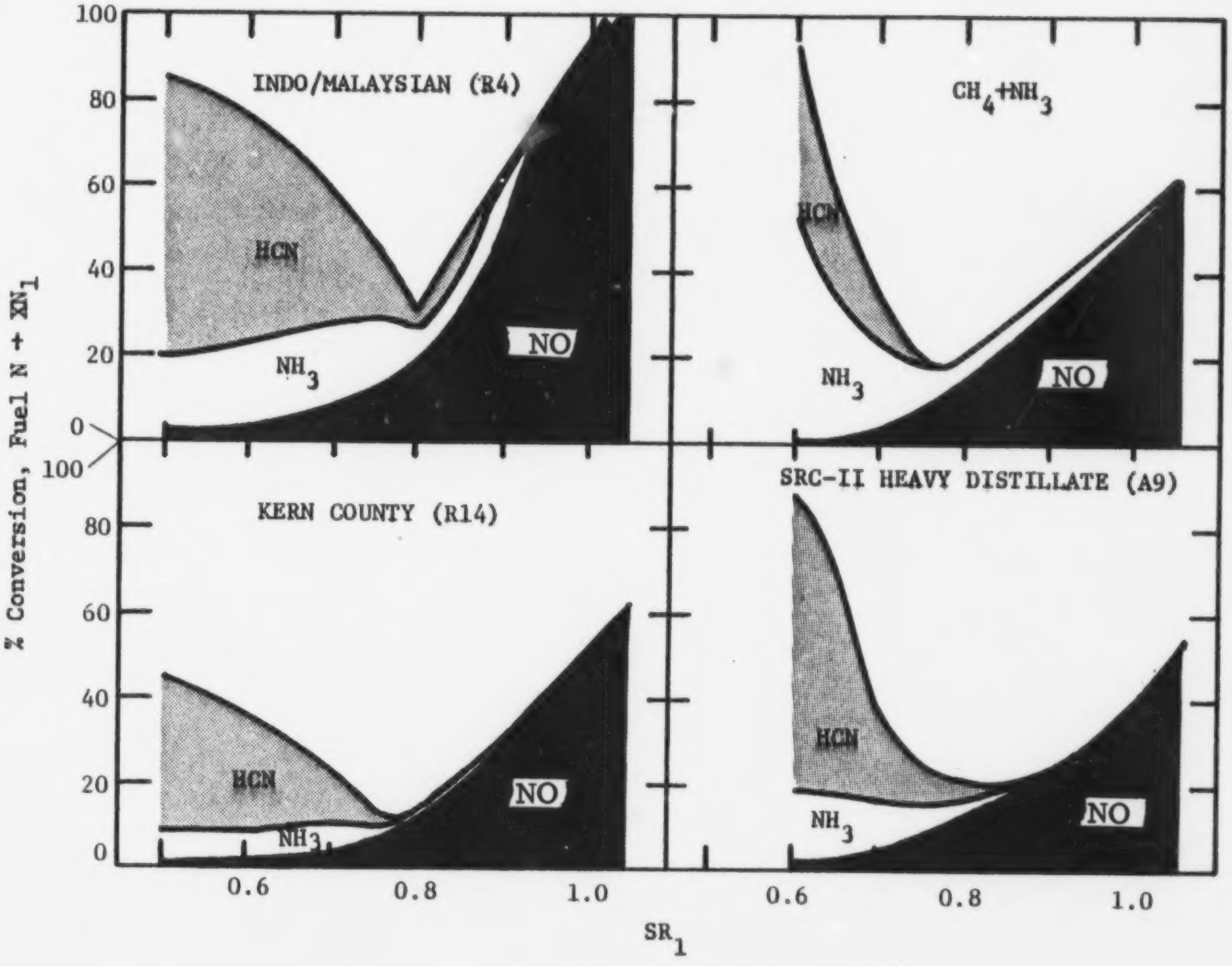

Figure 12. Distribution of First-Stage XN Species for Alternative and Petroleum Derived Fuels.

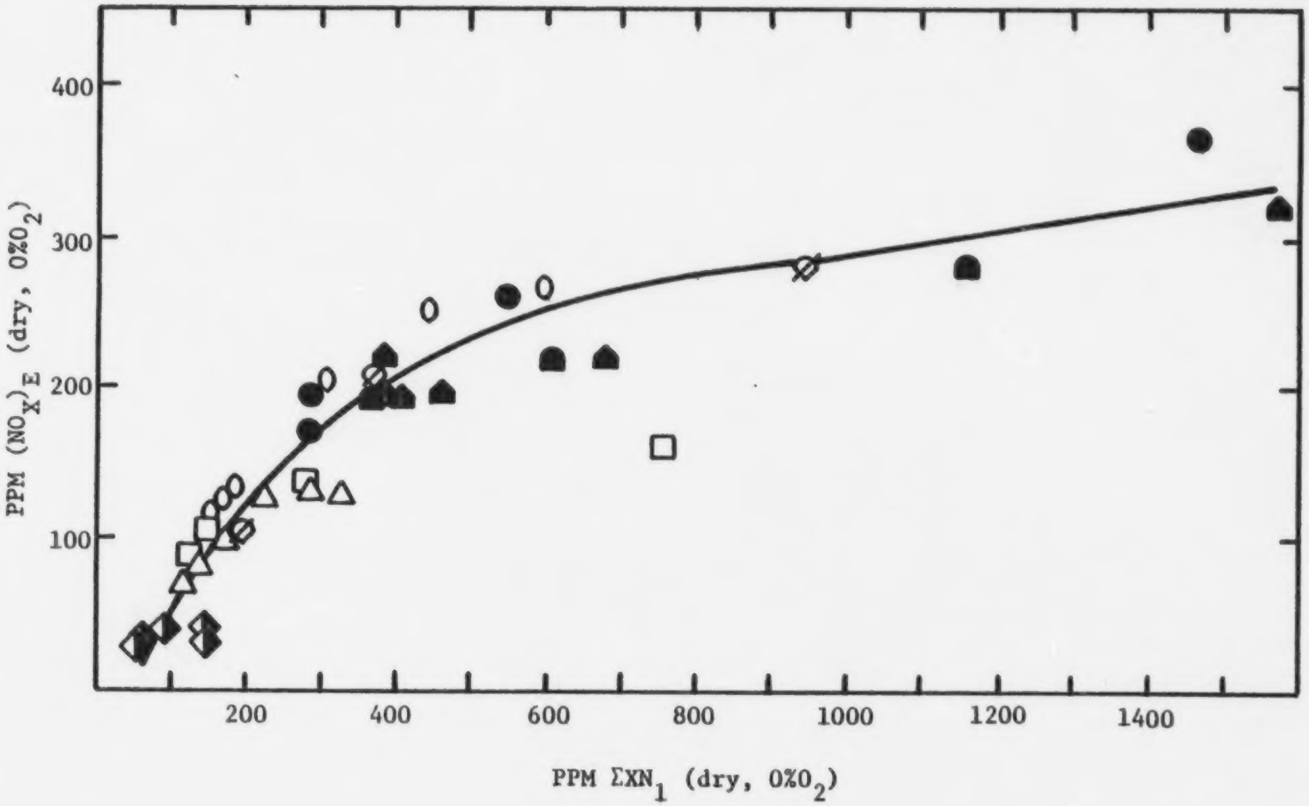

Figure 13. Exhaust NO_x Versus TFN at the Exit of the First Stage.

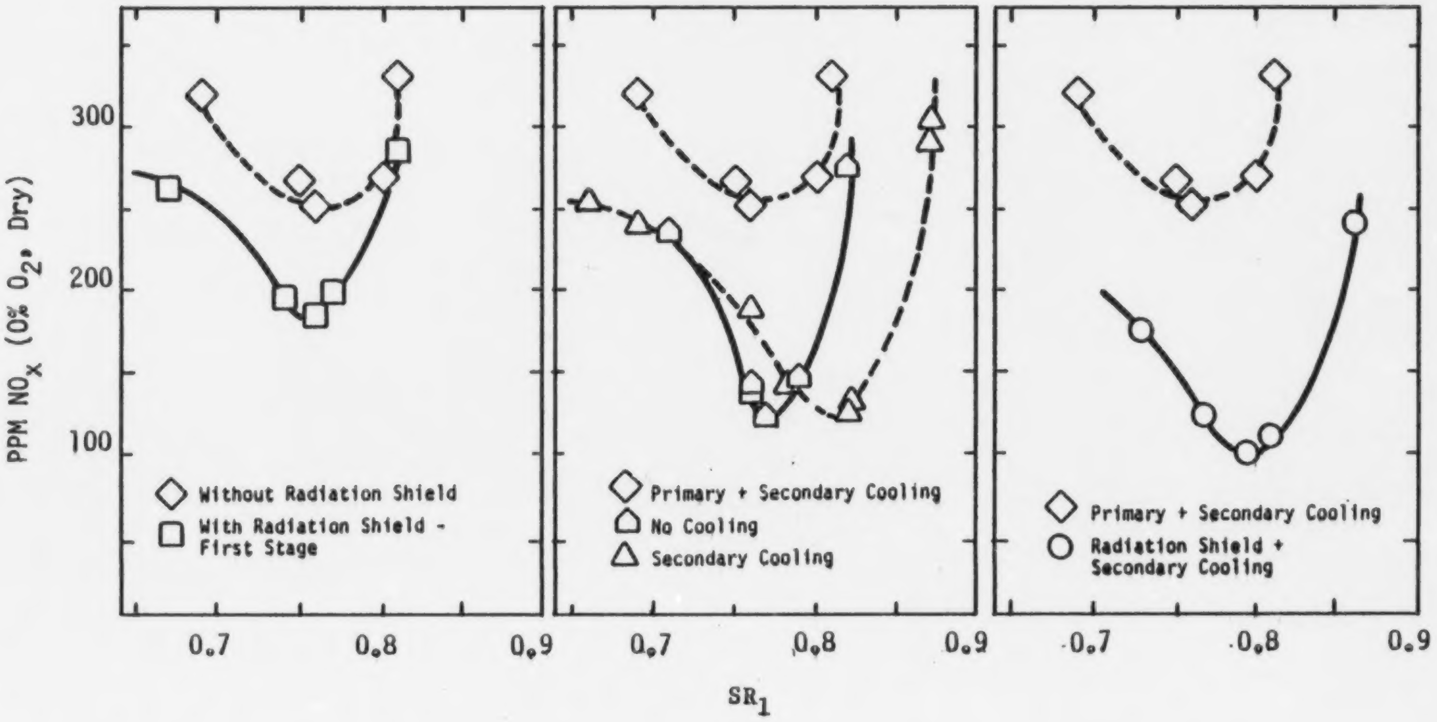

(a) (b) (c)

Figure 14. Influence of Heat Extraction Profile in the First and Second Stage upon Exhaust NO_x Emissions.

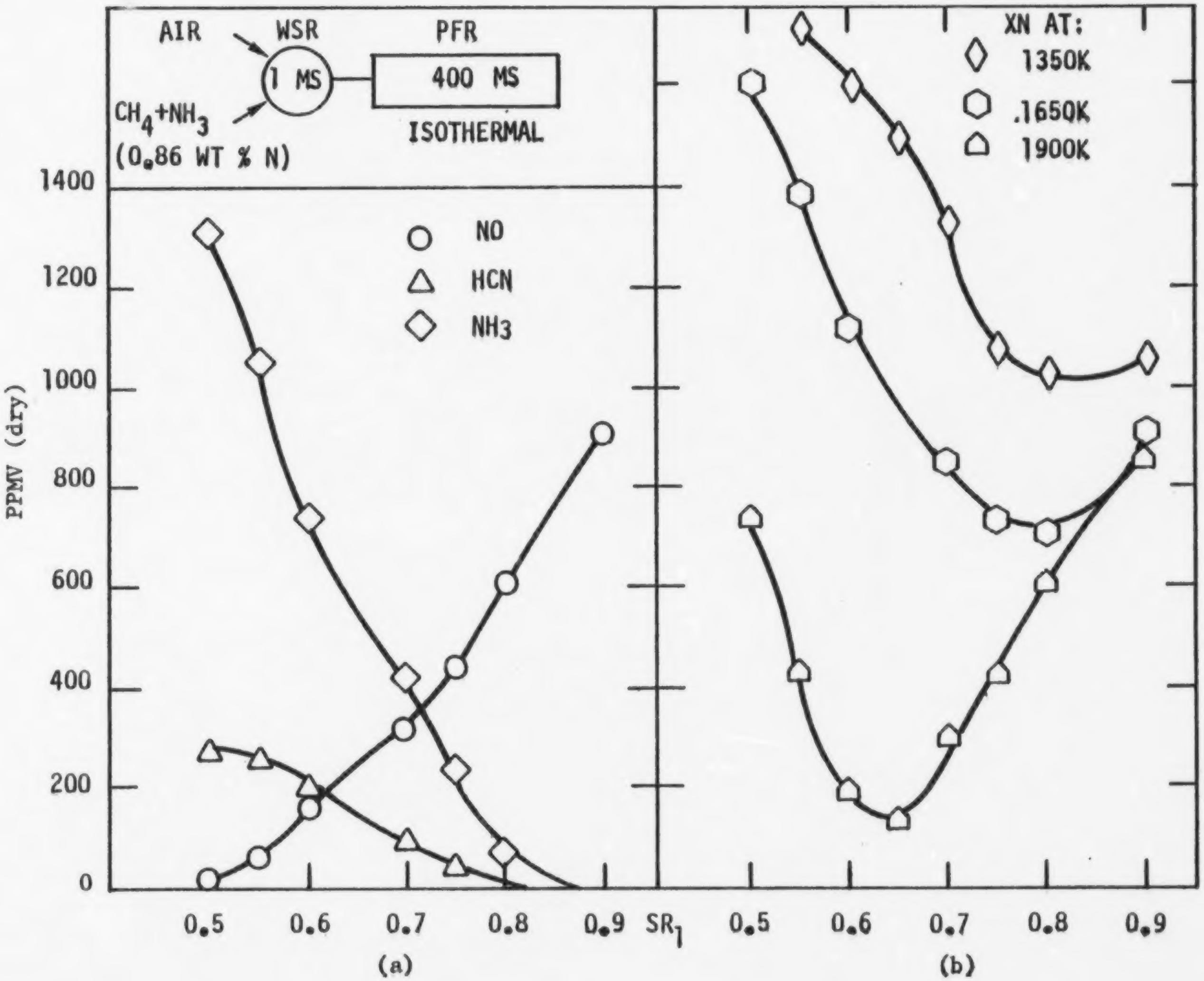

Figure 15. Calculated XN Species Distributions.

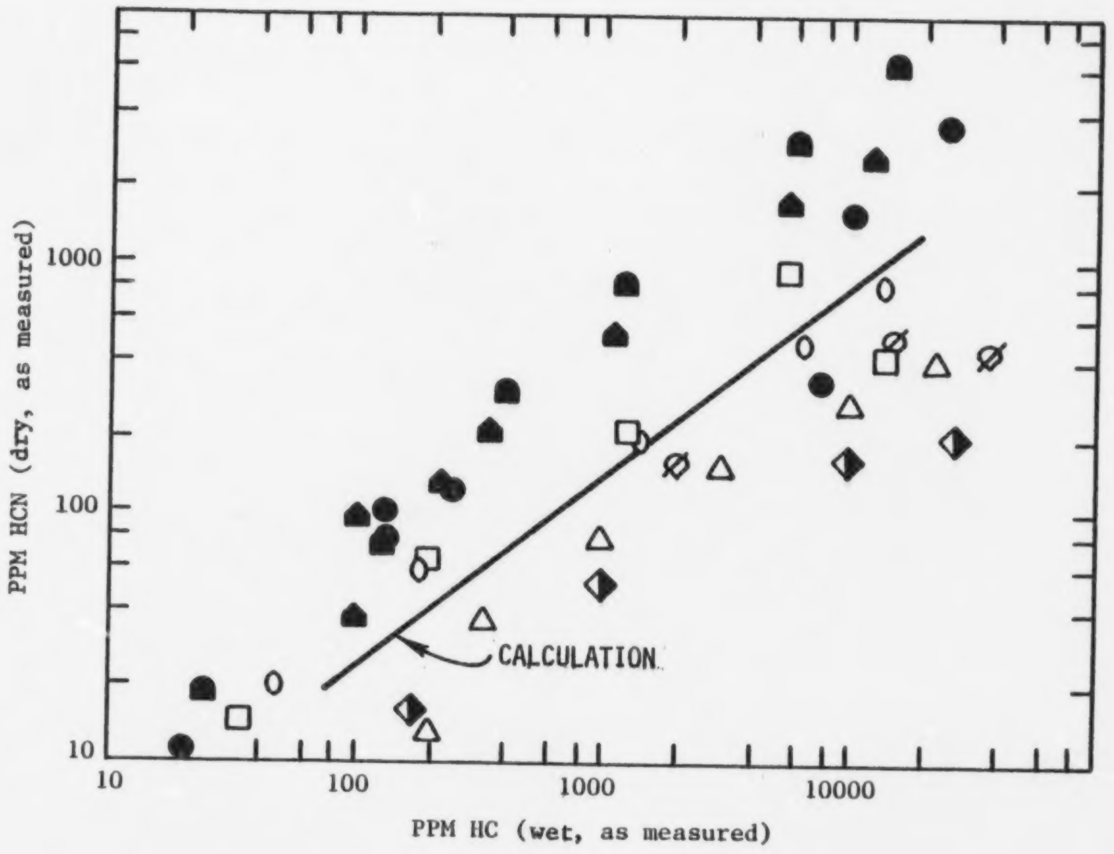

Figure 16. HCN Production Versus Hydrocarbons in the First Stage.

Table 1. Detailed Fuel Analyses

	D1	D2	D3	R1	R2	R3	R4	R5	R6	R7	R8	R9	R10
	Alaskan Diesel	W. Texas Diesel	California No. 2 Oil	East Coast	Middle East	Low Sulfur No. 6 Oil	Indo/ Malaysian	Venezuelan Desulphurized	Pennsylvania (Amarada Hess)	Gulf Coast	Venezuelan	Alaskan	California
Symbol	◆	▲	◐	⬡	◺	✙	△	∩	▵	◇	⌂	□	▽
Ultimate Analysis:													
Carbon, %	86.99	88.09	86.8	86.54	86.78	86.57	86.53	85.92	84.82	84.62	85.24	86.04	85.75
Hydrogen, %	12.07	9.76	12.52	12.31	11.95	12.52	11.93	12.05	11.21	10.77	10.96	11.18	11.83
Nitrogen, %	0.008	0.026	0.053	0.16	0.18	0.22	0.24	0.24	0.34	0.36	0.40	0.51	0.62
Sulfur, %	0.31	1.88	0.27	0.36	0.67	0.21	0.22	0.93	2.26	2.44	2.22	1.63	1.05
Ash, %	<.001	<.001	<.001	0.023	0.012	0.02	0.036	0.033	0.067	0.027	0.081	0.034	0.038
Oxygen, %	0.62	0.24	0.36	0.61	0.41	0.46	1.04	0.83	1.3	1.78	1.10	0.61	0.71
Conradson Carbon Residue, %				2.1	6.0	4.4	3.98	5.1	12.4	14.8	6.8	12.9	
Asphaltene, %				0.34	3.24	0.94	0.74	2.59	4.04	7.02	8.4	5.6	
Flash Point, °F				205	350	325	210	176	275	155	210	215	
Pour Point, °F				50	48	105	61	48	66	40	58	38	19.5
API Gravity at 60°F	33.1	18.3	32.6	24.9	19.8	25.1	21.8	23.3	15.4	13.2	14.1	15.6	246.1
Viscosity, SSU, at 140°F	33.0	32.0	30.8	131.2	490	222.4	199	113.2	1049	835	742	1,071	70.00
at 210°F	29.5	28.8	29.5	45	131.8	69.6	65	50.5	240	181	196.7	194	
Heat of Combustion:													
Gross Btu/lb			19,330	19,260	19,070	19,110	19,070	18,400	18,520	18,240	18,240	18,470	
Net Btu/lb				18,140	17,980	17,970	17,980	17,300	17,500	17,260	17,400	17,580	
Calcium, ppm				7.1	1.2	9.52	14	8.7	9.2	4.4	9.1	6.9	
Iron, ppm				16	2.6	123.6	16	6.5	13.2	19	11	24	
Maganese, ppm				0.09	0.02	0.46	0.13	0.09	0.10	0.13	0.09	0.06	
Magnesium, ppm				3.7	0.08	2.23	3.6	3.6	3.3	0.4	3.8	1.4	
Nickel, ppm				6.7	13	14.10	19		32.7	29	52	50	
Sodium, ppm				37	0.98	3.74	15		64.5	3.6	32	37	
Vanadium, ppm				14	25	3.11	101		81.5	45	226	67	

Table 1. Detailed Fuel Analyses (Continued)

	R11	R12	R13	R14	A1	A2	A3	A4	A5	A6	A7	A8	A9
	California	California	California	California (Kern County)	Shale-Derived DFM	Synthoil	Crude Shale	SRC II Blend	Shale Residual	SRC II	Shale Fraction (520-850°F)	Shale Fraction (+850°F)	SRC II Heavy Distillate
	○	◊	✧	⬯	◥	■	●	▲	◣	◆	◗	●	☗
Ultimate Analysis:													
Carbon, %	85.4	85.33	86.66	86.61	86.18	86.30	84.6	89.91	86.71	85.91	85.39	85.92	88.98
Hydrogen, %	11.44	11.23	10.44	10.93	13.00	7.44	11.3	9.27	12.76	8.74	11.53	10.61	7.64
Nitrogen, %	0.77	0.79	0.86	0.83	0.24	1.36	2.08	0.45	0.46	0.96	1.92	2.49	1.03
Sulfur, %	1.63	1.60	0.99	1.16	0.51	0.80	0.63	0.065	0.28	0.30	0.72	0.63	0.39
Ash, %	0.043	0.032	0.20	0.030	0.003	1.56	.026	0.004	0.009	0.04	0.002	0.24	0.058
Oxygen, %	0.71	1.02	0.85	0.44	1.07	2.54	1.36	0.30	0.03	4.08	0.44	0.11	1.90
Conradson Carbon Residue, %	8.72	9.22	15.2	8.3	4.1	23.9	2.9	6.18	0.19	0.51	0.07	9.3	
Asphaltene, %	5.18	5.18	8.62	3.92	0.036	16.56	1.33	4.10	0.083		0.12	4.24	
Flash Point, °F		150	180	255	162	210	250	70	235	1.73	255	370	265
Pour Point, °F	38	30	42	65	40	80	80	<-72	90	-55	70	95	8
API Gravity at 60°F	15.4	15.1	12.6	12.3	33.1	S=1.14	20.3	10.0	29.0		22.3	12.0	1.3
Viscosity, SSU, at 140°F	854	748.0	720	4630	36.1	10,880	97	40.6	54.3	39	62.9	3050	67.2
at 210°F	129	131.6	200	352	30.7	575	44.1	32.5	37.3		41.8	490	41.3
Heat of Combustion:													
Gross Btu/lb	18,470	18,460	18,230	18,430	19,430	16,480	18,290	17,980	19,350	17,100	18,520	18,000	17,120
Net Btu/lb	17,430	17,440	17,280	17,430	18,240	15,800	17,260	17,130	18,190		17,470	17,030	16,240
Calcium, ppm	21	14	90.6	4.4	0.13	1,670	1.5	0.33	4.20		<,05	238	
Iron, ppm	73	53	77.2	15	6.3	109	47.9	3.9	<0.5		2.9	86	
Manganese, ppm	0.8	0.1	0.87	0.15	0.06	6.2	0.17	<0.5	<0.5		0.033	1.3	
Magnesium, ppm	5.1	3.8	31.4	1.1		170	5.40	0.17	0.15		0.021	51	
Nickel, ppm	65	82	88.0	68	0.43	2.6	5.00	<0.5	<0.5		<0.5	7.4	
Sodium, ppm	21	2.6	22.3	3.4	0.09	148	11.71	0.31	2.51		<0.1	11	
Vanadium, ppm	44	53	66.2	39	<.1	6.5	<.3	<1.0	<1.0		<0.2	1.1	

FATE OF COAL NITROGEN DURING COMBUSTION

By:

S. L. Chen, M. P. Heap, D. W. Pershing, R. K. Nihart,
and D. P. Rees
Energy and Environmental Research Corporation
8001 Irvine Boulevard
Santa Ana, California 92705

ABSTRACT

Twenty-six coals covering all ranks have been burned under a wide variety of conditions to ascertain the impact of coal properties on the fate of fuel nitrogen. Three burner systems were used to vary the rate of fuel air mixing and fuel NO was identified by using a nitrogen free oxidant. It was found that fuel nitrogen content is not the only property controlling fuel NO formation. It appears that nitrogen volatility as well as total nitrogen content is important, particularly under well-mixed conditions.

Detailed specie concentration measurements were made under fuel rich conditions and it was found that:

- the partition of nitrogen between NO, NH_3 and HCN was dependent upon coal type;
- total gas-phase nitrogen specie (fuel rich) correlated with exhaust NO (fuel lean);
- reducing the temperature of the first stage increased gas-phase nitrogen specie concentrations but reduced fuel emissions.

This work will help in the generalization of low NO_x burner technology to a wide range of fuels.

ACKNOWLEDGMENTS

This work was supported under EPA Contract 68-02-2667. The authors are happy to acknowledge the contribution of their colleagues in the conduct of the experiments, particularly W. R. Seeker for his help with particle temperature measurement and also the encouragement and ideas resulting from discussions with A. Axworthy, A. F. Sarofim and P. Soloman.

SECTION 1

INTRODUCTION

The development of NO control strategies for coal-fired boilers has received considerable attention over the past decade. Pilot-scale studies[1] established that fuel/air mixing controlled by burner design dictated the formation of NO in pulverized coal flames, and that rapid mixing of coal volatiles and air promoted NO formation. Bench-scale and research studies further established the significance of fuel nitrogen oxidation,[2] the factors controlling fuel nitrogen evolution,[3,4] and the conditions that affect NO formation from pulverized coal under fuel-rich conditions.[5,6] Burner designs have been demonstrated at various scales[7,8,9] which are capable of minimizing emissions from field-operating boilers, and more advanced combustion control techniques have been proposed which will radically change current state-of-the-art boiler designs.[10] This study is directed toward an assessment of the impact of coal properties on the fate of fuel bound nitrogen under both fuel lean and fuel rich conbustion conditions.

The impact of coal properties on NO emissions from practical boilers is of considerable importance at a time when boiler operators are being faced with more stringent pollution control requirements, and the need to burn a wide range of fuels. Twenty-six coals from three continents have been burned under well-defined conditions using air and nitrogen-free mixtures as the oxidant. Experimental data has been obtained on the fate of fuel nitrogen specie under fuel-rich conditions as a means of establishing optimum time/temperature stoichiometry histories for minimum NO production under staged combustion conditions.

SECTION 2

EXPERIMENTAL

Figure 1 presents a schematic of the down fired tunnel furnace and the three burner systems used in this study. Complete details of both the furnace and the associated measurement systems have been presented elsewhere[11]. Pulverized coal was supplied pneumatically from a hopper-fed screw feeder to one of two burners which allowed the coal to be burned entirely premixed or as a diffusion flame. Premixing was achieved by direct impingement of the coal jets with the main combustion air supply in a premixing chamber which was separated from the combustion zone by a series of watercooled tubes which prevented flashback (see Fig. 1). The coal/air mixture burned in a plug flow mode with the ignition zone situated in the refractory divergent. The coal-plus-transport air could also be supplied to a variable swirl burner and injected either axially or radially, thus allowing experiments to be conducted with very different fuel/air mixing characteristics. Variable swirl was achieved by dividing the total oxidant flow into two streams, one of which flowed axially around the fuel injector and the other through swirl vanes. Swirling all the combustion air and injecting the coal/air mixture radially into the combustion airstream produced a flame with backmixed characteristics. An axial diffusion flame was obtained with a single-hole axial fuel injector and sufficient swirl in the combustion air to provide a stable ignition zone at the fuel injector. The characteristics of the solid fuels tested are presented in Table 1.

SECTION 3

FUEL-LEAN CONDITIONS

Figure 2 shows fuel NO emissions as a function of percent nitrogen in the original coal (dry, ash free) for 26 different coals ranging from anthracite through lignite. These data were obtained in the unmodified,[11] tunnel furnace at a nominal firing rate of 21 Kw (approximately 5 lbs/hr coal) with 5 percent excess O_2 and 550°K secondary-air preheat. The particle-size distribution was 65 percent through 200 mesh and the unpreheated primary air was maintained at 15 percent of stoichiometric air. Fuel NO was defined as the emission when molecular nitrogen was excluded from the oxidant and the fuel was burned in a mixture of argon, carbon dioxide, and oxygen.

The data obtained with the premixed burner (upper plot) indicate that in general fuel NO increases with increasing fuel nitrogen; however, within any rank there are other properties which have a significant impact on fuel nitrogen oxidation. For example, the Savage (△) and Beulah (□) lignites both contain approximately 1.05 weight percent nitrogen, yet their emissions differ by more than 60 percent. The German bituminous coal (Saar●) correlates well with the American bituminous coals; however, a predried Australian lignite (▼) gives uncharacteristically high emissions. As expected, the low volatile anthracite (▽) produces significantly less fuel NO than the high volatile bituminous coals.

Radial swirling and axial diffusion flames were also used to investigate the coupling between fuel properties and fuel/air contacting. These data (lower plots, Figure 2) indicate that fuel effects are also significant in diffusion flames. Fuel NO emissions produced with the radial diffusions burner also tend to increase with increasing fuel nitrogen content. The axial flame data show no obvious dependence on nitrogen content, but other composition parameters are obviously of major importance. The Australian lignite (▼) produced an extremely stable, well attached axial flame and uncharacteristically low NO emissions.

Comparison of data for the three burner types indicates that initial premixing of the fuel and air leads to the highest conversion of the fuel nitrogen to fuel NO, particularly with high volatile, bituminous coals. This can be attributed to the fact that as the coal/air mixing varies from premixed to axial diffusion there is less oxygen in contact with the volatile fuel nitrogen fractions, and, therefore, the formation N_2 from the volatile nitrogen specie is maximized. The anthracite data (◸) indicate that with the low volatile coal, initial fuel/air contacting has relatively little effect on the exhaust emissions.

Attempts to correlate the data shown in Figure 2 on the basis of the nitrogen lost in the ASTM volatile determination or with such basic fuel properties as % nitrogen, % volatiles or coal rank proved unsuccessful. Axworthy et al[12] carried out a series of inert pyrolysis experiments and measured the volatile nitrogen which was converted to HCN at 1373°K using six of the coals from this study and Figure 3 shows that this pyrolysis data agrees qualitatively with the experimental results obtained in the premixed and radial diffusion flames. The Savage lignite (△) has the highest percentage conversion of fuel nitrogen to NO in the combustion experiment and also has the highest fractional volatile nitrogen yield in the inert pyrolysis study. The slope of the correlation decreases with decreasing mixing rate (premixed to radial diffusion) as would be expected.

SECTION 4

FUEL-RICH CONDITIONS

The control of NO emissions from coal fired combustors involves operations under fuel rich conditions initially, therefore the optimization of the residence time, temperature and stoichiometry of this initial zone and the impact of fuel properties are of considerable practical significance.

PRIMARY ZONE STOICHIOMETRY

Figure 4 summarizes staged combustion results for a variety of fuels with both the radial diffusion and premixed burners. The second stage air was injected radially inward from two sides at a distance of 0.86m from the burner. All of the data were obtained at 5 percent overall excess O_2.

Figure 4a shows typical results for two bituminous coals (Utah, Gauley Eagle), two lignite coals (Savage, Beulah) and a Pennsylvania anthracite. For most of the coals tested, as the first stage stoichiometry is reduced the NO decreases, reaches a minimum before increasing as the stoichiometry is further reduced. Anthracite (and a Utah coal char, not shown) do not exhibit this minimum. Figure 4b summarizes this data in the form of minimum NO emissions as a function of the stoichiometric ratio at which the minimum occurs. Decreasing the initial fuel/air contacting rate decreases the minimum achievable NO emissions. Further, the optimum stoichiometric ratio depends both upon the fuel composition and the initial mixing rate. Detailed in-flame measurements of gas concentrations, solids composition and concentration, and temperature were made for nine coals to define the relationship between coal composition and first stage composition. Figure 5 shows a set of typical results for the Beulah, North Dakota lignite with the premixed burner. All gas-phase concentration measurements are shown on an as-measured (dry) basis, except the exhaust NO concentrations which have been reduced to 0 percent O_2 (SR = 1.0). As the first-stage stoichiometry is reduced, the NO exiting the first stage decreases, but ultimately this is compensated for by an increase in other oxidizable nitrogen specie (e.g., HCN and NH_3). The particle temperatures (measured at 0.53 m using two-color pyrometry)[13] also decrease and a significant amount of both the nitrogen and carbon remain in the solid phase and are carried into the second-stage flame.

Thus, there exists a minimum in exhaust NO concentrations because of the competition between decreased first-stage NO and increased oxidizable gas- and solid-phase nitrogen specie.

FUEL PROPERTIES

The relationship between fuel composition and the fraction of the fuel nitrogen retained in the solid phase under a given set of combustion conditions must be known if the optimum first-stage stoichiometry is to be predicted for a given fuel. Figure 6a shows the fraction of the initial nitrogen which remained in the char at 1.17m as a function of the initial nitrogen content for the premixed burner at a first-stage stoichiometry of 0.5. As expected, there is no obvious correlation with either total fuel nitrogen or rank. A standard ASTM proximate analysis of the original coal was made and the resulting solid was analyzed for nitrogen to determine the fraction of the initial nitrogen volatized under standard conditions. Figure 6b shows these results and indicates that there is at least qualitative agreement between the in-flame solids sampling results and the modified ASTM coal analysis. The Savage, North Dakota lignite (△) retained only approximately 33 percent of its original nitrogen in the char after the ASTM volatile determination, and a similar, small fraction of the initial nitrogen was found in the solid material exiting the first stage of the experimental furnace. In contrast, the Alabama, bituminous coal (Rosa, ▢) retained over 60 percent of its nitrogen in the ASTM test, and also had a much higher fraction of its initial nitrogen still in the solid phase at the end of the first stage of the furnace.

Figure 7 summarizes the total gas-phase fixed nitrogen (TFN = NO + NH_3 + HCN) measurements for the nine coals tested. These data were obtaine at a distance of 1.17m and a primary-zone stoichiometry of 0.75 with the premixed burner. In general, TFN increases with increasing fuel nitrogen content (Figure 7a) and correlates well with the exhaust NO emissions measured under unstaged (excess air) conditions (Figure 7b). Those coals which have high emissions under excess-air conditions, produce large amounts of gas-phase nitrogen specie under fuel rich conditions (e.g., the Utah, bituminous coal, ○). The low-volatile anthracite (▽) gave very low emissions under excess-air operation and produced little TFN under fuel rich conditions.

Figure 8 shows the influence of coal composition on the partition of the gas-phase nitrogen specie. The upper curves are for bituminous coals from the West (Utah), the South (Alabama), and Germany (Saar). The fraction of the TFN present as NH_3 was small for all of the bituminous-coal studies (including the Rosa, Alabama coal, not shown). The Utah coal produced a significant amount of HCN compared to the other bituminous coals.

The Pennsylvania anthracite (lower left) formed almost no HCN or ammonia; at all stoichiometries the dominant TFN specie was NO. The Western, sub-bituminous coals exhibited much the same behavior as the Western lignite coals. In each of these cases, the dominant TFN specie was NH_3 below a stoichiometric ratio of approximately 0.7. HCN concentrations at 1.17m were small for all of the sub-bituminous and lignite coals. The fraction of the TFN leaving the first stage as NO was also substantially smaller than in the case of the bituminous and anthracite coals.

TIME/TEMPERATURE HISTORY

Figure 9 shows detailed axial profiles for 3 coals at a common stoichiometric ratio ($SR_1 = 0.60$) without the addition of second-stage air. The burnout results (based on the CO and the CO_2 measurements) indicate that the anthracite burns much slower initially than the bituminous and lignite coals. The first-stage NO from the anthracite forms slowly and then subsequently decays. Similar decays were observed with the Utah, bituminous and the North Dakota lignite; however, the initial NO formation was too rapid to be measured.

Significant amounts of HCN or ammonia were not observed with the Pennsylvania anthracite. Large quantities of HCN were formed and subsequently decayed with the Utah coal; small, relatively constant amounts of HCN were measured with the lignite coal. Significant amounts of NH_3 were measured at all axial positions with the lignite and to a lesser extent with the bituminous coals. From these data it is clear that increasing the residence time in the first stage of a pulverized-coal combustor decreases the exhaust NO emissions because it allows time for the TFN concentrations to decrease from their early high values. It should be noted that although the input mixture is overall fuel rich, the gas-phase will be oxidizing in the early stages.

Figure 10 shows similar results for the Utah coal with the radial-diffusion burner at a first-stage stoichiometry of 0.8. The uncooled data (open symbols) are analygous to the premixed results presented in Figure 9. As noted previously, HCN concentrations exceed the NH_3 concentrations and the NO decays rapidly with axial distance. Figure 10 also shows data for a case in which the first stage was heavily cooled by inserting a water-cooled coil (see Figure 1). This coil reduced the gas temperature approximately 350K and appears to have frozen the NO concentration. However, the HCN and NH_3 concentration continued to decay with time. Overall reduction of the first-stage temperature increased the TFN concentration at 1.17m substantially, because of the decreased rate of NO reduction. However, when second-stage air was added at 1.17m the exhaust emissions were lower with the lower first stage temperature which gave the higher TFN concentration.

SECTION 5

CONCLUDING REMARKS

Results have been presented ongoing investigations to assess the impact of coal properties on nitrogen oxide formation in pulverized coal flames. The effort to date has concentrated upon providing information to answer the following questions:

- What are the fuel characteristics that dominate fuel NO formation? Are they entirely chemical in nature? What is the impact of physical properties such as the particle size of the thermal environment on fuel NO formation?
- To what extent does fuel/air contacting interact with fuel characteristics in the formation of fuel NO?
- Is it possible to assess the emission characteristics of fuels in practical systems without prior field tests?

Conclusions to date can be summarized as follows:

FUEL-LEAN

Tests with 26 different coals indicate that fuel nitrogen content is not the only fuel property controlling the fate of fuel bound nitrogen during combustion. The volatility of fuel nitrogen compounds appears to affect NO formation particularly under well mixed conditions. Fuel NO emissions are reduced as the rate of fuel/air mixing is reduced and become even less dependent upon total fuel nitrogen content.

FUEL-RICH

Detailed studies on the optimization of the fuel-rich stage suggest that the optimum stoichiometry for minimum emissions is a function of both fuel composition and primary-zone mixing. As first-stage stoichiometry is decreased, the NO formed in the first stage decreases, but the other oxidizable gas nitrogen specie increase as does nitrogen retention in the char. Nitrogen retention in the solid phase may be correlated with appropriate coal analyses, but the production of gas-phase nitrogen specie appears to correlate only with excess air emissions.

The distribution of the TFN specie is strongly dependent upon the coal composition. With bituminous coals NH_3 appears to be a substantially less fraction of the tota than with sub-bituminous and lignite coals. Of the nine coals tested in detail, only one (Utah bituminous) formed substantial amounts of HCN under well mixed conditions. Pennsylvania anthracite formed almost no HCN or ammonia, even under extremely fuel rich conditions.

Johnson, et al,[10] showed that heat extraction in the primary stage of low NO_x combustor decreased exhaust NO_x emissions. The results from the present study indicate that reducing the first stage temperature slowed the rate of decay of both NO and other XN specie. Although the lower temperature fuel rich stage produced a higher TFN concentration, this did not result in higher final NO emissions.

REFERENCES

1. Heap, M. P., T. M. Lowes and R. Walmsley. Emission of Nitric Oxide from Large Turbulent Diffusion Flames. In: Proceedings of the Fourteenth Symposium (International) on Combustion, The Combustion Institute, Pittsburgh, PA 1973. p. 883.

2. Pershing, D. W. and J.O.L. Wendt. Pulverized Coal Combustion, The Influence of Flame Temperature and Coal Composition on Thermal and Fuel NO_x . In: Proceedings of the Sixteenth Symposium (International) on Combustion, The Combustion Institute, Pittsburgh, PA, 1977. p. 389.

3. Pohl, J. H. and A. F. Sarofim. Devolatilization and Oxidation of Coal Nitrogen. In: Proceedings of the Sixteenth Symposium (International) on Combustion, The Combustion Institute, Pittsburgh, PA, 1977. p. 491.

4. Solomon, P. R. and M. B. Colket. Coal Devolatilization. In: Proceedings of the Seventeenth Symposium (International) on Combustion, The Combustion Institute, Pittsburgh, PA, 1979. p. 131.

5. Wendt, J.O.L., D. W. Pershing, J. W. Lee and J. W. Glass. Pulverized Coal Combustion, NO_x Formation Mechanisms under Fuel-Rich and Staged Combustion Conditions. In: Proceedings of the Seventeenth Symposium (International) on Combustion, The Combustion Institute, Pittsburgh, PA, 1979. p. 77.

6. Rees, D. P., L. D. Smoot and P. O. Hedman. Nitrogen Oxide Formation Inside a Laboratory Pulverized Coal Combustor. Submitted for Consideration to the Eighteenth Symposium (International) on Combustion, The Combustion Institute, Pittsburgh, PA, August, 1980.

7. Barsin, J. A. Pulverized Coal Firing NO_x Control. In: Proceedings of the Second NO_x Control Technology Seminar, Electric Power Research Institute, 1978.

8. Vatsky, J. Experience in Reducing NO_x Emissions in Operating Steam Generators. In: Proceedings of the Second NO_x Control Technology Seminar, Electric Power Research Institute, July, 1979.

9. Zallen, D. M., R. Gershman, R., M. P. Heap and W. H. Nurick. The Generalization of Low Emission Coal Burner Technology. In: Proceedings of the Third Stationary Source Combustion Symposium, Vol. II, San Francisco, CA, 1979. EPA-600/7-79-0506. p. 73.

10. Johnson, S. A., P. L. Cioffi, T. M. Sommer and M. W. McElroy. The Primary Combustion Furnace System, An Advanced Low NO_x Concept for Pulverized Coal Combustion. In: Proceedings of the Second NO_x Control Technology Seminar, Electric Power Research Institute, 1978.

11. Chen, S. L., et al. The Influence of Fuel Composition of the Formation and Control of NO_x in Pulverized Coal Flames. Western States Section, The Combustion Institute, Spring Meeting, Irvine, CA, April 1980.

12. Axworthy, A. Pyrolysis Products of Various Coals under Inert Conditions. EPA Fundamental Combustion Research Meeting, Newport Beach, CA, January 1980.

13. Seeker, W. R., G. S. Samuelsen, M. P. Heap and J. D. Trolinger. The Thermal Decomposition of Pulverized Coal Particles. Submitted for Consideration to the Eighteenth Symposium (International) on Combustion, Pittsburgh, PA, August, 1980.

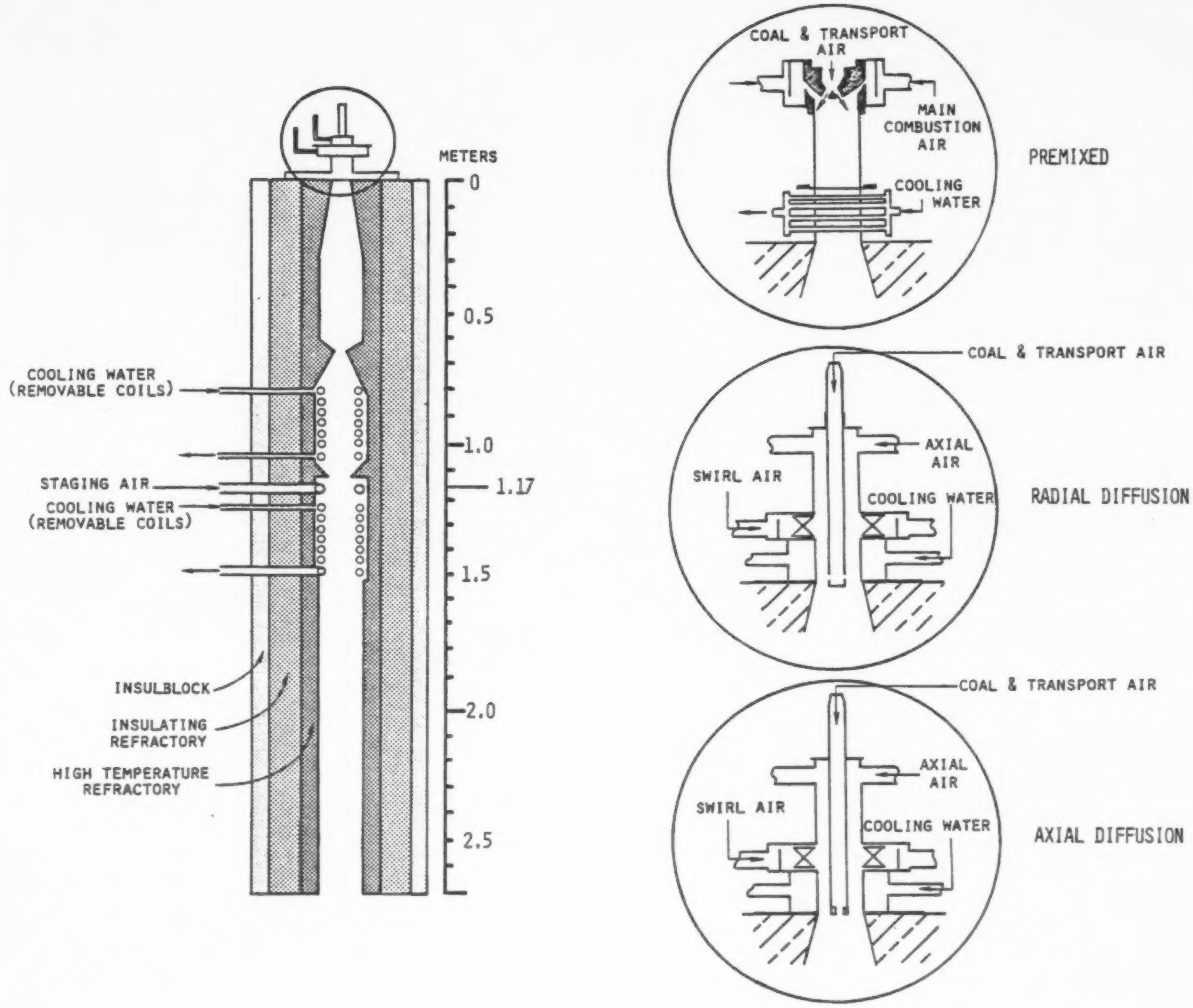

Figure 1. Schematic of Down Fired Tunnel Furnace and Burner Systems.

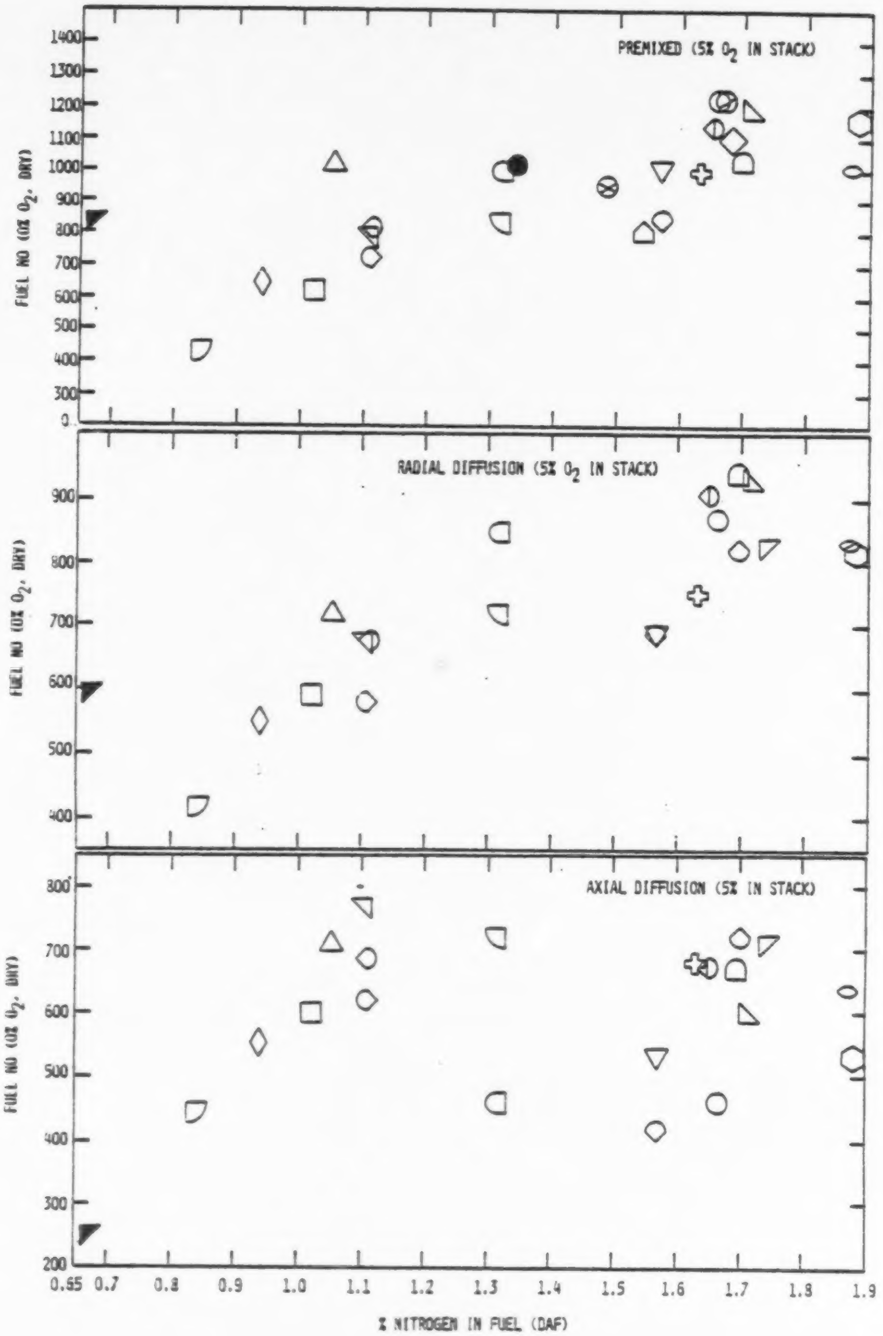

Figure 2. Fuel NO Formation as a Function of Coal Nitrogen Content and Fuel Air Mixing Characteristics.

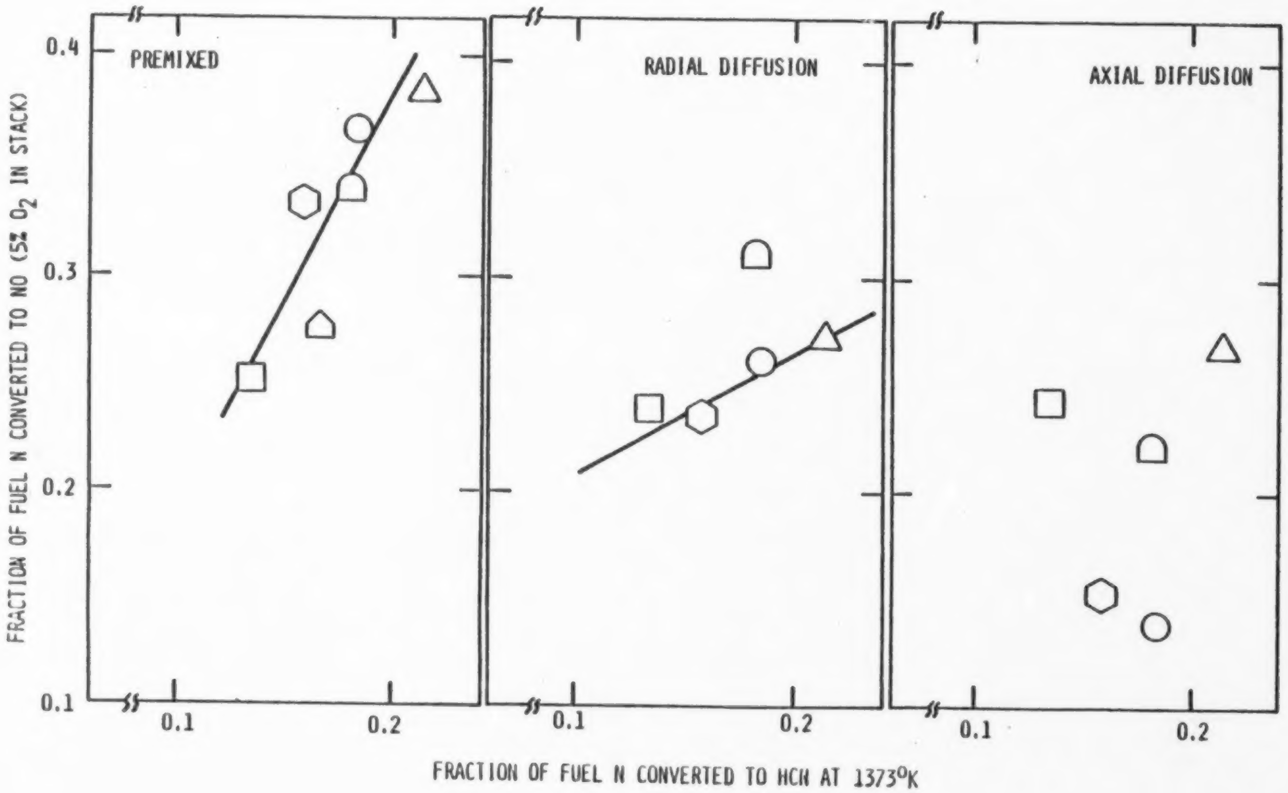

Figure 3. Fractional Conversion of Fuel Nitrogen to NO as a Function of HCN Formed During Inert Pyrolysis.[12]

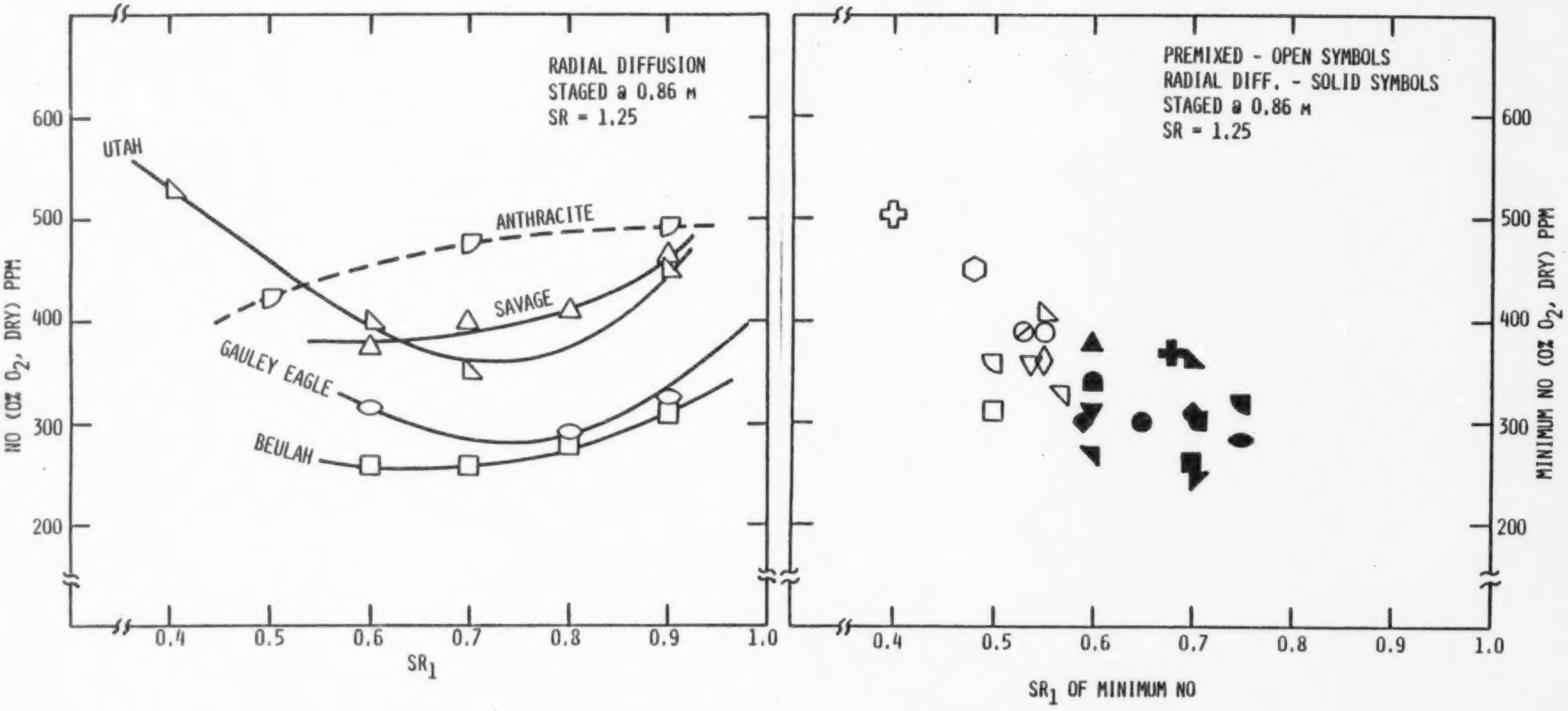

(a)

(b)

Figure 4. Staged NO Emissions: a) Effect of Coal Type, b) Effect of Mixing Characteristics.

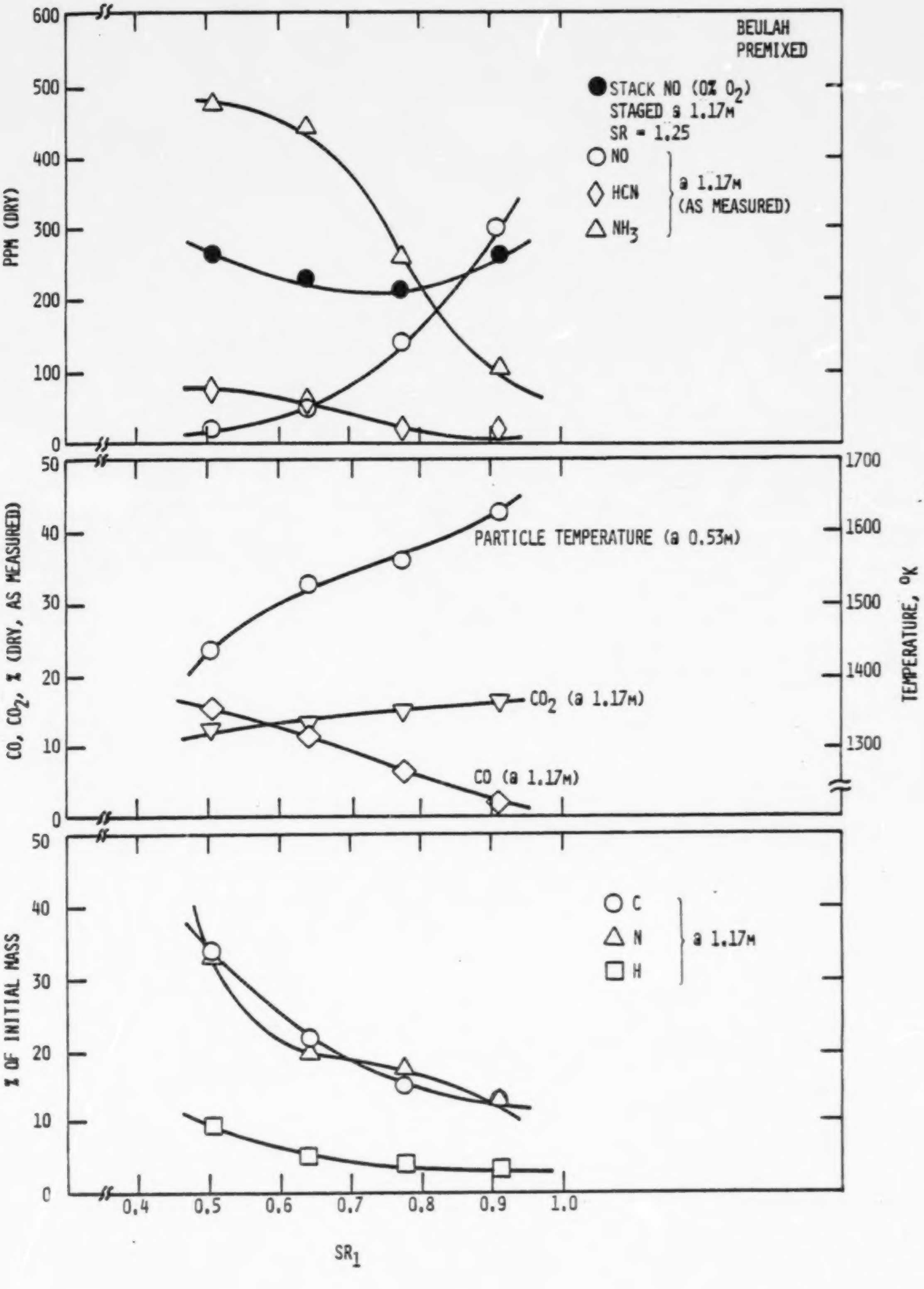

Figure 5. First Stage Exit Conditions.

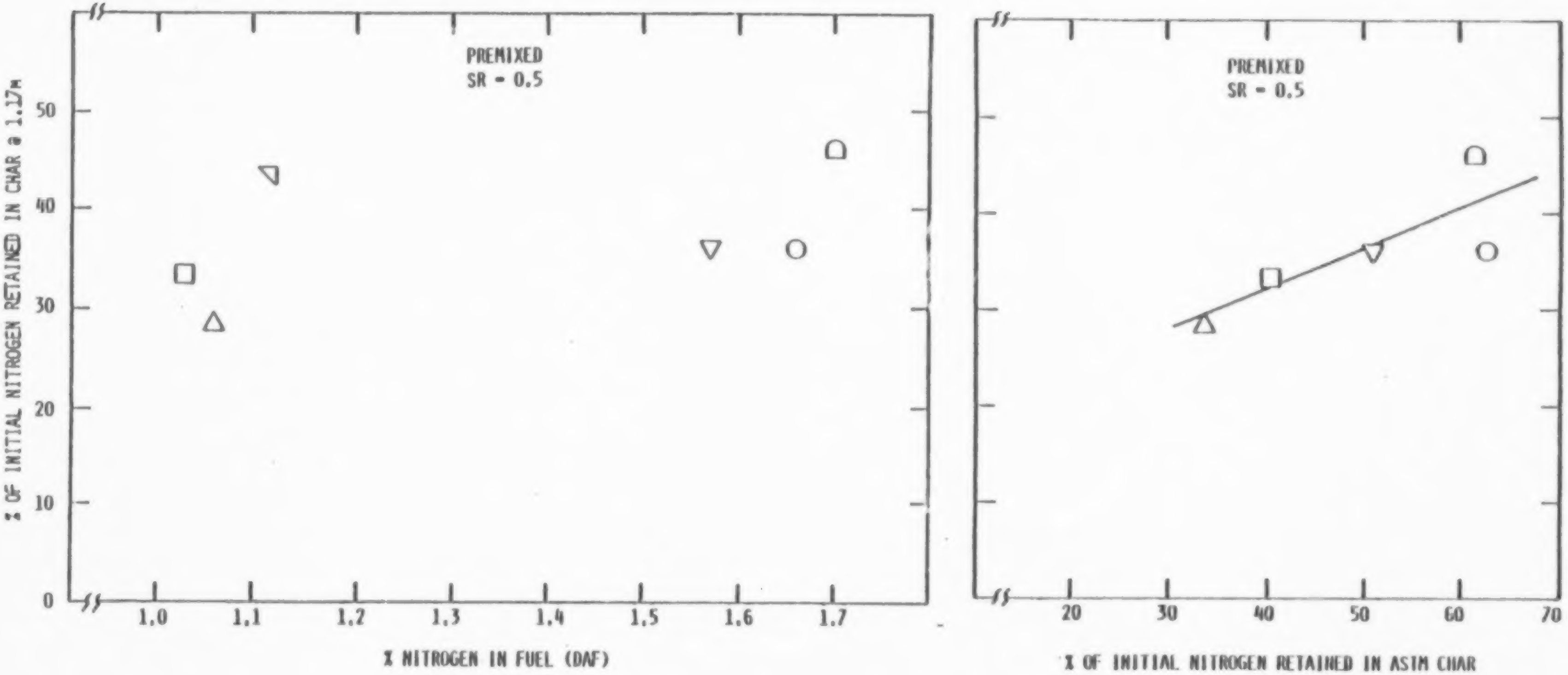

(a)

(b)

Figure 6. Nitrogen Remaining in Coal Char Under Staged Conditions.

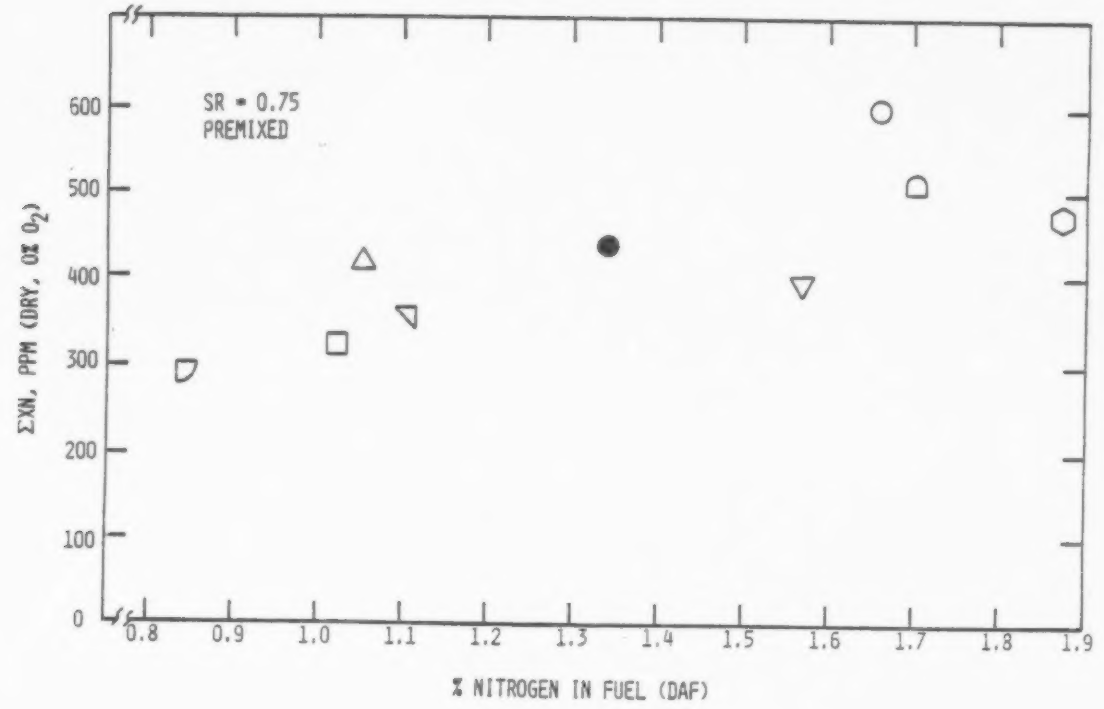

(a)

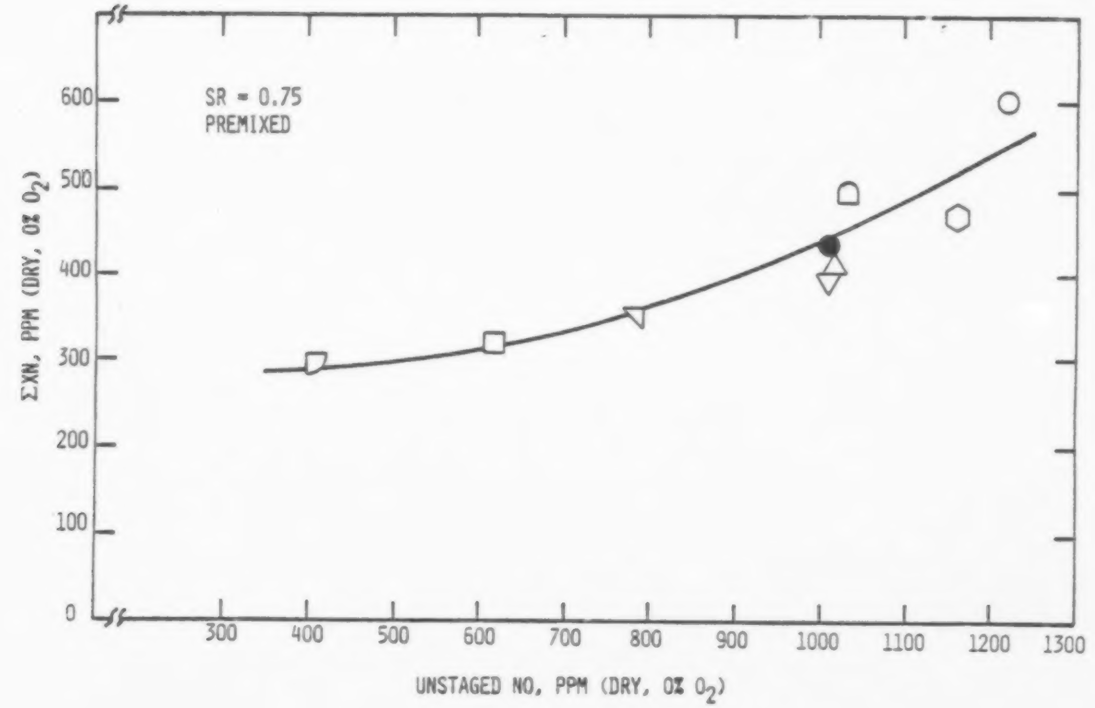

(b)

Figure 7. TFN Content as a Function of Coal Nitrogen Content and Unstaged NO Emissions.

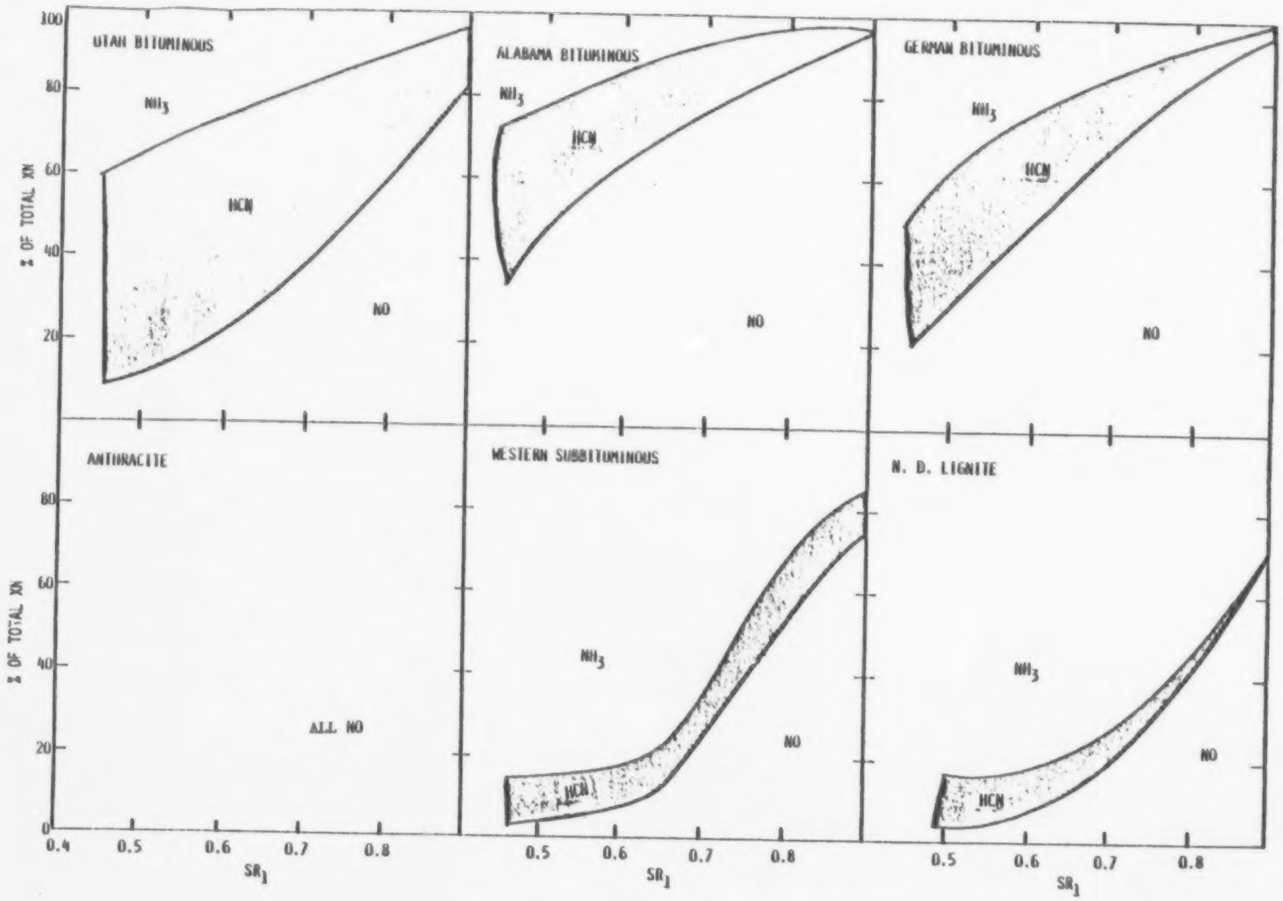

Figure 8. The Effect of Coal Composition on the Partition of Gas Phase Nitrogen Specie.

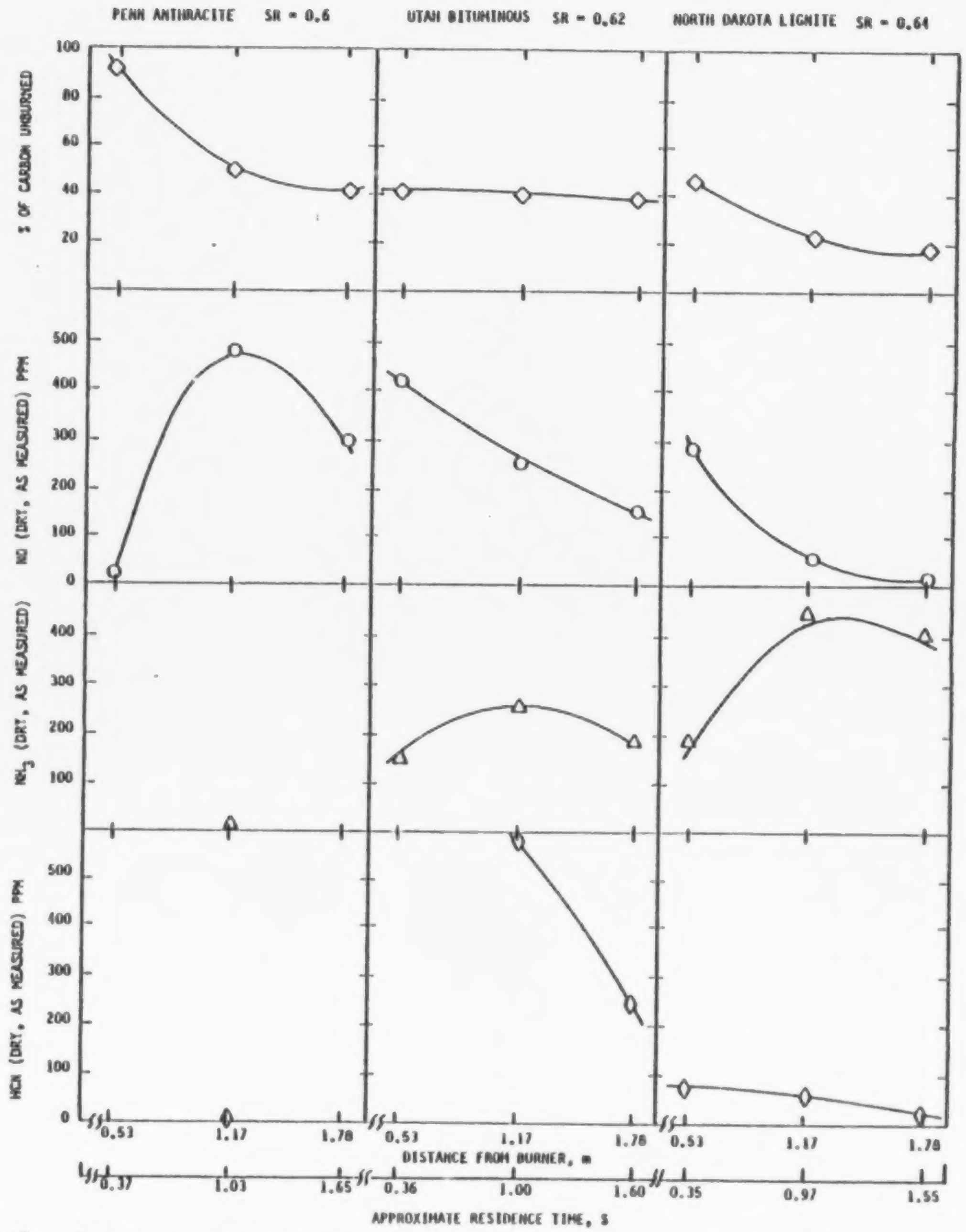

Figure 9. The Decay of Nitrogen Specie and Fixed Carbon with Time under Fuel Rich Conditions.

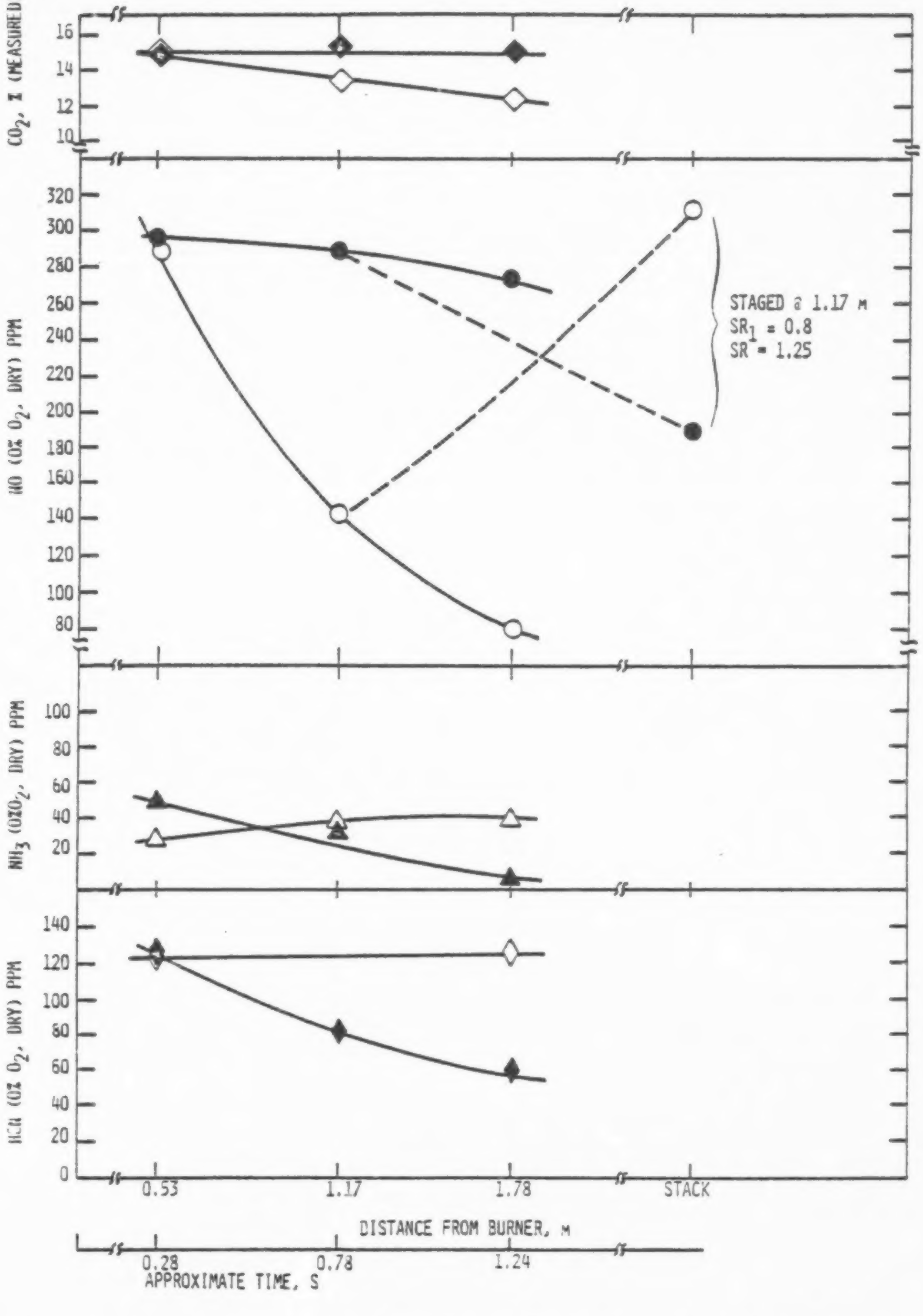

Figure 10. The Impact of First Stage Heat Removal.

TABLE I. FUEL ANALYSIS

Fuel Symbol	D	✙	⊡	⬡	◇	⌂	⬠	⬭	○	◺	⊘	⊗	▢
Fuel Source	Hazellon PA.	Upper Cliff Alabama	Rosa Alabama	Black Creek Alabama	W. KY.	W. VA.	Elkay W. VA.	Gauley Eagle W. VA.	Price Utah	Price Utah	Utah (Coal)	Utah (Char)	Cadiz Ohio
Proximate Analysis (% as received)													
Moisture	5.13	3.00	8.02	2.25	5.43	7.57	0.60	3.72	6.39	7.41	4.20	2.70	4.29
Ash	5.74	9.49	6.79	4.45	7.53	12.05	11.61	26.89	7.40	8.83	9.62	16.83	18.05
Volatile Matter	4.39	20.44	21.81	28.28	37.79	29.12	33.35	26.65	38.89	38.84	42.97	10.29	34.87
Fixed Carbon	84.74	67.07	63.38	65.02	49.25	51.26	54.44	42.74	47.32	44.92	43.21	70.18	42.79
Ultimate Analysis (% Dry)													
C	88.45	79.32	81.23	82.12	71.58	74.68	73.96	59.43	73.17	72.24	69.36	75.39	62.08
H	2.14	4.47	4.73	5.21	5.43	4.96	4.93	4.11	5.55	5.75	5.32	1.28	4.44
N	0.79	1.47	1.54	1.79	1.55	1.38	1.39	1.35	1.54	1.55	1.50	1.22	1.07
S	0.47	1.30	1.04	0.76	3.21	0.86	2.47	0.84	0.66	0.76	1.04	1.12	7.40
Ash	6.05	9.78	7.38	4.56	7.96	13.04	11.69	27.94	7.90	9.54	10.05	17.30	18.86
O	2.10	3.66	4.08	5.56	10.27	5.08	5.56	6.33	11.18	10.16	12.73	3.69	6.15
Heating Value (Btu/lb. Wet)	13,124	13,254	13,394	14,284	12,082	12,228	13,115	10,110	12,340	11,877	11,718	11,185	11,038
CLASSIFICATION (ASTM D388)	Anthracite	Medium Volatile Bituminous	Medium Volatile Bituminous	Medium Volatile Bituminous	High Volatile A Bituminous	High Volatile A Bituminous	High Volatile A Bituminous	High Volatile A Bituminous	High Volatile B Bituminous	High Volatile B Bituminous	High Volatile B Bituminous		High Volatile B Bituminous

TABLE I. FUEL ANALYSIS (Continued)

Fuel Symbol	◸	⦶	⬡	▽	⬡	◹	⛉	◇	○	□	△	◤	●
Fuel Source	Farmington N. M.	Four Corners N. M.	Fruitland N. M.	Colstrip Montana	Hardin Montana	Hardin Montana	Shell Texas	Scranton N. D.	Beulah N. D.	Beulah N. D.	Savage Montana	Morwell Australia	Saar Germany
Proximate Analysis (% as received)													
Moisture	7.76	5.24	11.02	21.27	22.70	20.49	25.23	34.96	33.10	34.63	36.36	9.07	
Ash	17.96	24.06	20.72	9.58	11.26	8.62	10.28	7.50	7.12	4.97	4.61	3.38	
Volatile Matter	34.95	35.94	31.66	30.82	31.26	33.24	35.31	28.85	28.65	27.02	28.48	48.79	
Fixed Carbon	39.33	34.76	36.60	38.33	34.88	37.65	29.18	28.69	31.13	33.38	30.55	38.76	
Ultimate Analysis (% Dry)													
C	63.06	55.99	58.71	67.52	65.54	67.88	60.99	64.61	65.29	66.15	64.99	66.25	78.06
H	4.65	4.71	4.21	4.36	4.15	4.65	4.49	4.17	3.96	4.20	4.04	5.01	4.86
N	1.40	1.23	1.30	1.38	0.95	0.99	1.13	0.83	0.99	0.96	1.00	0.65	1.25
S	0.81	1.03	0.93	0.63	0.79	1.07	1.02	1.52	1.14	0.37	0.42	0.28	0.80
Ash	19.47	25.39	23.29	12.17	14.57	10.84	13.74	11.53	10.64	7.60	7.25	3.72	6.46
O	10.61	11.65	11.56	13.94	14.00	14.57	18.63	17.34	17.98	20.72	22.30	24.09	8.57
Heating Value (Btu/lb, Wet)	10,391	9,425	9,344	9,169	8,603	9,229	8,131	6,446	7,245	7,254	6,995	10,051	13,657 (dry)
CLASSIFICATION (ASTM D388)	High Volatile C Bituminous	High Volatile C Bituminous	High Volatile C Bituminous	Sub-Bituminous B	Sub-Bituminous B	Sub-Bituminous B	Sub-Bituminous C	Lignite A	Lignite A	Lignite A	Lignite A		

SYSTEM APPLICATIONS OF CATALYTIC COMBUSTION

By:

J. P. Kesselring, W. V. Krill, S. J. Anderson,
and M. J. Friedman
Acurex Corporation
485 Clyde Avenue
Mountain View, California 94042

ABSTRACT

The development of catalytic combustion systems is continuing toward the prototype demonstration phase. Improved catalyst materials have shown higher maximum throughput capability and uniform axial temperature profiles. Special auxiliary components required for fuel injection, ignition, and catalyst temperature measurement have been developed and incorporated into system concept designs. The three combustor concepts developed to the system integration phase include a small gas turbine combustor, a watertube boiler concept, and a firetube boiler burner.

The model gas turbine combustor shows continued promise for low NO_x emissions with gaseous and distillate fuels. Greatest development difficulties are associated with introduction of the premixed fuel/air mixture and its interaction with catalyst lightoff systems. An integrated system has been developed, including a multiple nozzle, atomizing injector and an opposed jet lightoff burner. Testing of the concept is nearing completion to show its transient and steady-state capabilities.

The watertube boiler concept uses direct radiative transfer to watertubes in the combustion region. Structural problems of the radiative zone are currently being addressed, and final integration of the concept will follow. Thermal NO_x emissions are typically less than 2 ppm.

The firetube boiler burner also uses radiative heat transfer from a fiber matrix burner to the wall of the firetube. The matrix burner operates at a surface temperature below 1644K at low excess air levels to control the formation of thermal NO_x. Pad material screening tests have been conducted, and a mockup burner test is in preparation. Continuing program work will focus on prototype development of the watertube and firetube boiler concepts.

INTRODUCTION

The advancement of catalytic combustor concepts toward the system demonstration phase is continuing. Through a series of contracts with the Environmental Protection Agency (EPA), Acurex Corporation has continued the development of several system concepts. These concepts are being further developed under the current EPA contract 68-02-3122: (1) a model gas turbine combustor, (2) a watertube boiler system, and (3) a firetube boiler burner. This paper presents a brief history of each concept and progress since the Third Stationary Source Combustion Symposium (Reference 1).

The development of each of the three combustor types has been supported by other activities of the program. Catalyst development has continued to improve performance and operability of each of the combustors. The separate development of auxiliary systems has allowed fuel injection, lightoff, and temperature measurement problems to be solved. Data analysis and fundamental studies have provided greater ability to predict reactor performance. Finally, technology transfer through report publication, technical panel meetings, and workshops has allowed valuable interchange with the user industries. This multilevel approach is continuing, focusing on the prototype demonstration of watertube and firetube boiler systems.

CATALYST DEVELOPMENT

Catalytic combustors typically use ceramic or metallic honeycomb monolithic supports with many small diameter cells. Premixed fuel and air flow through the cells, where a catalyst coating on the interior surface promotes conversion of fuel and air to combustion products. Near the cell entrance, where most of the gas is at low temperature, gas-phase chemical reactions are unimportant. In this region, catalytic wall chemical reactions control heat release. Further down the channel, where wall reactions have preheated the gas to high temperature, gas-phase reactions become active. In this region, fuel is rapidly consumed by a "flame type" phenomenon that controls the amount of unburned hydrocarbon emissions that escape from the system.

The high throughput performance of graded cell catalysts had previously been documented (Reference 2), but a direct comparison between identical graded cell and single cell catalyst configurations had not been conducted. To compare the performance of the two systems, a series of comparative tests were run. Two catalyst configurations were supplied by UOP, Inc., on DuPont Torvex alumina honeycomb substrates. The graded cell system consisted of three 2.54-cm segments with cell sizes of 6.4 mm, 4.8 mm, and 3.2 mm. The single cell system used three 2.54-cm segments with a 3.2-mm cell size. Both systems were washcoated and catalyzed by UOP with a proprietary catalyst.

Pretest analysis of the single cell model indicated a surface area and dispersion of 4.88 m^2/g and 1.22 micromoles H_2/g, respectively, while the graded cell indicated 5.36 m^2/g and 17.63 micromoles/g catalyst. Although initially the graded cell had a much higher dispersion than the single cell, following 5 hours of aging, dispersion for both configurations should be essentially the same. This was verified by posttest analyses that indicated greatly reduced dispersions of 0.39 and 1.3 for the single and graded cell monoliths, respectively.

A comparison of the graded cell and single cell catalyst configurations, characterizations, and combustion performance on natural gas fuel is given in Table I. Both systems were operated in an identical manner during testing, which included 5 hours of steady-state operation under lean conditions at 1560K temperature, followed by maximum throughput tests. As a result of this testing, the following was noted:

- At a standard heat release rate of 105.5 MJ/hr, emissions from the graded cell and the single cell monoliths were approximately the same
- Volumetric heat release at maximum throughout for the graded cell was almost three times higher than for the single cell system (7.4×10^6 J/hr-Pa-m^3 versus 2.6×10^6 J/hr-Pa-m^3)
- Under fuel-rich conditions, both reactor types maintained combustion at preheat temperatures as low as 320K. However, hydrocarbon emissions from the single cell configuration were an order of magnitude higher than for the graded cell catalyst.
- At the standard heat release rate of 105.5 MJ/hr, the graded cell catalyst had a much more uniform axial temperature profile than the single cell system.

The HET code (Reference 3) was used to predict surface temperature profiles in the graded cell and single cell reactors, and the results are shown in Figure 1. Excellent agreement between code prediction and surface temperature as measured by in-depth thermocouples is noted. The more uniform temperature profile for the graded cell system is important, since to avoid poisoning effects, the catalyst should operate at as high a temperature as possible over its entire length. As shown in Figure 1, the single cell reactor has a high, relatively uniform temperature profile. In addition to running the risk of poisoning, the single cell reactor is also operating in an unstable mode. A slight change in inlet conditions could move the reaction zone downstream in the combustor, eventually resulting in blowout.

These comparative tests verify that combustors with high volumetric heat release rates can best be achieved with catalysts in the graded cell configuration with no penalties in combustible or NO_x emissions. In addition, the high uniform temperature of the catalyst walls throughout the length of the graded cell model may have important implications in avoiding catalyst poisoning or liquid fuel deposition on the walls.

AUXILIARY COMPONENTS

The auxiliary components developed under this program include fuel injection, ignition, and temperature measurement subsystems. Due to unique features of the catalytic combustor, special ignition techniques and premixed fuel and air are required. For catalyst lightoff, an ignitor must heat the catalyst to over 700K in a controlled manner. Once lightoff is achieved, the ignitor must be easily shut off. To effectively use all catalyst material and prevent excessive temperatures due to locally enriched reactant mixtures, air and fuel should be evenly distributed prior to entering the catalyst. Fuel injectors must provide thorough and rapid mixing to minimize mixing length, prevent recirculation that may lead to flameholding, and promote rapid prevaporization of liquid fuels. Finally, catalyst temperature must be carefully monitored during startup and steady-state operation to maintain catalyst materials within allowable operating limits. Correspondingly, a reliable system must be developed to continuously measure catalyst surface temperature.

Fuel Injection Concepts

Several fuel injection techniques exist that can provide rapid fuel/air mixing and fine liquid fuel atomization. Aerodynamic fuel injectors for both gaseous and liquid fuels and atomizing spray nozzles for liquid fuels were selected as candidate injectors. While the aerodynamic fuel injectors showed excellent performance with gaseous fuels, performance with distillate fuels has resulted in operational problems that require great care to ensure uniform injection in all aerodynamic zones under varying fuel flowrates. To avoid these problems, atomizing spray nozzle injectors were developed for liquid fuels.

A multiple point atomizing spray injection system, shown in Figure 2, has been developed for the gas turbine combustor system. The three air-atomizing nozzles produce mean drop sizes of approximately 60 to 100 micrometers with distillate fuel. The spray nozzles are mounted on extensions approximately 5 cm away from the injector plate. The injector plate is mounted between flanges of the test facility. Vaporization or mixing are nearly complete in the allowed mixing length without autoignition difficulties.

During initial testing of the multiple injectors, the nozzles' wide spray angle caused fuel to impinge directly on the wall of the combustor can. Some thermal NO_x was produced, apparently as a result of upstream burning of the distillate fuel on the wall. This was confirmed by cold water model tests using a clear acrylic combustor can. Fuel contact with the wall was suppressed by reducing the nozzle spray angle from 77 to 15°. Subsequent combustion testing with a low spray angle was quite successful. The injection system provided a uniform fuel mixture without upstream burning.

In summary, aerodynamic fuel injectors provide rapid and complete fuel-air mixing of gaseous fuels over a wide range of flowrates. If system pressure drop is not important, a single injector is sufficient. To minimize pressure drop, multiple point injection may be necessary. Aerodynamic injectors do not adequately atomize liquid fuel, however. Consequently, spray nozzles are recommended for these applications. In addition, for large systems, multiple point injection should be employed to reduce mixing length while maintaining uniform fuel-air distribution.

Combustor Ignition Concepts

Catalyst lightoff occurs when a minimum catalyst temperature is achieved. The lightoff temperature varies primarily with catalyst and fuel type and secondarily with stoichiometry and mass throughput. In general, temperatures in excess of 700K (800°F) are necessary for lightoff. For example, noble metal catalysts such as platinum and palladium require 617 to 784K (650° to 950°F) lightoff temperatures, while metal oxide catalysts such as nickel and cobalt require 866 to 1367K (1100° to 2000°F) temperatures. In early EPA testing, lightoff temperature was achieved using electric air preheaters. However, air preheat temperatures at this level are not available in boiler and gas turbine systems. Consequently, alternate techniques for lightoff were investigated.

The preferred technique is the opposed jet system where a jet of premixed fuel and air (approximately 1 percent of the total mainstream mass flow) is injected counterflow to the main stream of reactants, producing a stagnation point flow condition. An upstream spark plug ignites the jet and a bow flame front stabilizes in the jet region. By consuming the mainstream reactants, the opposed jet acts as an aerodynamic flameholder, providing a preheated fuel-air mixture to the catalyst located downstream. When the desired ignition temperature is achieved, the jet fuel and air are turned off, thereby extinguishing the flame. The opposed jet ignitor was evaluated using both gaseous and prevaporized liquid fuel in the mainstream.

Optimum performance of the jet was identified initially without a catalyst by varying mainstream and jet stoichiometry. Catalyst lightoff capability was then evaluated with a catalyst. Although tests were conducted mainly with natural gas in the jet and mainstream, similar results are achievable for other gases with similar heating values (e.g., propane). Opposed jet stability depended primarily on the relative magnitude of gas momentum in the mainstream duct and the jet. Based on visual observation, the most stable jet operating condition occurred at a jet-to-mainstream velocity ratio of 7.4 and a jet-to-mainstream mass flowrate ratio of 0.01 to 0.02. Preheat temperatures delivered by the opposed jet show small variations with jet stoichiometry and large variations with mainstream stoichiometry. At a nominal 105 MJ/hr (100,000 Btu/hr) heat release rate with natural gas under lean mainstream conditions, the jet operated at stoichiometries between 5.6 and 17.0 percent theoretical air. Exit temperature varied from 28 to 56K (50^{o} to 100^{o}F) with changes in jet stoichiometry. Smaller temperature variations occurred at decreasing mainstream stoichiometries.

The jet operated effectively over a range of mainstream stoichiometries from 180 to 270 percent theoretical air. This temperature range appears suitable for ignition of both noble metal and metal oxide catalysts. Figure 3 plots exit temperature as a function of mainstream stoichiometry for 10.9 percent theoretical air in the jet. The opposed jet demonstrated excellent catalyst lightoff capability under lean conditions with natural gas. A comparison of an opposed jet lightoff sequence with a typical lightoff using preheated air and fuel is given in Figure 4. As shown, the preheated air technique with a noble metal catalyst required a bed temperature near 750K (900°F) for startup under typical flowrate conditions with the lightoff rate controlled by the stoichiometry of the reactant stream (two are shown). In contrast, the opposed jet can operate with a reactant stream at ambient temperature while the heating rate is controlled by jet and mainstream stoichiometry and the thermal mass of the particular combustion system. For a specific application, the desired heating rate is dictated by both catalyst material and other system startup constraints.

Catalyst Temperature Measurement Techniques

To maintain efficient, stable combustion and not exceed its material temperature limitations, a catalyst must be operated within a relatively narrow range of steady-state temperatures. Thus, measurement of the catalyst surface temperature is a key parameter in system control. The instrument used for temperature measurement must be accurate within 28 to 56K (50° to 100°F), maintain adequate life at low cost, and respond quickly to temperature transients. Furthermore, it should be simple to install and readily accessible for easy maintenance.

Techniques used to date include in-depth thermocouples attached directly to the substrate wall, thermocouple probes that measure gas-phase temperature, and optical pyrometers.

Based on the testing done with each of these techniques, it was found that all systems require further development for system applications. In-depth thermocouples are too fragile and may adversely affect the structural integrity of the honeycomb. Pyrometers can accurately measure catalyst temperature (within 30K) if surface emissivity is known as a function of temperature. Because the sensor is external to the combustion zone, it does not suffer reliability problems due to direct exposure to high temperatures (as do thermocouple probes). Temperature measurement by thermocouple probes located downstream of the catalyst bed depend in a complicated manner on gas velocity and system geometry. Consequently, they are not an accurate method of temperature measurement. In contrast, at the gas velocities investigated, interbed thermocouple probes do appear to accurately measure catalyst temperature.

The integration of catalyst and auxiliary system components into the three combustion concepts has resulted in further system testing, as described in the following section.

MODEL GAS TURBINE COMBUSTOR

The demand for low NO_x gas turbine combustors is increasing. Potential applications include utility power systems, pipeline pumping, transportation vehicles, and future combined cycle processes. As a result, government and private development activities have greatly increased. Among selective catalytic reduction, thermal $DeNO_x$, and NO_x scrubbing, catalytic combustion may prove to be the most cost-effective NO_x control technique.

Under early work with fuel-lean combustors, Acurex developed a model gas turbine can combustor (Reference 4). The combustor consisted of a stainless steel can, multiple cone fuel injector (based on a concept developed at NASA, Reference 5), and the catalyst element. The concept was tested under steady-state operatng conditions in both Acurex and Pratt and Whitney test facilities. Fuels used were natural gas, propane, and No. 2 oil at test pressures from 0.101 to 0.808 MPa (1 to 8 atmospheres). Very low thermal NO_x emissions (less than 5 ppm) were achieved throughout the test series. The combustor was also tested with nitrogen-doped fuels to investigate fuel nitrogen conversion to NO_x. Lean conversion rates were generally high (greater than 50 percent) at all test conditions.

The greatest system operational problem was injection of fuel to obtain a well-mixed, prevaporized reactant stream at the catalyst. The injector design resulted in flameholding under some operating conditions that would be encountered in machine applications. Therefore, the range of operability required improvement.

A second distillate fuel injector was designed and constructed, as described previously. The injector incorporated three air-assist atomizing spray nozzles spraying through a perforated air distribution plate. Cold flow and combustion tests were run on the configuration to verify the injector performance. Flameholding caused by the fuel introduction to the air stream was alleviated following optimization of the spray pattern into the combustor.

To further advance the combustor design, an opposed jet lightoff system was incorporated to simulate typical turbine ignition and startup requirements. The advanced concept is shown in Figure 5. In application, the jet would be ignited during low air flow conditions and produce energy to accelerate the machine and preheat the catalyst to its lightoff temperature. As the machine approaches a loaded condition, the jet is extinguished by depletion of its flow, and combustion occurs totally in the catalyst. To date, the overall concept has been tested to simulate startup without the catalyst element to investigate operating characteristics of the fuel injector and opposed jet.

Tests were conducted with premixed air and natural gas in the opposed jet and atomized diesel fuel in the mainstream air. The lightoff temperature that could be achieved was determined by varying the amount of diesel flow and hence the mixture adiabatic flame temperature. Tests were run at atmospheric pressure with a mainstream reference velocity of 4.6 m/sec (15 ft/sec) and a preheat temperature of 547K (525°F).

The test data is shown in Figure 6. As the mixture stoichiometry (including jet and mainstream fuels) is decreased toward stoichiometric, the lightoff temperature increases. The increasing adiabatic flame temperature of the mixture is shown for comparison. The actual temperature achieved at a given stoichiometry is dependent on the degree of mainstream fuel consumed. Less fuel is consumed near stoichiometric conditions due to increasing difficulty of burning liquid fuel droplets at 547K preheat. Increasing the preheat would result in greater fuel consumption and higher lightoff temperatures at a given mixture stoichiometry.

At 400 percent theoretical air, the combustor is operating with only jet fuel at a temperature of 1005 K (1350°F). Above 400 percent, flame cannot be stabilized in the combustor. At 100 to 150 percent theoretical air, the majority of the fuel is diesel. Below 150 percent theoretical air at the preheat and velocity conditions described, the stabilized flame could not be extinguished upon depletion of the jet flow.

The wide range of jet operability should allow smooth turbine startup in applications. At low air flow, the jet fuel would be introduced and ignited. During acceleration (and increasing compressor discharge temperature), mainstream fuel would be increased to the catalyst lightoff temperature and the jet extinguished. Final acceleration and loading could then be achieved catalytically by further fuel increases. Testing of the startup and steady-state operation of the combustor with a catalyst is in progress.

WATERTUBE BOILER SYSTEM

The effect of NO_x control on boiler systems is even more significant than for gas turbines. Whereas stationary gas turbine combustors contribute approximately 3 percent of the total U.S. NO_x inventory, packaged and utility boilers are estimated to contribute 20 percent and 48 percent, respectively (Reference 6). Clearly, controls developed for watertube and firetube boilers are an important factor in reducing this country's NO_x emissions.

A catalytic watertube boiler system has been devised and extensively tested. Combustion occurs on the exterior surface of catalyzed cylinders in crossflow to the premixed reactant stream. Energy is transferred to watertubes by radiation from the combustion surfaces.

The concept is shown in Figure 7. A stoichiometric fuel/air mixture is fed to the radiative section which contains a close-packed array of catalyst elements and watertubes. The mixture is partially combusted by the catalyst which is kept at a low surface temperature by radiation heat loss to the watertubes. The combustion products and remaining unburned fuel and air are then passed to a downstream catalytic adiabatic combustor to complete combustion reactions. A final convective section extracts energy from the fully combusted gases. Both catalyst sections operate well below the maximum use temperature of the catalyst supports — the radiative section by radiative cooling and the adiabatic section by dilution of the fuel/air mixture with exhaust products from the radiative section.

The radiative section has been constructed and tested independently of the downstream adiabatic combustor and convective sections. In early testing, the staggered tube arrangement (separate catalyst tubes and watertubes) was used. Later tests were conducted with a concentric tube design. The results for the staggered tube configuration were reported in

Reference 2. The radiative section was run with natural gas at varying stoichiometry (40 to 220 percent theoretical air), heat release rate (1.09×10^8 to 3.44×10^8 J/hr), and preheat to establish its combustion efficiency, thermal and fuel NO_x emissions, and heat transfer characteristics at varying conditions. The catalyst was a platinum preparation on alumina tubes.

At stoichiometric conditions, the combustion efficiency of the staggered tube combustor was approximately 37 percent. This result was slightly lower than the anticipated level of 50 percent necessary to avoid flame temperatures above the temperature capability of the adiabatic section. The thermal NO_x emissions were very low, however, never exceeding 2 ppm at these conditions. To evaluate the conversion of fuel nitrogen to NO_x, natural gas was doped with ammonia (NH_3). A minimum conversion level of 20 percent was measured at approximately 55 to 60 percent theoretical air.

These early combustion test results suggested several design modifications for improvement of the radiative section. Closer spacing of the catalyst tubes would improve the combustion efficiency. It would also be desirable to isolate the cold surfaces of the watertubes from the combustion zone to avoid fouling when firing with fuel oils. To meet these requirements, a concentric tube design was completed where the catalyst tube surrounds the water tube with an air gap between the two. Therefore, combustion energy generated on the catalyst tube outside surface would be transferred by conduction to its inner surface and by radiation across the air gap to the watertube.

The concentric configuration was first tested under conditions similar to those for the staggered arrangement with a platinum catalyst on alumina tubes. Combustion efficiency was markedly improved, reaching a high of 93 percent fuel conversion at stoichiometric conditions as shown in Figure 8. Thermal NO_x emissions were again less than 2 ppm, and fuel nitrogen conversion was below 30 percent under fuel-rich conditions. Tests were not performed with fuel oil to verify that capability, however.

Despite the improved combustion performance of the concentric watertube design, structural problems were encountered. The configuration develops a substantial temperature gradient across the walls of the ceramic tubes. The temperature difference results in nonuniform radial expansion and, ultimately, fracturing of the material. The stresses that would be encountered in application were calculated as 198 x 10^6 Pa (28,700 psia) to 257 x 10^6 Pa (37,300 psia), clearly greater than the 190 x 10^6 tensile strength of alumina tubes at 1367K (2000°F).

Only one other ceramic can be made with adequate strength and is appropriate for combustion applications. Silicon carbide not only has a high strength of over 400 x 10^6 Pa at the above conditions, but it has a higher thermal conductivity than alumina and therefore results in lower temperature gradients and developed stresses. As a result, tubes of silicon carbide were purchased from the Norton Company in the proper dimensions and coated with a chromia (Cr_2O_3) and platinum catalyst preparation for an additional test series. Testing of the concept is in progress.

FIRETUBE BOILER BURNER

A large percentage (approximately 50 to 65 percent) of the commercial size boiler market is composed of firetube boilers. These smaller units account for over 30,000 gas-fired boilers and an equal number of distillate oil-fired boilers in the 3.2 x 10^9 J/hr (3 x 10^6 Btu/hr) size alone (Reference 7). In fact, of all commercial and industrial size boilers in the field, the majority are firetubes. These applications are principally gas- and distillate oil-fired.

Thus, firetube boilers represent another area for significant NO_x reduction. A catalytic burner would be especially attractive if it were retrofitable into the large number of boilers already installed or at least presented only minor changes to current designs.

A number of catalytic burner designs were conceptualized and reviewed with major firetube boiler manufacturers. The simplest and most acceptable to the manufacturing community utilizes a fiber matrix material that is molded into a cylindrical surface burner for insertion into the firetube.

The burner concept is shown schematically in Figure 9. A fuel/air mixture is passed into the central region of the cylindrical fiber matrix. The cylinder construction is best described by Figure 10. The matrix is approximately 2.5 cm (2 inches) in thickness, is closed with similar material at the downstream flow end, and is sealed at the upstream end by a combustion chamber flange. The matrix material is rigid, is supported at the upstream end, and has internal flow passages as shown in Figure 10, maintaining concentricity with the boiler firetube.

In the described configuration, premixed fuel and air are forced to flow into an annulus between the fiber matrix and an internal cylinder. The fuel may be gaseous or vaporized liquid. The mixture then flows through the matrix and is ignited at the outer cylinder surface to start the burner. A heterogeneous surface reaction zone is established on the cylinder outer surface, within a depth of only a few millimeters of the matrix thickness. The majority of the matrix thickness remains at the temperature of the incoming reactants and promotes no additional reaction.

Heat is transferred directly from the matrix outer surface to the firetube as shown in Figure 9. The transfer is primarily radiative although convective transfer also contributes. This heat transfer limits the matrix surface temperature to less than 1644K (2500°F), the temperature limitation of the material, although the adiabatic flame temperature of the reactive mixture exceeds 2200K. The heat is transferred through the metal firetube wall to the boiler water to heat the water or raise steam. Flue gases are forced to the end of the firetube and out to the additional firetube passes.

Catalytic fiber matrix materials have demonstrated low NO_x emissions and high combustion efficiency with gaseous fuels (Reference 8). However, the optimum matrix material, appropriate heat transfer configuration, and ability to operate on distillate fuel required additional study. A series of tests on fiber matrix disks was conducted to evaluate these parameters.

Figure 11 shows the matrix surface temperature of the combustion zone as a function of theoretical air for three values of face velocity. Lower face velocities result in lower surface temperatures at low excess air levels (100 to 130 percent theoretical air) where firetube boilers normally operate. This low surface temperature is advantageous in reducing NO_x emissions as shown in Figure 12. Emissions of less than 10 ppm at 115 percent theoretical air are possible. Tests also indicate high combustion efficiency (low CO and HC) can be achieved simultaneously with low NO_x emissions.

The low surface temperatures of Figure 11 also demonstrate the effective radiative heat transfer away from the combustion zone. The indicated temperatures of 1478K to 1644K (2200°F to 2500°F) at 100 percent theoretical air are within the use temperature capabilities of the alumina silicate fibers and far below the adiabatic flame temperature of

2228K. From these tests, the optimum flow velocity for the selected matrix material appears to be 10 to 15 cm/sec (1/3 to 1/2 ft/sec).

The catalytic burner was also operated on diesel fuel. To achieve stable combustion with similar results to natural gas, it was necessary to partially vaporize the oil. This was accomplished by preheating the air stream to 492K (425°F) prior to admitting the fuel. Current firetube boiler designs operate without air preheating systems. Therefore, operation of the matrix burner with fuel oil in a firetube boiler will require additional development of an air preheating technique.

These flat disk burner tests identified the operating requirements of the matrix material. To further develop the concept, a cylindrical burner as in Figure 10 was constructed for testing in a simulated firetube. Results of the tests are pending. The fiber matrix burner does appear attractive for further development and should be applicable to many firetube designs with only minor modifications.

CONCLUSIONS

The development of catalytic gas turbine, watertube boiler, and firetube boiler combustors is rapidly progressing. The potential for near-term reduction of thermal NO_x emissions with clean fuels is promising.

An integrated model gas turbine combustor has been tested to simulate both startup and steady state operating conditions, following refinement of fuel injection and lightoff techniques. Only further refinement of the concept is required for small machine applications. The concept may also be scalable to larger combustor sizes.

The watertube boiler concept shows promise for further development despite being a radically different design from present systems. Production units would probably differ further from those tested. Stress analyses on the catalyst supports determine silicon carbide as the most appropriate ceramic in the preferred concentric tube design. Ongoing testing will verify the material recommendations and lead to testing of the integrated concept.

The firetube boiler burner is a retrofitable design for gas-fired units. For distillate-fired firetubes, the fiber matrix concept requires preheated air for acceptable operation. Detailed tests on fiber materials have shown low NO_x emissions due to surface cooling with concurrent low CO and hydrocarbon emissions. A cylindrical burner of the most acceptable material is being fabricated for testing.

The development of burners for these three classes of equipment addresses a large portion of the NO_x emissions in this country. Further EPA program development will focus on prototype demonstration of catalytic boiler systems.

REFERENCES

1. Kesselring, J. P., et al. Catalytic Combustion System Development for Stationary Source Applications. In: Proceedings of the Third Stationary Source Combustion Symposium; Volume II. Advanced Processes and Special Topics. EPA-600/7-79-050b, February 1979, pp. 207-240.

2. Krill, W. V. and Kesselring, J. P. The Development of Catalytic Combustors for Stationary Source Applications. In: Proceedings: Third Workshop on Catalytic Combustion. EPA-600/7-79-038, February 1979, pp. 239-268.

3. Kendall, R. M., et al. An Analysis of Catalytic Combustion in Monolithic Honeycomb Beds. In: Proceedings: Third Workshop on Catalytic Combustion. EPA-600/7-79-038, February 1979, pp. 197-238.

4. Kesselring, J. P., et al. Design Criteria for Stationary Source Catalytic Combustion Systems. EPA-600/7-79-181, August 1979.

5. Tacina, Robert R. Degree of Vaporization Using an Airblast Type Injector for a Premixed-Prevaporized Combustor. NASA TM-7883b, August 1978.

6. Mason, H. B. and Waterland, L. R. Environmental Assessment of Stationary Source NO_x Combustion Modification Techniques. In: Proceedings of the Second Stationary Source Combustion Symposium. EPA-600/7-77-073a, July 1977.

7. Evaluation of National Boiler Inventory. EPA-600/2-75-067, 1975.

8. Martin, G. Blair. Prototype Surface Combustion Furnace Evaluation. EPA-600/7-79-038, February 1979, pp. 175-196.

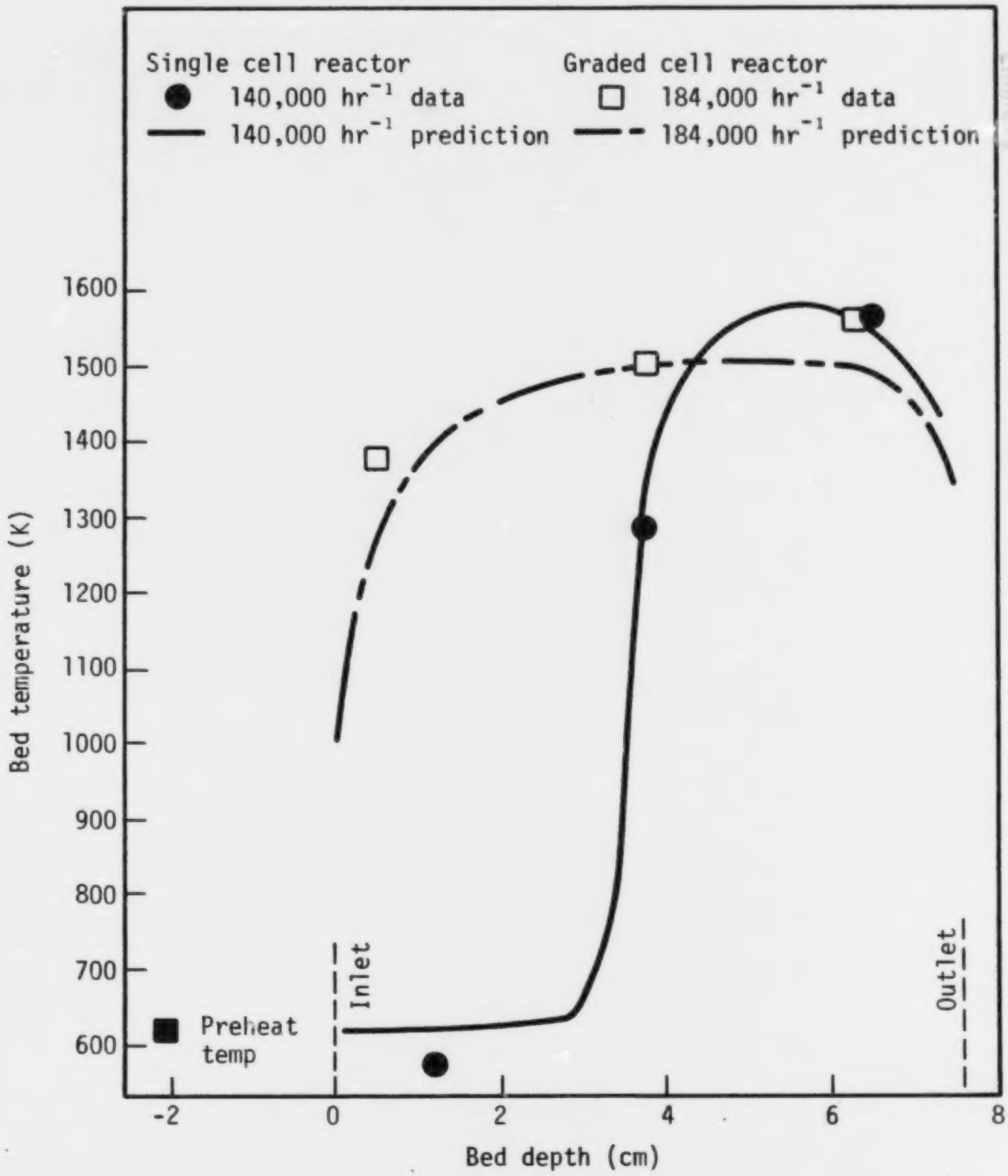

Figure 1. Comparison of graded cell and single cell reactor temperature profiles with HET code predictions.

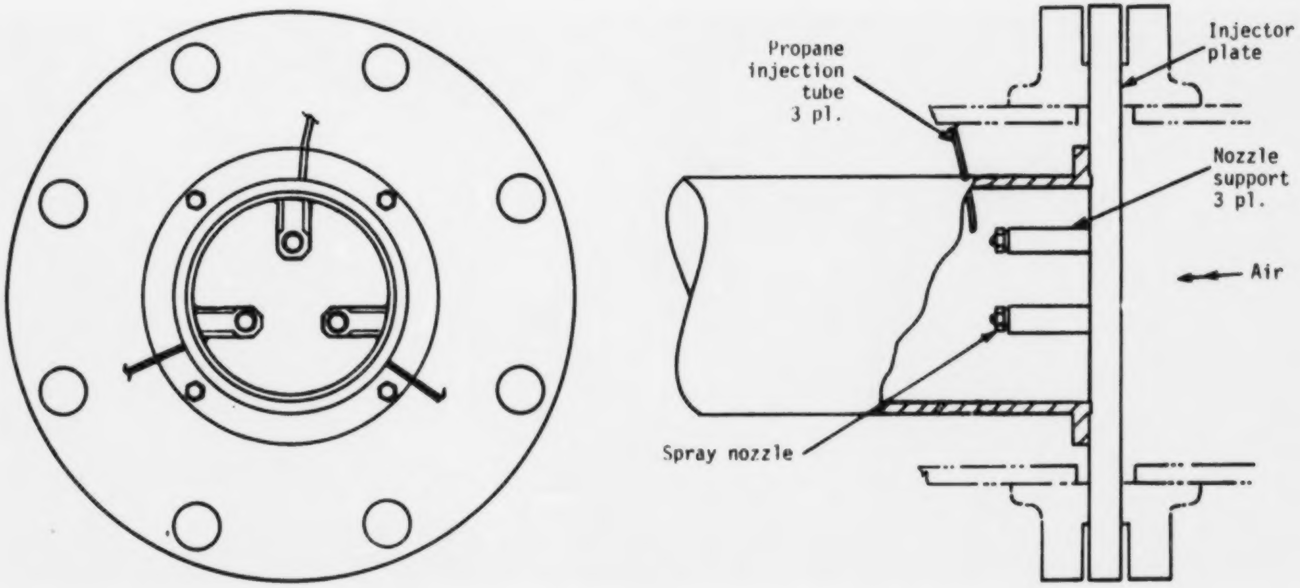

Figure 2. Multiple spray fuel injector.

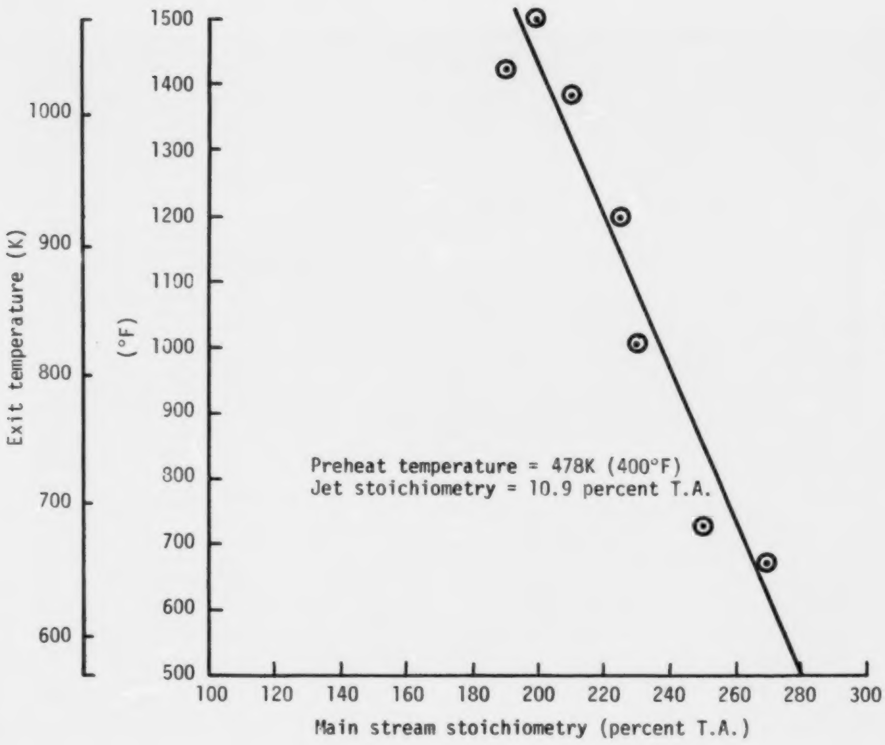

Figure 3. Opposed jet ignitor -- exit temperature versus mainstream stoichiometry.

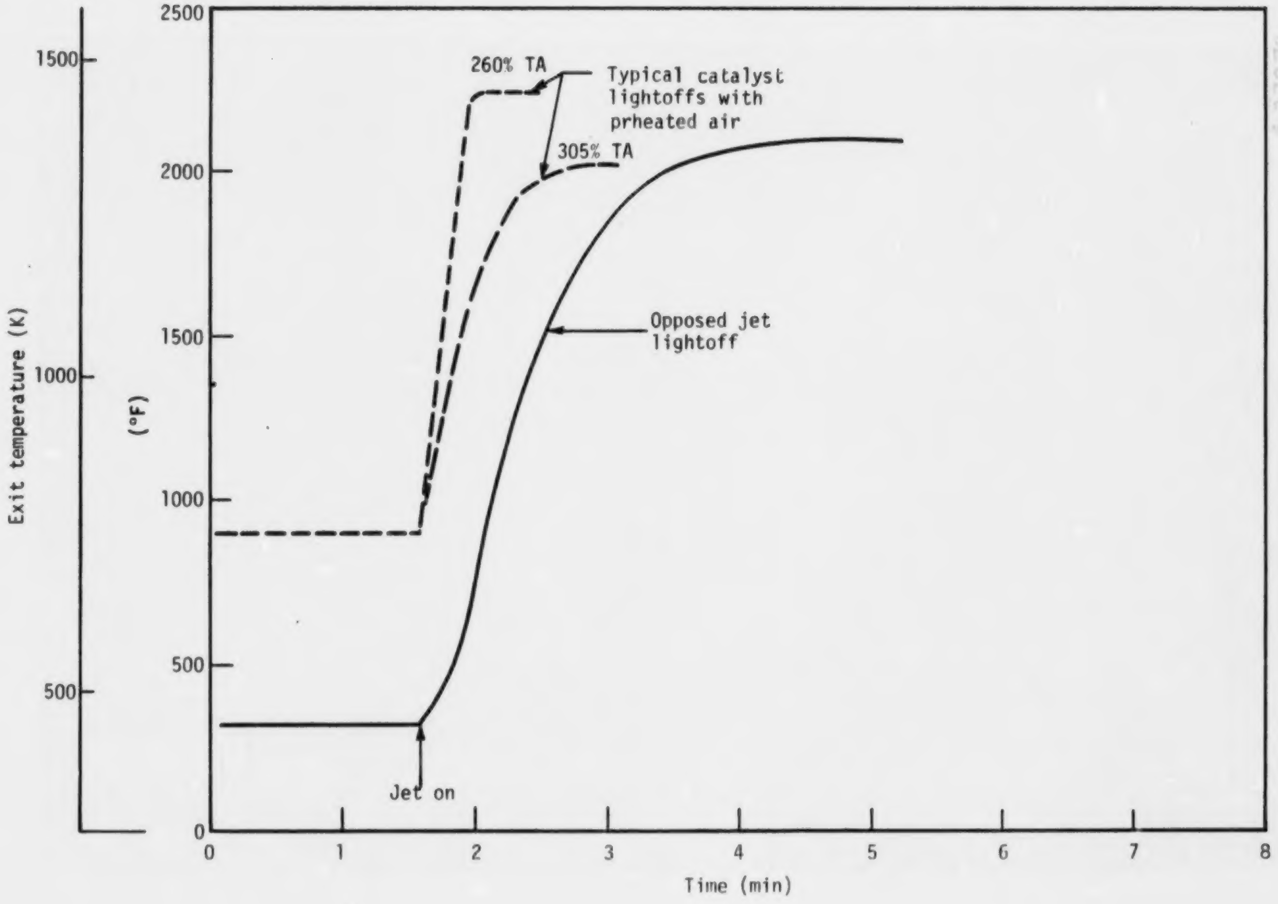

Figure 4. Lightoff time comparison.

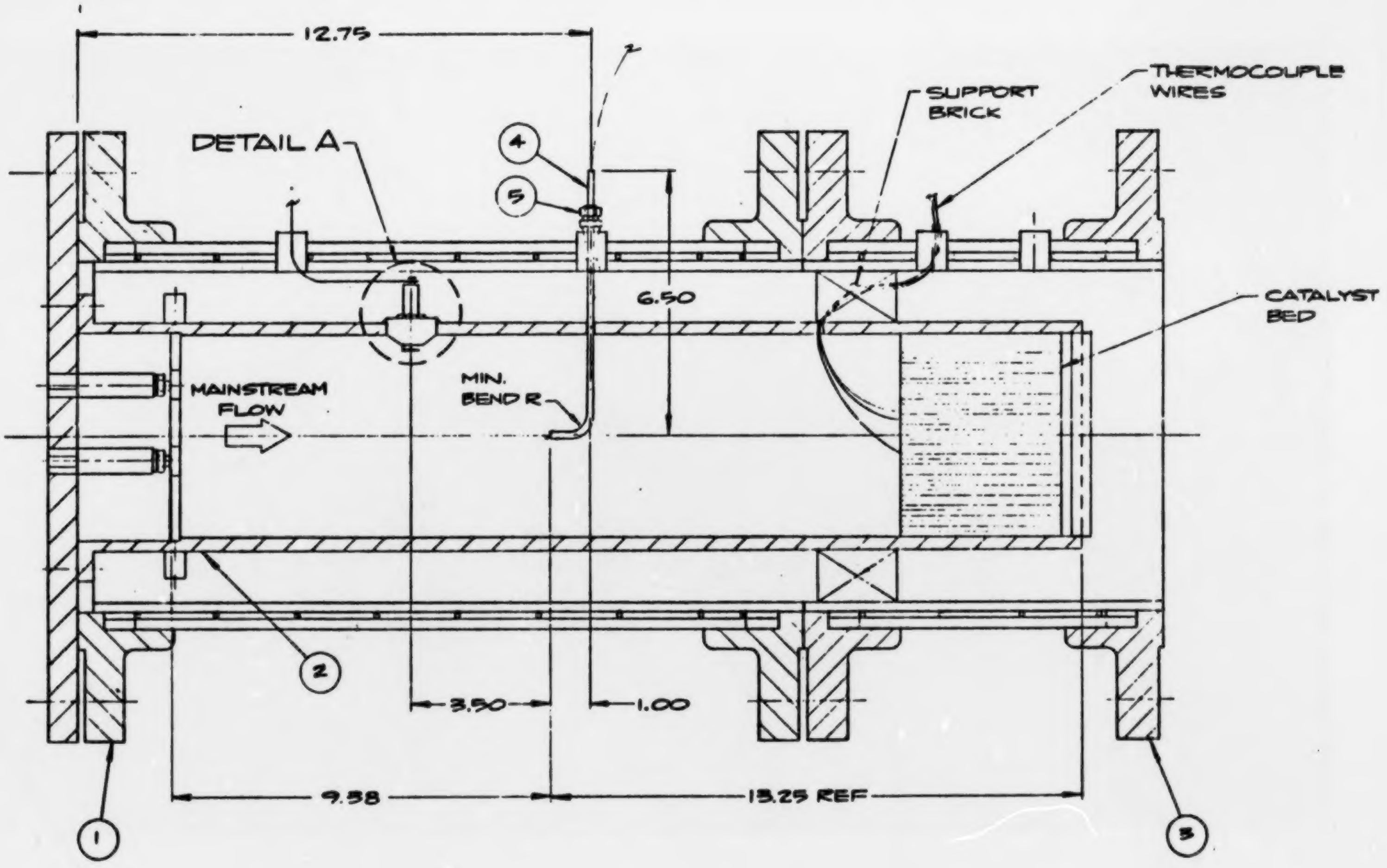

Figure 5. Model gas turbine combustor with opposed jet startup system.

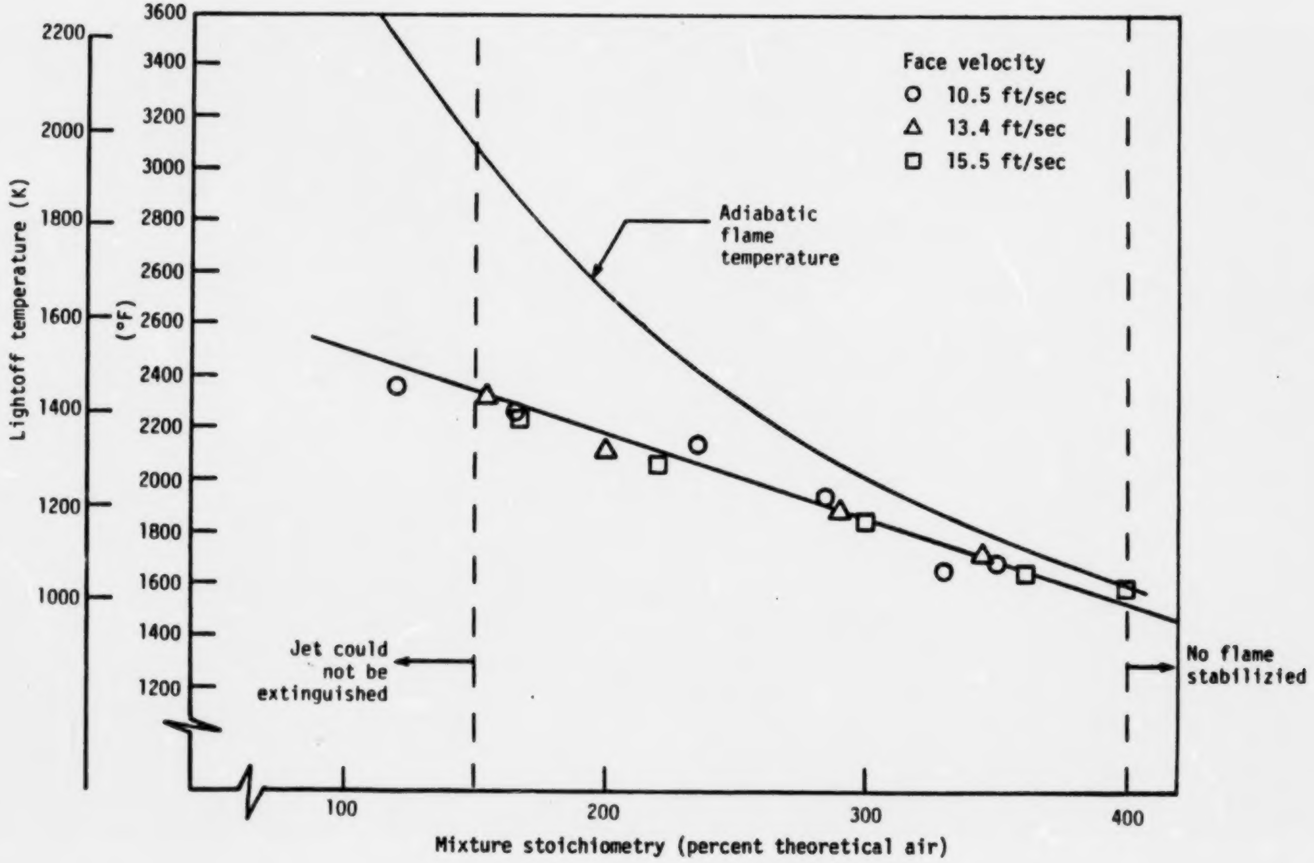

Figure 6. Gas turbine opposed jet results.

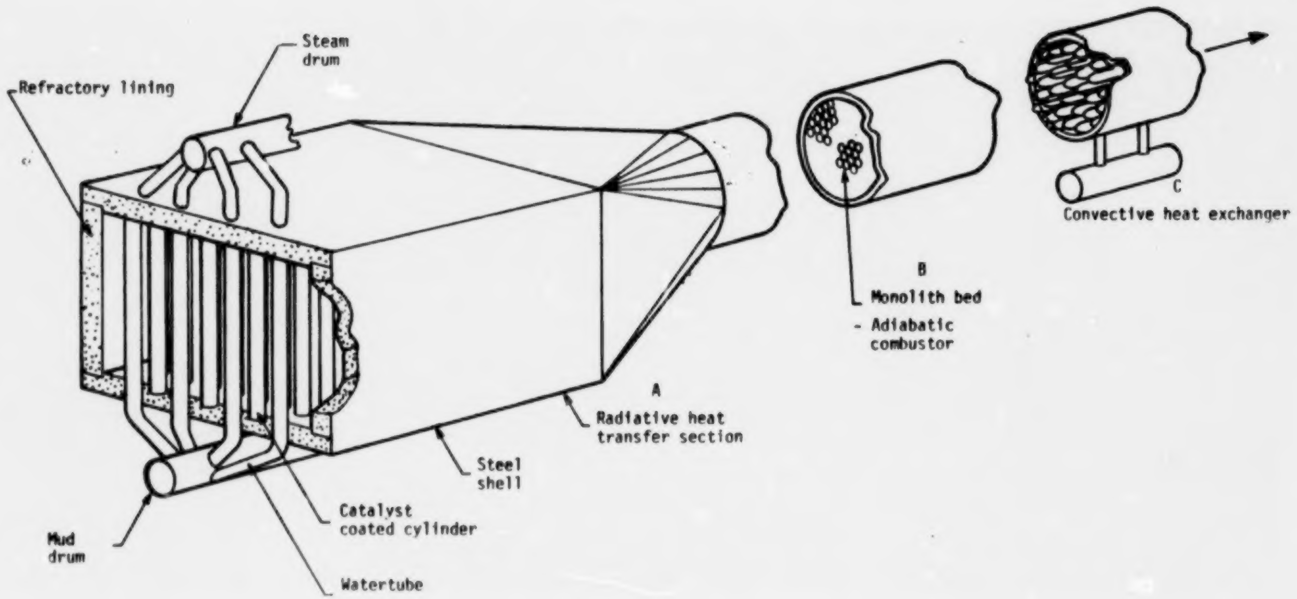

Figure 7. Radiative watertube boiler concept.

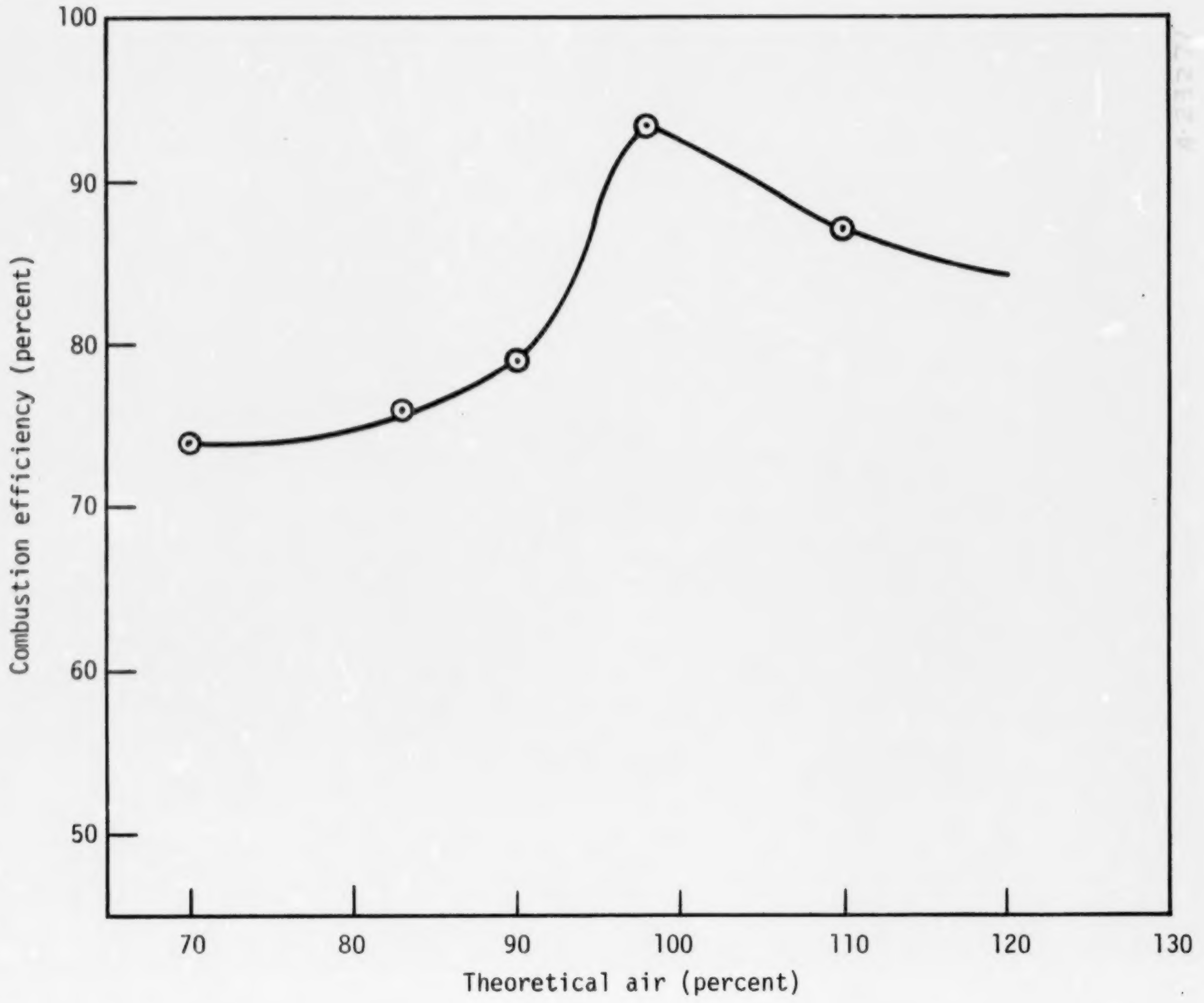

Figure 8. Concentric watertube boiler combustion efficiency.

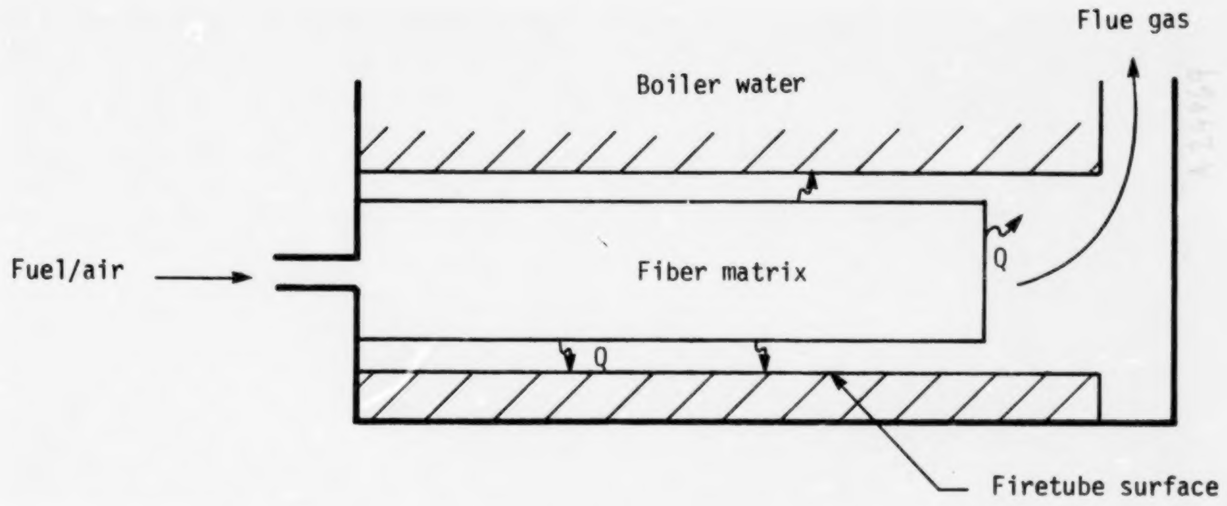

Figure 9. Firetube boiler catalytic burner concept.

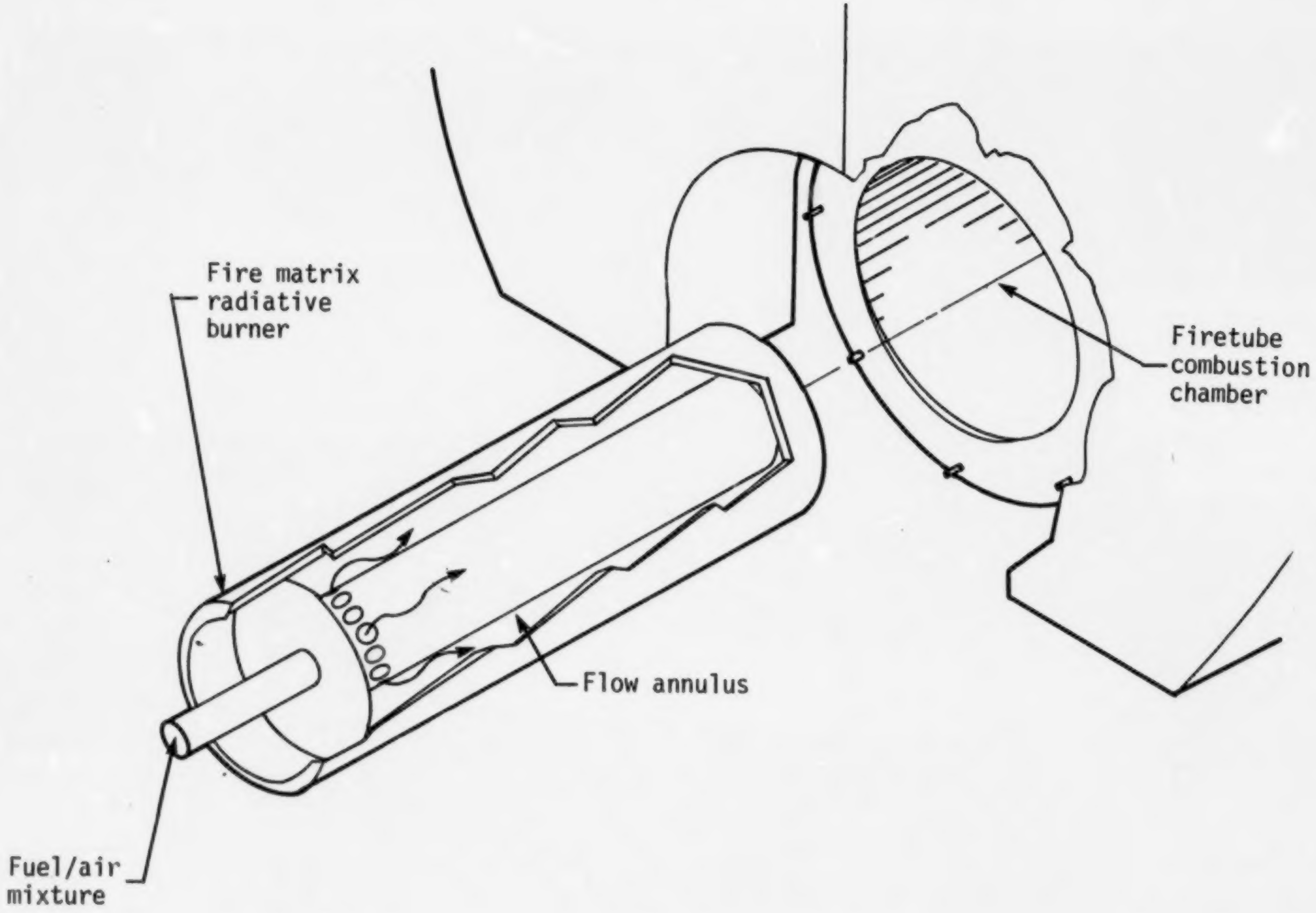

Figure 10. Catalytic firetube boiler burner.

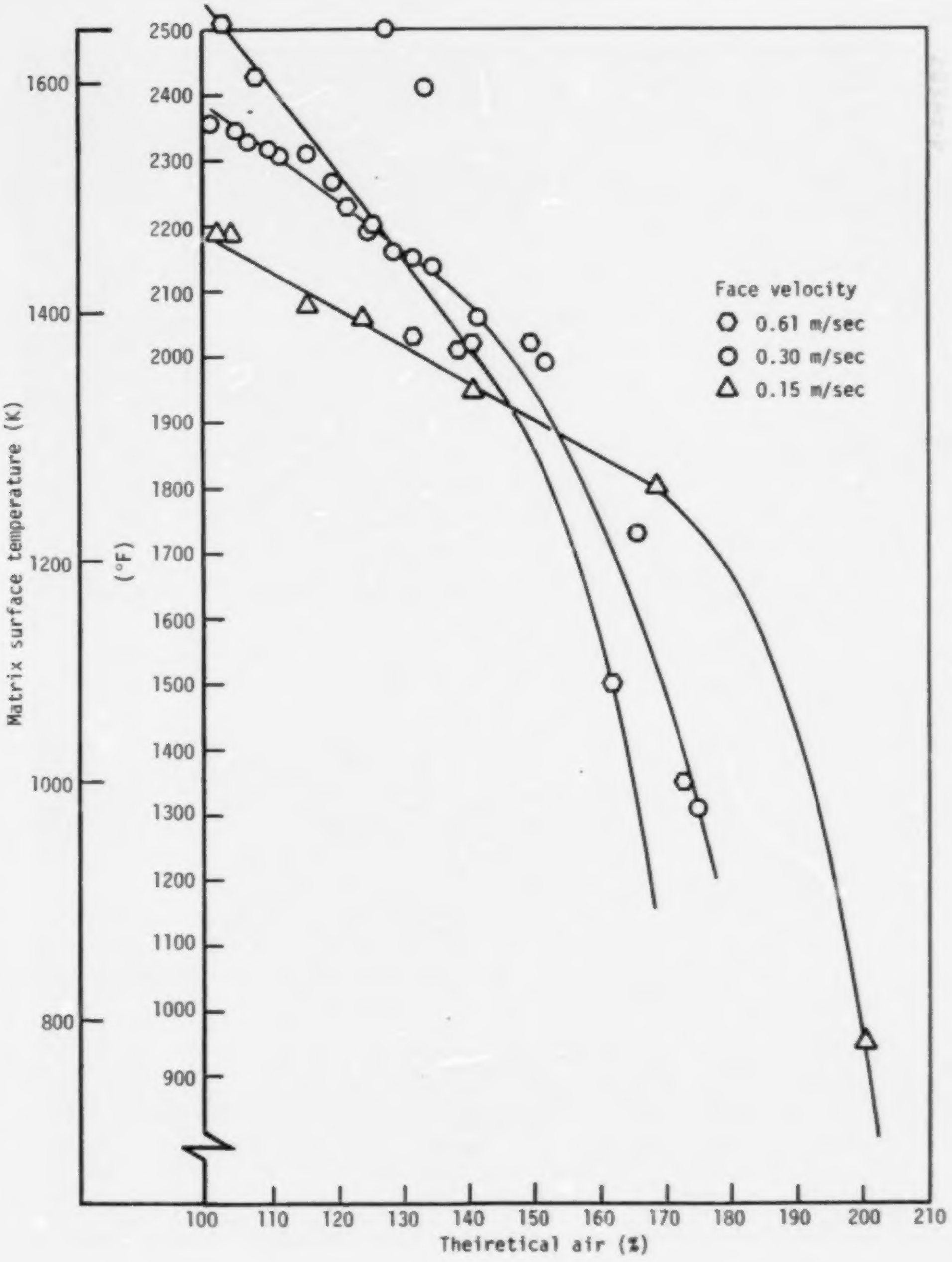

Figure 11. Fiber matrix operating temperature.

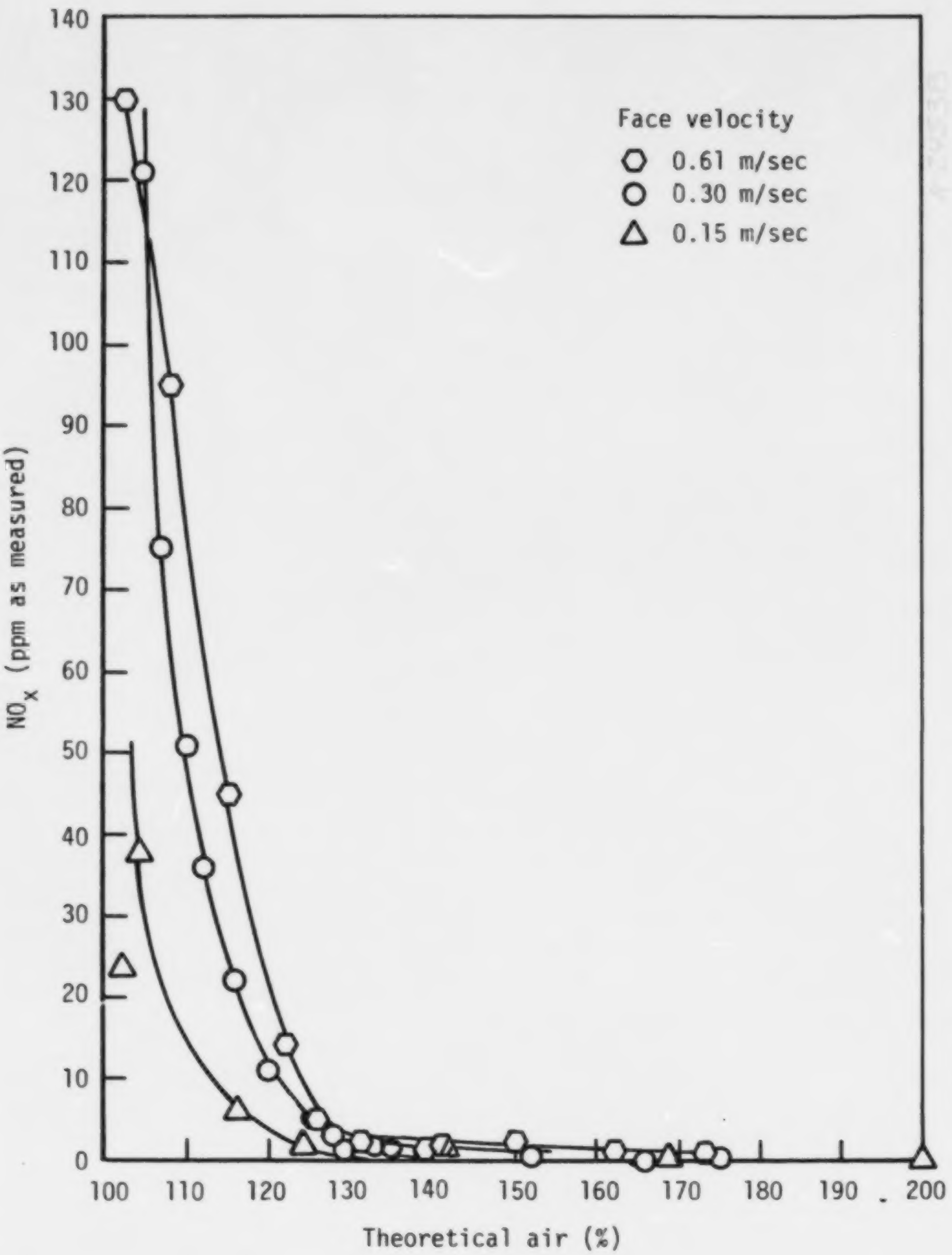

Figure 12. Fiber matrix NO$_x$ emissions.

TABLE I. COMPARISON OF SINGLE CELL AND GRADED CELL CATALYST PERFORMANCE

Parameter	Graded Cell Catalyst	Single Cell Catalyst
Catalyst manufacturer	UOP	UOP
Cell geometry	(3) 25.4-mm long segments of 6.4, 4.8, and 3.2-mm cell size	(3) 25.4-mm long segments of 3.2-mm cell size
Substrate	DuPont alumina	DuPont alumina
Surface area (m^2/g)		
Pre-test	5.36	4.88
Post-test	0.986	0.05
Dispersion (moles H_2/g)		
Pre-test	17.63	1.22
Post-test	1.30	0.39
Operating temperature (K)	1561	1561
Maximum heat release rate ($J/hr-Pa-m^3$)	7.4×10^6	2.6×10^6
Typical emissions (ppm)		
NO_x	1	2
CO	30	60
HC	12	35

FIXED-BED AND SUSPENSION FIRING OF COAL

By:

S. P. Purcell, D. M. Slaughter, J. M. Munro, G. P. Starley,
S. L. Manis, and D. W. Pershing
Department of Chemical Engineering
University of Utah
Salt Lake City, Utah 84112

ABSTRACT

This paper summarizes the progress made during the second year of a grant to study the formation of pollutant species, particularly nitrogen and sulfur oxides in fixed-bed and suspension combustion of coal. During this period, the suspension furnace was completed and preliminary experiments conducted. The results suggest that the large particles are essentially unreacted when they reach the stoker bed. The burning rate of the small particles increased with increased local oxygen concentration and increased heating rate.

The fixed-bed furnace was also completed and initial results were obtained. These data suggest that the nitrogen volatiles evolve from the bed early in the combustion process and form significant amounts of nitrogen oxides. Staged combustion appears to be a potentially effective means of controlling NO_x emissions from a fixed-bed system. Increased clinkering problems were not observed under staged combustion conditions; however, this is a potential problem in the application of this technology to larger scale units. Both overall excess-air level and overfire-air height were studied, but neither appeared to be of first-order importance at the conditions investigated.

The model spreader stoker was designed and the fabrication drawings prepared. Construction should be completed in late 1980.

ACKNOWLEDGMENTS

This research was supported by the United States Environmental Protection Agency under Grant No. R-805899. The considerable help and advice of G. Blair Martin, EPA Project Officer, is sincerely appreciated. In addition, input from the engineering staff at Delco-Remy Division, General Motors: Dr. David Junge, Oregon State University; Robert Giammar, Battelle; Mr. Niel Johnson and the engineering staff at Detroit Stoker; and, Dr. M. P. Heap, Energy and Environmental Research, is gratefullly acknowledged. Thanks are also due to the Vibra Screw Corporation for providing the very accurate solids-metering system used in this work. Last, but certainly not least, the authors gratefully acknowledge Mrs. Colleen Anderson for her help in managing the project, and preparing the required manuscripts, and Blake Beckstrom and Robert Brodbeck for their assistance in building the equipment and gathering the data.

SECTION 1

INTRODUCTION

Clean, liquid and gaseous fuels have substantially increased in price and have become more difficult to obtain during the past decade. These trends, along with a heightened environmental awareness, have resulted in a renewed interest in coal as a domestically available alternative fuel. Considerable research has been focused on utility coal combustion; however, mid-range commercial and industrial coal-fired systems have been largely ignored.

Industrial users have three potential alternatives available for burning coal to raise steam for industrial process utilization or facility space heating. These coal-firing methods include:

- pulverized coal-fired boilers;
- fluid-bed coal-fired boilers; and,
- stoker coal-fired boilers.

In general, pulverized-coal (PC) firing is restricted to very large industrial installations (above 500,000 pph steam), because of the high capital cost associated with the pulverization equipment, and the large inherent maintenance costs of this equipment. In addition, many industrial and commercial users desire coal-firing systems which can utilize the fuel as it is delivered without additional preparation.

Fluid-bed combustion (FBC) is a promising new technology that utilizes large coal particles (relative to PC) and provides very high heat transfer rates. FBC may eventually dominate the industrial sector; however, to date it has experienced very limited acceptance in the United States.

Stoker coal-fired systems are recognized as the current field technology for medium capacity steam generation facilities. Stoker coal-fired furnaces are most often located in densely populated, urban centers because of size classification and method of utilization (i.e., factory space heating, hospital heating, etc.). The presently operating installations represent major stationary polluting sources and increased future utilization of stoker-fired boilers poses a serious threat to ambient air quality in metropolitan areas. It is important, therefore, that further knowledge be obtained on the formation and control of nitrogen and sulfur oxides under conditions typical of stoker firing.

Recent large-scale pilot and field tests have at least partially demonstrated the potential of combustion modifications for NO_x control in stoker-fired boilers. Giammar, et al (1) have conducted tests on a 25,000 pph steam spreader stoker with a water-cooled vibrating grate and found that decreased overall excess air resulted in lower NO_x emissions (at a constant load). Gabrielson and Langsjoen (2, 3) have tested several, large-scale industrial stokers and reported little effect of overfire air percentage on NO_x emissions and an apparent increase in NO_x with increasing load. However, the fundamental mechanisms controlling these effects are not well defined.

SECTION 2

PROJECT OVERVIEW

PURPOSE

The overall objective of this program is to study the formation of nitrogen and sulfur oxides under carefully controlled experimental conditions typical of stoker-fired boilers. In particular, this program is considering the following major research areas:

1. the evolution and oxidation of fuel nitrogen and sulfur;
2. the retention of sulfur oxides by ash and/or solid-chemical sorbents in both suspension and fixed-bed burning;
3. the effectiveness of combustion modifications for NO_x control in stoker-fired coal systems.

In addition, the study will attempt to quantify the combustion process in a stoker environment and consider possible detrimental effects of control technology on boiler operation.

APPROACH

This project is considering both spreader and mass-burning (thick bed) stoker systems. Conceptually, the combustion process in a spreader stoker can be divided into two major parts:

- suspension burning and
- fixed-bed burning.

As the particles pass through the overthrow zone, they are heated, partially devolatilized, and may even burn completely if they are small enough. The large particles form a thin (2 to 4 inches) active fuel bed and burn out heterogeneously. In a mass burning stoker (e.g., underfeed) the particles may be partially devolatilized by radiant heating prior to actual ignition.

The approach in this study has been to divide the processes into the separate pieces for individual study before attempting research on the coupled system. In particular, the program consists of three major tasks:

Task 1. An experimental investigation of suspension burning of bituminous coal;

Task 2. An experimental investigation of fixed-bed burning of bituminous coal; and,

Task 3. An experimental optimization of combustion modification technology using a model stoker system.

Although the primary thrust of the study is experimental, each of the furnace studies will be supported by analytical modeling.

SECTION 3

SUSPENSION BURNING

SUSPENSION FURNACE

The purpose of this task is to investigate the formation of pollutant emissions during the suspension-burning phase of the combustion process. Figure 1 illustrates the furnace system which was fabricated for these studies. The inner combustion chamber is six inches in diameter and the outer shell is 28-inches square. The walls of the main furnace sections consist of an outer steel shell, five inches of 1900°F insulating block, four inches of 2500°F insulating refractory, and two inches of 3400°F high-temperature castable refractory. Each of the mid-sections contain five, two-inch diameter ports for second-stage air injection and/or insertion of species and temperature probes.

The side walls have provision for auxiliary heating (or cooling) by firing natural gas or passing cooling air through outer channels. These channels are two inches in width and cover 50 percent of the circumference. This allows partial independent control of the radiant heat transfer to the particles and more complete control of wall temperature.

A high-intensity gas burner is attached to the horizontal extension at the furnace bottom. This burner produces hot combustion gases which flow vertically upward and simulate the combustion products leaving the stoker bed. Large, stoker-size particles are fed into a water-cooled collar at the furnace top via an auger/vibrating tray system (Figure 1a). The partially burned particles are collected at the bottom of the furnace in a water-spray trap (Figure 1b). The trap contains six commercial spray nozzles which create a water screen through which the particles must fall. A water bath at the bottom of the trap insures complete quenching.

Exhaust gas samples are continuously withdrawn through a water-cooled, stainless steel probe positioned in the flue. NO and NO_x are measured with a chemiluminescent analyzer while CO, CO_2, and O_2 are determined by NDIR's and paramagnetic analyzers. Coal and char compositions are determined with a Perkin-Elmer 240 B Elemental Analyzer.

EXPERIMENTAL RESULTS

The experimental results from the suspension phase experiments are both direct and indirect. During the actual experiment, real-time data on the nature and extent of combustion are obtained indirectly by measurement of the composition of the flue gases leaving the furnace. Subsequent to the actual experiments, the coal and partially burned particles are analyzed to directly establish the carbon, hydrogen and nitrogen loss.

Table I shows the ultimate and proximate analyses of the coal being used throughout this program. It is a high-volatile, bituminous coal from southern Utah, and it contains 1.68 percent N (DAF). Figure 2 shows the particle-size-distribution data for this coal plotted on the standard, spreader stoker size chart.

In the first experimental tests, the normal size distribution coal was fed at a rate of 12 lbs/hr, and the gas burner (bottom) was fired at 150,000 Btu/hr. The upper curve in Figure 3 summarizes these results. As the mean free-stream-oxygen concentration was increased from two percent to 10 percent, the coal burning rate increased significantly, indicating a strong dependence on oxygen partial pressure. However, at all conditions, the burning rate was low; less than 10 percent of the 12 lbs/hr being fed were actually consumed.

Analysis of the solid particles collected at the bottom of the furnace indicated that:

- nitrogen was being preferentially evolved; and,
- the larger particles were essentially unreacted.

These results suggested that the fines (particles less than 0.1 inch) were very important in the suspension-phase burning. To investigate this, the standard coal was sieved with an 0.096-inch screen. This removed approximately 15 percent of the coal (by weight). The remaining large particles were then fed into the furnace, and the experiments repeated. The lower curve of Figure 3 shows these results which confirmed that under the conditions of these tests (1700°F walls, 6 ft vertical drop), only the smallest particles reacted.

To investigate the influence of particle-heating rate, similar tests were conducted with the auxiliary burners each firing at 40,000 Btu/hr. Figure 4 shows the influence of these burners on the wall-temperature profile. The auxiliary heating both raises the overall temperatures and makes the profile more uniform. Figure 5 shows the influence of the increased heating rate on the large particles (greater than 0.1 inch). In these tests, the coal-feed rate was 10 lbs/hr; hence, less than three precent of the coal was burning.

PRELIMINARY CONCLUSIONS

Based on the limited data obtained to date, it appears that the overthrow phase of a spreader stoker may have a significant impact on the fines, but it probably has little effect on the bulk of the coal feed. Further, nitrogen evolved from the small particles may be converted to NO_x in much higher proportions than nitrogen evolved in the bed; hence, the fines may be of exaggerated importance in terms of NO_x formation.

SECTION 4

FIXED-BED COMBUSTION

FURNACE DESIGN

The fixed-bed furnace was designed to provide a Lagrangian simulation of the time/temperature/environmental history seen by a small section of the stoker bed as it moves through a large, mass-burning chain-grate or vibrating-grate stoker. In this way, the horizontal, planer dimensions were reduced dramatically compared to the full-size unit; however, the vertical dimension was scaled 1:1. Figure 6 shows a side view of the fixed-bed furnace which was designed to have a maximum superficial firing rate of approximately 600,000 Btu/hr-ft^2. The furnace itself is 27 inches by 23 inches by eight feet outside, and the inner combustion chamber is 11 inches by 15 inches.

The furnace is composed of four, separate, flanged sections. Section A, the upper most section, contains the six-inch circular flue, and a three-inch, expanding quartz window to provide a view of the combustion chamber from above. Sections B and C are the central furnace pieces and contain overfire-air slots, large observation ports, and probe ports. All three of the upper furnace sections have composite walls consisting of one-eight-inch carbon steel, four inches of block insulation, and two inches of high temperature refractory.

The lower furnace section, labeled D, contains the experimental coal bed. The bed proper is 10 inches wide and six inches deep with the total surface area of 0.42 ft^2. Immediately adjacent and surrounding the bed is a one-inch, high temperature, refractory wall, which is used to confine the coal. Just outside the wall, there are porous stainless steel, methane burners with an equivalent surface area (0.42 ft^2). These gas burners are used to provide uniform heating of the combustion chamber when coal is not being burned. The coal bed and gas burners are mounted in a "drawer-like" assembly which rolls out of Section D to permit easy loading of the coal particles.

The combustion air is distributed between the underfire-air plenum and two levels of overfire-air ports. In this study, the air was metered with 600 mm rotameters, but was not preheated.

Exhaust concentration measurements were made in the flue above Section A with a water-cooled, stainless steel probe. The instrumentation described in the previous section was also used for the fixed-bed experiments.

TYPICAL EXPERIMENTAL RESULTS

Figure 7 shows typical experimental results obtained for coal-burning rates as a function of run time. The run was conducted with the Utah coal (Table I), sized at one-half inch through one inch. The data are presented in terms of superficial burning rate; the rate of heat release per unit area of bed surface. The superficial burning rate was computed from exhaust oxygen concentrations and air-supply flow rates. The data show that as the run proceeded the burning rate increased, reached a maximum, and then decreased. It is believed that the burning rate increase is attributable to an increase in bed temperature. Limited temperature measurements indicated that the coal bed burned in excess of 2400°F. The average coal-burning rate over the control interval (six minutes to 25 minutes in this case) was 311,000 Btu/hr-ft^2 for this particular run.

In order to separate parametric effects, it was necessary to keep both total and bed-region stoichiometries constant during a coal run, even though the burning rate changed significantly. This required precise control of the air supply, which was achieved by continuously monitoring the carbon dioxide concentrations in the exhaust gases.

Figure 8 gives the overall and bed-region stoichiometries as a function of run time. The stoichiometric ratios were computed from effluent gas oxygen concentrations and air-supply-flow rates at one-minute intervals. Both the overall and bed-region stoichiometries were controlled to within approximately ± 0.1 of their respective average stoichiometries for the run, except in the early stages of the experiment. A control interval was defined for each run on the basis of these narrowly bounded, average stoichiometries. Average values for NO emissions and burning rates were computed for this interval only.

Figure 9 shows the effluent-gas concentration of NO converted to zero percent exhaust O_2 as a function of run time. The exhaust gas concentration of NO increased rapidly in the initial stages of the run, passed through a maximum and then decayed toward the termination of the run. Comparison of Figures 7 and 9 indicates that NO formation peaks prior to achieving the maximum combustion rate. This "early" NO generation is typical of all the coal runs.

INFLUENCE OF BED STOICHIOMETRY

Figure 10 shows NO emission results (plotted as lbs $NO_2/10^6$ Btu) for three different bed stoichiometries. In each test, the overall stoichiometry was held constant at 1.35 ± 0.03, and the firing rate was approximately 500,000 $Btu/hr\text{-}ft^2$. The overfire air was added in two volumetrically equivalent portions through opposing jets at 15½ inches and 44 inches above the coal bed. Neither the overfire nor underfire air was preheated in these experiments.

As the combustion was staged, with the total air supply held constant, the NO emissions decreased substantially. Based on these limited data the dependence of NO_x on primary zone stoichiometry appears to be approximately linear, and this is in marked contrast to pulverized-coal combustion. No problems with clinkering or incomplete combustion were encountered; CO emissions were always less than 0.03 percent.

BURNING RATE

Figure 11 shows the integral superficial firing rates for two cases with nearly identical stoichiometric distributions ($S.R._B = 0.83 \pm 0.02$, $S.R._T = 1.37 \pm 0.05$), yet widely different burning rates. The lower burning rate experiment was conducted by significantly cooling the walls of the bed prior to charging the reactor with coal. For each experiment, the data are presented for the combustion of 4.5 pounds of coal (hence, in Figure 11, the high burning rate case ends first at 16 minutes). An average burning rate of 546,000 Btu/hr-ft^2 was achieved for the "hot" run, while a corresponding burning rate of only 398,000 Btu/hr-ft^2 was attained for the "cold" run.

Figure 12 shows NO emissions for both the "hot" and "cold" experiments. The rate of NO formation was substantially greater for the "hot" case, in spite of the fact that in both experiments the bed was fired without excess air. The disparity in rates of NO formation cannot be attributed simply to a difference in the amount of coal consumption since the data were normalized to the same basis (lbm $NO_2/10^6$ Btu) independent of coal-feed rate. The integrated emission factor over the control interval for the high temperature run was 0.273 lbm $NO_2/10^6$ Btu as compared with the respective average emission factor for the low temperature experiment of 0.180 lbm $NO_2/10^6$ Btu. The marked difference in NO emissions between high and low load firing was observed during oxidant-rich combustion as well, indicating a strong dependence of NO formation upon bed heat-release rates.

The dependence of NO emissions upon bed heat-release rates suggests that as the burning rate increases, local bed temperatures increase. This may result in higher volatile nitrogen yields and, hence, higher NO_x emissions.

PRELIMINARY CONCLUSIONS

The following tentative conclusions have been reached regarding the formation of nitrogen oxides in a fixed-bed combustion system:

1. NO formation is not uniform throughout the burning time of the bed. The formation maximizes early in the process, prior to the peak combustion rate and then gradually decreases.
2. Staged air addition is a potentially effective means of NO control. Exhaust concentrations decrease approximately linearly with decreasing bed stoichiometry.

3. Increasing the bed heat-release rate increases the NO_x emissions with staged-air conditions.

SECTION 5

MODEL SPREADER STOKER

The purpose of the third task is to apply the pollutant reduction concepts developed in Tasks 1 and 2 to an actual stoker system in which the suspension and fixed-bed burning phases are coupled. A model spreader stoker has been designed based on the following parameters which were scaled 1:1 with current commercial practice:

- bed heat-release (approximately 750,000 Btu/hr-ft^2);
- spreader-to-grate distance (approximately 32 inches); and,
- grate-to-convective passage distance.

The bed heat-release rate is a direct reflection of the local burning rate and, hence, the particle temperatures, local oxygen availability, etc. The spreader-to-grate distance determines the residence time of the particles in the suspension phase and, therefore, the amount of devolatilization that occurs prior to the bed. The grate-to-convective passage distance controls the gas-phase residence time prior to strong quenching.

The overall furnace design is illustrated in Figure 13. As shown, the furnace will stand 10.8-ft high, which corresponds approximately to the height of the radiant section in a spreader stoker furnace. Section 1 is the ash storage secton and will be equipped with an ash drawer capable of holding ash from a 14-hour run.

Section 2 is the grate-burning bed section. The 1 ft^2 coal grate will actually be a type of dumping grate design in which the ash is allowed to build up to some predetermined depth and then dumped. After dumping, two inches of ash will remain on the grate to partially insulate the metal grate from excessive heat. Section 2 will contain ports for flame and solids sampling, a large removable section for access to the bed, and a 4-inch window for observation of the bed.

Section 3 will contain two horizontally opposed gas burners (300,000 Btu/hr each) for use between experimental runs and overnight when the coal-feed system will be shut down. Overfire-air ports will be located in both front and back walls and there will be a large slot port for insertion of probes or cooling coils. The side walls will contain 2-inch diameter ports for a pilot burner and ultraviolet flame detectors.

Section 4 will include the coal distribution system. Coal from a sealed storage hopper will be metered into the furnace at a rate of up to 60 lbs/hr via an auger. The coal will then drop onto a vibrating tray which will serve to dampen any pulsations from the auger, and also to distribute the coal uniformly to a width of eight inches. At the end of the tray, the coal will drop into the furnace shell and onto the rotating spreader. An adjustable plate will be used to vary the exact position at which the rotating spreader strikes the coal particles. The variable-speed spreader will be air-cooled.

Sections 5 and 6 will be equipped with slot ports for overfire air, gas-sampling probes, or cooling coils. Although it is anticipated that the furnace will be operated in an uncooled mode of operation, the capability of inserting cooling coils will allow simulation of the bed adjacent to a water-tube wall.

Section 7 will contain probe ports for temperature, particle mass and size distribution, and gas-species concentration measurements.

The model spreader stoker is currently being fabricated and should be ready for initial shakedown testing in October, 1980. Initial experiments will be conducted to define the interaction between the suspension burning and the fixed-bed combustion since each of these will have been considered separately in the previous tasks. Later, testing will be directed toward defining and optimizing new combustion control technology.

REFERENCES

1. Giammar, R. D. Evaluation of Emissions and Control Technology for Industrial Stoker Boilers. In: Proceedings of the Third Stationary Source Combustion Symposium, EPA-600/7-79-050, NTIS, Springfield, Virginia, 1979.

2. Gabrielson, J. E. Field Tests of Industrial Stoker-Fired Boilers for Emission Control. In: Proceedings of the Third Stationary Source Combustion Symposium, EPA-600/7-79-050a, NTIS, Springfield, Virginia, 1979.

3. Langsjoen, P. L. Characterization of Emissions from Industrial Stoker Boilers. Presented: APCA Conference on Industrial Boilers, Research Triangle Park, North Carolina, December, 1979.

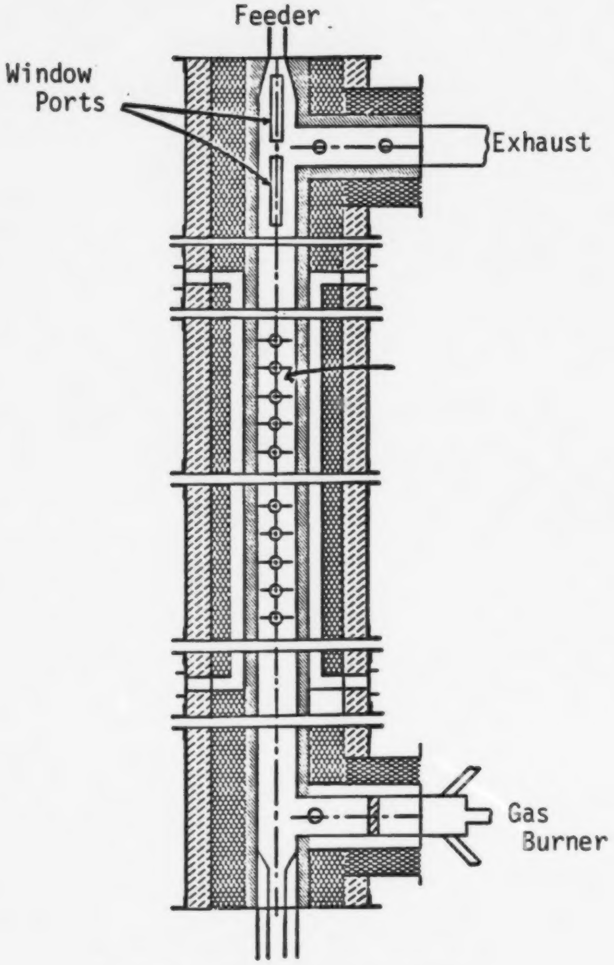

Particle Collection System

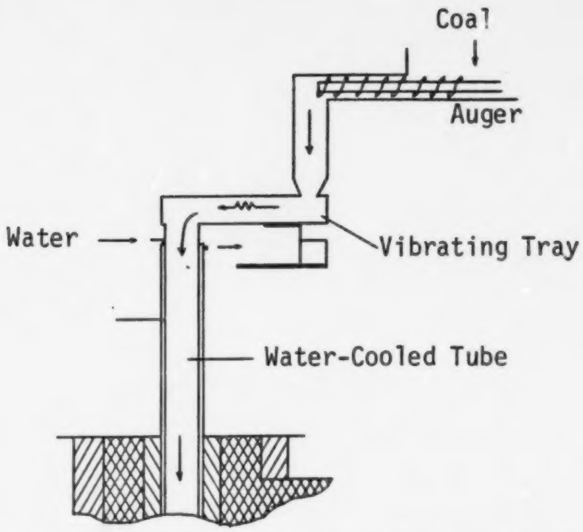

Figure 1a. Feeding System Detail

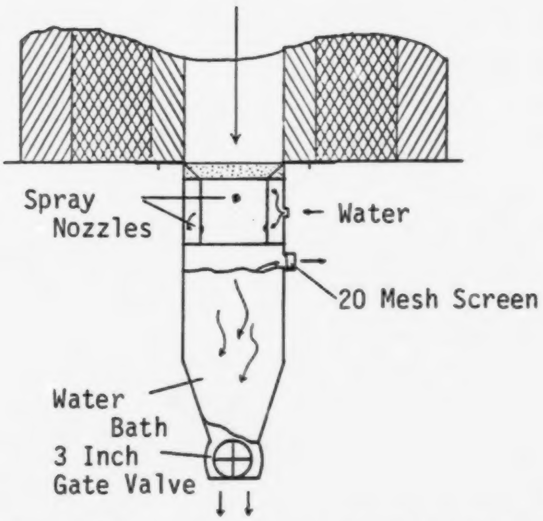

Figure 1b. Particle Collection System

Figure 1. Suspension Furnace

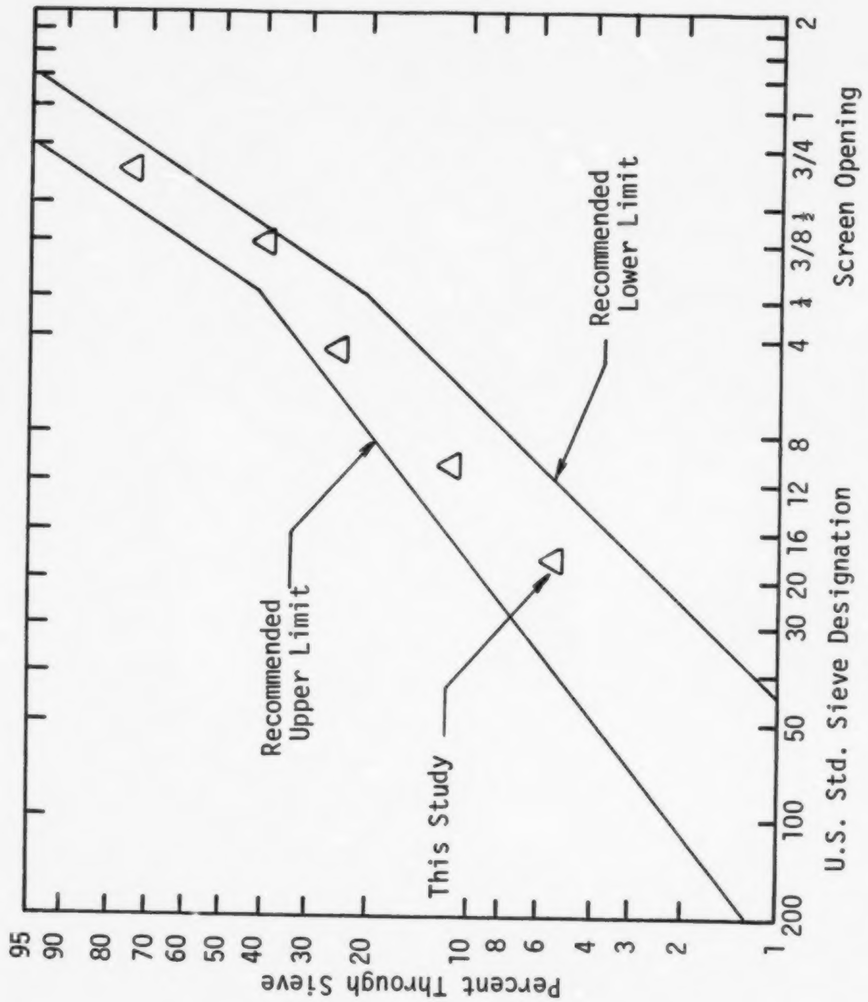

Figure 2. Particle-Size Distribution

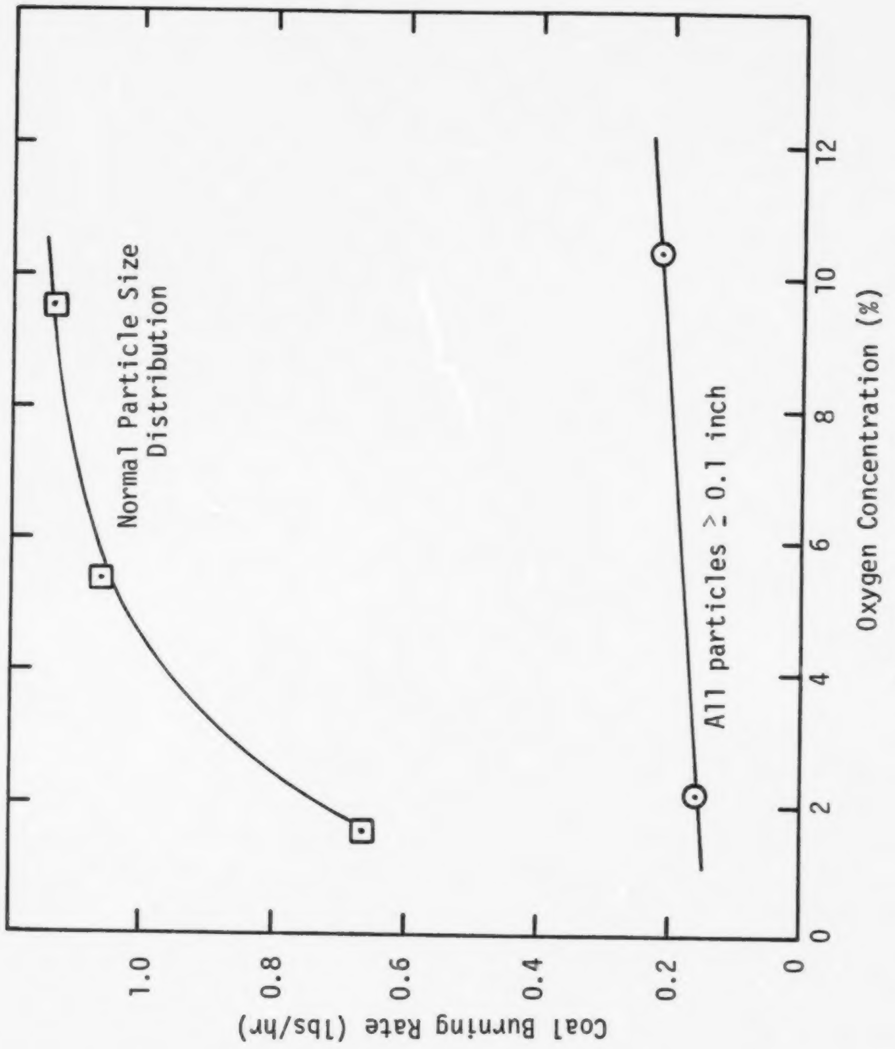

Figure 3. Importance of Fines

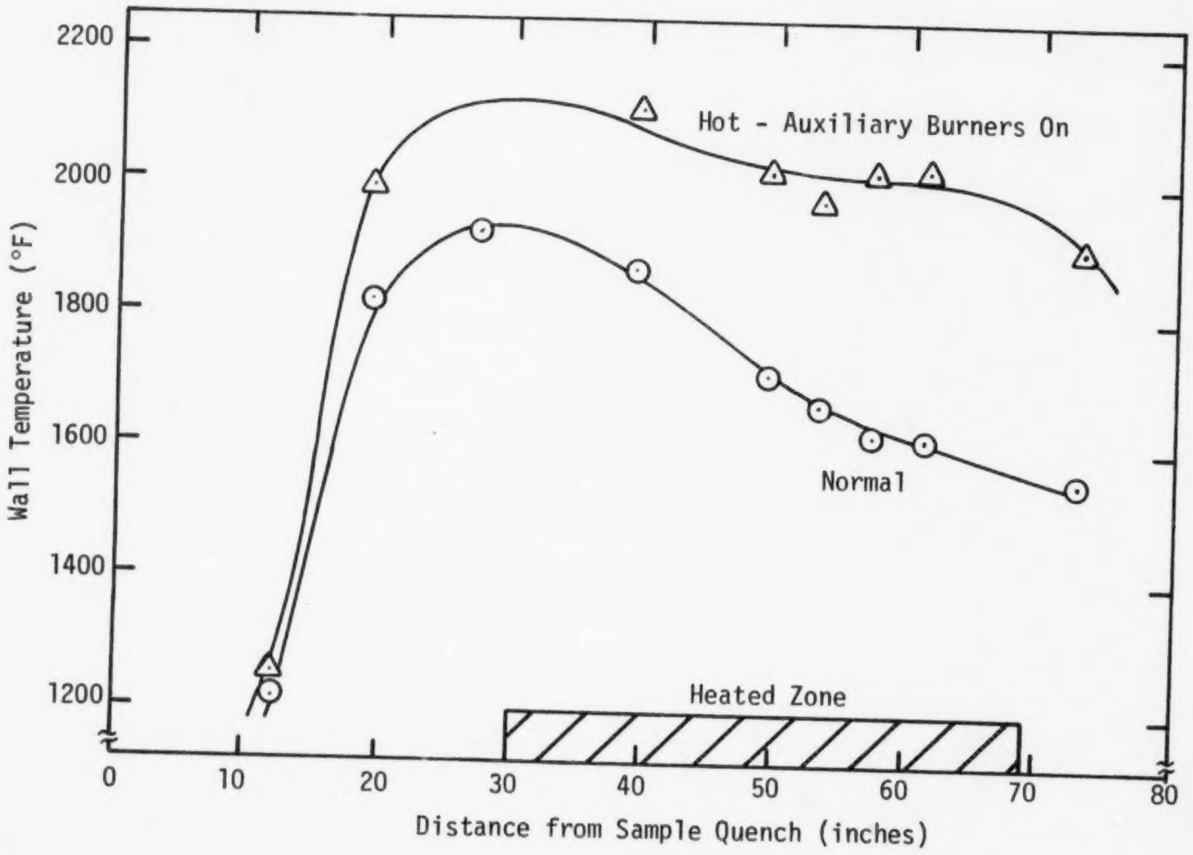

Figure 4. Wall-Temperature Distributions

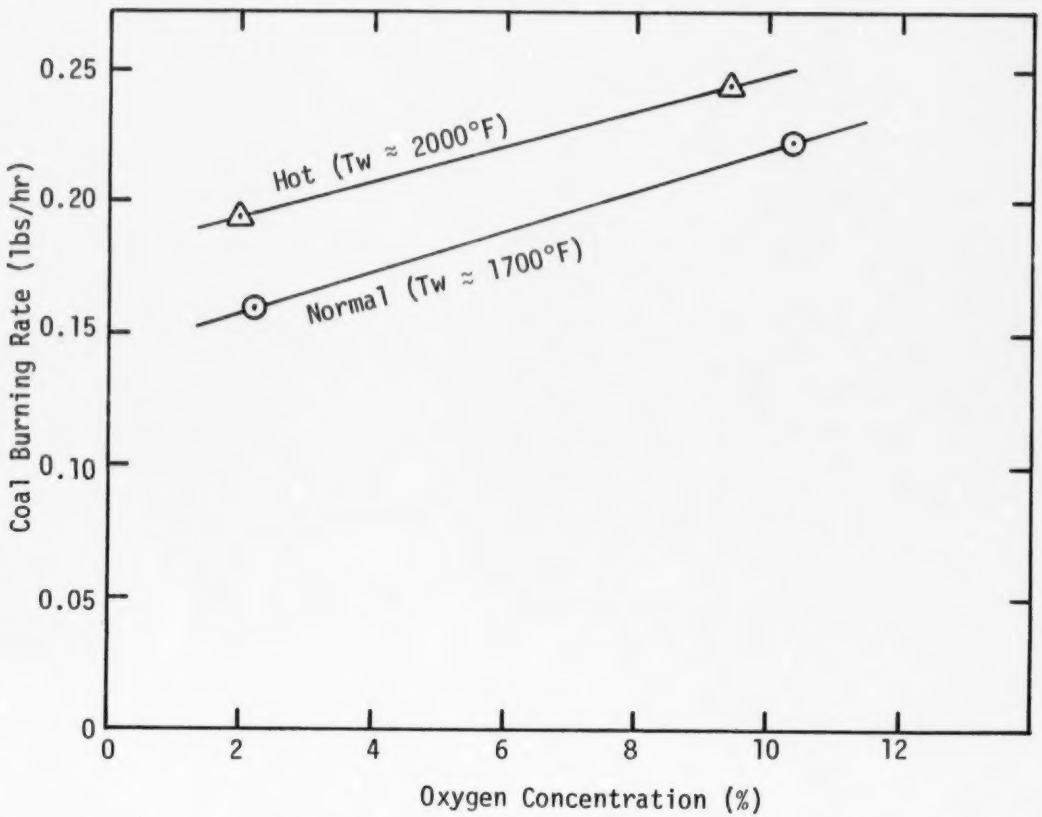

Figure 5. Influence of Particle Heating Rate

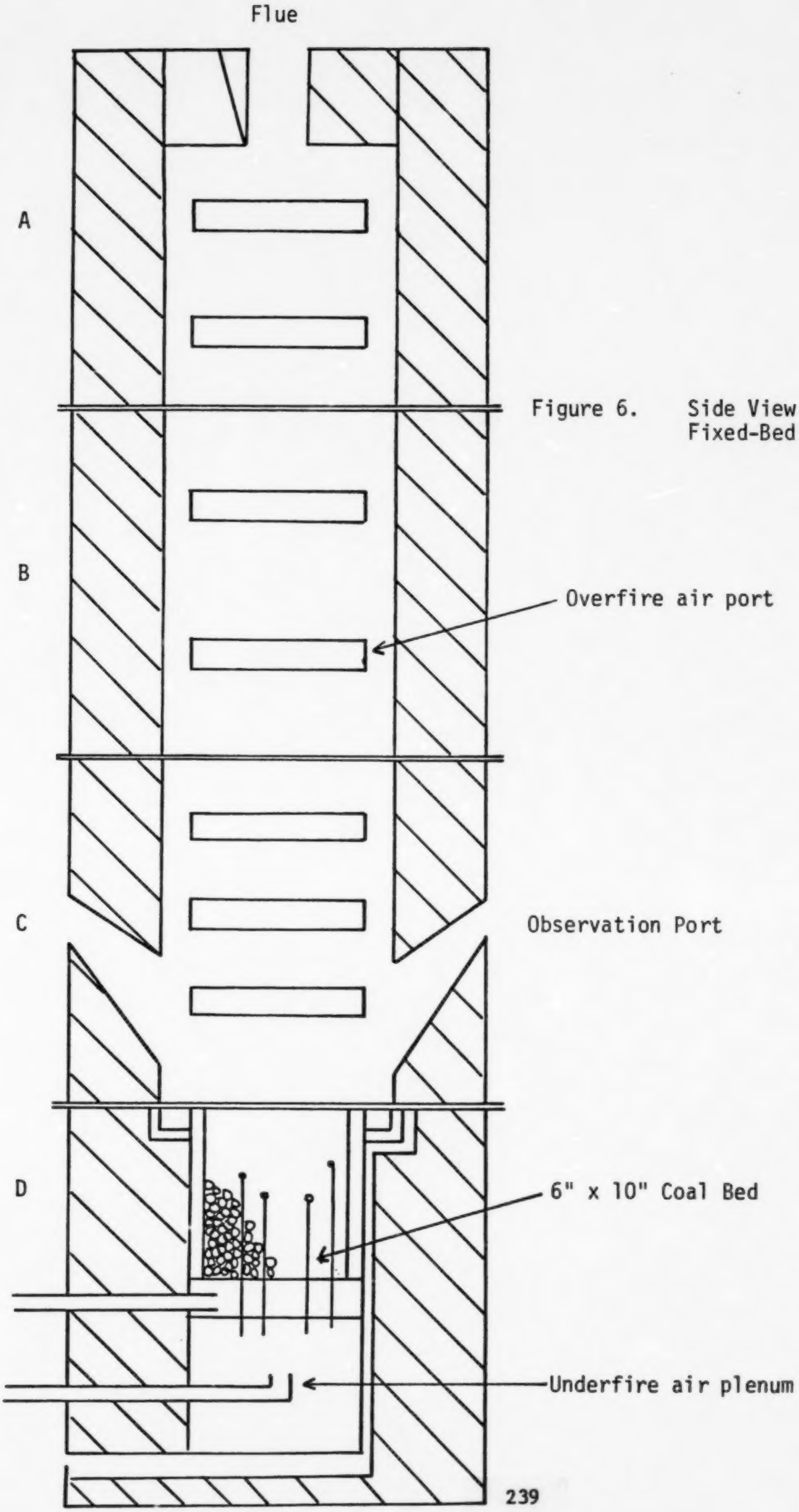

Figure 6. Side View of the Fixed-Bed Furnace

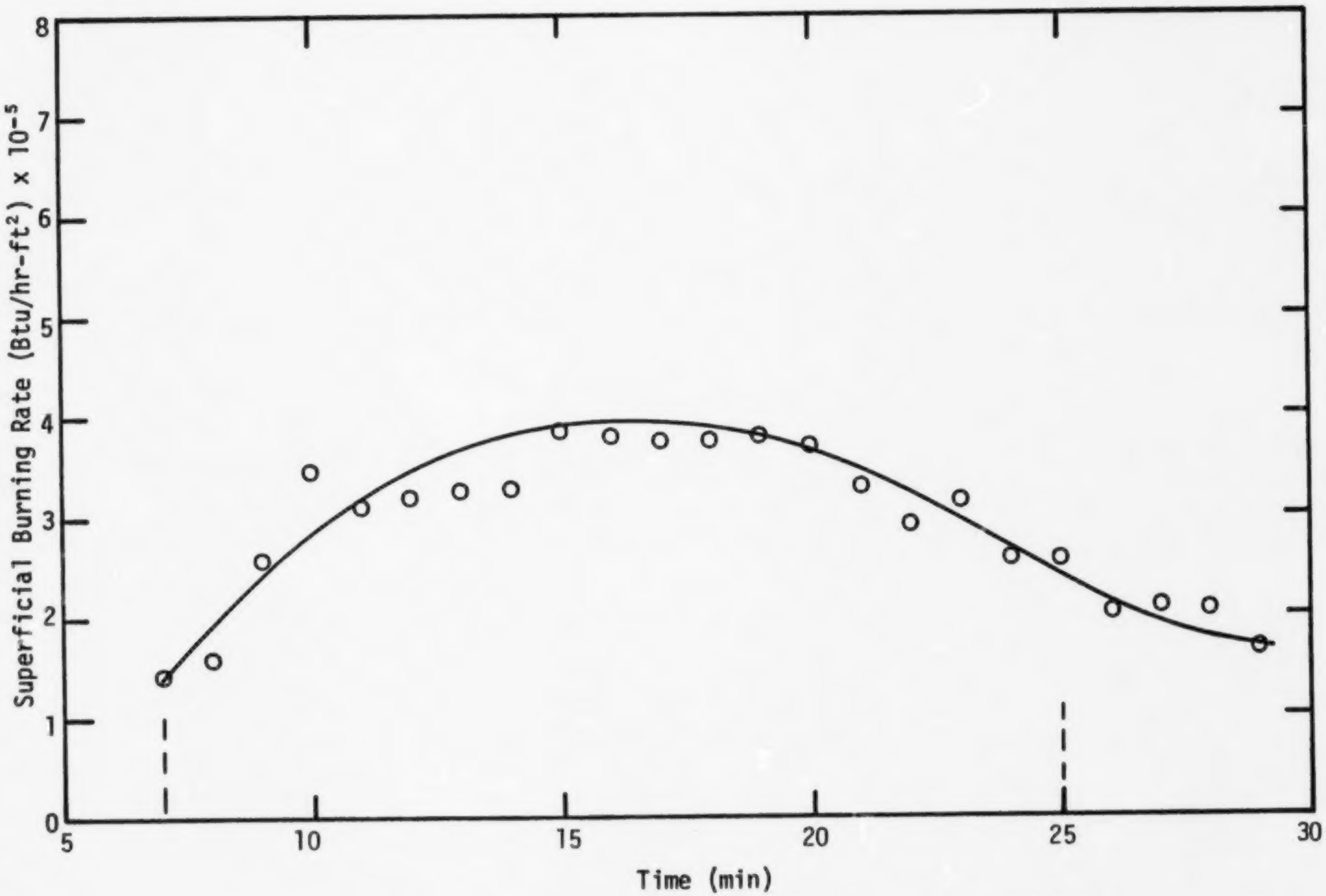

Figure 7. Superficial Burning Rate: UBS - 1/9/80-4

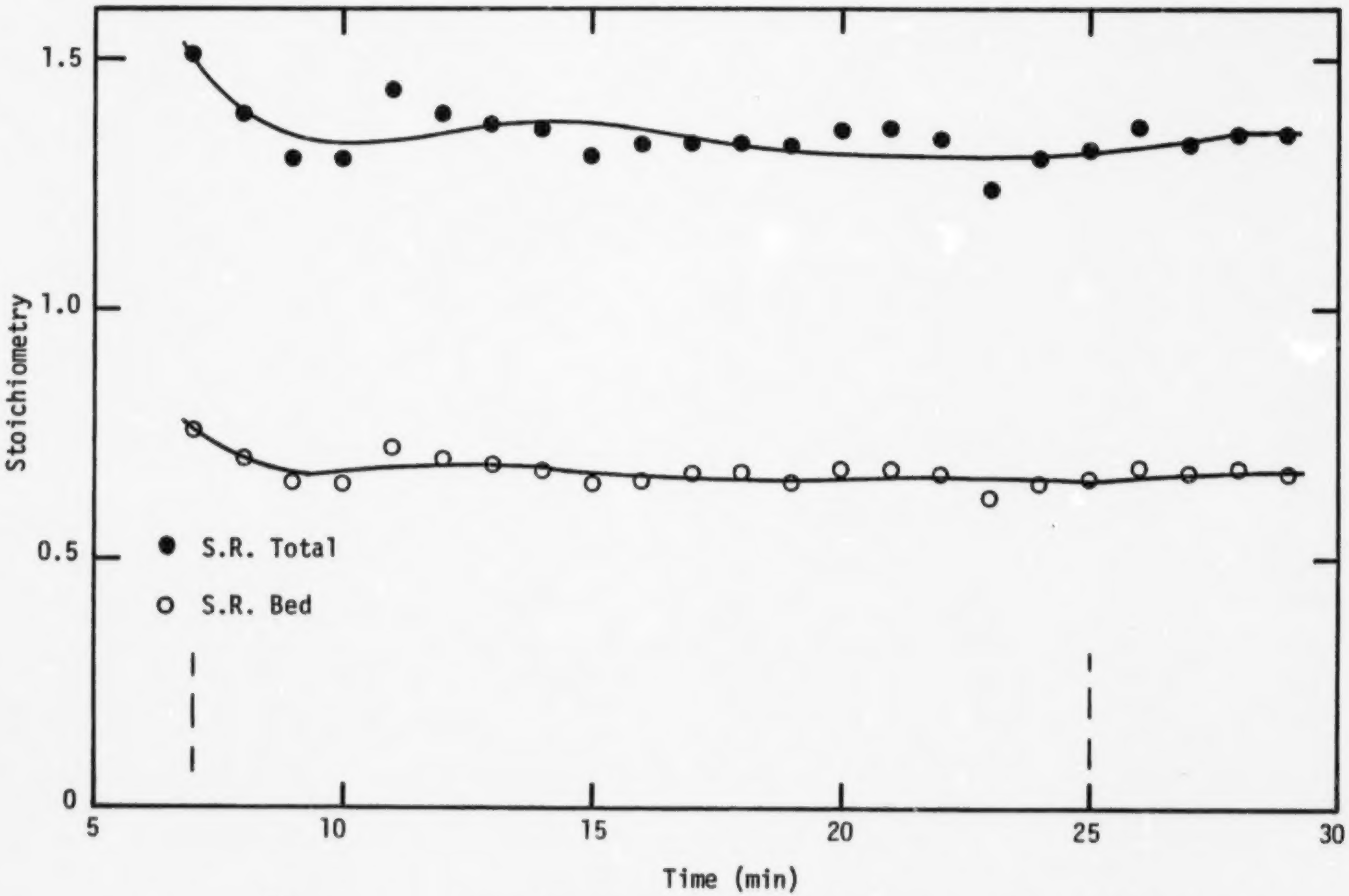

Figure 8. Overall and Bed-Region Stoichiometry: UBS - 1/9/80-4

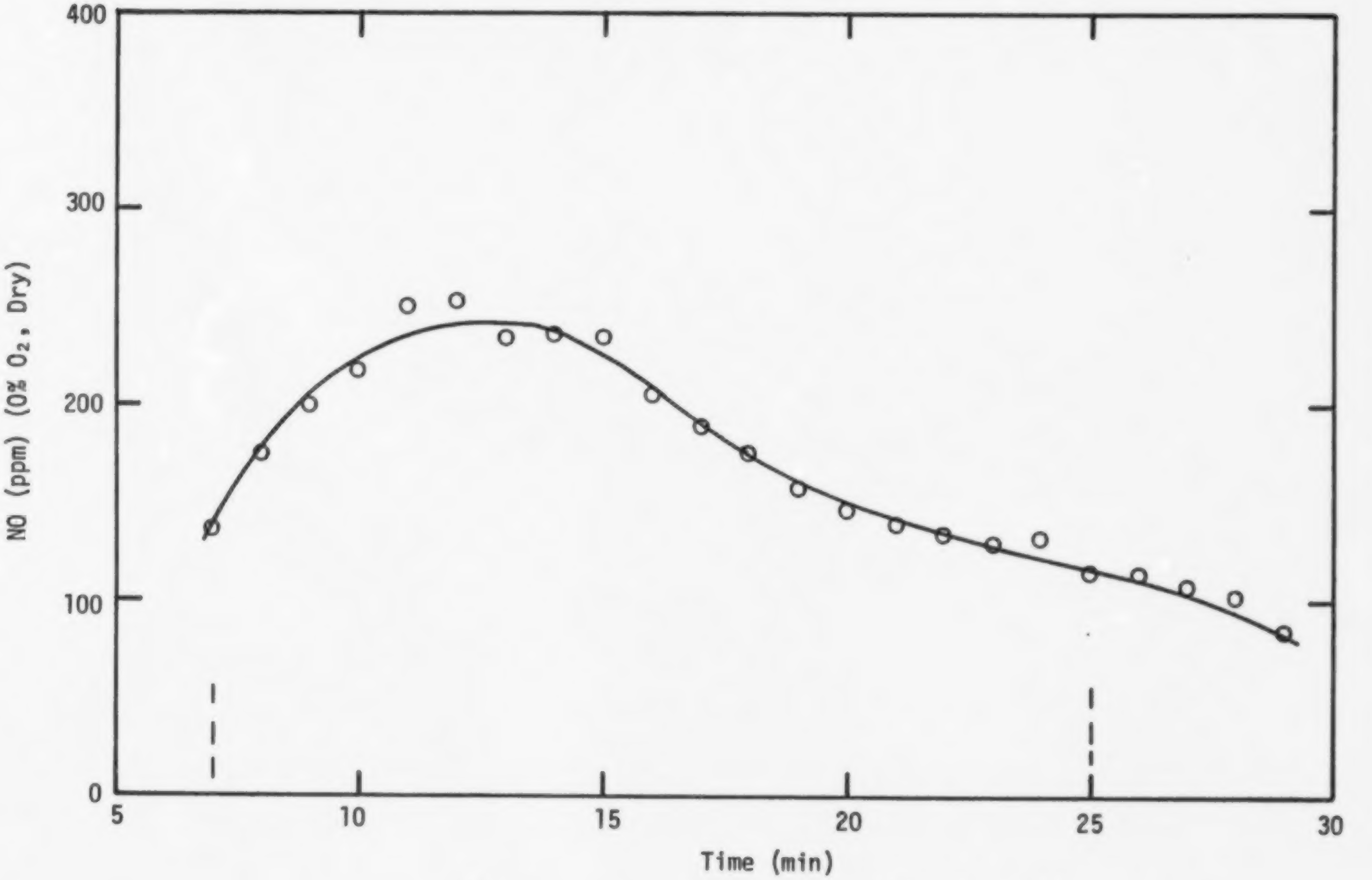

Figure 9. NO Emissions: UBS - 1/9/80-4

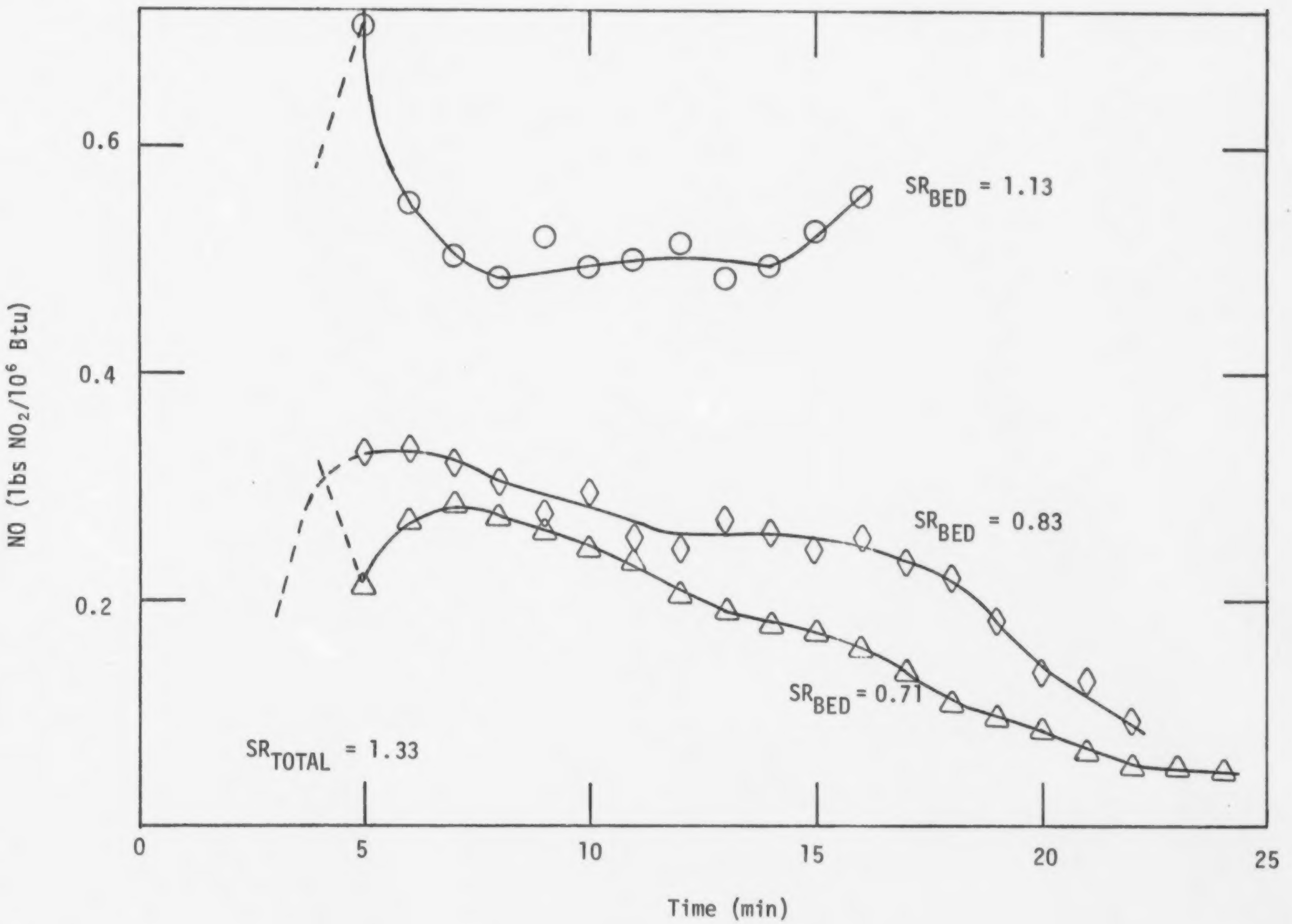

Figure 10. NO Emission Results for Three Different Bed Stoichiometries

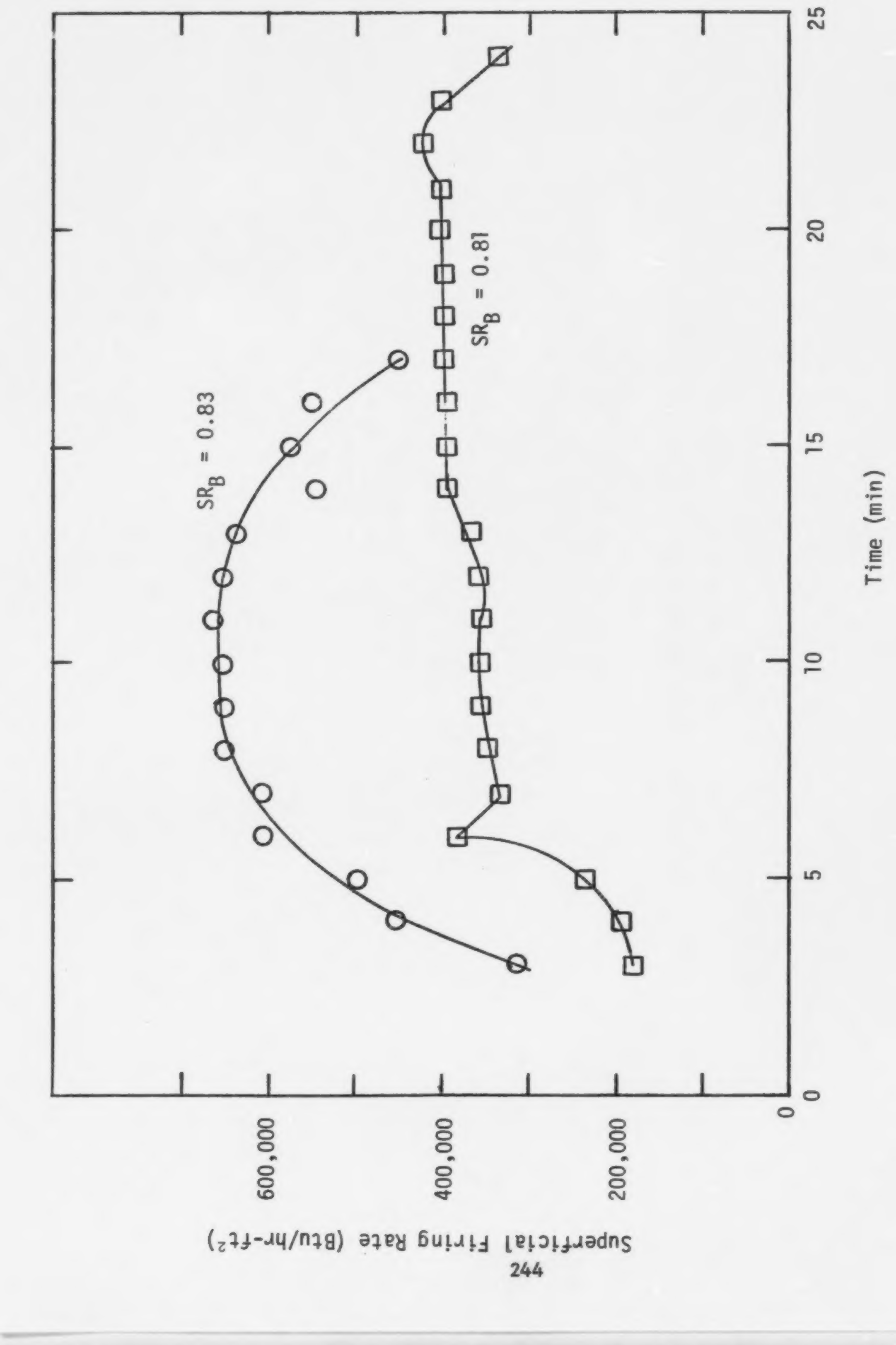

Figure 11. Firing Rate Results

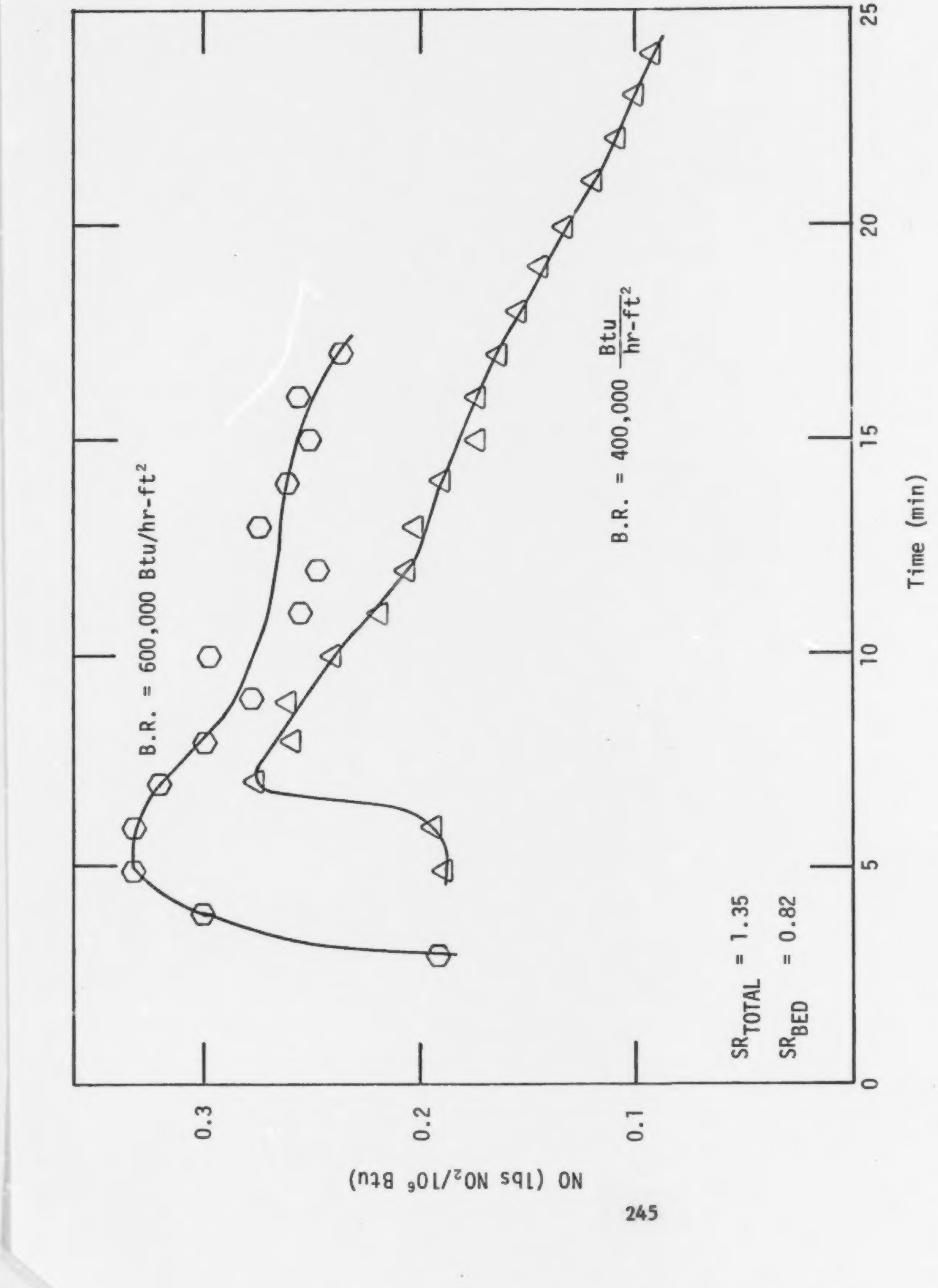

Figure 12. Influence of Burning Rate on NO Emissions

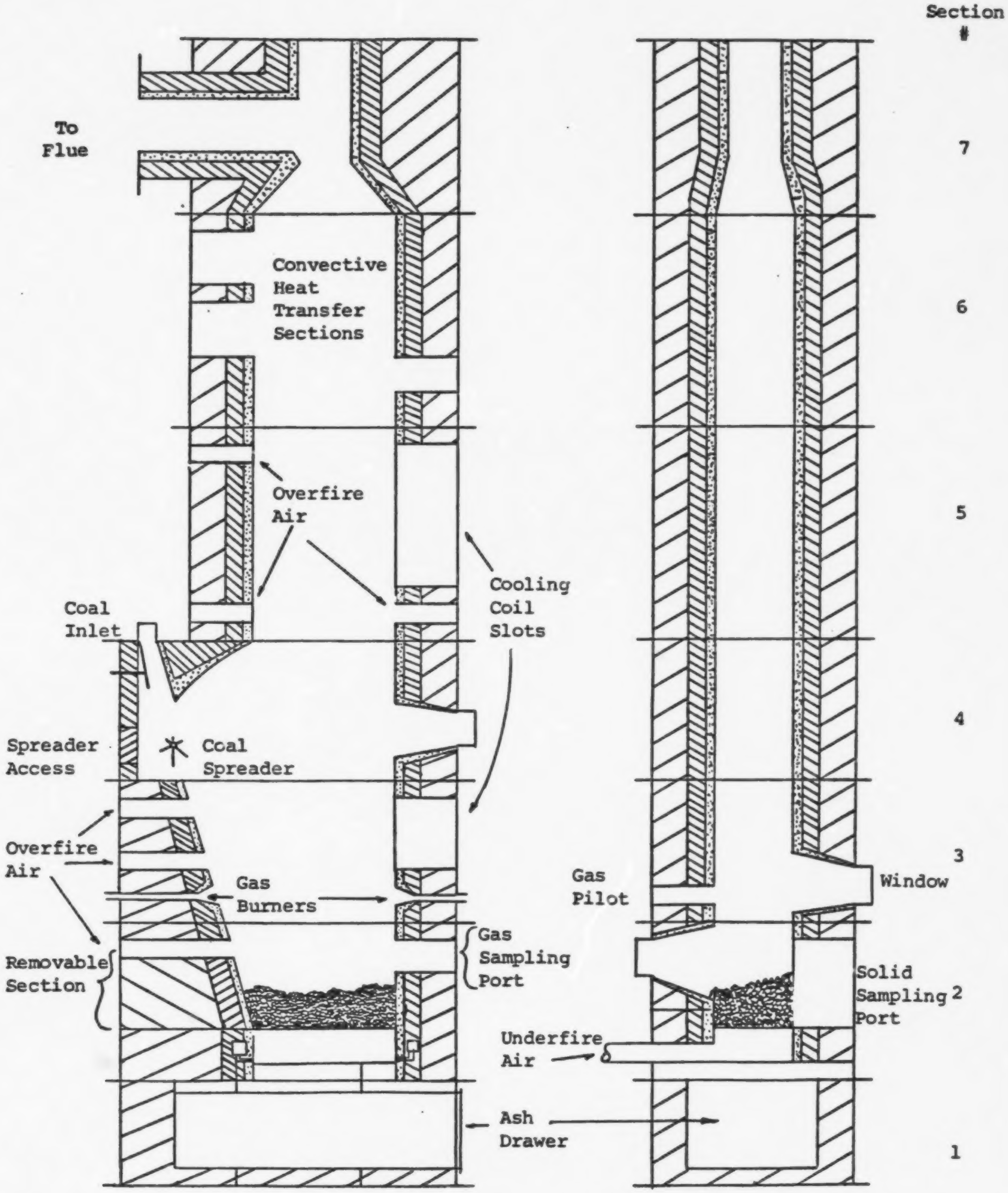

Figure 13. Model Spreader Stoker

Table I

Chemical Analysis - Utah B Coal

Proximate Analysis

Weight %	As Received	Dry Basis
Moisture	6.22	- -
Ash	9.59	10.23
Volatile Matter	37.84	40.35
Fixed Carbon	46.35	49.42
Total	100.00	100.00
Calorific Value (Btu/lb)		
Proximate Value	11,658	12,432
Mineral Matter Free	- -	14,004

Ultimate Analysis

Weight %	As Received	Dry Basis
Moisture	6.22	- -
Carbon	66.44	70.85
Hydrogen	4.86	5.19
Nitrogen	1.42	1.51
Sulfur	0.88	0.94
Ash	9.59	10.23
Oxygen (difference)	10.59	11.28
Total	100.00	100.00

PRESSURIZED BENCH SCALE TESTING OF LOW NO_x LBG COMBUSTORS

By:

W. D. Clark, B. A. Folsom, W. R. Seeker,
C. W. Courtney, and M. P. Heap
Energy and Environmental Research Corporation
8001 Irvine Boulevard
Santa Ana, California 92705

ABSTRACT

The high efficiencies obtained in a combined gas turbine-steam turbine power cycle burning low Btu gas (LBG) make it a potentially attractive alternative to the high sulfur emitting direct coal-fired steam cycle. In the gasification process, much of the bound nitrogen in coal is converted to ammonia in the LBG. This ammonia is largely converted to nitrogen oxides (NO_x) in conventional combustors. This paper examines the bench scale performance of reactors previously demonstrated to produce low NO_x emissions in laboratory scale experiments. Low Btu gas was synthesized in a catalytic reformer and fired in two primary combustors: a diffusion flame and a platinum/nickel oxide catalytic combustor. Effects of scale, primary stoichiometry, pressure, throughput, and primary residence time were examined. Lowest NO_x emissions were produced in rich/lean combustion, utilizing either the diffusion flame or the catalyst in the fuel rich primary stage.

ACKNOWLEDGMENT

The investigations described in this paper were carried out under EPA contract 68-02-2196. The authors wish to express their appreciation to Mr. G. B. Martin, the EPA Project Officer, to Dr. J. Kesselring of the Acurex Corporation for his help in obtaining the catalysts, and to Mister M. Maser of Energy and Environmental Research Corporation for his assistance in conducting the experiments.

SECTION 1

INTRODUCTION

The limited availability and the increasing cost of petroleum based fuels have generated an increased interest in coal as a primary power source. The potential for low sulfur emissions makes combustion of gasified coal an environmentally attractive alternative to direct fired coal combustion. However, low Btu coal gases can contain ammonia concentrations a high as 0.38 percent (1). In a conventional combustor, much of this ammonia may be converted to nitrogen oxides resulting in significant pollutant emission: up to 1370 ng/J (3.2 lbm/10^6 Btu) for full conversion of NH_3 to NO_2.

The gas turbine - steam turbine combined cycle is an efficient method of low Btu gas combustion. The current New Source Performance Standard (NSPS) for steam generators firing coal-derived gaseous fuels with greater than 73.3 MW (250 X 10^6 Btu/hr) heat input is 210 ng/J (0.5 lbm $NO_2/10^6$ Btu)(2). For a combined cycle firing an LBG with 3800 ppm NH_3 to NO would have to be less than 15.7 percent. With the advent of new combustor and cleanup technology it is reasonable to expect that future NSPS will be more stringent; therefore, in the development of energy-efficient LBG combustion systems it is important to achieve the lowest NO_x emissions possible.

Equilibrium and kinetic calculations on fuel nitrogen processing in LBG combustion have been tested at atmospheric pressure in laboratory scale experiments (3-4) resulting in the development of several low NO_x combustor concepts. This paper describes experiments performed on scaled-up LBG combustors, utilizing these low NO_x concepts, operated at pressures more nearly approximating gas turbine combustors, Sections are included to discuss background, experimental systems, results and conclusions.

SECTION 2

BACKGROUND

Coal-derived low Btu gas comprises a family of fuels of varying composition, ranging in heating value from 3.0×10^6 to 7.5×10^6 J/m^3 (80 to 200 Btu/ft^3), produced by reforming coal with air and steam. Its principle components are CO, H_2 and light hydrocarbons as combustibles; and N_2, H_2O and CO_2 as inerts. Significant amounts of ammonia, sulfur compounds and particulate matter may also be present. These impurities may be partially removed in several alternative gas cleaning systems prior to combustion (5). The most energy efficient cleanup systems operate hot, removing a majority of sulfur products and particulates, but some systems do not remove much of the ammonia from the LBG.

Figure 1 is a simplified schematic of an LBG-fired gas turbine-steam turbine combined cycle power plant with integrated gasifier. In the high pressure gas turbine topping cycle, LBG is produced in a gasifier and burned in an adiabatic gas generator to produce the hot pressurized gas that turns the gas turbine. Heat in the exhaust gas is recovered in a waste heat boiler and utilized to drive a steam turbine bottoming cycle. Under optimum operating conditions utilizing current technology including high-temperature sulfur removal, an overall efficiency of 40% can be achieved in the combined cycle. Future generation systems, operating at higher pressures and temperatures, could achieve efficiencies up to 48%. Variations of the combined cycle which can improve the performance of the bottoming cycle and increase the overall efficiency include utilizing the gas generator as a super-charged boiler and reheating the gas turbine exhaust. A more detailed discussion of combined cycle optimization is included in reference 6. A low NO_x LBG combustor would function as the gas generator of the combined cycle. It must operate at high pressure and its effluent gas should be low in NO_x, CO and hydrocarbons.

Figure 2 shows that minimum equilibrium fixed nitrogen concentrations of less than 1 ppm occur in the adiabatic combustion of a 3.35×10^6 J/m^3 (90 Btu/ft^3) LBG between 60 and 80% theoretical air. The location and value of this minimum change with adiabatic flame temperature, depending upon the composition and preheat temperature of the LBG. Lower temperatures push the minimum to leaner stoichiometries. An ideal low NO_x combustor, shown in Figure 3, would operate in two stages. In the fuel rich-primary stage, sufficient holdup time would allow ΣXN ($\Sigma XN = NH_3 + HCN + NO + NO_2$) to approach an N_2 favored equilibrium. In the fuel-lean secondary stage, the remnants of the fuel would be burned out, meeting the low CO and HC requirements.

In a practical combustor, the mechanics of primary fuel/air contacting affect the fuel nitrogen processing. Laboratory scale flame reactor experiments, discussed in detail in references 3, 4 and 7, to investigate and optimize these effects were performed in a previous part of this program. Promising results were achieved utilizing either a catalytic reactor or a diffusion flame reactor.

Use of a catalyst in the rich stage could shorten the holdup time required to reach low ΣXN levels, reducing the size of the combustor. Studies of NO reduction in automotive exhaust have shown that platinum effectively promotes the reduction of NO to NH_3 and in combination with an NH_3 to N_2 catalyst, such as nickel, can speed the complete reduction of NO to N_2 (8). Catalytic combustion studies have indicated the potential of several catalysts for XN reduction in rich combustion, including platinum and nickel oxide (9). For gas turbine combustion application, pressure-drop must be kept to a minimum. The graded cell catalyst concept has been developed to maximize throughput while keeping emissions and pressure-drop low (10). Ceramic honeycomb monoliths are coated with the catalyst and stacked in the order of decreasing cell size. The coarse upstream cells tend to hold the flame while the fine downstream cells tend to complete the reaction.

In a lean-diffusion flame, a single fuel nitrogen molecule passes through the entire range of stoichiometries: from an initially very rich zone, through the stoichiometric flame front, into the lean post flame zone. Thus a lean diffusion flame is, in effect, a multistage combustor. Low conversions of fuel nitrogen to NO_x ahve been observed in fuel-lean laminar diffusion flames. Turbulence tends to increase NO_x emissions (11).

In a fuel-rich laminar diffusion flame, part of the fuel never passes through the flame front; thus, depending on downstream temperatures and mixing conditions, it is possible for some of the fuel nitrogen to pass through unprocessed. High NH_3 concentrations have been measured in the products of an NH_3-doped fuel-rich laminar diffusion flame (12). Turbulence in a rich diffusion flame would be expected to enhance mixing in the hot region within the flame and immediately downstream, increasing the reduction of fuel nitrogen.

SECTION 3

EXPERIMENTAL SYSTEMS

The apparatus for the bench scale experiments can be divided into four subsystems: LBG supply, modular combustors, sample train and control systems. A simplified schematic of the facility can be seen in Figure 4.

LBG is synthetically produced from hot air premixed with vaporized water and heptane passed through a catalytic reformer. The reformer is operated at pressures between 6.4 and 11.9 atmospheres at a stoichiometry of 45% theoretical air, the richest stoichiometry attainable without excessive sooting. The water acts as a diluent to maintain the maximum catalyst bed temperature at around 1370° K. Table I shows measured and equilibrium LBG compositions at the standard operating point. The reformer product gas passes through a variable heat exchanger, cooling it to the desired preheat temperature. Ammonia and methane are added to trim the gas to the desired fuel nitrogen and hydrocarbon content. The LBG passes through a soot filter and into a valve system, controlling the fraction of the LBG which goes to the combustors and the fraction which is bypassed. If none of the gas is bypassed, maximum combustor capacity is 60,000 J/s (200,000 Btu/hr).

The combustors consist of a series of modules with 5 cm (2 in) ID reaction/flow chambers enclosed in 15 cm (6 in) OD low-density insulation and housed in flanged steel pipe. Primary ignition modules include the catalyst and the diffusion flame. Secondary burnout is achieved in the jet-stirred secondary air injector. Plug flow modules of various lengths allow control of primary and secondary residence times. Platinum/rhodium thermocouples in each module allow primary and secondary temperature measurements. The interchangeable modules can be combined to model and optimize a variety of combustor concepts. The primary ignition modules are shown in Figure 5. In the catalyst module, premixed LBG and primary air pass through a stainless steel flow straightener/flame arrestor and into the graded cell catalyst. The catalyst, supplied by Acurex, consists of three zironia honeycomb monoliths of decreasing cell size, coated with nickel oxide. Platinum has been added to the coating of the upstream monolith to promote ignition. Thermocouples detect flashback and measure catalyst bed and wall temperatures. In the concentric diffusion flame module, LBG is introduced through a removeable fuel tube of variable diameter. Straightened primary air passes annularly around the fuel tube in the direction of the fuel flow.

Samples are taken in the secondary region, through a water-cooled stainless steel probe situated on the centerline of the flow chamber. The cooling water is preheated and the stainless steel sample lines are wrapped with heat tape to maintain the sample system above the dewpoint of the exhaust gases. The sample stream is throttled to nearly atmospheric pressure. Batch wet samples can be taken by two bubblers in series and later analyzed by specific ion techniques to determine the ammonia and hydrogen cyanide content of the gas. Low NH_3 and HCN concentrations have been measured (less than 10% of ΣXN), indicating that the secondary zone is long enough for nearly complete processing to NO_x. Continuous gas samples are passed through a water trap maintained at 0°C, through a teflon-lined sample pump and into the emissions console which measures CO and CO_2 by infrared analysis, NO and NO_x by chemiluminescence, O_2 by paramagnetic analysis, and hydrocarbons by flame ionization. LBG samples are taken downstream of the soot filter in a similar system.

Air, water, heptane, methane and ammonia streams are measured by rotameter. LBG flow to the combustors and primary and overall stoichiometry are calculated by oxygen balance, utilizing the secondary O_2 concentration and the primary and secondary air flows. Reformer pressure is controlled by a valve on the LBG bypass line. Combustor pressure is maintained by passing the exhaust gases through a small orifice downstream of the combustors. The pressure upstream of the orifice is a function of the mass flow rate and the temperature of the exhaust gases. Constant pressure tests are performed by keeping the LBG flow and the total air flow constant. The primary stoichiometry can be changed by varying the ratio of primary to secondary air, but the overall stoichiometry is maintained constant. The exhaust gas temperature in the nearly adiabatic system is a function primarily of the overall stoichiometry. Variable pressure tests are performed by varying the total flow. The opposing effects of increased pressure and increased flow tend to keep residence times constant for variable pressure tests. Variable pressure tests at constant flow (variable residence time) can be performed by changing the size of the flow-restricting orifice.

SECTION 4

RESULTS

Encouragingly low NO_x levels have been achieved on the bench scale utilizing a catalytic reactor and a diffusion flame reactor. An effective fuel nitrogen-reducing catalyst was identified in laboratory scale experiments and the effects of scale and stoichiometry were examined in the bench scale experiments. A fuel-lean diffusion flame was identified as an attractive low NO_x combustor concept in laboratory scale experiments and effects of scale, stoichiometry, hydrocarbon content of the fuel, fuel tube size, pressure, and primary residence time were examined in the bench scale experiments.

Effects of catalyst type on fuel nitrogen processing in LBG combustion were examined on the laboratory scale in an unstaged catalytic reactor operated at a constant adiabatic flame temperature of 1473°K. Figure 6 shows the variable stoichiometry results for two catalysts. The alumina supported platinum catalyst converted almost all fuel nitrogen to NO_x in fuel-lean combustion and had a minimum conversion of 40% in fuel-rich combustion. At stoichiometries richer than 60% theoretical air, decreasing NO concentrations were overwhelmed by increasing NH_3, and HCN concentrations, causing a sharp rise in ΣXN. The zirconia supported platinum/nickel oxide catalyst converted 80% of the fuel nitrogen to NO_x in lean combustion, but had very low conversions in rich combustion. For a 500 ppm NH_3 in LBG dopant level, less than 10 ppm ΣXN were measured at stoichiometries as rich as 40% theoretical air. Tests of the platinum/nickel oxide catalyst over a range of adiabatic flame temperatures (1273-1673°K) and with CH_4 as the fuel yielded similar results.

A rich/lean series staged platinum/nickel oxide primary catalytic reactor was selected as a potential low NO_x concept for bench scale testing. The scale-up results were in general agreement with the laboratory scale results. Figure 7 compares the results of staged combustion of a 500 ppm NH_3 doped LBG at two scales: 1200 and 20,000 J/sec (4000 and 70,000 Btu/hr). Each had high conversions of NH_3 to NO_x in fuel-lean combustion. Minimum conversions occurred in rich/lean staged combustion when the primary was operated close to stoichiometric. At a primary stoichiometry of 90% theoretical air, the laboratory scale catalytic reactor converted 8% of the input NH_3 to NO_x while the bench scale combustor had an average conversion of 14%. Conversions in the bench scale combustor remained low (less than 18%) over all rich primary stoichiometries under normal operation; but breakthrough occurred if the primary was operated richer than 75% theoretical air: the temperatures on the walls of the catalyst monoliths dropped and the conversion rose sharply. Breakthrough was not observed in the laboratory scale experiment where the adiabatic flame temperature was maintained at a constant 1473°K by varying the amount of nitrogen diluent in the reactants. The undiluted flame reactor LBG had a higher heating value (HHV) of 6.7×10^6 J/m^3 (180 Btu/ft^3) while the HHV of the bench scale LBG was only 3.0×10^6 J/m^3 (80 Btu/ft^3). This indicates that raising the heating value of the gas could extend the operating range of the Pt/NiO catalyst, and that catalyst effectiveness is limited by a threshold flame temperature below which breakthrough occurs.

It is difficult to compare the laboratory and the bench scale diffusion flame combustors. Figure 8 shows laboratory and bench scale results for diffusion flame combustion of LBG containing about 500 ppm NH_3 and varying amounts of methane. In the unstaged laboratory scale experiment, performed at atmospheric pressure in a cold wall reactor under attached laminar flow conditions, the hydrocarbon content of the LBG had the most significant effect on XN conversion. Conversions as low as 10% were observed for combustion of hydrocarbon-free LBG under nearly stoichiometric conditions. Under richer conditions, conversion increased due primarily to increasing ammonia concentrations. However, under leaner conditions conversions remained quite low. Similar trends were observed in combustion of LBG containing 5% methane, but XN conversion was much higher. In the staged bench scale experiment, performed at 8 atmospheres in a nearly adiabatic combustor under turbulent flow conditions, effects of hydrocarbon content and stoichiometry were not so pronounced.

The bench scale flame was not visible and there was no reliable indicator as to whether the flame was attached or lifted. However, throughput and tube size ranged from conditions where the flame should definitely be attached to conditions where the flame should definitely be lifted. No sharp changes were observed in NO_x emissions or in other measured parameters, indicating that the attached/lifted transition was not an important factor. This agreed with previous variable throughput laboratory scale tests of a hydrocarbon containing diffusion flame, where a smooth NO_x transition was observed as the flame became detached (3).

Figure 9 shows the effect of fuel tube size on XN conversion in the bench scale diffusion flame operated at eight atmospheres. In constant pressure operation at a fixed stoichiometry, fuel flow and primary residence time were independent of fuel tube size, while Reynolds number was inversely proportional to the fuel tube I.D., fuel tube size had little effect on XN conversion in fuel rich combustion. However, in lean combustion, increasing tube size (decreasing Reynolds number) decreased NH_3 conversion to NO_x. Increased tube size also decreased the NO_x noise level (high frequency concentration fluctuation shown by the error bars in the figure), perhaps an indication of flame stability.

Figure 10 shows the effect of pressure on rich/lean and lean diffusion flames. In the bench scale system, pressure is maintained by passing the exhaust gases through a critical flow orifice. For a fixed stoichiometry, fuel flow and Reynolds number are proportional to pressure while primary residence time is independent of pressure. The staged tests were performed at a primary stoichiometry of about 95% theoretical air. For low hydrocarbon LBG, NH_3 conversion to NO_x remained constant at 33% over pressures ranging from 4 to 8 atmospheres. For LBG containing 2.1% CH_4, conversions remained constant around 40% with changing pressure. The lean tests were performed at a stoichiometry of about 150% theoretical air. Noise levels were higher than in the staged case. Conversions increased slightly with increasing pressure in low hydrocarbon combustion. Little change in conversion was seen with changing pressure for the 2.1% CH_4 LBG.

Primary residence time appeared to have the most pronounced effect on XN conversion in a staged diffusion flame. Residence time was varied at constant pressure by changing the pressure control orifice size. In constant pressure operation at a fixed stoichiometry, fuel flow and Reynolds number were inversely proportional to primary residence time. Figure 11 shows XN conversion with primary stoichiometry for two different primary residence times. Using a large pressure control orifice, a pressure of 8 atm was achieved at fuel tube Reynolds numbers around 40,000 and primary residence times around 120 msec. A minimum XN conversion of 34% was observed at a primary stoichiometry around 90% theoretical air. Using a smaller pressure control orifice, a pressure of 8 atm was achieved at fuel tube Reynolds numbers around 20,000 and primary residence times around 250 msec. A minimum XN conversion of about 22% was observed at a primary stoichiometry around 90% theoretical air. For a 553 ppm doped LBG burned out to 150% theoretical air, this XN minimum corresponded to a NO_x concentration of 100 ppm.

Figure 12 shows NO_x concentration as a function of NH_3 in the LBG for rich/lean staged combustion in a diffusion flame and in a platinum/nickel oxide catalytic combustor. For both the catalytic and the diffusion flame combustors, NO_x emissions increased with increasing fuel nitrogen content, but the increase in NO_x was much less than proportional to the increase in fuel nitrogen content. The 3/8 OD tube diffusion flame, operated at a primary stoichiometry of 76% theoretical air and a pressure of 4.4 atmospheres, converted 40% of its fuel nitrogen to NO_x at 553 ppm NH_3 in the LBG and had conversions of only 11% at a 3800 ppm doping level. The catalyst, operated at a primary stoichiometry of 80% theoretical air and a pressure of 2.4 atmospheres, had XN conversions of 16% at the low NH_3 doping level and 6% at the high doping level. Similar trends, but higher NO_x concentrations, were observed for both combustors in fuel lean combustion.

SECTION 5

DISCUSSION OF RESULTS

A rich/lean series staged combustor with a platinum/nickel oxide primary was the most promising low NO_x combustor investigated. It had low conversions of fuel nitrogen to NO_x over a wide range of fuel rich primary stoichiometries. Thus, it could be operated rich enough to maintain the adiabatic flame temperature relatively cool, prolonging the life of the catalyst. However, catalyst coated ceramics are often short-lived due to loss of activity of the coating and structural problems of the support caused by thermal shock. During the course of the bench scale experiments there was a great change in the appearance of the Pt/NiO catalyst. A green coating formed on the surface. Also, the zirconia honeycombs became quite fragile after repeated thermal cycling, especially the fine-cell downstream monolith which was almost completely destroyed in the final experiments. Further investigation is necessary of catalyst aging and of pressure and throughput effects under optimized combustor conditions before a catalytic combustor could be considered a serious candidate for a gas turbine combustor.

A rich/lean series staged combustor with a diffusion flame primary also had low conversions of fuel nitrogen to NO_x. Primary stoichiometry and residence time had the most significant effects on fuel nitrogen conversion. Minimum NO_x emissions were achieved at primary stoichiometries around 90% theoretical air for long primary residence times (250 msec or longer). Pressure and Reynolds number had little effect on NO_x in a staged diffusion flame, while an increase in the hydrocarbon content of the LBG caused a slight increase in NO_x emissions. Combustion of a hydrocarbon-free LBG was not tested on the bench scale, but laboratory scale tests indicated that the absence of hydrocarbons in the fuel could cause a significant reduction in NO_x emissions.

A lean unstaged diffusion flame produced higher NO_x emissions than the rich/lean staged diffusion flame. However, because of its simplicity, it remains an attractive low NO_x combustor concept. The influence of Reynolds number on NO_x levels in the lean flame suggests that NO_x emissions could be lowered by utilizing larger fuel tubes, perhaps approaching the levels achieved by the staged diffusion flame.

It is planned to investigate other combustor configurations including a premixed backmixed simulated stirred reactor and a combination diffusion flame/catalyst hybrid combustor. The zero dimensional stirred reactor is easy to model. It will provide experimental feedback for the fuel nitrogen processing kinetics code to be used in future prototype combustor design. The hybrid system will input low ΣXN containing fuel rich diffusion flame exhaust into a Pt/NiO cleanup catalyst prior to secondary burnout.

REFERENCES

1. Robson, F. L., W. A. Blecher and A. J. Giramonti. Combined - Cycle Power Systems. EPA-600/2-76-149, U. S. Environmental Protection Agency, Washington, D.C., 1976. p.359.

2. Environmental Protection Agency Title 40, Chapter 1, Subcharter C, Part 60 - Standards of Performance for New Stationary Sources, Federal Register, Vol. 44, No. 113, June 11, 1979.

3. Folsom, B. A., C. W. Courtney, T. L. Corley and W. D. Clark. Advanced Combustion Concepts for Low Btu Gas Combustion. In: Proceedings of the Third Stationary Source Combustion Symposium, Vol. 2, Advanced Processes and Special Topics, EPA-600-17-79-050b, February 1979.

4. Folsom, B. A., W. D. Clark, C. W. Courtney, M. P. Heap, and W. R. Seeker. Fuel Nitrogen Conversion - The Impact of Catalyst Type. In: Proceedings - Fourth Workshop on Catalytic Combustion, EPA Publication not yet in print.

5. Dravo Corporation, Handbook of Gasifiers and Gas Treatment Systems, NTIS Report No. FE-1772-11, February 1976.

6. Folsom, B. A., T. A. Corley, M. H. Lobell, C. J. Kau, M. P. Heap, and T. J. Tyson. Evaluation of Combustor Design Concepts for Advanced Energy Conversion Systems. In: Proceedings of the Second Stationary Source Combustion Symposium, Vol. 5, Addendum, EPA-60017-77-073, July 1977.

7. Folsom, B. A., C. Courtney and M. P. Heap. Environmental Aspects of Low Btu Gas-Fired Catalytic Combustion. In: Proceedings - Third Workshop on Catalytic Combustion, EPA-60017-79-038, February 1979.

8. Klimisch, R. L. and K. C. Taylor, Ammonia Intermediacy as a Basis for Catalyst Selection for Nitric Oxide Reduction. Environmental Science & Technology 7 (2): 127-131, February 1973.

9. Chu, E. K. and J. P. Kesselring. Fuel NO_x Control by Catalytic Combustion. In: Proceedings - Third Workshop on Catalytic Combustion, EPA-60017-79-038, February 1979.

10. Krill, W. V. and J. P Kesselring. The Development of Catalytic Combustors for Stationary Source Applications. In: Proceedings - Third Workshop on Catalytic Combustion, EPA-60017-79-038, February 1979.

REFERENCES (cont.)

11. Fenimore, C. P. Effects of Diluents and Mixing on Nitric Oxide from Fuel-Nitrogen Species in Diffusion Flames. In: Proceedings of the Sixteenth Symposium (International) on Combustion, The Combustion Institute, Pittsburgh, Pa., 1976.

12. Folsom, B. A., C. W. Courtney and M. P. Heap. The Effects of LBG Composition and Combustor Characteristics on Fuel NO_x Formation. In: Proceedings of the Twenty-Fourth International Gas Turbine Conference, ASME, San Diego, Ca., 1979.

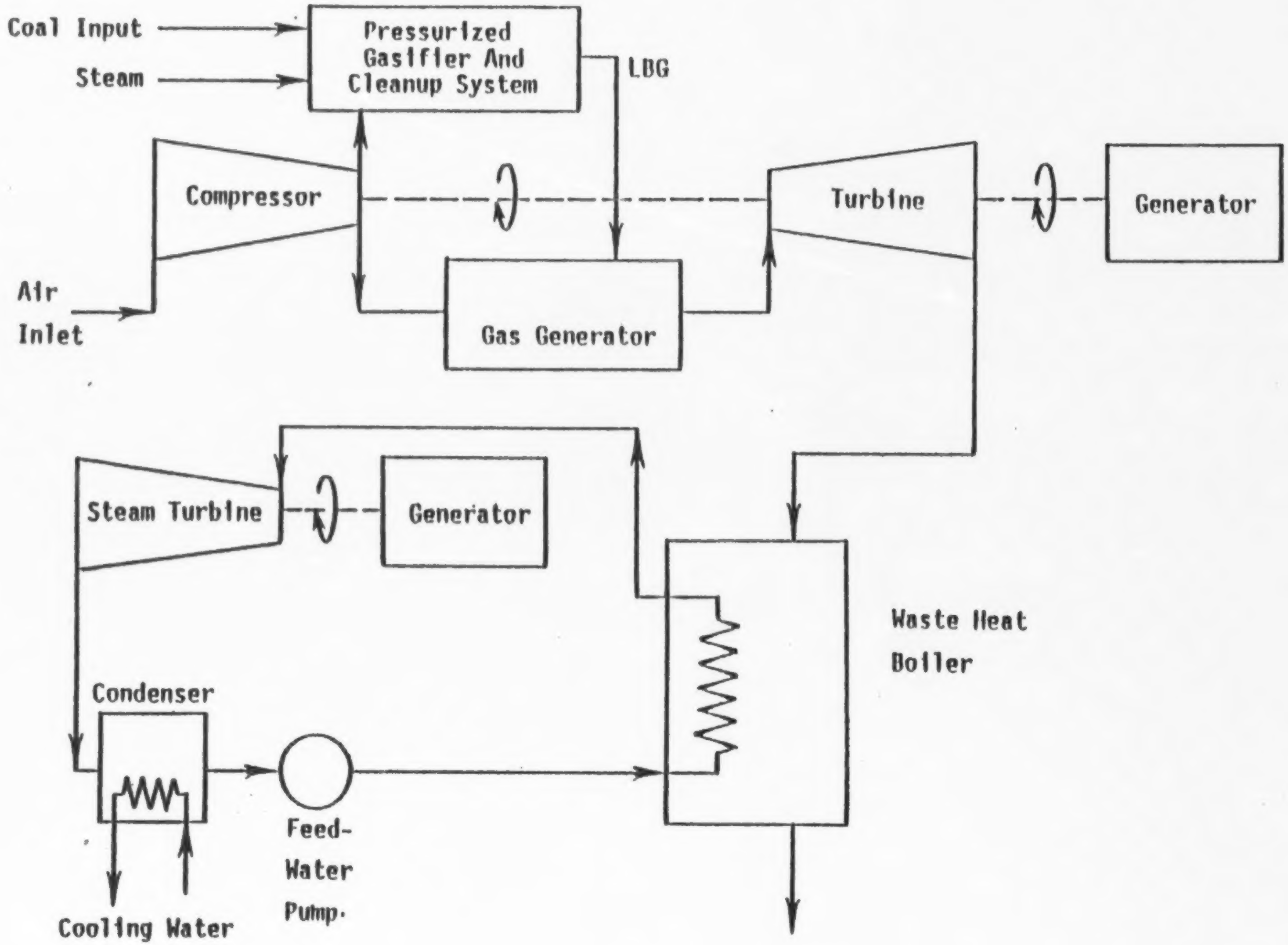

Figure 1. Combines Cycle Power Plant

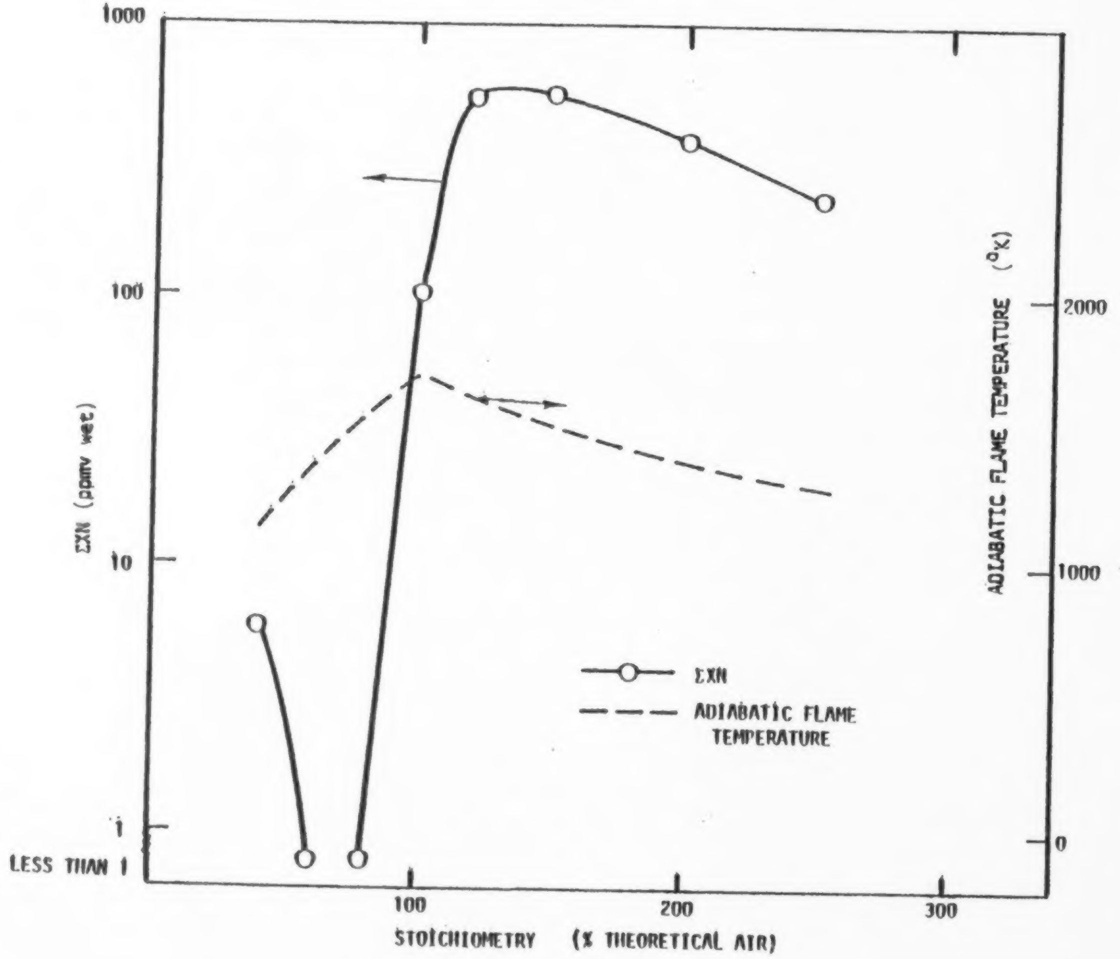

Figure 2. Equilibrium ΣXN and Adiabatic Flame Temperature for LBG.

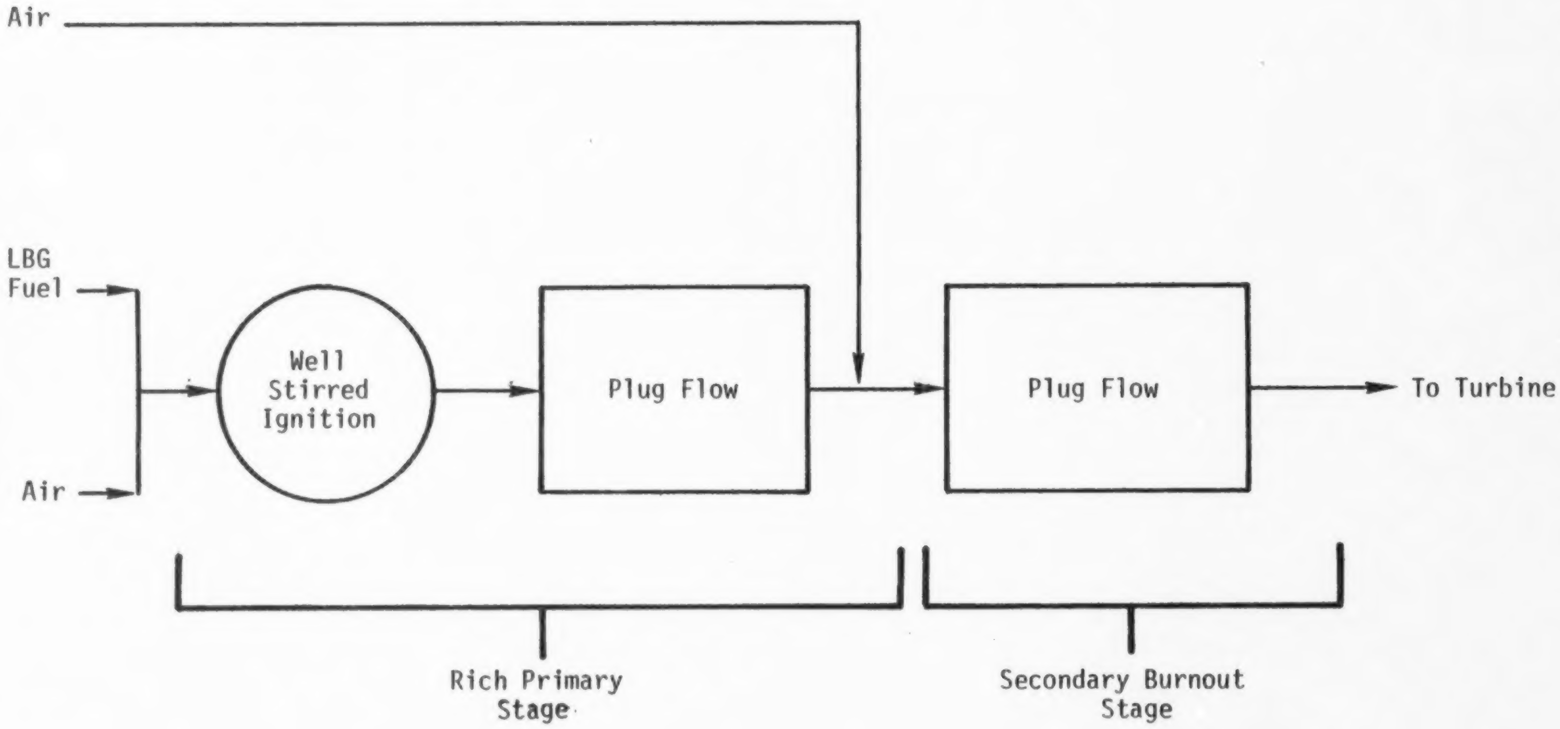

Figure 3. Rich/Lean Series Staged Combustor.

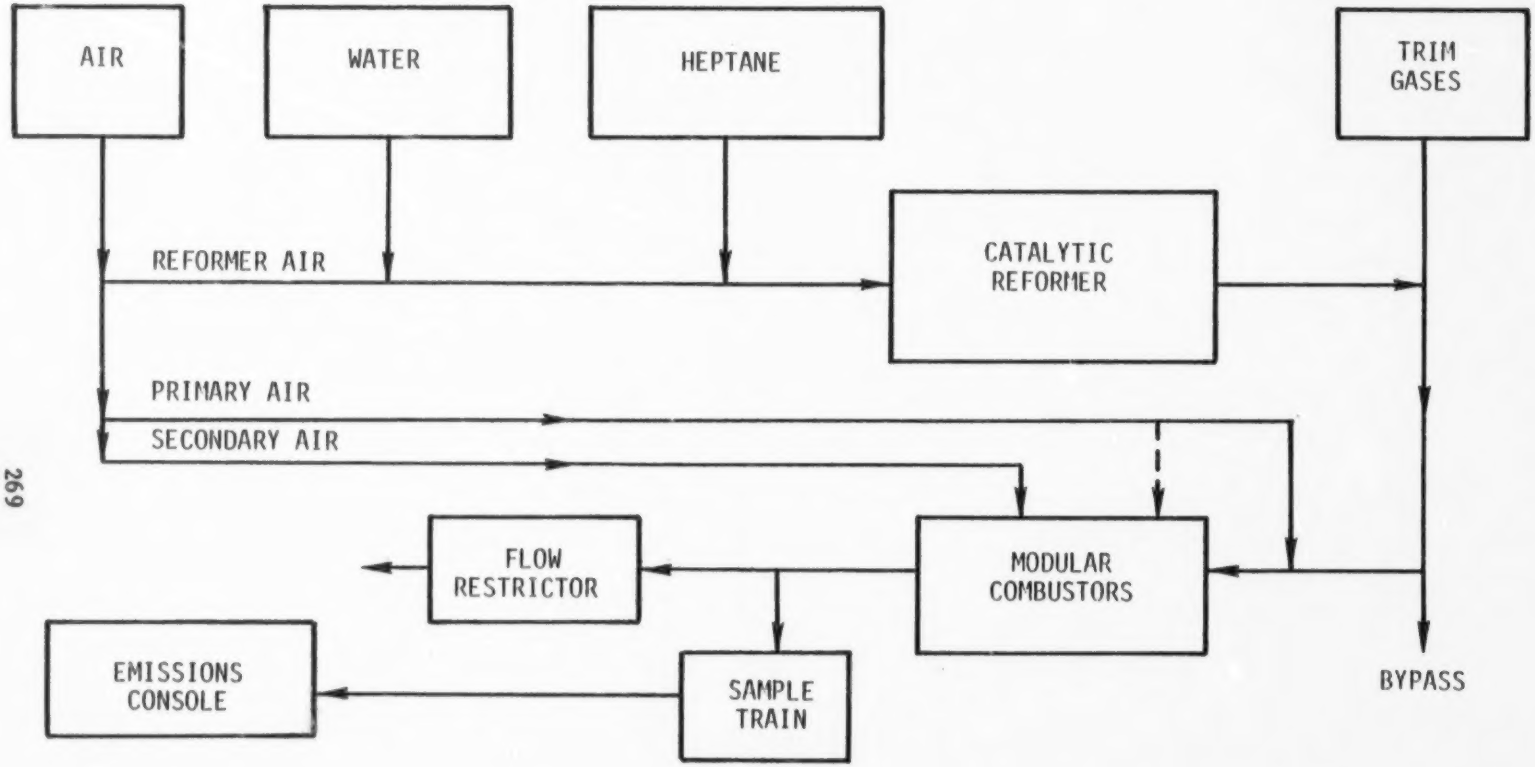

Figure 4. Bench Scale Pressurized Test Facility.

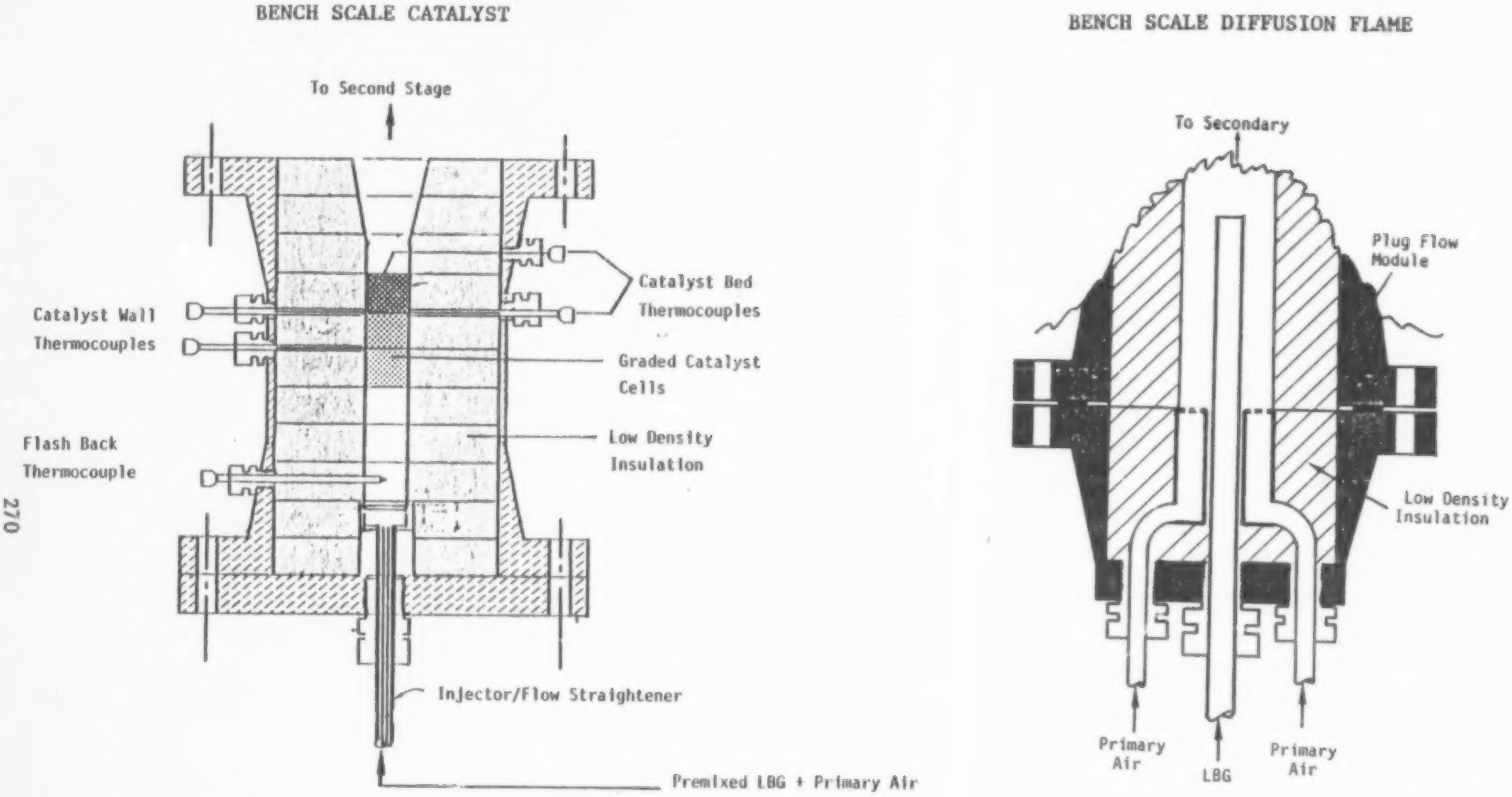

BENCH SCALE CATALYST

BENCH SCALE DIFFUSION FLAME

Figure 5. Primary Ignition Modules.

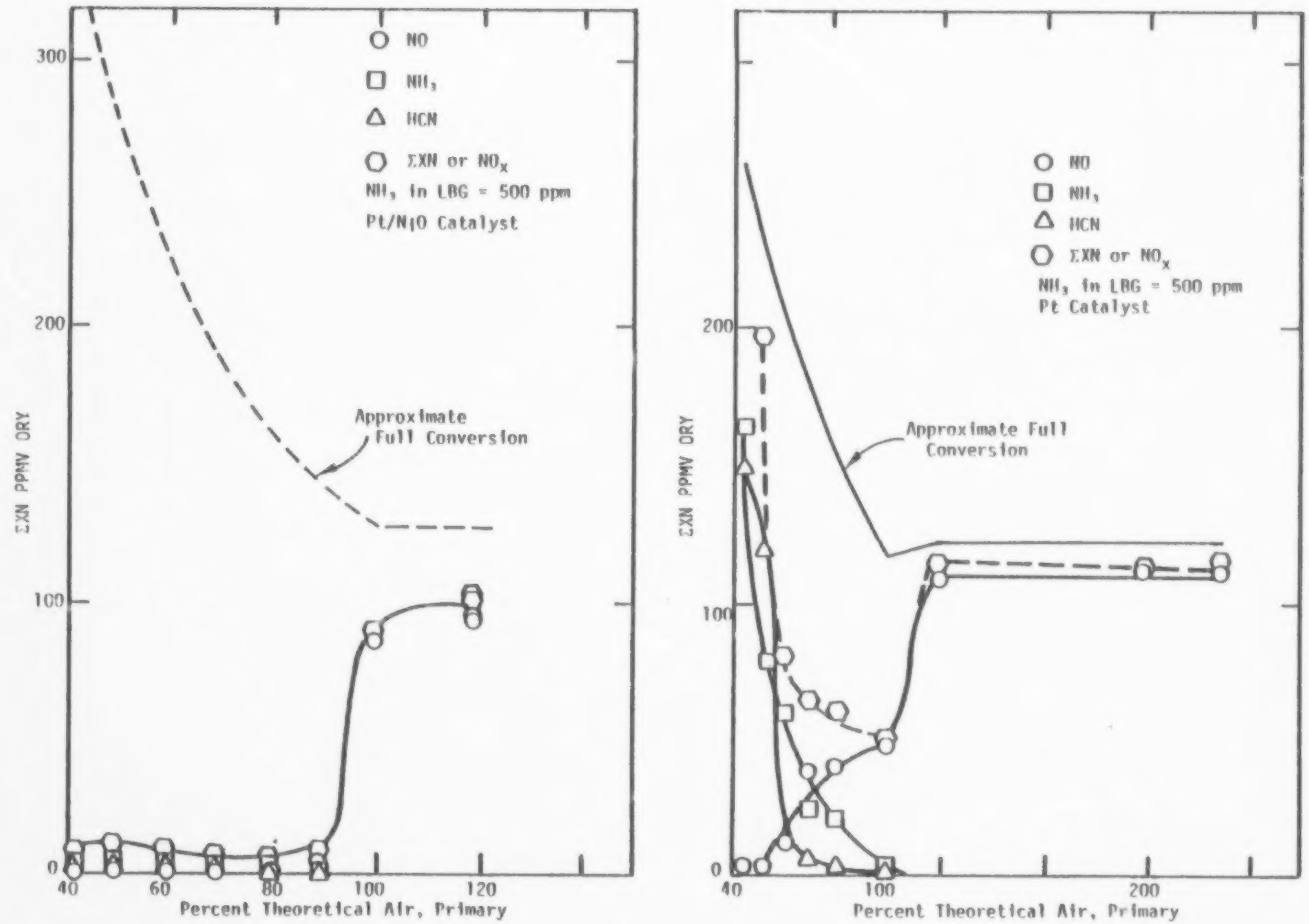

Figure 6. Laboratory Scale Catalyst Comparison.

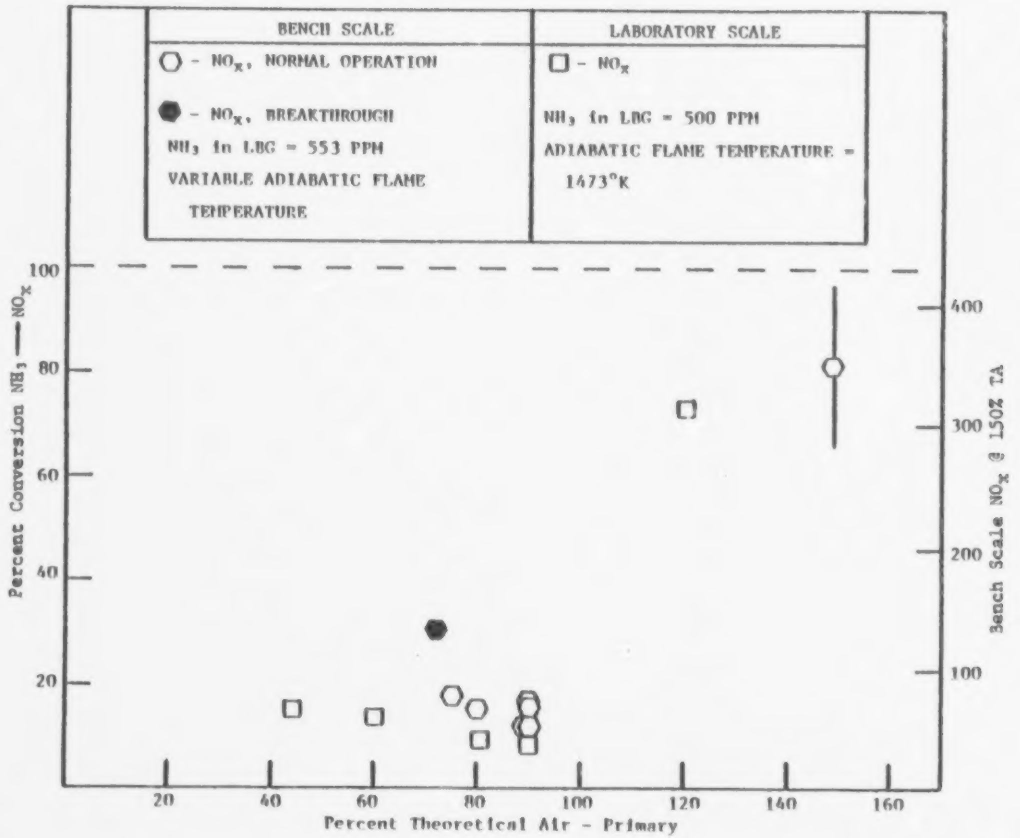

Figure 7. Pt/NiO Catalyst Scale-up.

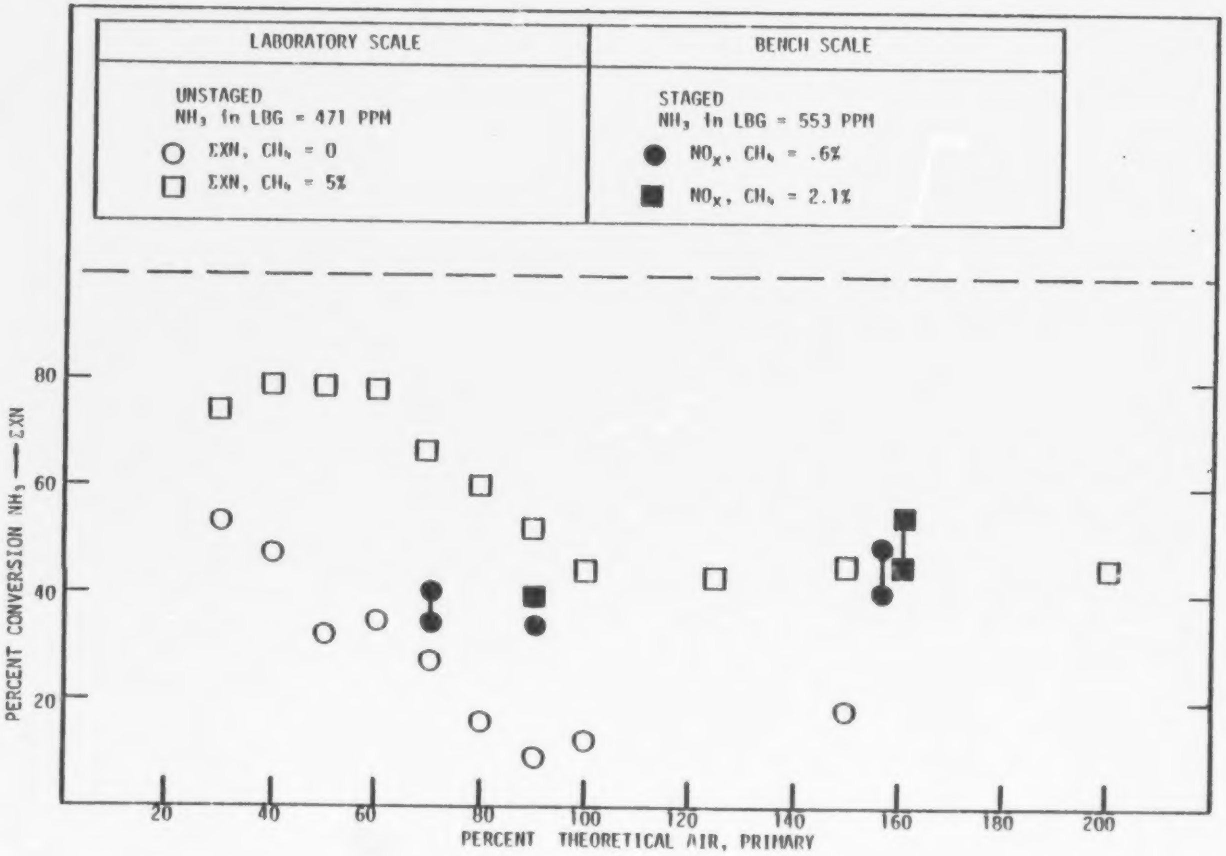

Figure 8. Diffusion Flame Scale-up.

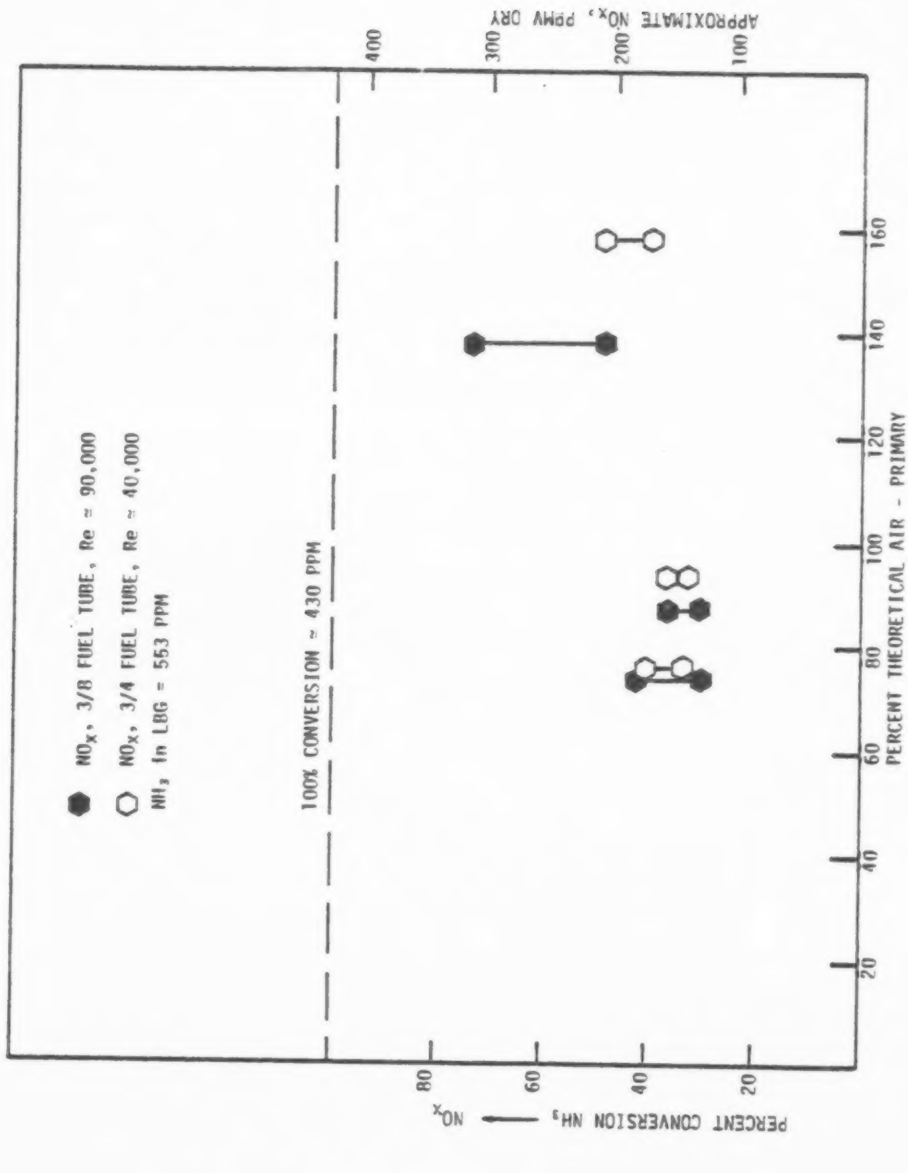

Figure 9. Bench Scale Diffusion Flame: Effect of Reynolds Number.

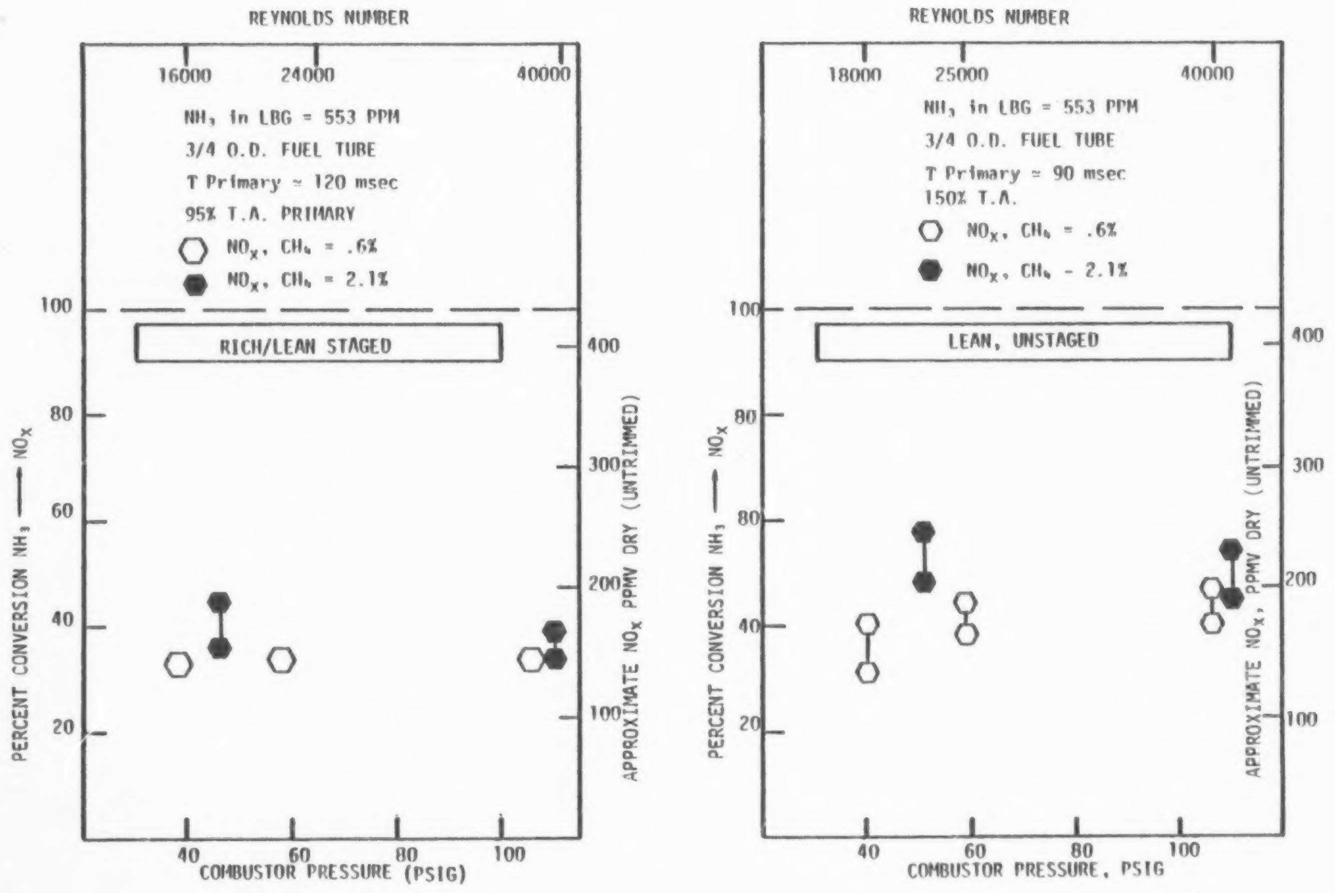

Figure 10. Bench Scale Diffusion Flame: Variable Pressure/Reynolds Number.

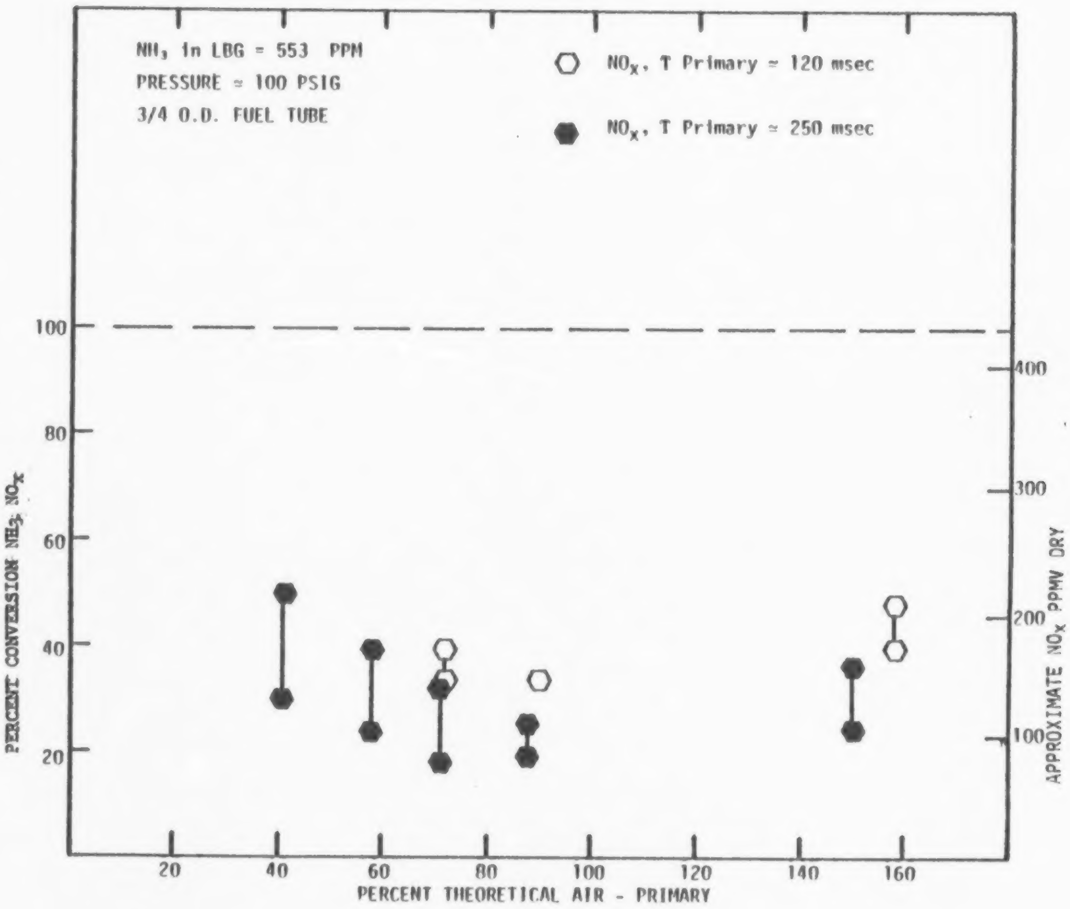

Figure 11. Bench Scale Diffusion Flame: Effect of Residence Time.

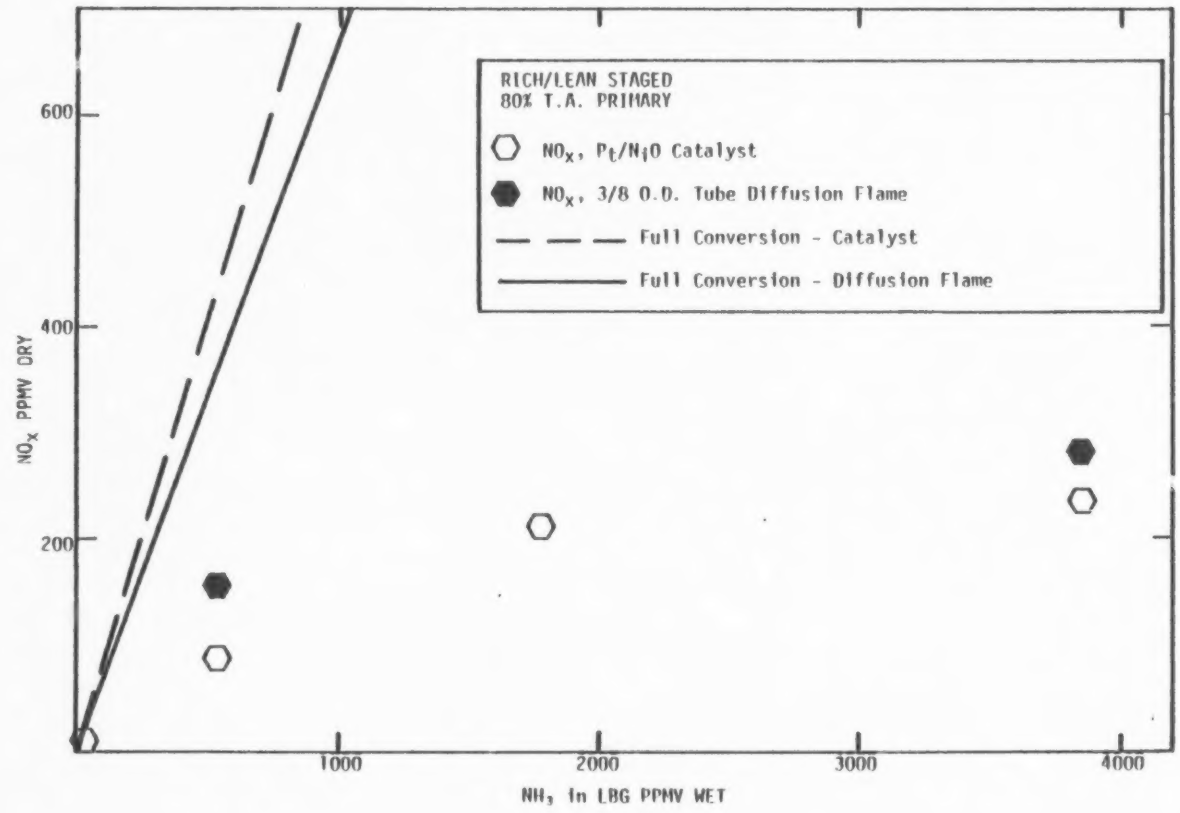

Figure 12. Bench Scale Reactor Comparison: Effect of Dopant Level.

Table I. Reformer-produced Low BTU Gas Composition

Product	Measured 80 psig	Measured 120 psig	Equilibrium 160 psig
NO (ppm)	2	1	0
NH_3 (ppm)	44	50	66
HCN (ppm)	1	1	0
O_2 (%)	0.0	0.0	0.0
CO (%)	7.4	7.1	7.8
CO_2 (%)	8.8	8.7	7.0
CH_4 (%)	0.3	0.3	0.0
H_2O (%)	27.0	27.1	28.4
H_2 (%)	19.9*	19.5*	17.7
C(S) (%)	0.0*	0.0*	0
N_2 (%)	36.6*	37.3*	39.2
Heating Value(Btu/ft^3)	89.4	87.2	80.7

---

* By difference between measured output and input reformer feed stock - heptane.

CONTROL OF NO_x AND PARTICULATES EMISSION FROM SRC-II SPRAY FLAMES

By:

J. M. Beér, M. T. Jacques, S. Hanson, A. K. Gupta
Massachusetts Institute of Technology
Department of Chemical Engineering and the Energy Laboratory
Cambridge, Massachusetts 02139

W. Rovesti
Electric Power Research Institute
Palo Alto, California 94303

ABSTRACT

Experiments were carried out with SRC-II fuels in a laboratory scale laminar flow reactor and in the 4ft x 4ft MIT Combustion Research Facility. In the laminar flow reactor monosize droplet arrays are pyrolyzed in an inert atmosphere at variable temperatures and the time resolved evolution of the fuel nitrogen is determined. This information is needed for the development of an NO_x control strategy by staged combustion. Parallel with the laboratory studies, experiments are carried out with SRC-II liquid fuel sprays in unstaged and staged turbulent diffusion flames in a thermal environment similar to that in a utility boiler. The NO_x and particulates emission is determined in unstaged flames for the effects of the rate of fuel/air mixing, air preheat and the quality of atomization. The results show that low overall excess air in a long slowly mixing turbulent flame with a low degree of swirl in the air for flame stabilization, can reduce the NO_x emission level to about 250 ppm from 550 ppm obtained for high intensity fast mixing flames. A significant further reduction of NO_x can be achieved with staged combustion by physically separated stages. In these latter experiments a computer analysis of the fuel nitrogen conversion is used to guide the experiments carried out using the MIT Combustion Research Facility. The distributions of NO_x and particulates in the flames are determined for the effects of the primary stage fuel/air ratio, temperature and atomization quality. The mixing in both the fuel rich and lean stages and the heat extraction along the flame is closely controlled in these experiments. Results show that NO_x (3% O_2) levels below 100 ppm can be achieved without excessive emission of particulates. The experimental data show the same general trends for NO_x emission as a function of fuel equivalence ratio, as that predicted by the computer model. While the NO_x and particulate levels achieved in these studies are most encouraging, it is the development of a strategy of NO_x and particulate emission control, that is the main objective of the present study. The emission levels achieved in this study can be considered as lower

bounds for conditions in which the mixing in the flame is controlled more closely than can be achieved in practical utility boiler combustion chambers.

SECTION 1

INTRODUCTION

It is generally accepted that staged combustion techniques currently offer the most attractive strategy for the control of NO_x emission from the combustion of high nitrogen content fuels. Several experimental studies [1-3] have demonstrated the potential of these techniques for achieving environmentally acceptable emissions from the combustion of the lighter coal derived liquid fuels. However, there is still some concern over the potential for soot emission from the heavier, highly aromatic, high C/H ratio coal derived liquids when fired under staged combustion conditions. The high temperature, fuel-rich flame conditions required to suppress conversions of fuel-nitrogen to NO_x, result in the formation of a significant amount of soot. Complete burn-out of this soot must be achieved in the fuel-lean flame zone by ensuring good mixing and sufficient residence time at elevated temperatures.

Consequently, it is of considerable interest to establish both theoretical and practical lower limits of NO_x and soot emissions which can be achieved by employing staged combustion techniques for the utilization of coal derived liquid fuels.

A research program is underway at MIT under EPRI sponsorship. The program objectives are to identify and quantitatively describe the critical steps involved in the processes of fuel-nitrogen evolution and conversion in order to develop a design strategy for minimizing NO_x and particulate emissions from the combustion of coal derived liquid fuels. The research complements a fundamental study on the kinetics of fuel nitrogen evolution from pyrolysing fuel particles and droplets sponsored by EPA [4] and on fuel nitrogen conversion in fuel rich flames, under the sponsorship of DOE [5].

The research presented in this paper involves a combination of laboratory scale experiments on the pyrolysis of single droplet streams, computer modeling of the fuel-nitrogen conversion reactions, and an experimental study using the pilot-scale MIT Combustion Research Facility on the effect of staged combustion on the NO_x and particulate emissions from a blended SRC-II fuel oil (2.9 parts by weight middle distillate to 1 part heavy distillate).

SECTION 2

DROPLET PYROLYSIS STUDIES

The important fuel-nitrogen conversion reactions, which form the basis of the staged combustion NO_x control strategy, i.e., those leading to the formation of N_2, are dominated by gas phase reactions involving the nitrogen containing fuel vapors. Consequently the rate of vaporization and yield of fuel-nitrogen species from the parent droplet represent a critical first step in the fuel-nitrogen conversion process. Fuel-nitrogen present in the form of high molecular weight heterocyclic compounds may concentrate in the heavy liquid fractions or become locked-up in solid residues formed during the pyrolysis of the fuel [1]. Any fuel-nitrogen which escapes unreacted from the fuel-rich flame zone will be readily oxidized to NO_x in the fuel-lean flame zone. It is, therefore, of considerable interest to understand the factors that determine the rate at which fuel-nitrogen evolves from liquid fuel droplets during pyrolysis under conditions of rapid heating.

2.1 The Experimental Apparatus

The experimental apparatus and the measurement techniques were developed within the scope of an EPA grant to MIT entitled: "Reduction of Pollutant Formation in Coal Particle and Liquid Fuel Flames;" brief description is given in the following.

For the study of fuel-nitrogen evolution from liquid fuel droplets during pyrolysis and oxidation, a laminar flow reactor (Fig. 1) was designed with provision for feeding a monosize droplet array into a laminar gas stream and the capability of intercepting the droplets, after a chosen residence time, by a fast quenching sampling probe. Optical access to the pyrolyzing, burning oil droplet array through quartz windows along the full length of the uniformly heated section of the reactor enables photographic and schlieren-interferometric measurements to be made of droplet size variation, droplet velocity and the temperature distribution in the droplet boundary layer.

The objective of carrying out experiments with droplet arrays of heavy residual fuel oils, posed significant experimental problems concerning the fuel preparation and droplet generation and also the sampling.

A vibrating orifice-type droplet generator was chosen for the introduction of fuel droplets into the reactor. A monosized droplet array is injected vertically downward into the furnace through a small (50 or 100 μm) orifice mounted in a piezo-electric vibrator. The vibrator is driven by a variable frequency signal generator. The variation of oil flow rate, vibrator frequency and orifice size permits the control of droplet size and interdrop distance. The droplets are injected into a laminar co-flowing gas stream; in recent studies helium was chosen to give a chemically inert environment for the vaporizing-pyrolyzing drops.

The sampling probe inserted through the base of the furnace is aligned with the drop generator by means of a small laser.

The sampling probe takes the total gas flow, the residual droplet array and the vapor.

A transpiring type of probe following the conceptual design by Mims [7], combined with a cascade impactor was used.

2.2 Experimental Results

Results of experiments carried out with the pyrolysis of 150 μm SRC-II droplet streams in helium at furnace temperatures of 975, 1050, 1160 and 1270 K are presented in the form of the percentage of fuel bound nitrogen evolved versus mass loss by vaporization, in Fig. 2. The data points are calculated from the weight loss due to vaporization between the droplet generator and the sampling position and from the nitrogen concentration of the liquid residue collected at that sampling position. Equilibrium distillation data are also given in Fig. 2; these were determined at atmospheric pressure by slow heating of the SRC-II fuel. The equilibrium distillation curve is close to a 45° line showing that under slow heating conditions the nitrogen is nearly uniformly distributed amongst the different boiling fractions of the fuel. Under conditions of rapid heating, however, the rate at which nitrogen is released relative to that of vaporization becomes dependent on the rate of heating of the fuel droplet.

In the case of equilibrium distillation under well mixed conditions, the evolution of a particular component is given by the following thermodynamic expression,

$$y_i = \frac{x_i}{P_\alpha} \exp\{\frac{\Delta H_v}{R}(\frac{1}{T} - \frac{1}{T_{bi}})\}$$

where y_i is the vapor phase mole fraction of i

x_i is the liquid phase mole fraction of i

P_α is the ambient pressure

ΔH_v is the enthalpy of vaporization

R is the ideal gas constant

T is the liquid temperature

T_{bi} is the normal boiling point for pure i

The vapor phase contribution of the component in question is influenced by its liquid phase mole fraction and temperature. The overall composition determines the temperature and competition with other species of differing relative volatilities can shift the contribution of any particular component in its attempt to satisfy the constraints $\Sigma x_i = 1$ and $\Sigma y_i = 1$. Thus, a fuel containing a single nitrogenous compound may, due to the influence of the other species, produce a nitrogen distillation curve similar to that presented for the SRC-II middle fraction. For the SRC-II middle fraction, it is known that there are many nitrogen containing species and what is observed is the summation of the nitrogen evolved by all of them. The utility of the distillation curve is not that it identifies what nitrogenous species are present, but that it represents one extreme of vaporization from droplets where diffusive mixing is rapid relative to weight loss by vaporization.

When a 150μm droplet of SRC-II middle fraction is exposed to a hot inert environment, the light boiling fractions, which contain little nitrogen, are vaporized from the surface. This depletion causes a concentration gradient to be established which permits more light material to travel to the surface. The more rapidly one vaporizes the droplet, the steeper are the gradients and the greater the light fraction contribution in the volatile fraction. Thus one observes an initial retention of fuel nitrogen with increasing mass vaporization rate. What has been said so far is true up to the point where mass vaporization is so rapid that diffusion cannot keep up with the removal of low boiling fractions. Nitrogen containing species concentrated at the surface of the droplet now contribute to the mass evolved and the more rapid the vaporization thereafter the earlier the nitrogen will evolve. Needless to say, the description just given has been greatly simplified. The effects of changing surface temperature and relative volatility with changing surface composition are implicit in the discussion. Liquid phase reactions, superheating within the droplet and other effects are recognized to be present but are not considered.

SECTION 3

KINETICS OF FUEL-NITROGEN CONVERSION-MODELING STUDIES

Nitrogen oxides emission from combustion processes originates from two main sources: the fixation of atmospheric nitrogen at high combustion temperatures ("thermal-NO_x") and the oxidation of fuel bound nitrogen ("fuel NO_x"). When burning high nitrogen content fuels ($N > 0.2\%$), an increasing proportion of the NO_x emitted will be of "fuel NO" type. In contrast to "thermal NO" the rate of formation of which is a strong function of temperature, the formation rate of "fuel NO" is only slightly dependent upon temperature but increases markedly with increased oxygen concentrations in the flame. This is because the conversion efficiency of fuel nitrogen to NO is thought to depend on the rate of competing reactions involving nitrogen fragments to produce NO or N_2. The exact mechanism of fuel nitrogen conversion is not known, but there is now a significant body of knowledge for general conclusions to be drawn with respect to the development of a design strategy for reducing NO emissions from combustion processes when burning high nitrogen content fuels. Details of the chemistry of the formation and destruction of "fuel-NO" are discussed in a recent survey by Levy et al. [8]. Figure 4 illustrates the various pathways of fuel-nitrogen during pyrolysis and oxidation reactions in a flame. In liquid fuels the fuel nitrogen evolved during vaporization converts in fast reactions to HCN, which will react further via oxycyanide intermediates to form amines. At every step of the reaction sequence, if oxidants such as OH or O are available NO will be formed. However, in the absence of other oxidants the nitrogenous species react either with NO, or with each other to form N_2. These latter reactions form the basis of NO_x control by staged combustion techniques in which the conditions in the fuel-rich zone favor the conversion of the fuel-nitrogen species to N_2 rather than NO_x. Information on the thermodynamics and chemical kinetics of the above mentioned reaction sequence suggests that such a control strategy requires the pyrolysis of the fuel vapor under fuel-rich conditions at sufficiently high temperature to ensure rapid conversion of the fuel-nitrogen to N_2. To achieve complete combustion and to minimize soot emission, the fuel-rich zone has to be followed by the introduction of additional combustion air. In this fuel lean flame zone, any fuel-nitrogen fragments not converted to N_2 will be rapidly oxidized to form NO_x. Consequently an important parameter is the sum of bound nitrogen species present in the combustion gases leaving the fuel-rich flame zone.

The bound nitrogen species considered include all nitrogen species present in the combustion products, i.e., N, NH, NO, N_2O, HCN, CN, NCO and HNCO with the notable exception of N_2. Hence a decrease in total bound nitrogen species represent conversion of fuel-nitrogen to N_2.

A simplified computer model, incorporating the kinetics of gas phase nitrogen reactions under plug-flow conditions developed by Taylor [9] was used by Farmayan [10] to identify the influence of important fuel-rich stage parameters on the sum of bound nitrogen species within the flame. The kinetic mechanism contained in the combustion model consists of reactions (shown in Table I) which are believed to dominate the conversion of bound nitrogen species under high temperature fuel-rich combustion conditions. The initialization of the kinetic calculations was obtained by assuming that the hydrocarbon/air rections are partially equilibrated, yielding a mixture of CO, CO_2, H_2, H_2O, O, OH, and O_2. In addition, the fuel nitrogen was assumed to be instantaneously pyrolyzed to HCN and CN which are also in partial equilibrium with the hydrocarbon combustion products.

This model was employed by Farmayan [10] first in an extensive computer study to determine the influence of fuel-rich zone parameters, namely, fuel equivalence ratio, adiabatic flame temperature and residence time, on the rate of fuel-nitrogen conversion during the combustion of a high-nitrogen content #6 fuel oil (0.73 wt% N).

Figure 5 shows results of this computer study on the high-nitrogen content #6 fuel oil in terms of the predicted sum of bound nitrogen species mole fraction as a function of the fuel-rich zone residence time. Data are presented for three fuel equivalence ratios, $\phi = 1.4$, 1.6 and 1.8 and air inlet temperatures 298K, 500K and 700K. This latter variable influences the adiabatic flame temperature which is shown in parenthesis for each condition. These data clearly show that the bound nitrogen species mole fraction can be reduced by at least an order of magnitude below the initial value within residence times of practical significance (approx. one second). Furthermore they show that the inlet air temperature, and hence the adiabatic flame temperature, has a significant influence on the extent of fuel-nitrogen conversion. At a fuel equivalence ratio of 1.4 increasing the inlet air temperature from 298K to 700K decreases the initial rate of bound nitrogen decay and would result in higher NO_x emissions. This behavior can be explained by the fact that at $\phi = 1.4$ increasing flame temperature increases the equilibrium mole fraction of bound nitrogen species to a level close to the initial mole fraction in the mixture. However, at $\phi = 1.6$ and 1.8 the equilibrium mole fraction of bound nitrogen species is much lower than that in the initial mixture and increasing flame temperature increases the rate at which bound nitrogen species are converted to N_2. At $\phi = 1.8$ it can be seen that high air preheat levels are required to achieve significant fuel nitrogen conversion within 4 sec residence time, clearly indicating that the gas phase reactions may well be kinetically limited at these equivalence ratios.

Similar computer calculations performed for the SRC-II 2.9/1 blend showed that the partial equilibrium assumptions employed to initialize the kinetic calculations yielded initial bound nitrogen species mole fraction very close to those obtained with the high-nitrogen #6 fuel. Consequently it was decided to select only a few critical fuel-rich zone parameters for the SRC-II fuel and compare the results with those obtained for the high-nitrogen #6 fuel oil.

Figure 6 shows a comparison of the extent of fuel nitrogen conversion between the two fuels at $\phi = 1.4$ and 1.6 with inlet air temperature of 500K. These data show that the two fuels exhibit very similar trends in fuel nitrogen conversion under these conditions, particularly for $\phi = 1.6$ where the bound nitrogen species decay rate and final values after 1 second residence time are almost identical. The slightly higher final value at $\phi = 1.4$, of bound nitrogen species mole fraction for the SRC-II is attributed to the higher initial value resulting from the higher adiabatic flame temperature.

Figure 7 further illustrates the sensitivity of the rate of decay of bound nitrogen species to adiabatic flame temperature. At $\phi = 1.6$ and an inlet air temperature of 298K the SRC-II exhibits a much faster rate of decay than the #6 fuel oil, indicating that reduced residence times are possible at the lower air preheat levels for the same extent of fuel-nitrogen conversion. The general conclusion from these comparative studies are that both fuels behave in a very similar manner, particularly with respect to the extent of fuel-nitrogen conversion at residence times of $\simeq$ 1sec. Consequently it was felt that the computer model results contained for #6 fuel oil could be used to guide the choice of experimental parameter values for SRC-II studies.

Of particular interest is the influence of fuel equivalence ratio on the extent fuel nitrogen conversion. Figure 8 shows the results obtained for the #6 fuel oil and it can be clearly seen that the total bound nitrogen mole fraction achieves a minimum with a fuel equivalence ratio within the range of 1.6 - 1.8 depending upon air preheat level and residence time. Furthermore the minimum values of total bound nitrogen which are attainable are, in terms of equivalent NO_x of the order of 10ppm (at 3% O_2). The minima of the curves representing the sum of bound nitrogen species is seen to shift towards higher fuel/air ratios with increasing air preheat temperature. The air preheat temperature is given for characterization of the flame temperatures because these latter are varying along the curves as a result of the variation of the fuel/air ratio. The absolute value of the minimum of bound nitrogen species decreases with increased residence time indicating the controlling influence of chemical kinetics.

SECTION 4

PILOT SCALE FLAME STUDIES

The experimental combustion program involved the use of the MIT Combustion Research Facility (CRF) which was designed specifically to facilitate detailed experimental investigations of large turbulent flames. The MIT-CRF consists of a 4 ft x 4 ft cross-section, 30 ft long combustion tunnel equipped with a single burner having a 3MW, multi-fuel firing capability. Figure 9 shows the general arrangement of the CRF as used in the present SRC-II flame studies. The burner consists of a variable swirl generator, of the 'movable - block' design developed by the International Flame Research Foundation at Ijmuiden. The fuel gun and atomizer nozzle are inserted through the swirl generator for location at the burner throat. The furnace chamber comprises a number of individual, 1 ft wide, water-cooled, refractory lined or bare metal interchangeable sections, an arrangement of which permits variable heat sink for control of heat extraction along the length of the flame. This variable heat sink permits simulation of the thermal environment of a wide range of industrial flames. In the present study, in which interest is in utilization of SRC-II fuels in utility boilers, the condition needed to ensure chemical similarity between utility boiler flames and MIT-CRF flames required the use of hot wall conditions.

Experiments were performed using two SRC-II fuel types. The blend of 2.9 parts of middle distillate to one part of heavy distillate (2.9/1) and the unblended heavy distillate. The properties of these fuels are given in Table II. Both unstaged and staged combustion conditions were investigated. The unstaged experiments were designed to provide baseline data on NO_x and particulate emissions from these two SRC-II fuel types.

For the discussion of the arrangement used for staged combustion studies we refer to Fig. 9. Primary zone air was admitted through the swirl generator/burner assembly and secondary zone air was introduced perpendicular to the burner/furnace axis at an axial distance of 8.5 ft from the burner, through two sets of injector nozzles arranged directly opposite each other and mounted in the furnace side walls as shown in Fig. 10. Each nozzle injection assembly consists of five interchangeable stainless steel pipes which extend to the inner surface of the refractory lined furnace wall, thus permitting air injection through single of multiple nozzles to provide a wide range of air injection velocities.

Measurements of temperature and gaseous species concentrations (NO_x, O_2, CO, CO_2) were made along the axis of the unstaged flames by the use of water cooled probes which are inserted through rectangular slots centrally located in the side walls of each furnace section. Solids and NO_x concentrations and Baccarach smoke number were measured in the exhaust gas at the exit of the experimental section.

4.1 Unstaged Flame Studies

Baseline data were obtained for two types of unstaged flames: a long, slow mixing low swirl flame, typical of corner fired boiler units; and a short, fast mixing, high swirl flame characteristic of front or side wall fired units. The effects of design and operating variables on NO_x and particulate emissions were investigated for two types of atomizer, a twin fluid, steam assisted Y-jet atomizer and a steam assisted Sonicore atomizer; two levels of air preheat 500 and 850°F and two burner swirl numbers 0.53 (low swirl) and 2.70 (high swirl). (The swirl number is the value of a nondimensional group characterizing the degree of rotation in the jet).

A total of twelve flames were studied, six of which were obtained using the SRC-II 2.9/1 blend of middle to heavy distillate and six using the SRC-II heavy distillate. The input conditions for these twelve flames are summarized in Table III. The MIT-CRF was operated with hot (refractory lined) walls, a total of 15 wall sections were used giving a combustor length of 15 ft. The thermal input was maintained constant at 1MW and excess air was controlled at 2-10% to give 0.5-1.9% O_2 in the flue gas. Furnace wall temperatures were typically 2200°F and the flue gas exit temperature from the combustion chamber was ≈2400°F.

The SRC-II 2.9/1 blend was fired without heating the fuel, the temperature at the atomizer being 100°F, with a corresponding viscosity of 40 SSU. The SRC-II heavy distillate was heated using in-line electric heaters, to maintain a temperature of 210°F at the atomizing nozzle to maintain the viscosity at 40 SSU. The axial NO_x profiles shown in Fig. 11 are characteristic of the two flame types studied. Both profiles are relatively flat indicating that most of the NO_x is formed very early in the flames. There is a significant increase in NO_x emission for the high swirl flame, in this case from 300 ppm, in flame #3, to 550 ppm in flame #4, (both at 3% O_2). This increase in NO_x emission is due entirely to the change in flame aerodynamics resulting from the increase in swirl of the combustion air. It is not possible to distinguish the fraction of NO_x produced from fuel-nitrogen in these flames from that produced as thermal NO_x. In addition to the expected increase in fuel-nitrogen conversion to NO_x due to faster mixing of fuel and air near the burner there is possibly an increase in thermal NO_x formation due to an increase in peak flame temperature in the high swirl flame.

Solids emissions were measured by two separate techniques. Firstly, the flue-gas was sampled intermittently using a Baccarach Smoke Tester to obtain the smoke number. Samples were taken at 5 minute intervals during steady-state conditions for each flame. Secondly, a high-volume flue-gas sampling system was employed which consisted of a 1" diameter quartz glass tube placed in the exhaust gas, through which the flue gas was aspirated. A glass fibre filter was used to capture all particulates in the flue gas above 0.1 μm.

Solids emissions data are presented in Table 4 together with those of NO_x emission. It can be seen that the concentration of solids in the flue gas is well below the current solids emission standards for all the flames studied, and that in general the SRC-II heavy distillate gave higher solids concentrations than the 2.9/1 blend.

The variability in Smoke # does not correlate well with the measured solids concentrations, and it is felt that this is due to the fact that most flames were run at close to minimum possible excess air levels, where periodic fluctuations in fuel or air flow rate resulted in puffs of smoke being emitted. Smoke #'s measured during these periods gave higher values than the mean, whereas the continuous sampling for solid concentration averaged these intermittent smoke emissions over the entire sampling period.

An attempt was made to characterize the onset of smoke formation for the two types of SRC-II fuel. Test conditions were chosen which would tend to minimize smoke formation, i.e., high swirl and high air preheat using the Sonicore atomizer. Smoke numbers were measured as the O_2 concentration in the flue-gas was reduced, until CO appeared in the flue-gas. The results of these brief tests are shown in Fig. 12 where it is clear that the heavy distillate has a considerably higher tendency to form smoke. Under the conditions of these experiments excess air levels greater than 5% are required to reduce the smoke number below a value of 2. The 2.9/1 blend exhibited less of a tendency to form smoke under these high intensity combustion conditions, and excess air could be reduced to zero without the smoke number exceeding a value of 2.

4.2 Staged Combustion Flame Studies

The results obtained from computer modeling of the phase reactions, together with experimental data obtained from a previous study on a high-nitrogen content #6 fuel oil [11], indicated that the design and operating variables which influence NO_x emissions under staged combustion conditions are:

- fuel-rich zone fuel equivalence ratio ϕ_b.
- fuel-rich zone mixing pattern as influenced by burner air swirl number, S.
- flame temperature as influenced by combustion air preheat.

Throughout the staged combustion experiments the following operating conditions were maintained constant:

- thermal input - 1MW (3.4×10^6 Btu/hr)
- overall excess air -10% (2% O_2 in the flue-gas)
- furnace wall temperature -2200°F (exhaust gas temperature -2400°F)
- atomization conditions - a twin fluid, Y-jet steam atomizer.

The effects of varying ϕ_b upon flue gas NO_x concentration and Baccarach Smoke # were determined at constant air preheat and burner swirl number. Air preheat temperature was 100°F and burner air swirl number $S = 0.65$, [illegible] was found to be the minimum swirl number required to maintain good flame stability over the range of fuel equivalence ratios being studied. Five staged combustion conditions corresponding to ϕ_b = 1.20, 1.30, 1.44, 1.62, and 1.76 were examined. The results obtained are shown in Fig. 13 where it can be seen that the concentration of NO_x in the flue gas changes from the unstaged value of ≈ 290 ppm @ 3% O_2 to a minimum of ≈ 95 ppm @ O_2 as ϕ_b is increased to between 1.3 and 1.4. Increasing ϕ_b beyond a value of 1.4 resulted in a slight increase in NO_x emissions.

Smoke #, as measured with the Baccarach smoke tester, is seen to increase significantly as the burner fuel equivalence ratio is increased beyond ϕ_b = 1.3. However, it is felt that smoke number measurements should be used only to indicate trends in solids emissions, since individual measurements made under constant furnace operating conditions can exhibit considerable scatter.

The influence of swirl on NO_x and smoke emissions was investigated by maintaining staged combustion conditions with ϕ_b = 1.3 (minimum observed NO_x) and varying the swirl number from 0 to 2.7. Air preheat was maintained at 100°F. Flue-gas NO_x concentration and Baccarach smoke number were measured at six swirl settings.

The results are shown in Fig. 14, and it is seen that a significant change in NO_x emissions occurs as the swirl number is changed from 0.25 to 0.45. NO_x emissions changed from 260 ppm to 90 ppm at 3% O_2, and smoke number increased. The high NO_x values at low swirl settings are very similar to the unstaged values, and it appears as through fuel/air mixing is sufficiently influenced in the primary zone under these conditions as to cancel out the effects of staging at swirl numbers less than 0.45.

Visual observation of the flame clearly showed that the change in swirl from 0.25 to 0.45 corresponded to a change from a "lifted" to a "non-lifted" flame. The "lifted" flame was stabilized 2-3 ft from the spray nozzle while the "non-lifted" flame was stabilized close to the spray nozzle. It is not clearly understood why the position of the flame has such a strong influence on NO_x emission under staged combustion conditions.

The effect of air preheat temperature, upon NO_x and smoke emissions was measured for constant values of ϕ_b = 1.3 and S = 0.65 which were identified as giving minimum NO_x emissions and low smoke levels. Increasing air preheat resulted in a decrease in both NO_x and Smoke # as shown in Fig. 15. NO_x emission was reduced by ≃ 20%, when air preheat was increased from 100°F to 800°F. The fact that increasing air preheat has resulted in the reduction of flue gas NO_x concentration is an indication that higher temperatures in the fuel rich zone were instrumental to lowering the sum of bound nitrogen species entering the lean stage, and that little or no incremental thermal NO was formed as a result of higher air preheat. This is likely due to the fast mixing at the introduction of the high velocity secondary air stream resulting in a lowering of the mixture temperature before the lean stage combustion takes place.

The trend of decreasing Smoke # with air preheat was verified by the measurement of flue-gas particulate concentration using a high-volume sampling probe/filter arrangement. Particulate concentration was measured at only two air preheat levels; and the results are given below:

Air Preheat °F	Particulate Concentration lb/10^6 BTU
260	$.32 \times 10^{-2}$
800	$.28 \times 10^{-2}$

It is encouraging to note that these particulate concentration levels obtained with staged combustion conditions are well below the emission standard and are of the same order as those for single stage combustion.

SECTION 5

CONCLUSIONS

5.1 Drop Tube Studies

- The extent of nitrogen evolution depends upon the rate of vaporization.
- Under typical droplet heating conditions, the initial products of vaporization are deficient of nitrogen.
- The nitrogen poor product, as a fraction of the total mass of the fuel droplet, is increasing with increasing heating rate up to a limit above which this trend is reversed.
- No carbonaceous residue is formed by the rapid heating of 150 μm droplets.

5.2 Computer Modeling Studies

- A model to predict total bound nitrogen species as a function of fuel rich stage fuel equivalence ratio, temperature and residence time was developed.
- The model shows that the fuel equivalence ratio of the fuel rich stage is the primary variable controlling fuel-nitrogen conversion and that the process is chemical kinetically limited.
- The model exhibited the ability to obtain significant reductions in bound nitrogen species for residence times (less than one second) typical of many utility boilers and industrial furnaces.

5.3 Combustion Research Facility Experiments

5.3.1 Single Stage Combustion Studies

- NO_x emission changed from 500 ppm (3% O_2) for a highly swirling jet flame to about 250 ppm (3% O_2) for a long turbulent jet diffusion flame. Solids emissions were well below existing standards for both the blend and heavy distillate fuel.

5.3.2 Staged Combustion Studies

- NO_x levels were reduced to below 100 ppm (at 3% O_2) by staged combustion.
- NO_x reduction was most strongly affected by fuel rich stage fuel equivalence ratio. Minimum NO_x emissions occured in the range of ϕ_b = 1.3-1.5 in agreement with computation.
- Swirl affected NO_x emissions only so far as it modified the flow pattern. For values of swirl number near the critical (onset of recirculation) NO_x emission was sensitive to flame stability. Both staged and unstaged flame studies demonstrated stepwise increase in NO_x emission when the flame "lifted" upon reduction of swirl degree.
- Air preheat, increasing air inlet temperature from 100°F to 800°F, reduced NO_x emission by approximately 20% and is in agreement with computation.
- The Baccarach Smoke number increased with increasing fuel equivalence ratio and increasing burner swirl number. Nevertheless, at optimum staged combustion conditions (ϕ_b = 1.3, S = 0.65) particulate loading was found to be well below emission standards.

REFERENCES

1. Downs, W., and A. J. Kubasco, "Characterization and Combustion of SRC-II Fuel Oil," EPRI Report FP-1028, June 1979.

2. Piper, B. F., et al., "Combustion Demonstration of SRC-II Fuel Oil in a Tangentially Fired Boiler," EPRI Report FP-1029, May 1979.

3. Muzio, L. J., J. K. Avand and W. C. Rovesti, "Combustion and Emission Characteristics of SRC-II Fuels," Western States Section, The Combustion Institute 1980 Spring Meeting, April 1980.

4. Beér, J. M., A. F. Sarofim, S. Hanson and A. K. Gupta, "High Temperature Pyrolysis of Oil Droplet and Coal Particle Streams," EPA Fundamental Combustion Workshop, Newport Beach, CA., January 1980. Grant No. R805552-01.

5. "Control of NO_x Emissions from Combustion of Fuels Derived from Shale and Coal." DOE Contract EX76-A-A-01-2205 T036 at M.I.T.

6. Martin, G. B., and E. E. Berkau, "An Investigation of the Conversion of Various Fuel Nitrogen Compounds to Nitrogen Oxides in Oil Combustion," AIChE Symp. Ser. Air Pollution and Its Control, 68 (1972).

7. Mims et al., "Laboratory Studies of Trace Element Transformations during Coal Combustion." Paper presented at the National 87th AIChE Meeting, August 1979.

8. Levy, J. M., J. P. Longwell and A. F. Sarofim, "Conversion of Fuel-Nitrogen to Nitrogen Oxides in Fossil Fuel Combustion: Mechanistic Considerations." Report submitted to the Energy and Environmental Research Corporation by the M.I.T. Energy Laboratory, April 1978.

9. Taylor, B. R., Sc.D. Thesis (to be submitted) Massachusetts Institute of Technology, Cambridge, Mass., (1980).

10. Farmayan, W. F., M.Sc. Thesis, "The Control of Nitrogen Oxides Emissions by Staged Combustion," Massachusetts Institute of Technology, Cambridge, Mass., April 1980.

11. Jacques, M. T., and J. M. Beér, "Experimental Studies on the Conversion of Fuel-Nitrogen in Staged Combustion." Paper presented at the Italian Flame Day Meeting, Naples, June 1980.

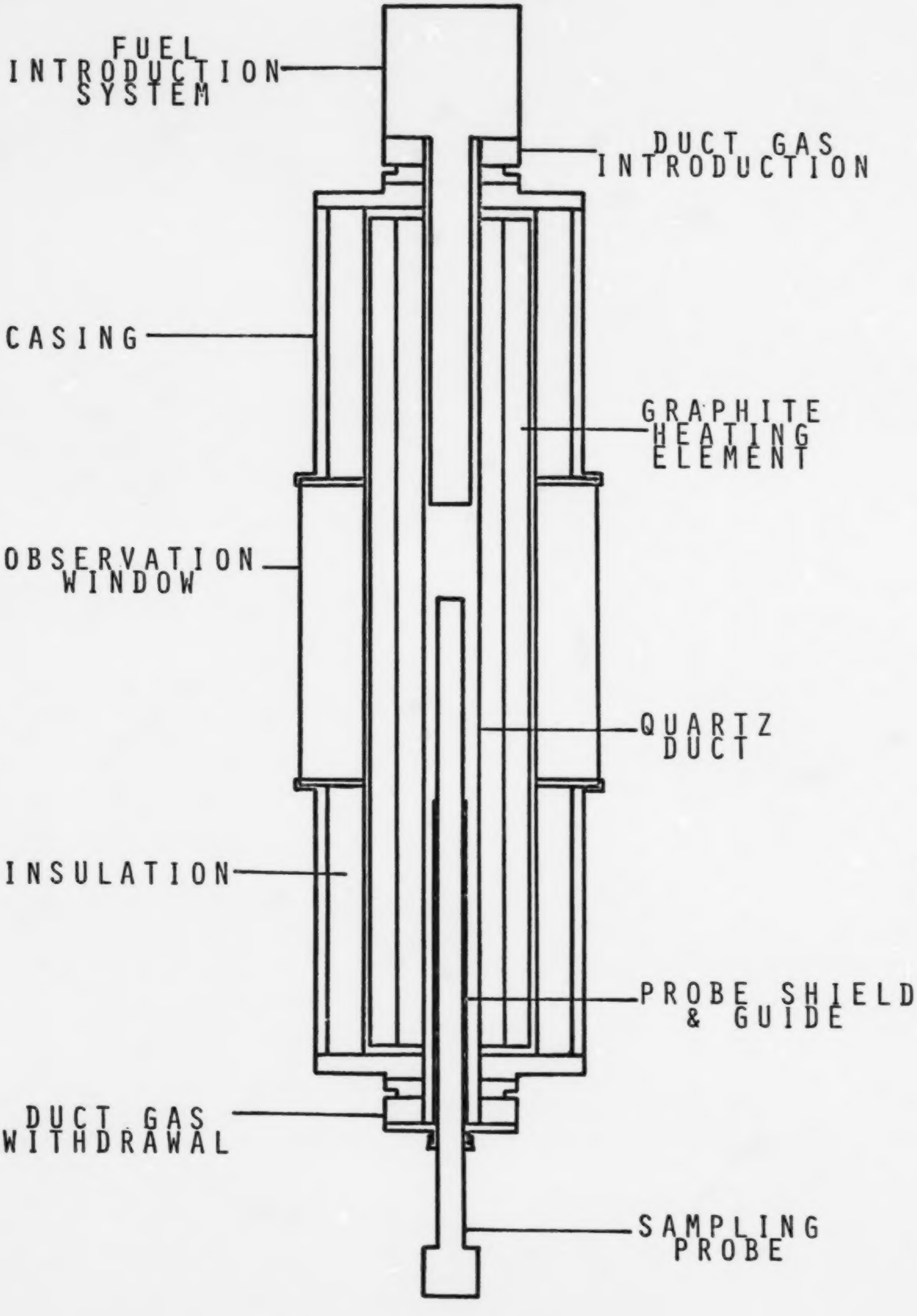

FIGURE 1: THE EXPERIMENTAL SYSTEM

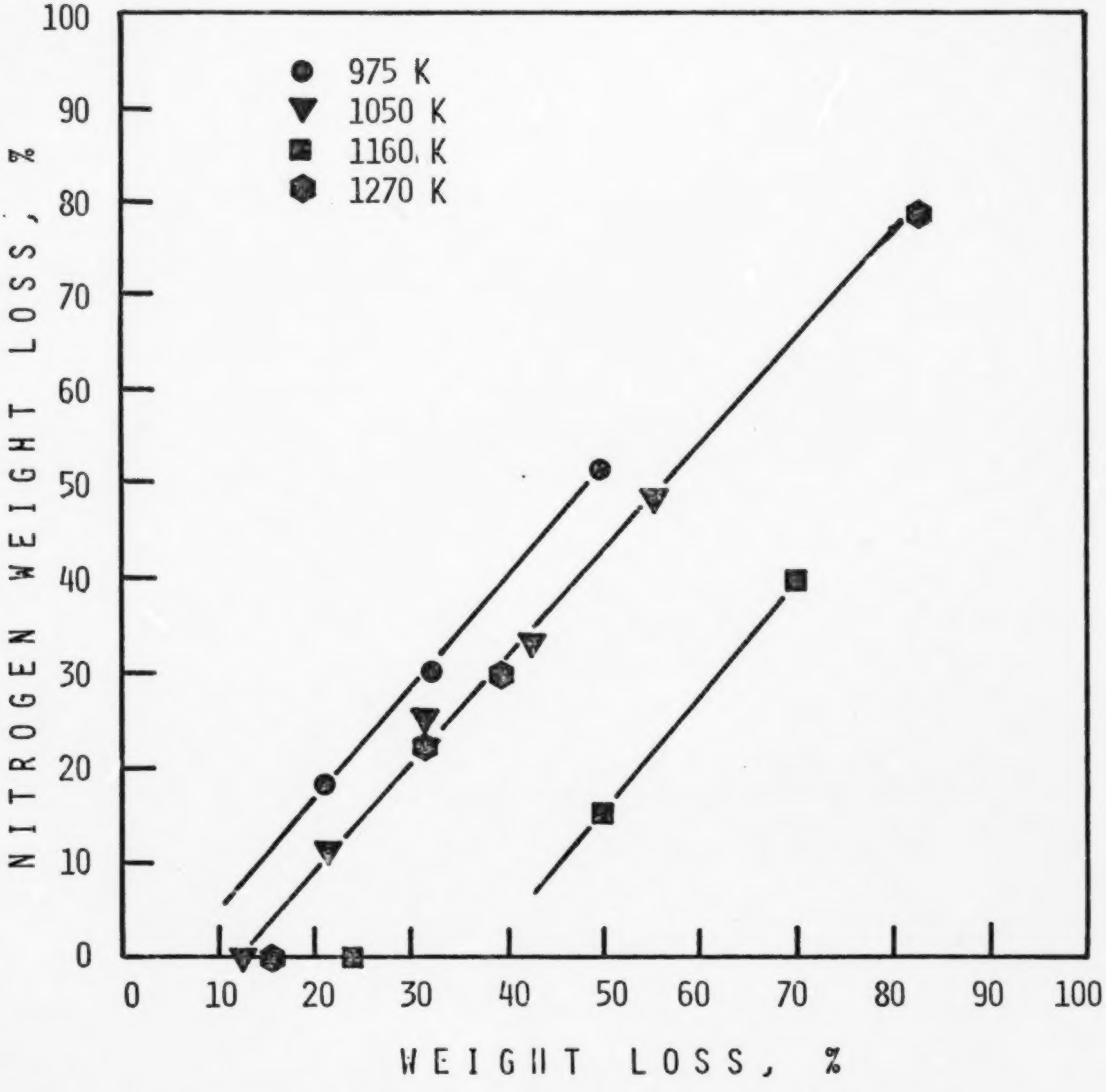

FIGURE 2: NITROGEN EVOLUTION FROM 150μm DROPLET ARRAY OF SRC II (MIDDLE DISTILLATE)

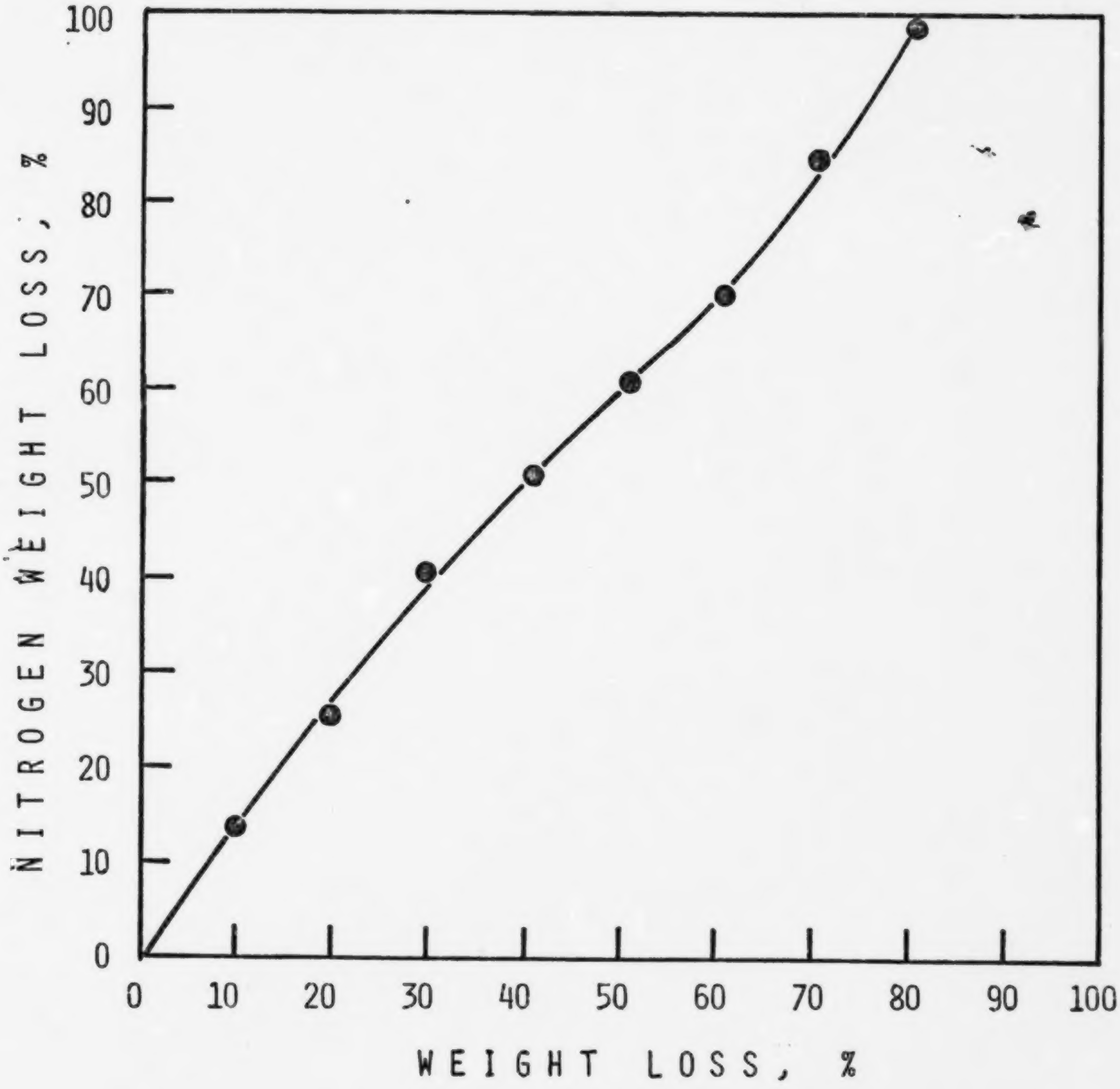

FIGURE 3 : NITROGEN EVOLUTION FROM THE EQUILIBRIUM DISTILLATION OF SRC II (MIDDLE DISTILLATE) AT ATMOSPHERIC PRESSURE

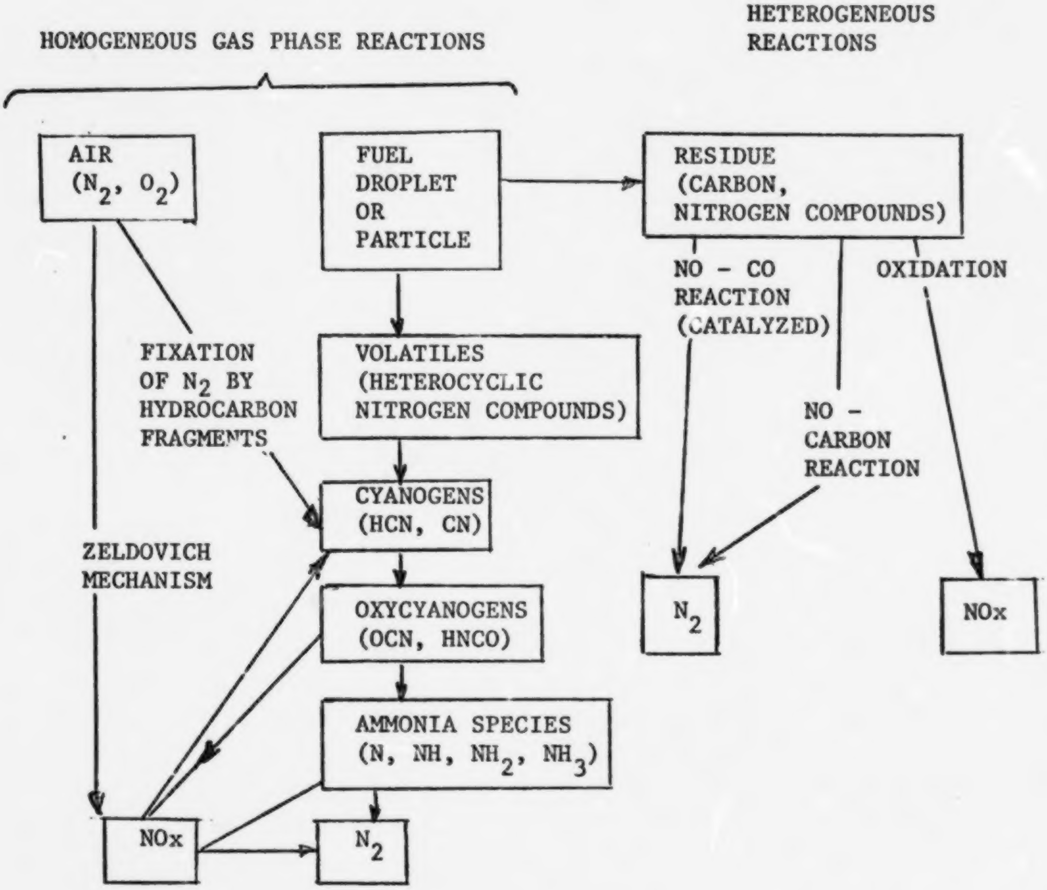
HOMOGENEOUS GAS PHASE REACTIONS
HETEROGENEOUS REACTIONS
AIR (N_2, O_2)
FUEL DROPLET OR PARTICLE
RESIDUE (CARBON, NITROGEN COMPOUNDS)
NO - CO REACTION (CATALYZED)
OXIDATION
FIXATION OF N_2 BY HYDROCARBON FRAGMENTS
VOLATILES (HETEROCYCLIC NITROGEN COMPOUNDS)
NO - CARBON REACTION
CYANOGENS (HCN, CN)
ZELDOVICH MECHANISM
N_2
NOx
OXYCYANOGENS (OCN, HNCO)
AMMONIA SPECIES (N, NH, NH_2, NH_3)
NOx
N_2

Figure 4. The formation of nitrogen oxides in fossil fuel combustion: mechanistic pathways.

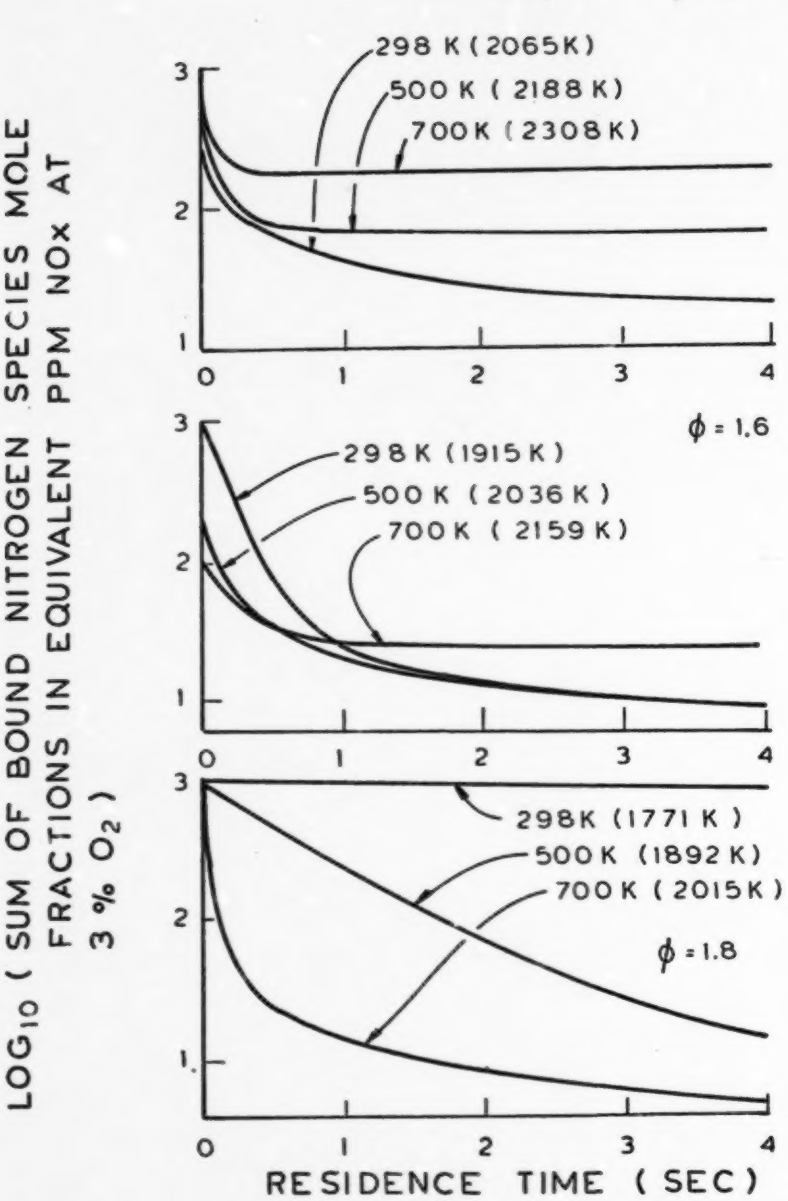

Figure 5 Bound Nitrogen Species Mole Fractions vs Residence Time, (0.7 % N # 6 Fuel Oil)

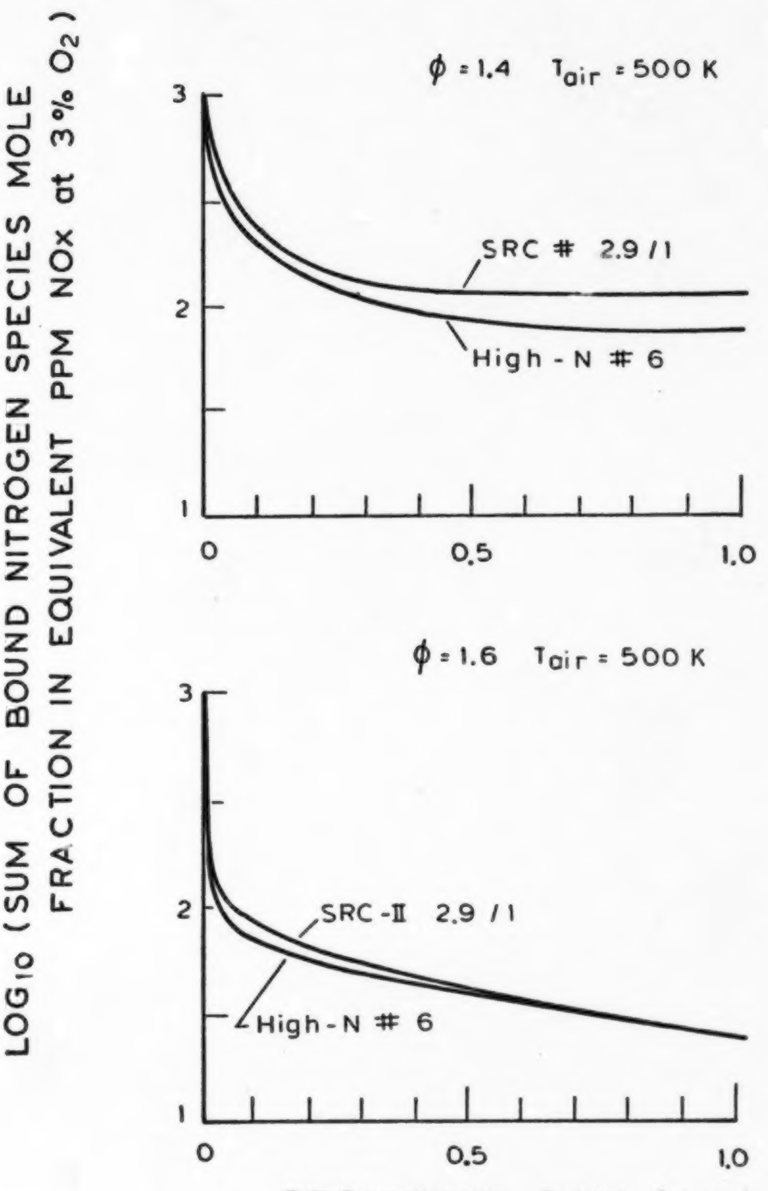

Figure 6 Comparison of SRC # (2.9/1) and High Nitrogen Content # Computer Model Predictions for Effect of ϕ

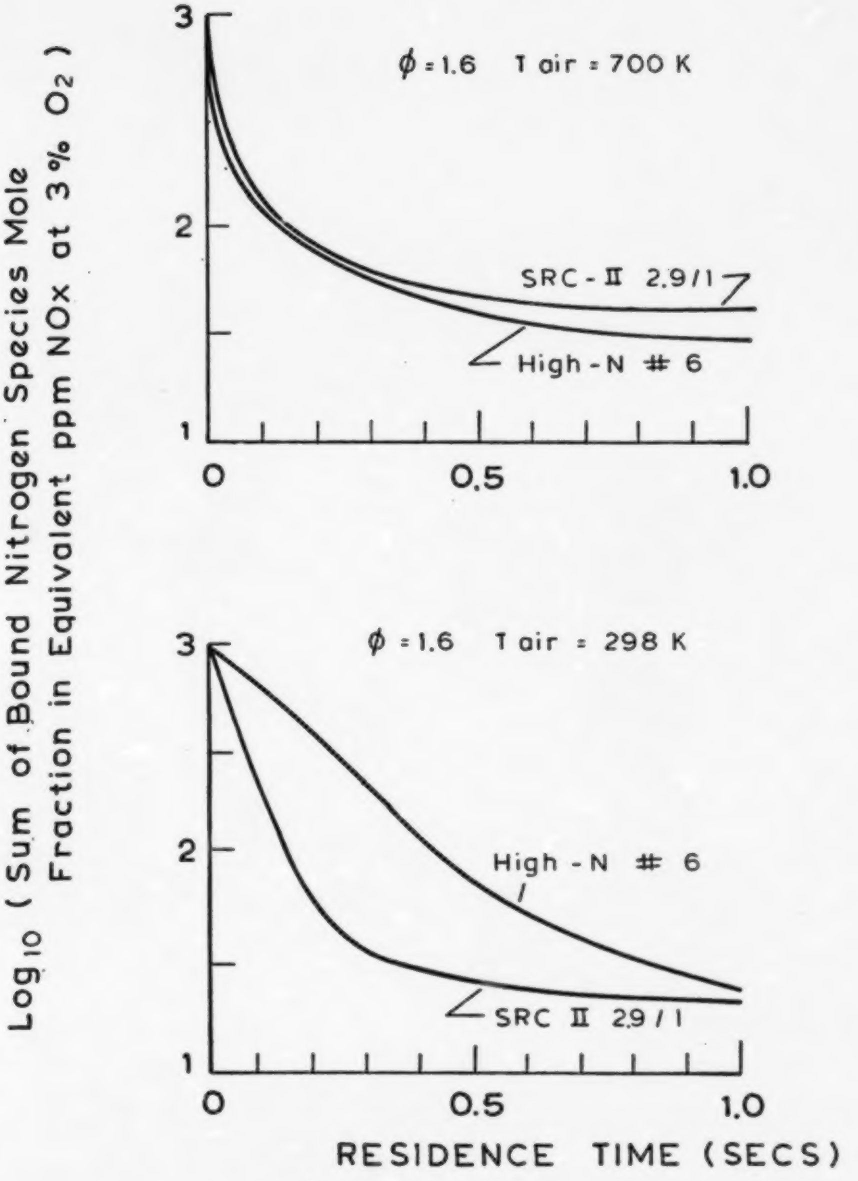

Figure 7 Comparison of SRC - II (2.9/1) and High Nitrogen Content # 6 Computer Model Predictions for Effect of Air Preheat

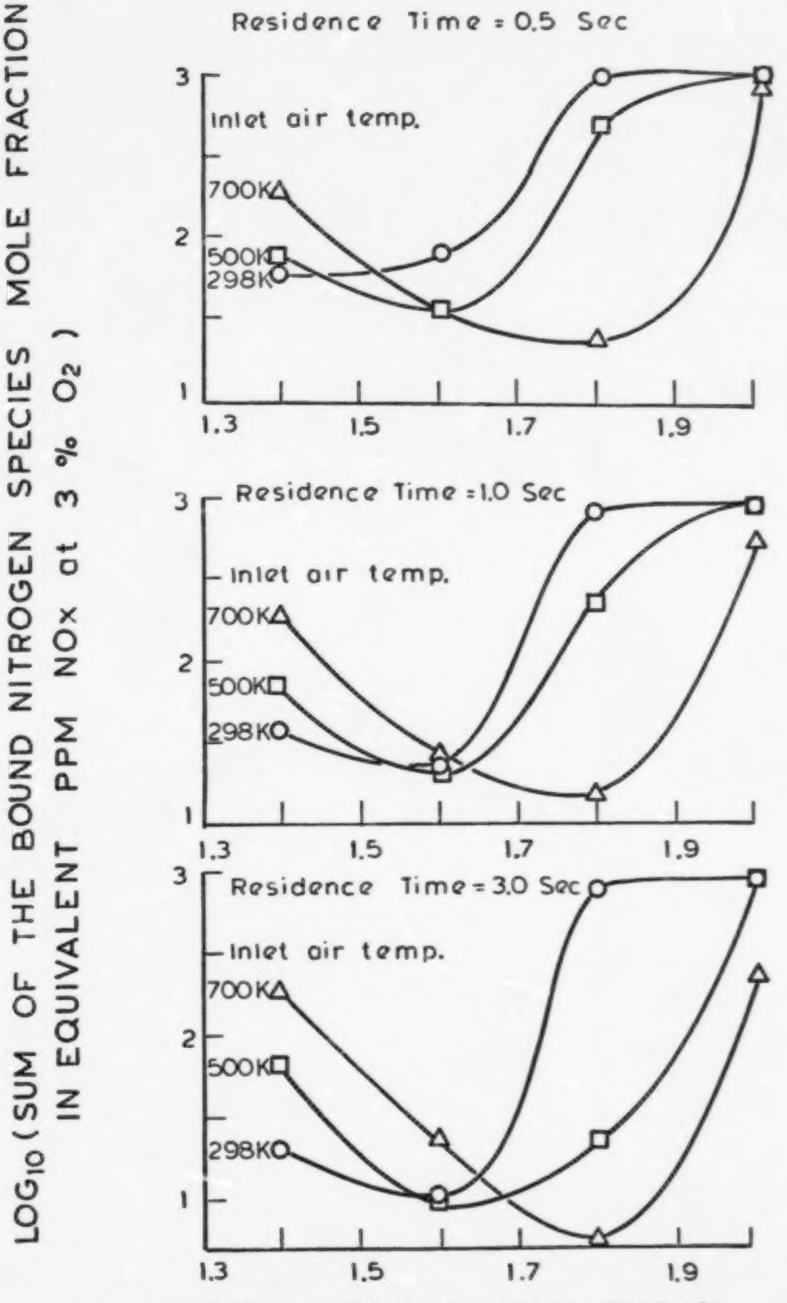

Figure 8 Bound Nitrogen Species Mole Fraction vs Fuel Equivalence Ratio

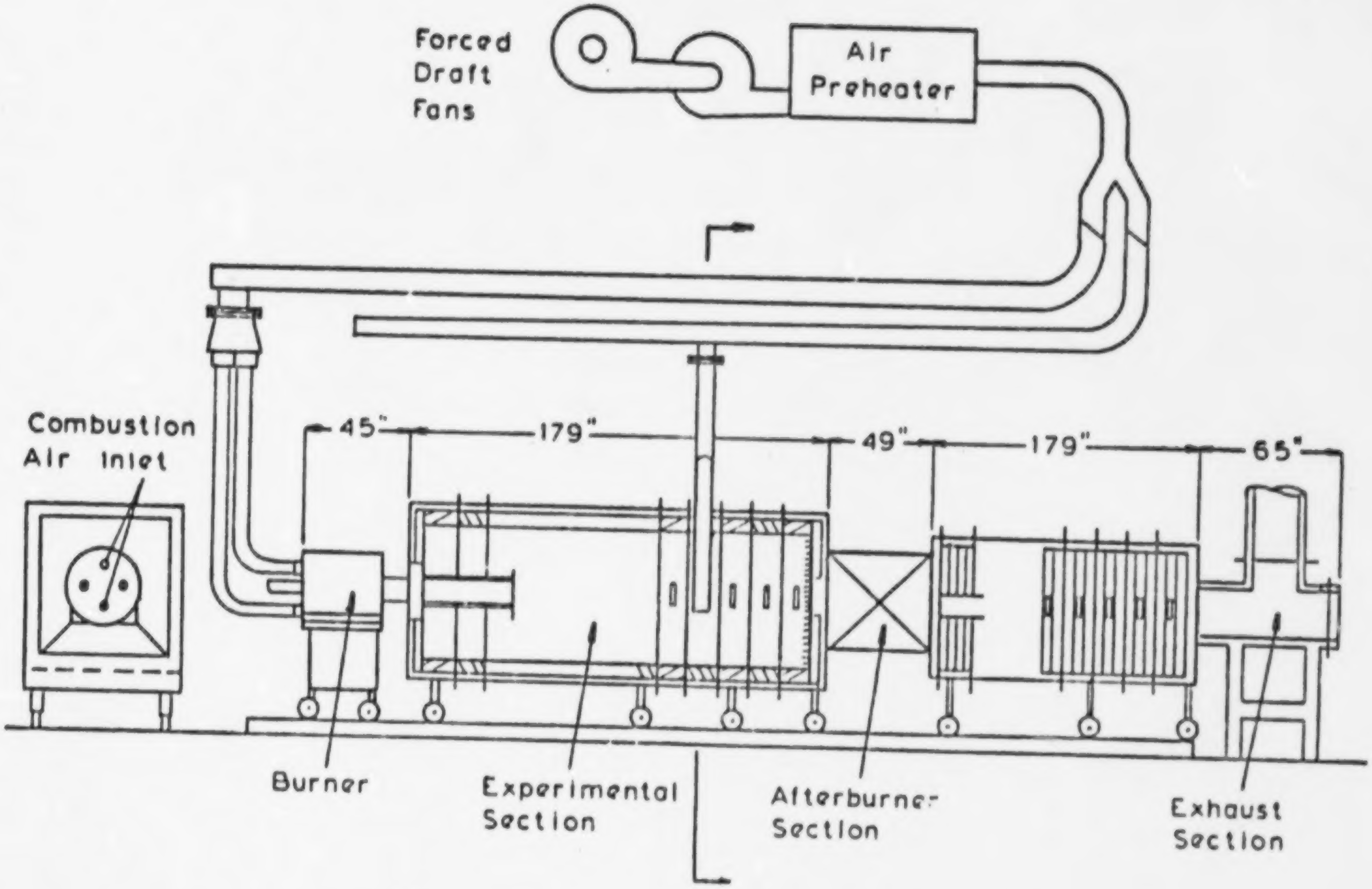

Figure 9. The MIT-Combustion Research Facility

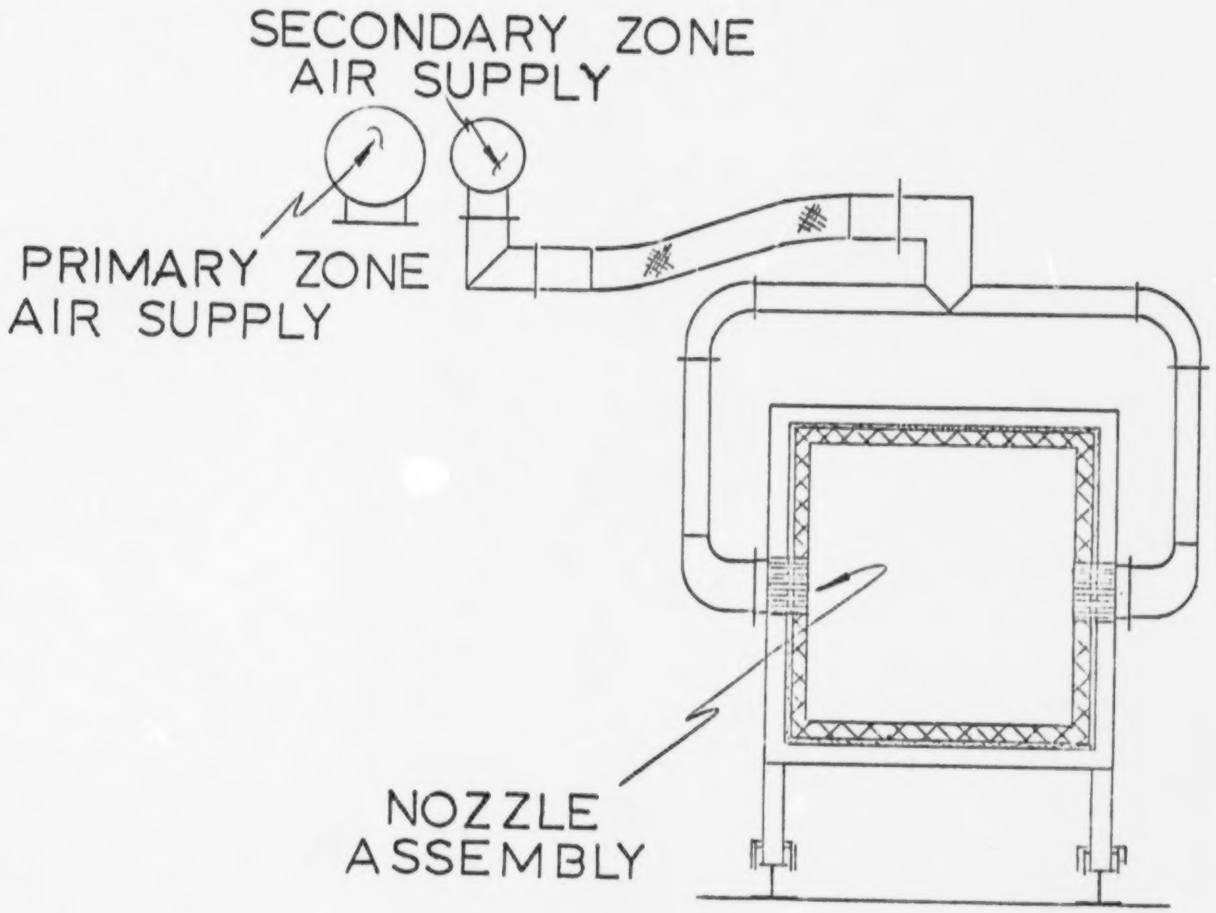

Figure 10. Sectional View of the MIT Combustion Research Facility showing a Schematic of the Secondary Zone Air Supply to the Furnace.

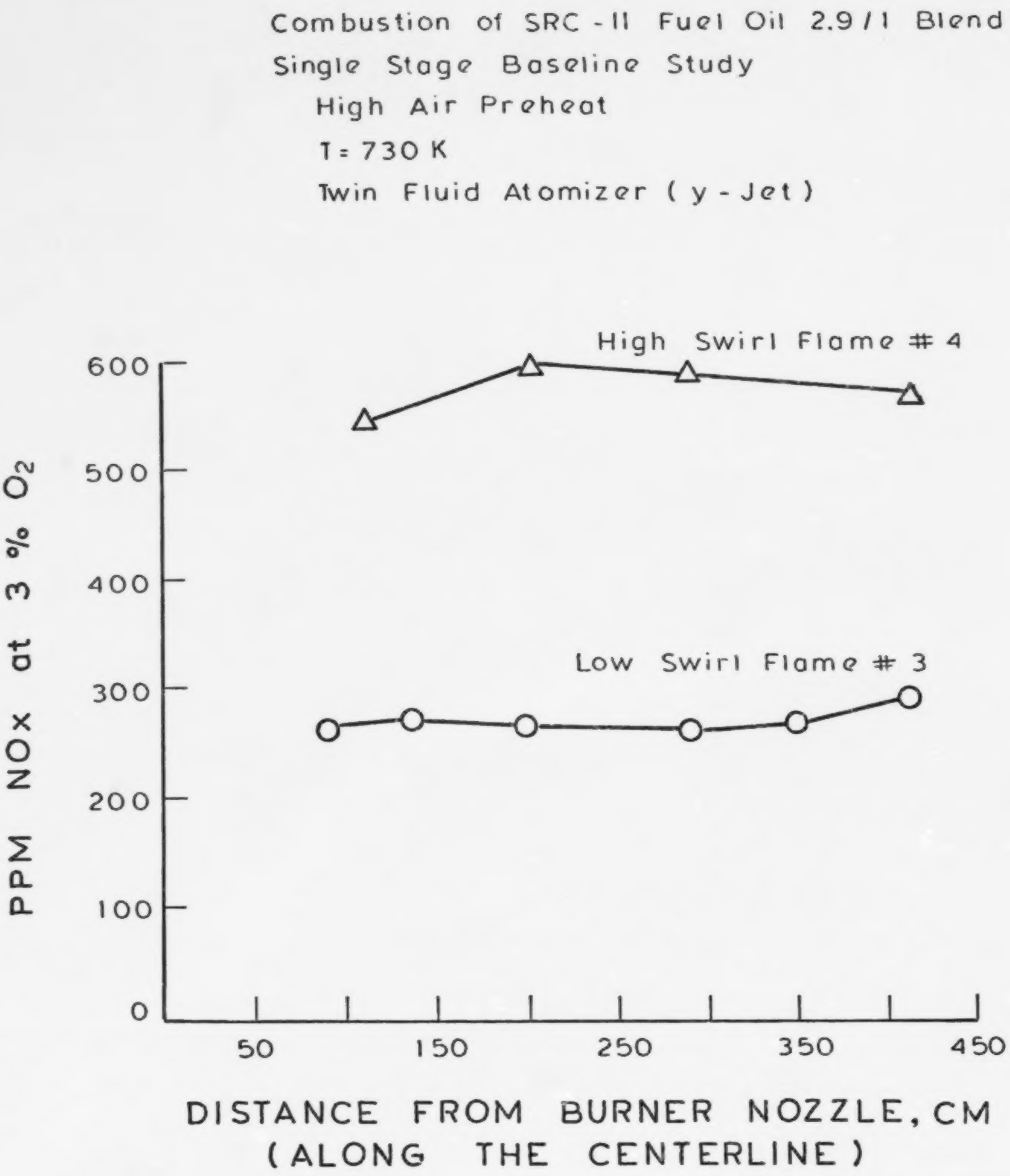

Figure 11 Axial NOx Concentration Profiles

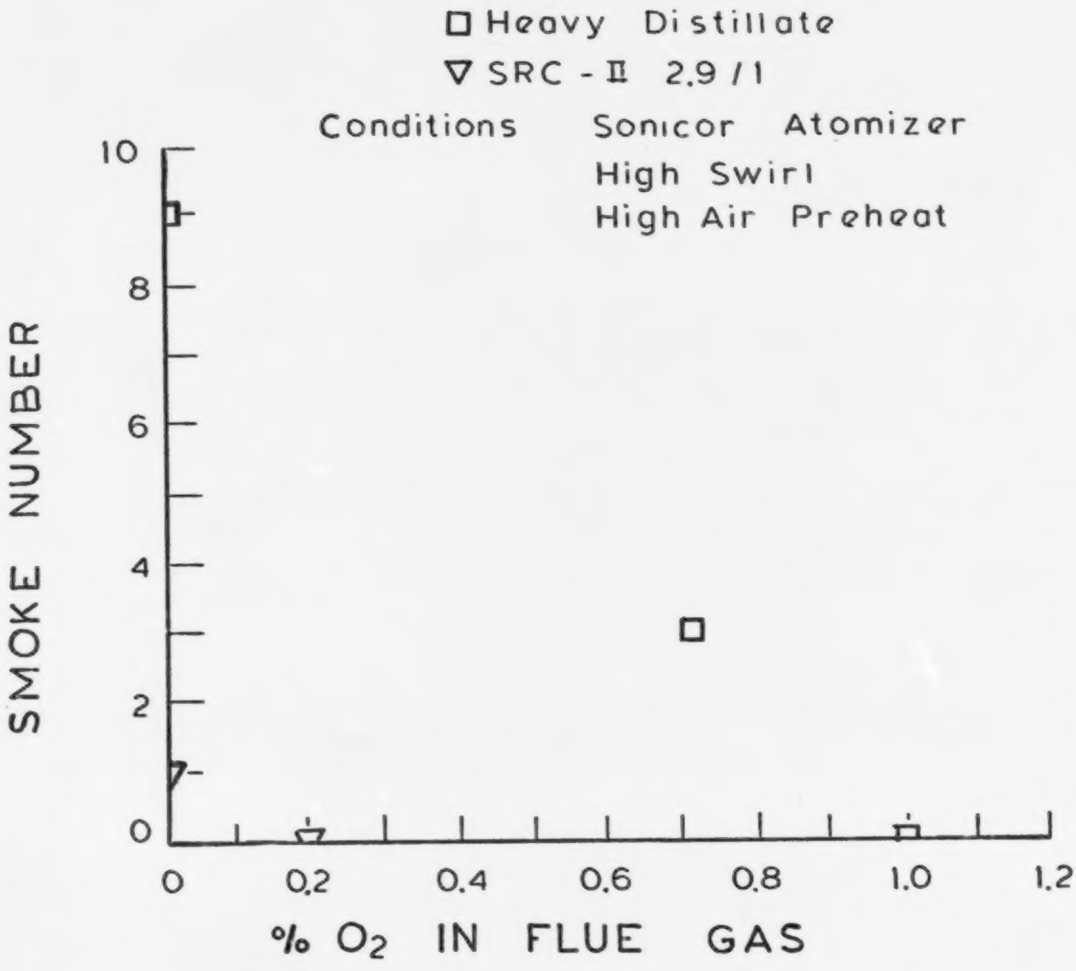

Figure 12 Smoke Number Versus % O_2 in Flue - Gas

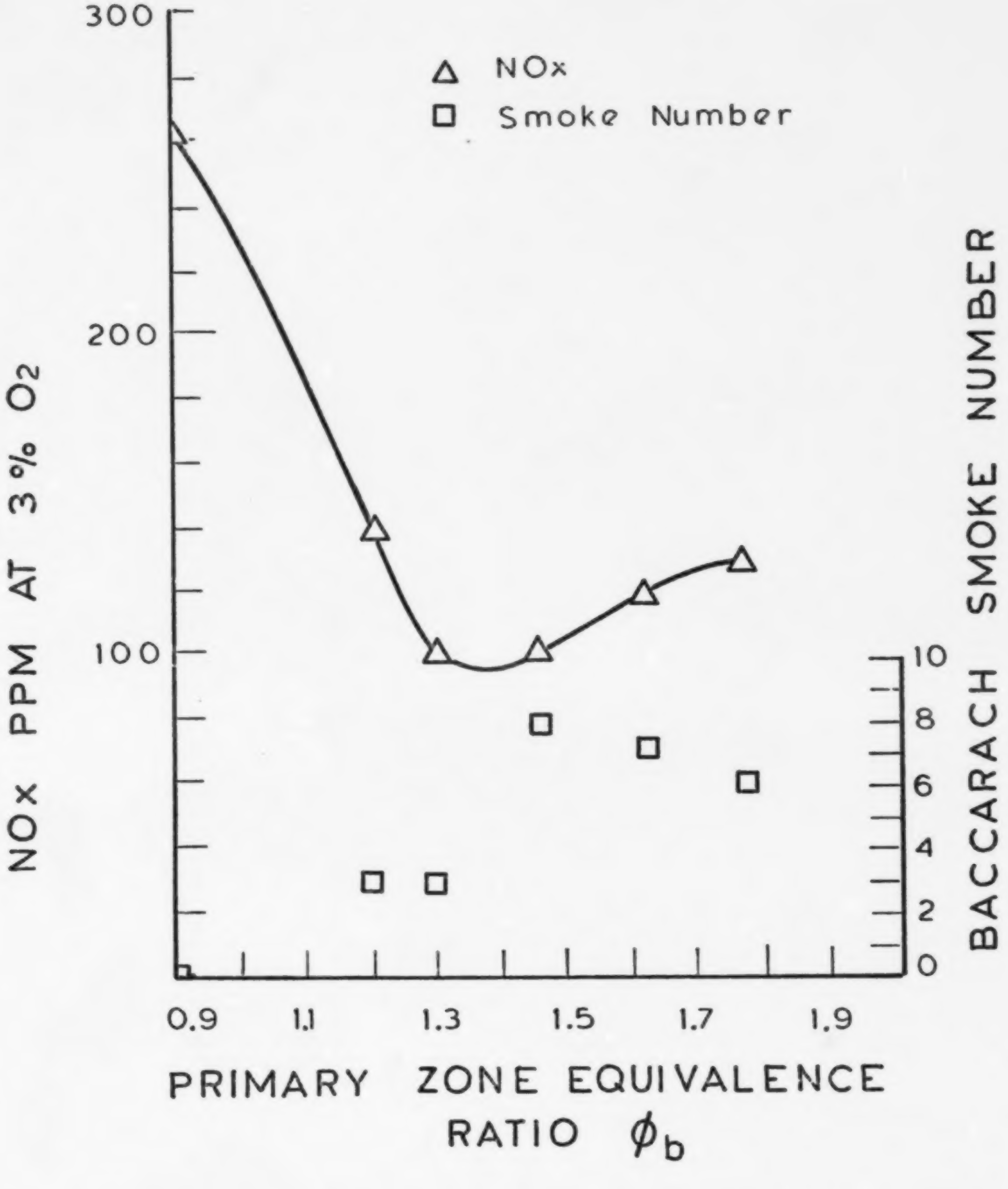

Figure 13 Measured NOx and Smoke Number vs Primary Zone Fuel Equivalence Ratio, ϕ_b (Swirl Number = 0.65)

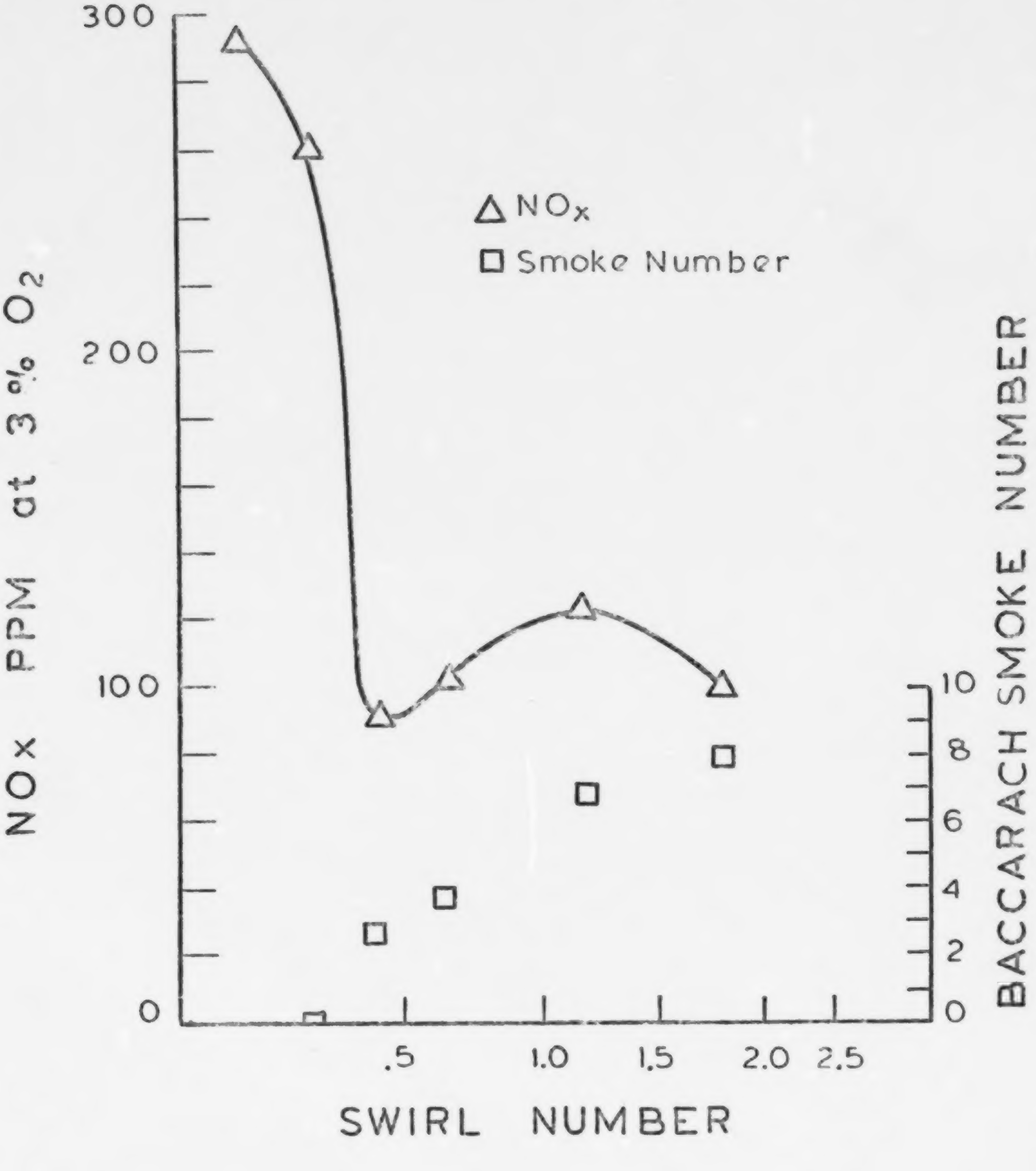

Figure 14 Measured NOx and Smoke Number vs. Swirl Number ($\phi_b = 1.3$)

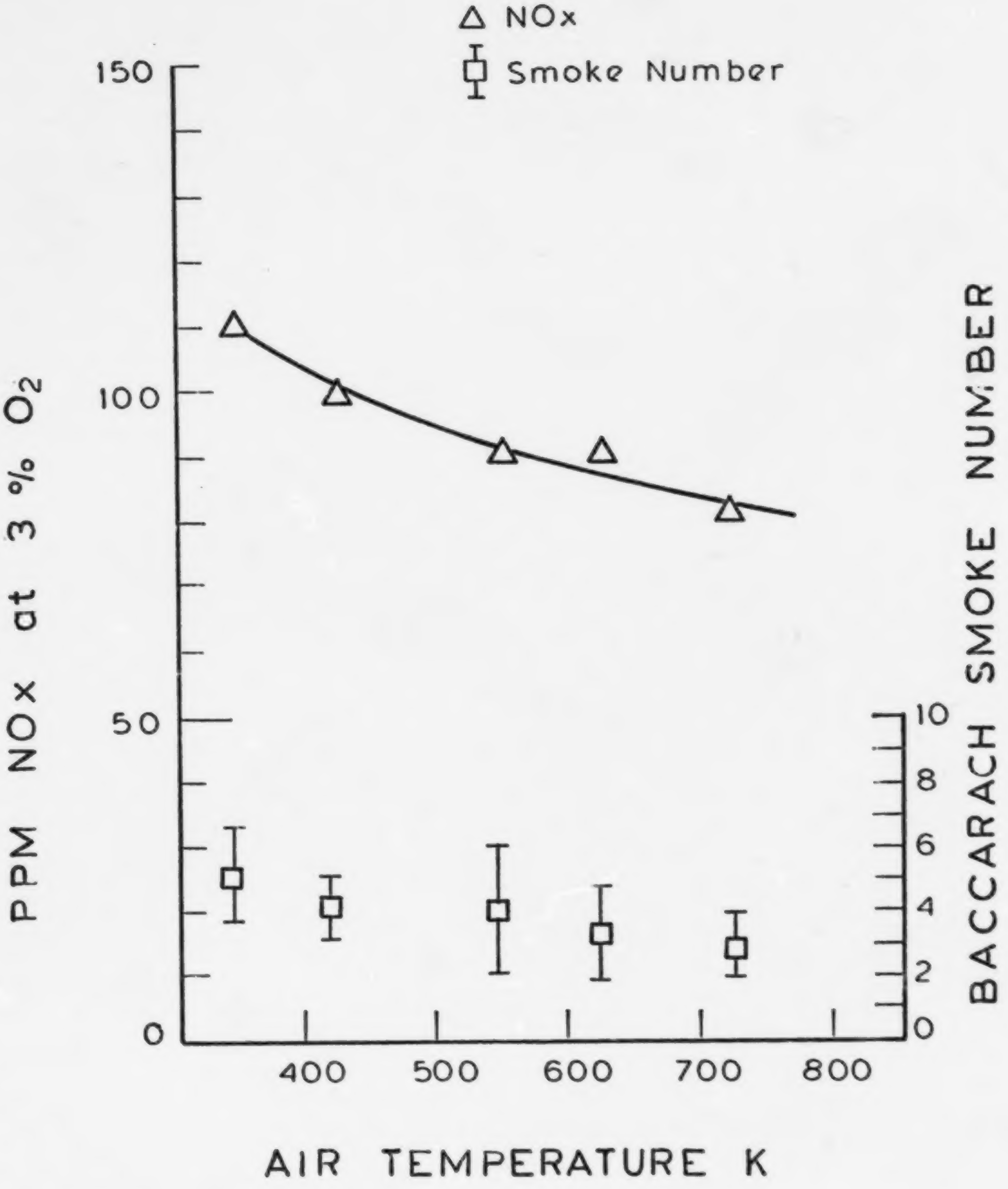

Figure 15 Measured NOx and Smoke Number vs Air Preheat (ϕ_b = 1.3 , S = 0.65)

TABLE I *

REACTIONS AND ACCOMPANYING RATE DATA INCORPORATED INTO THE PLUG FLOW KINETIC MODEL FOR MODELLING OF NO_X FORMATION RATES

$$k_f = AT^N \exp(-E/RT)$$

Reaction	A cm^3/mole s	N	E cal/mole
$CN + H_2 = HCN + H$	3.16 E + 12	0.0	5000
$HCN + OH = CN + H_2O$	2.00 E + 11	0.6	5000
$CN + O = CO + N$	6.31 E + 11	0.5	0
$CN + OH = NCO + H$	5.60 E + 13	0.0	0
$CN + O_2 = NCO + O$	3.20 E + 13	0.0	1000
$HCN + OH = HNCO + H$	2.00 E + 11	0.0	0
$HCN + O = NCO + H$	5.20 E + 12	0.0	8100
$NCO + H_2 = HNCO + H$	3.20 E + 11	0.0	0
$NCO + H = NH + CO$	3.00 E + 14	0.0	0
$HNCO + H = NH_2 + CO$	1.40 E + 13	0.0	0
$NO + O = N + O_2$	1.59 E + 09	1.00	38640
$NO + H = N + OH$	1.34 E + 14	0.0	49200
$NH_3 + OH = NH_2 + H_2O$	1.26 E + 10	0.68	1100
$NH_3 + O = NH_2 + OH$	1.50 E + 12	0.0	6000
$NH_2 + O = NH + OH$	9.20 E + 11	0.50	0
$NH + OH = N + H_2O$	5.00 E + 11	0.50	2000
$NH + O = N + OH$	6.31 E + 11	0.50	8000
$NH + H = N + H_2$	1.00 E + 12	0.68	1900
$NH_2 + OH = NH + H_2O$	3.00 E + 10	0.68	1300
$NH_2 + H = NH + H_2$	3.50 E + 10	0.79	4460
$NH_3 + H = NH_2 + H_2$	5.00 E + 11	0.50	2000
$NH + NH_2 = NH_3 + N$	1.00 E + 11	0.50	4107

Table I continued

Reaction	A	N	E
$NH + NO = N_2O + H$	9.00 E + 09	0.75	0
$N_2O + H = N_2 + OH$	7.60 E + 13	0.0	15101
$N_2O + M = N_2 + O + M$	5.00 E + 14	0.0	58000
$NH + N = N_2 + H$	6.30 E + 11	0.50	0
$NO + N = N_2 + O$	3.10 E + 13	0.0	334
$NH + O = NO + H$	6.30 E + 11	0.50	0
$NCO + O = NO + CO$	2.00 E + 13	0.0	0
$H_2 + O = H + OH$	1.82 E + 10	1.00	8900
$H_2O + O = OH + OH$	6.76 E + 13	0.0	18350
$H_2 + OH = H_2O + H$	2.51 E + 13	0.0	5200
$O_2 + H = O + OH$	2.24 E + 14	0.0	16800
$H + OH + M = H_2O + M$	4.70 E + 16	0.0	0
$H + H + M = H_2 + M$	4.70 E + 16	0.0	0
$H + O + M = OH + M$	7.94 E + 15	0.0	0
$O_2 + M = O + O + M$	2.51 E + 18	-1.00	118700
$CO_2 + H = CO + OH$	1.48 E + 14	0.0	26440

---

* Rate data was compiled by B. R. Taylor from the literature.

TABLE II. SRC-II FUEL OIL ANALYSES

	SRC-II (Middle)	SRC-II (2.9/1)	SRC-II (Heavy)	Source of Analysis
API Gravity	13.4	10.4	1.3	Truesdail Labs
Viscosity ssu @ 70°F	-	-	-	
ssu @ 100°F	-	-	-	
ssu @ 140°F	36.4	36.8	67.2	
ssu @ 210°F	31.8	33.0	41.3	
Flash Point °F	147	150	265	
Pour Point °F	<-20	<-20	+8	
Normal Boiling Range °F	350-550	350-850	550-850	
Heat of Combustion				
Gross BTU/Lb	17,000	17,110	17,120	
Net BTU/Lb	16,190	16,340	16,420	
Elemental Analysis				
Carbon %	83.79	86.28	88.37	MIT
Hydrogen %	9.04	8.83	7.38	
Nitrogen %	0.94	0.96	1.17	
Sulfur %	0.23	0.28	0.43	Galbraith Labs
Ash %	<0.01	<0.01	<0.07	
Oxygen %	4.84	3.68	1.17	

TABLE III

INPUT AND OPERATING CONDITIONS FOR THE 12 FLAMES STUDIED

Flame #	SRC-II Fuel Type	Thermal Input	Atomizer Type	Air Preheat	Swirl #
1	2.9/1	1MW	y-jet	500°F	0.53
2	2.9/1	1MW	y-jet	500°F	2.70
3	2.9/1	1MW	y-jet	850°F	0.53
4	2.9/1	1MW	y-jet	850°F	2.70
5	2.9/1	1MW	Sonicore	500°F	0.53
6	2.9/1	1MW	Sonicore	500°F	2.70
7	Heavy	1MW	y-jet	500°F	0.53
8	Heavy	1MW	y-jet	500°F	2.70
9	Heavy	1MW	y-jet	850°F	0.53
10	Heavy	1MW	y-jet	850°F	2.70
11	Heavy	1MW	Sonicore	500°F	0.53
12	Heavy	1MW	Sonicore	500°F	2.70

TABLE IV. SOLIDS EMISSIONS DATA

Flame #	SRC-II Fuel Type	Solids Conc. Lb/M BTU	Smoke # (Baccarach)	NO_x ppm @ 3% O_2	% Excess Air
1	2.9/1	0.006	0	240	3-8%
2	2.9/1	0.006	0	525	5-8%
3	2.9/1	0.008	0-4	300	2-10%
4	2.9/1	0.004	0	575	2-5%
5	2.9/1	0.005	0-3	250	3-7%
6	2.9/1	0.005	0	500	4-7%
7	Heavy	0.006	0	250	2-5%
8	Heavy	0.010	0	425	2-5%
9	Heavy	0.008	0-2	275	4-8%
10	Heavy	0.008	0	600	5-10%
11	Heavy	0.008	0-2	250	2-8%
12	Heavy	0.008	0-1	515	4-7%